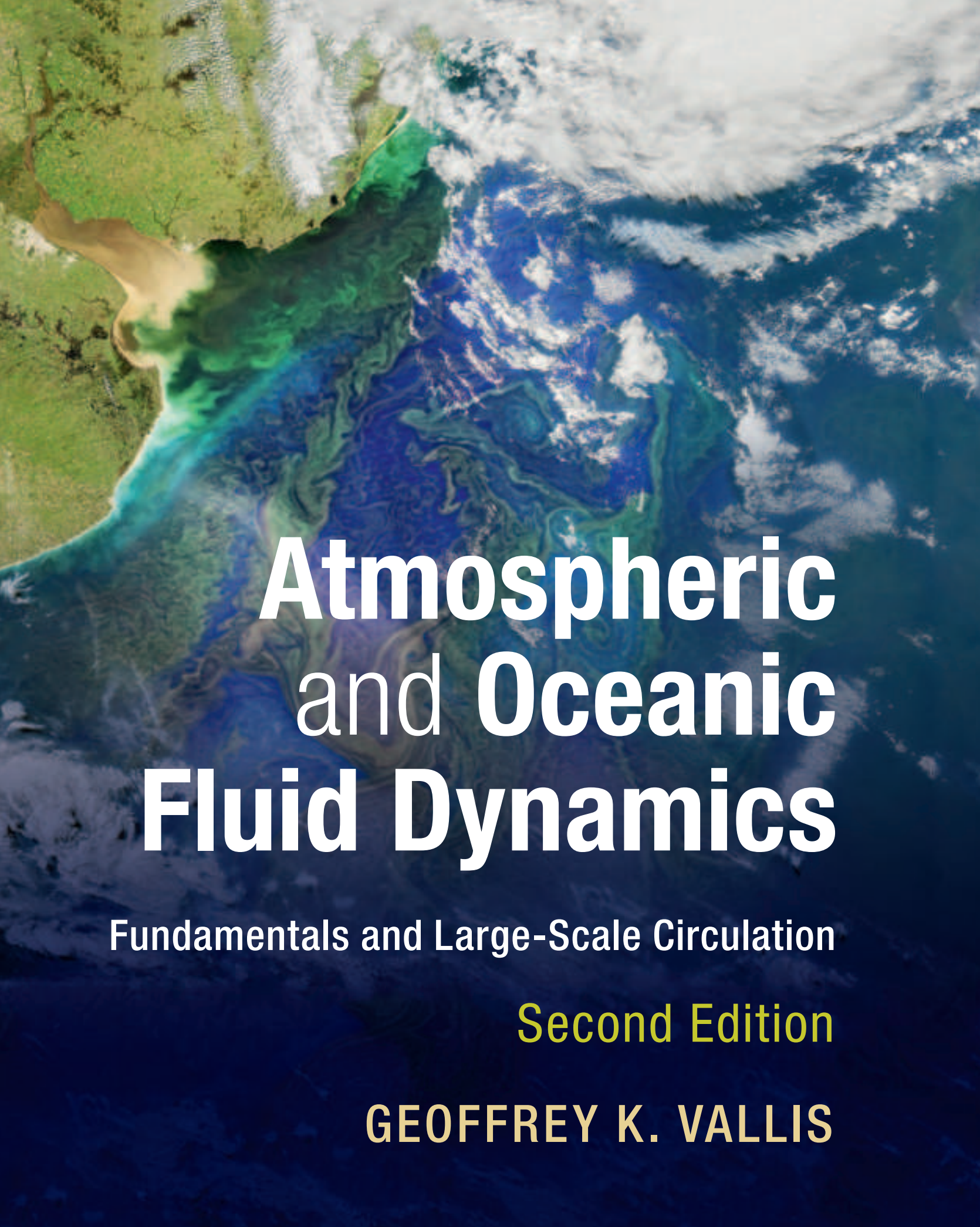

Atmospheric and Oceanic Fluid Dynamics

Fundamentals and Large-Scale Circulation

Second Edition

GEOFFREY K. VALLIS

Atmospheric and Oceanic Fluid Dynamics

Fundamentals and Large-Scale Circulation

Second Edition

The atmosphere and ocean are two of the most important components of the climate system, and fluid dynamics is central to our understanding of both. This book provides a unified and comprehensive treatment of the field that blends classical results with modern interpretations. It takes the reader seamlessly from the basics to the frontiers of knowledge, from the equations of motion to modern theories of the general circulation of the atmosphere and ocean. These concepts are illustrated throughout the book with observations and numerical examples. As well as updating existing chapters, this second, full-colour edition includes new chapters on tropical dynamics, El Niño, the stratosphere and gravity waves. Supplementary resources are provided online, including figures from the book and problem sets, making this new edition an ideal resource for students and scientists in the atmospheric, oceanic and climate sciences, as well as in applied mathematics and engineering.

Geoffrey K. Vallis is a professor of applied mathematics at the University of Exeter, UK. Prior to taking up his position there, he taught for many years at Princeton University in the USA. He has carried out research in the atmospheric sciences, oceanography and the planetary sciences, and has published over 100 peer-reviewed journal articles. He is the recipient of various prizes and awards, including the Adrian Gill Prize (Royal Meteorological Society) in 2014, and the Stanislaw M. Ulam Distinguished Scholar award (Los Alamos National Laboratory) in 2013.

"Vallis writes explanations as clear as tropical ocean waters, bringing fresh new light to complex concepts. This expanded text will be immediately useful both for graduate students and seasoned researchers in the field."

Dargan M. W. Frierson, *University of Washington*

"In 2006, Vallis' first edition of AOFD offered the atmospheric and oceanic sciences community a truly great book, marking a milestone in our discipline. Well, Vallis has done it again! This second edition of AOFD represents the pinnacle of a maturing discipline. It is **The Great Book** of the field, and it will remain so for a generation or longer. AOFD-2 dives deep into atmospheric and oceanic fluid dynamics, spanning a wealth of topics while offering the reader lucid, pedagogical, and thorough presentations across a universe of knowledge. There are really three books here: one focused on geophysical fluid dynamic fundamentals; a second on atmospheric dynamics; and a third on oceanic dynamics. Each part offers new material relative to the first edition, as well as the reworking of earlier presentations to enhance pedagogy and update understanding based on recent research. . . . the reader is privileged to receive a unified presentation from a master scientific writer whose pedagogy is unmatched in the discipline. This book is a truly grand achievement. It will be well used by fluid dynamicists, oceanographers, atmospheric scientists, applied mathematicians, and physicists for decades to come. Each sentence, paragraph, section, chapter, and figure, are thoughtful and erudite, providing the reader with insights and rigor needed to truly capture the physical and mathematical essence of each topic."

Stephen M. Griffies, *Geophysical Fluid Dynamics Laboratory and Princeton University*

"Vallis speaks my language. He successfully weaves together fundamental theory, physical intuition, and observed phenomena to tell the story of geophysical fluid behavior at local and global scales. This multi-pronged approach makes this an ideal text for both beginners and experts alike - there is something for everyone. This is why it is the book I use for my class, the book I recommend to incoming graduate students (no matter their background) and the book I go to first when I need clarity on GFD topics. The first edition of this book has been my go-to text since it was first published . . . With the new edition, we now get an even more comprehensive view of how the fundamental processes that dictate the evolution of our atmosphere and oceans drive the complex phenomena we observe."

Elizabeth A. Barnes, *Colorado State University*

"The first edition . . . provided an exceptionally valuable introduction to the dynamical theory of the large-scale circulation of the atmosphere and ocean . . . This second edition is a further major achievement ... It includes significant new material on the atmosphere and on the ocean, presented in two separate later sections of the book, but building carefully and clearly on the 'unified' material in the first part of the book ... The second edition will be an exceptionally valuable resource for those designing advanced-level courses, for the students taking those courses and for researchers, many of whom will surely be stimulated by the clear presentation of existing theory to identify what such theory does not explain and where progress is needed."

Peter Haynes, *University of Cambridge*

"This second edition is even more comprehensive than the first. It now covers subjects such as the derivation of the first law of thermodynamics, the fundamental physics involved in the meridional overturning of the ocean, and equatorial oceanography. The book concentrates on the fundamentals of each subject, with sufficient motivation to make the exposition clear. For good reason, the first edition is now the standard text for courses in oceanography, and this will clearly continue with this second edition, helping all of us, not just students, to clarify our understanding of this field."

Trevor J. McDougall, *University of New South Wales*

"Researchers looking for an informative and coherent treatment of the dynamics of the atmosphere and ocean, starting at a fundamental level, and proceeding to advanced topics, will find that this book is a truly superb resource. The book is particularly notable for its even-handed treatment of the ocean and the atmosphere and its synthetic discussion of observations, numerics and analytic methods."

William R. Young, *Scripps Institution of Oceanography*

Atmospheric and Oceanic Fluid Dynamics

Fundamentals and Large-Scale Circulation

Second Edition

Geoffrey K. Vallis
University of Exeter

CAMBRIDGE
UNIVERSITY PRESS

CAMBRIDGE
UNIVERSITY PRESS

University Printing House, Cambridge CB2 8BS, United Kingdom

One Liberty Plaza, 20th Floor, New York, NY 10006, USA

477 Williamstown Road, Port Melbourne, VIC 3207, Australia

4843/24, 2nd Floor, Ansari Road, Daryaganj, Delhi – 110002, India

79 Anson Road, #06–04/06, Singapore 079906

Cambridge University Press is part of the University of Cambridge.

It furthers the University's mission by disseminating knowledge in the pursuit of education, learning, and research at the highest international levels of excellence.

www.cambridge.org
Information on this title: www.cambridge.org/9781107065505
DOI: 10.1017/9781107588417

First published 2017

Printed in the United Kingdom by Clays, St Ives plc

A catalogue record for this publication is available from the British Library

ISBN 978-1-107-06550-5 Hardback

The Falconer

Turning and turning in the widening gyre
W. B. Yeats.

Soaring and diving in the spiraling gyre
The freed falcon divines
Earth's air and water.

B. A. Wingate, 2017.

Contents

Preface xiii
Notation xvii

PART I FUNDAMENTALS OF GEOPHYSICAL FLUID DYNAMICS 1

1 Equations of Motion 3
1.1 Time Derivatives for Fluids 3
1.2 The Mass Continuity Equation 7
1.3 The Momentum Equation 11
1.4 The Equation of State 13
1.5 Thermodynamic Relations 14
1.6 Thermodynamic Equations for Fluids 21
1.7 Thermodynamics of Seawater 30
1.8 Sound Waves 40
1.9 Compressible and Incompressible Flow 41
1.10 The Energy Budget 42
1.11 An Introduction to nondimensionalization and Scaling 46
Appendix A: Thermodynamics of an Ideal gas from the Gibbs function 47
Appendix B: The First Law of Thermodynamics for Fluids 49

2 Effects of Rotation and Stratification 55
2.1 Equations of Motion in a Rotating Frame 55
2.2 Equations of Motion in Spherical Coordinates 59
2.3 Cartesian Approximations: The Tangent Plane 69
2.4 The Boussinesq Approximation 70
2.5 The Anelastic Approximation 75
2.6 Pressure and other Vertical Coordinates 79
2.7 Scaling for Hydrostatic Balance 83
2.8 Geostrophic and Thermal Wind Balance 87
2.9 Gradient Wind Balance 94
2.10 Static Instability and the Parcel Method 97
Appendix A: Asymptotic Derivation of the Boussinesq Equations 101

3 Shallow Water Systems 105

3.1 Dynamics of a Single Shallow Layer of Fluid 105
3.2 Reduced Gravity Equations 110
3.3 Multi-Layer Shallow Water Equations 112
3.4 From Continuous Stratification to Shallow Water 114
3.5 Geostrophic Balance and Thermal Wind 118
3.6 Form Stress 119
3.7 Conservation Properties of Shallow Water Systems 120
3.8 Shallow Water Waves 123
3.9 Geostrophic Adjustment 127
3.10 Isentropic Coordinates 134
3.11 Available Potential Energy 137

4 Vorticity and Potential Vorticity 143

4.1 Vorticity and Circulation 143
4.2 The Vorticity Equation 145
4.3 Vorticity and Circulation Theorems 147
4.4 Vorticity Equation in a Rotating Frame 153
4.5 Potential Vorticity Conservation 156
4.6 Potential Vorticity in the Shallow Water System 162
4.7 Potential Vorticity in Approximate, Stratified Models 163
4.8 The Impermeability of Isentropes to Potential Vorticity 165

5 Geostrophic Theory 171

5.1 Geostrophic Scaling 171
5.2 The Planetary-Geostrophic Equations 176
5.3 The Shallow Water Quasi-Geostrophic Equations 180
5.4 The Continuously Stratified Quasi-Geostrophic System 187
5.5 Quasi-Geostrophy and Ertel Potential Vorticity 195
5.6 Energetics of Quasi-Geostrophy 198
5.7 The Ekman Layer 201

PART II WAVES, INSTABILITIES AND TURBULENCE 213

6 Wave Fundamentals 215

6.1 Fundamentals and Formalities 215
6.2 Group Velocity 220
6.3 Ray Theory 224
6.4 Rossby Waves 226
6.5 Rossby Waves in Stratified Quasi-Geostrophic Flow 231
6.6 Energy Propagation and Reflection of Rossby Waves 234
6.7 Group Velocity, Revisited 240
6.8 Energy Propagation of Poincaré Waves 244
Appendix A: The WKB Approximation for Linear Waves 247

7 Gravity Waves 251

7.1 Surface Gravity Waves 251
7.2 Shallow Water Waves on Fluid Interfaces 257
7.3 Internal Waves in a Continuously Stratified Fluid 259
7.4 Internal Wave Reflection 268

7.5 Internal Waves in a Fluid with Varying Stratification 271
7.6 Internal Waves in a Rotating Frame of Reference 276
7.7 Topographic Generation of Internal Waves 283
7.8 Acoustic-Gravity Waves in an Ideal Gas 293

8 Linear Dynamics at Low Latitudes 297
8.1 Co-existence of Rossby and Gravity Waves 298
8.2 Waves on the Equatorial Beta Plane 303
8.3 Ray Tracing and Equatorial Trapping 314
8.4 Forced-Dissipative Wavelike Flow 316
8.5 Forced, Steady Flow: the Matsuno–Gill Problem 321
Appendix A: Nondimensionalization and Parabolic Cylinder Functions 330
Appendix B: Mathematical Relations in the Matsuno–Gill Problem 333

9 Barotropic and Baroclinic Instability 335
9.1 Kelvin–Helmholtz Instability 335
9.2 Instability of Parallel Shear Flow 337
9.3 Necessary Conditions for Instability 345
9.4 Baroclinic Instability 347
9.5 The Eady Problem 351
9.6 Two-Layer Baroclinic Instability 356
9.7 A Kinematic View of Baroclinic Instability 363
9.8 The Energetics of Linear Baroclinic Instability 367
9.9 Beta, Shear and Stratification in a Continuous Model 369

10 Waves, Mean-Flows, and their Interaction 379
10.1 Quasi-Geostrophic Wave–Mean-Flow Interaction 380
10.2 The Eliassen–Palm Flux 383
10.3 The Transformed Eulerian Mean 387
10.4 The Non-Acceleration Result 394
10.5 Influence of Eddies on the Mean-Flow in the Eady Problem 399
10.6 Necessary Conditions for Instability 403
10.7 Necessary Conditions for Instability: Use of Pseudoenergy 406

11 Basics of Incompressible Turbulence 413
11.1 The Fundamental Problem of Turbulence 413
11.2 The Kolmogorov Theory 416
11.3 Two-dimensional Turbulence 423
11.4 Predictability of Turbulence 433
11.5 Spectra of Passive Tracers 437

12 Geostrophic Turbulence and Baroclinic Eddies 445
12.1 Differential Rotation in Two-dimensional Turbulence 445
12.2 Stratified Geostrophic Turbulence 454
12.3 A Scaling Theory for Geostrophic Turbulence 460
12.4 Phenomenology of Baroclinic Eddies in the Atmosphere and Ocean 464

13 Turbulent Diffusion and Eddy Transport 473

13.1 Diffusive Transport 473
13.2 Turbulent Diffusion 475
13.3 Two-Particle Diffusivity 480
13.4 Mixing Length Theory 484
13.5 Homogenization of a Scalar that is Advected and Diffused 487
13.6 Diffusive Fluxes and Skew Fluxes 490
13.7 Eddy Diffusion in the Atmosphere and Ocean 493
13.8 Thickness and Potential Vorticity Diffusion 502

PART III LARGE-SCALE ATMOSPHERIC CIRCULATION 509

14 The Overturning Circulation: Hadley and Ferrel Cells 511

14.1 Basic Features of the Atmosphere 511
14.2 A Steady Model of the Hadley Cell 516
14.3 A Shallow Water Model of the Hadley Cell 524
14.4 Asymmetry Around the Equator 525
14.5 Eddy Effects on the Hadley Cell 528
14.6 Non-local Eddy Effects and Numerical Results 532
14.7 The Ferrel Cell 534

15 Zonally-Averaged Mid-Latitude Atmospheric Circulation 539

15.1 Surface Westerlies and the Maintenance of a Barotropic Jet 540
15.2 Layered Models of the Mid-Latitude Circulation 549
15.3 Eddy Fluxes and an Example of a Closed Model 562
15.4 A Stratified Model and the Real Atmosphere 566
15.5 Tropopause Height and the Stratification of the Troposphere 572
15.6 A Model for both Stratification and Tropopause Height 579
Appendix A: TEM for the Primitive Equations in Spherical Coordinates 581

16 Planetary Waves and Zonal Asymmetries 585

16.1 Rossby Wave Propagation in a Slowly Varying Medium 585
16.2 Horizontal Propagation of Rossby Waves 588
16.3 Critical Lines and Critical Layers 594
16.4 A WKB Wave–Mean-Flow Problem for Rossby Waves 598
16.5 Vertical Propagation of Rossby waves 599
16.6 Vertical Propagation of Rossby Waves in Shear 606
16.7 Forced and Stationary Rossby Waves 609
16.8 Effects of Thermal Forcing 615
16.9 Wave Propagation Using Ray Theory 621

17 The Stratosphere 627

17.1 A Descriptive Overview 627
17.2 Waves in the Stratosphere 634
17.3 Wave Momentum Transport and Deposition 639
17.4 Phenomenology of the Residual Overturning Circulation 642
17.5 Dynamics of the Residual Overturning Circulation 644
17.6 The Quasi-Biennial Oscillation 652
17.7 Variability and Extra-Tropical Wave–Mean-Flow Interaction 663

18 Water Vapour and the Tropical Atmosphere 673

18.1 A Moist Ideal Gas 673
18.2 The Distribution of Relative Humidity 680
18.3 Atmospheric Convection 691
18.4 Convection in a Moist Atmosphere 695
18.5 Radiative Equilibrium 700
18.6 Radiative-Convective Equilibrium 703
18.7 Vertically-Constrained Equations of Motion for Large Scales 708
18.8 Scaling and Balanced Dynamics for Large-Scale Flow in the Tropics 711
18.9 Scaling and Balance for Large-Scale Flow with Diabatic Sources 714
18.10 Convectively Coupled Gravity Waves and the MJO 717
Appendix A: Moist Thermodynamics from the Gibbs Function 720
Appendix B: Equations of Radiative Transfer 724
Appendix C: Analytic Approximation of Tropopause Height 725

PART IV LARGE-SCALE OCEANIC CIRCULATION 729

19 Wind-Driven Gyres 731

19.1 The Depth Integrated Wind-Driven Circulation 733
19.2 Using Viscosity Instead of Drag 740
19.3 Zonal Boundary Layers 744
19.4 The Nonlinear Problem 745
19.5 Inertial Solutions 747
19.6 Topographic Effects on Western Boundary Currents 753

20 Structure of the Upper Ocean 761

20.1 Vertical Structure of the Wind-Driven Circulation 761
20.2 A Model with Continuous Stratification 767
20.3 Observations of Potential Vorticity 770
20.4 The Main Thermocline 774
20.5 Scaling and Simple Dynamics of the Main Thermocline 776
20.6 The Internal Thermocline 779
20.7 The Ventilated Thermocline 785
Appendix A: Miscellaneous Relationships in a Layered Model 796

21 The Meridional Overturning Circulation and the ACC 801

21.1 Sideways Convection 802
21.2 The Maintenance of Sideways Convection 808
21.3 Simple Box Models 813
21.4 A Laboratory Model of the Abyssal Circulation 818
21.5 A Model for Oceanic Abyssal Flow 821
21.6 A Model of Deep Wind-Driven Overturning 829
21.7 The Antarctic Circumpolar Current 836
21.8 A Dynamical Model of the Residual Overturning Circulation 845
21.9 A Model of the Interhemispheric Circulation 853

22 Equatorial Circulation and El Niño 861

22.1 Observational Preliminaries 861
22.2 Dynamical Preliminaries 862
22.3 A Local Model of the Equatorial Undercurrent 865
22.4 An Ideal Fluid Model of the Equatorial Undercurrent 876
22.5 An Introduction to El Niño and the Southern Oscillation 886
22.6 The Walker Circulation 891
22.7 The Oceanic Response 893
22.8 Coupled Models and Unstable Interactions 895
22.9 Simple Conceptual and Numerical Models of ENSO 898
22.10 Numerical Solutions of the Shallow Water Equations 902
Appendix A: Derivation of a Delayed-Oscillator Model 904

References 909

Index 936

In the main text, sections that are more advanced or that contain material that is peripheral to the main narrative are marked with a black diamond, ✦. Sections that contain material that is still not settled or that describe active areas of research are marked with a dagger, †.

The sea obscured by vapour that … slid in one mighty mass along the sea shore … The distant country, overhung by straggling clouds that sailed over it, appeared like the darker clouds, seen at a great distance apparently motionless, while the nearer ones pass quickly over them, driven by the lower winds. I never saw such a union of earth, sky and sea. The clouds beneath our feet spread to the water, and the clouds of the sky almost joined them.
Dorothy Wordsworth, *Alfoxden Journal*, 1798.

Preface

THIS IS A BOOK ON THE DYNAMICS OF THE ATMOSPHERE AND OCEAN, with an emphasis on the fundamentals and on the large-scale circulation. By 'large-scale' I mean scales between that of the weather (a few hundred kilometres in the atmosphere and a few tens of kilometres in the ocean, which indeed has its own weather) and the global scale. My focus is our own planet Earth, for that is where we live, but the principles and methodology used should be appropriate for the study of the atmospheres and oceans of other planets. And even if we stay at home, I try to take the reader on a journey — from the most basic and classical material to the frontiers of knowledge.

The book is written at a level appropriate for advanced undergraduate or graduate courses; it is also meant to be a useful reference for researchers, and some aspects of the book have the nature of a research monograph. Prior knowledge of fluid dynamics is helpful but is not a requirement, for the fluid equations are introduced in the first chapter. Similarly, some knowledge of thermodynamics will ease the reader's path, but is not essential. On the other hand, the reader is assumed to have a working knowledge of vector calculus and to know what a partial differential equation is.

Atmospheric and oceanic fluid dynamics (AOFD) is both pure and applied. It is a pure because it involves some of the most fundamental and unsolved problems in fluid dynamics — problems in turbulence and wave–mean flow interaction, in chaos and predictability, and in the general circulation itself. It is applied because the climate and weather so profoundly affect the human condition, and the practice of weather forecasting is a notable example of a successful (yes it is) applied science. The field is also broad, encompassing such subjects as the general circulation, instabilities, gyres, boundary layers, waves, convection and turbulence. My goal in this book is to present a coherent selection of these topics so that the reader will gain a solid grounding in the fundamentals, motivated by and with an appreciation for the problems of the real world. The book is primary a theoretical one, but in a number of places observations are used to illustrate the dynamics and define the problems. And I have tried to lead the reader to the edge of active areas of research — for a book that limits itself to what is absolutely settled would, I think, be rather dry, a quality best reserved for martinis and humour.

This book is a major revision of one that first appeared in 2006, and about half of the material here is new or rewritten. Some of the changes were motivated by the fact that half of the planet lies equatorward of 30°, that about 20% of the mass of the atmosphere lies above 10 km, and that it rains. Overall, I have tried to encompass the most important aspects of the dynamics and circulation of both atmosphere and ocean, for the similarities and differences between the two are so instructive that even if one's interest is solely in one there is much to be learned by studying the other. Where the subject matter verges on areas of research, I have focused on ideas and topics that, I think, will be of lasting value rather than of current fashion; however, this choice is undoubtedly influenced by my own interests and expertise, not to mention my prejudices.

How to Use this Book

This book is a long one, but it might help to think of it as four short ones with a common theme. These books are on the fundamentals of geophysical fluid dynamics (GFD); waves, instabilities and turbulence; atmospheric circulation; and ocean circulation. Each short book forms a Part in this book, and each might form the basis for a course of about a term or a semester, although there is more material in each than can comfortably be covered unless the course hums along at a torrid pace. The ordering of the topics follows a logical sequence, but is not the order that the book need be read. For example, Chapter 1 covers the basic equations of motion for a fluid, including the requisite thermodynamics. The thermodynamics of seawater belongs to and is included in that chapter, but this material is quite advanced and is not needed to understand many of the later chapters, and may be skipped on a first reading. Typically, sections that are more advanced or that are peripheral to the main narrative are marked with a black diamond, ✦, and sections that contain matters that are not settled or that describe active areas of research are marked with a dagger, †, but there is some overlap and arbitrariness in the markings. In some of these areas the book may be thought of as a entrance to the original literature and it gives my own view on the subject.

Putting the various topics together in one book will, I hope, emphasize their coherence as part of a single field. Still, there are many paths through the woods and the following notes may help steer the reader, although I do not wish to be prescriptive and experienced instructors will chart their own course. In a nutshell, the material of Part I forms the basis of all that follows, and subsequent Parts may then be read in any order if the reader is willing to cross refer, often to Part II. With care, one may also construct a single course that combines aspects of Parts II, III and/or IV.

A basic GFD course

A first course in GFD might cover much of Part I and, in many cases, Rossby waves and possibly baroclinic instability from Part II. If the students have already had a course in fluid dynamics then much of Chapter 1 can be skipped. Some of the thermodynamics may in any case be omitted on a first reading, and a basic course might encompass the following:

For students with no fluid mechanics:

Equations of motion, Sections 1.1–1.6, omitting starred sections.
Compressibility, Sections 1.8 and 1.9.
Energetics, Section 1.10 (optional).

Then, for all students:

Rotational effects and Boussinesq equations, Sections 2.1–2.4.
Pressure coordinates, Section 2.6 (optional, mainly for meteorologists).
Hydrostatic and geostrophic balance, Sections 2.7 and 2.8.
Static instability, Section 2.10.

Shallow water equations and geostrophic adjustment: Sections 3.1, 3.2, 3.5, 3.7–3.9.

Vorticity, Sections 4.1–4.4 (for students with no fluids background).
Potential vorticity, some or all of Sections 4.5 and 4.6.

Geostrophic theory, Sections 5.1–5.5.
Ekman layers, Section 5.7.

Rossby waves, Sections 6.4 and 6.5, and possibly Section 16.5 on vertical propagation.
Jet formation, Section 15.1.
Baroclinic instability, Sections 9.5 and/or 9.6.

One option is to use only the Boussinesq equations (and later the shallow water equations) and the beta plane, eschewing pressure co-ordinates and sphericity, coming back to them later for atmospheric applications. This option also makes the derivation of quasi-geostrophy a little easier.

But meteorologists may well prefer to introduce these topics from the outset, and use pressure coordinates and not the Boussinesq approximation. Many first courses will end after Rossby waves, although a rapidly-moving course for well-prepared students might cover some aspects of baroclinic instability. If waves are being covered separately, then an alternative is to cover some aspect of the general circulation of the atmosphere or ocean, for example the Stommel model of ocean gyres in Section 19.1, which is a pedagogical delight.

Subsequent reading

The other three short books, or Parts to this book, are loosely based on more advanced courses that I have taught at various times, and taken together are an attempt to pull together classical ideas and recent developments in the field into a coherent whole. Each Part is more-or-less self-contained, although some aspects of Parts III and IV build on Part II, especially the sections on Rossby waves and baroclinic instability. An understanding of the essentials of geostrophic turbulence and turbulent diffusion will also help. Provided these sections and the material in Part I is mastered the remaining Parts may be read in any order if the reader is willing to flip pages occasionally and consult other sections as needed. I won't suggest any specific syllabus to follow apart from the contents of the book itself, but let me make a few remarks.

Part II: Waves, instabilities and turbulence

Rossby waves, gravity waves and baroclinic instability could form the first half of a second course on GFD, with wave–mean-flow interaction and/or turbulence the second half. Any one of these topics could be a full course, especially if supplemented from other sources. WKB methods are very useful in a variety of practical problems and can readily be taught in an elementary way. If needs be equatorial waves (Chapter 8) could be treated separately, for it is a little mathematical, and perhaps folded into a course covering equatorial circulation more generally. One might also construct a course based around geostrophic turbulence and the mid-latitude circulation of the atmosphere and/or ocean.

Part III: Atmospheric circulation

My focus here is on the large scale, and on the fundamental aspects of the general circulation — how wide is the Hadley Cell? why do the surface winds blow eastward in mid-latitudes? why is there a tropopause and why is it 10 km high and not 5 or 50 km? and so forth. A basic knowledge of GFD, such as is in the sample course above, is a pre-requisite; other sections of Part II may be needed but can be consulted as necessary. Chapters 14 and 15 form a pair and should be read consecutively, and Chapter 16 is in some ways a continuation of Chapter 5 on waves. There are numerous ways to navigate through these chapters — one might omit the stratosphere chapter, or it could form the basis for an entire course if other literature were added. The same applies to Chapter 18 on the tropics, and here especially the material cuts close to the bone of what is known and other researchers might write a very different chapter.

Part IV: Oceanic circulation

Many of the above comments on atmospheric circulation apply here, as my goal is to describe and explain the fundamental dynamical processes determining the large-scale structure and circulation of the ocean — why go gyres have western boundary currents? what determines the structure of the thermocline? why does El Niño occur? As for Part III, a basic knowledge of GFD, such as is in the sample course above, is a pre-requisite. Chapter 19 on wind-driven gyres is the foundation of much that follows, and Chapter 20 flows naturally from it. The chapters on the meridional overturning circulation and El Niño delve into active areas of research, and again others might have written differently. Both here and in my discussion of atmospheric circulation I take the position of a *practical theoretician;* such a person seeks theories or explanations of phenomena, but they should be relevant to the world about us.

Miscellany and Acknowledgements

The book was written in LaTeX using Minion fonts for text and Minion Math from Typoma for equations. I fear that the references at the end disproportionately represent articles written in English and by British and North American authors, for that is the community I have mainly socialized with. The references are simply those with which I happen to most familiar — but this is a lazy choice and I apologize for it. Student exercises, various codes, and all of the figures, may be downloaded from the CUP website or my own website, which is best obtained using a search engine.

Many, many, colleagues and students have helped in the writing of this book, both by offering constructive suggestions and by gently and not so gently pointing out errors and misconceptions. Many thanks to all of you! I acknowledge your input in the endnotes after each chapter, although I am afraid that I have omitted many of you. If you have additional input or find mistakes, please email me. I would also like to thank three of my predecessor authors. The pioneering books by Joe Pedlosky and Adrian Gill paved the way and if those books had not existed I would have had neither the knowledge nor the courage to write mine. And the book by Rick Salmon taught me that careful arguments can be couched in plain language, and that an easy-to-read style can at the same time be clear and precise. I have tried to follow that example.

As with the first edition, this book ultimately owes its existence to my own hubris and selfishness: hubris to think that others might wish to read what I have written, and selfishness because the enjoyable task of writing such a book masquerades as work.

NOTATION

Variables are normally set in italics, constants (e.g, π, i) in roman (i.e., upright), differential operators in roman, vectors in bold, and tensors in bold sans serif. Thus, vector variables are in bold italics, vector constants (e.g., unit vectors) in bold upright, and tensor variables are in bold slanting sans serif. A subscript denotes a derivative only if the subscript is a coordinate, such as x, y, z or t, or when so denoted in the text. A subscript 0 generally denotes a reference value (e.g., ρ_0). The components of a vector are denoted by superscripts. If a fraction contains only two terms in the denominator then brackets are not always used; thus $1/2\pi = 1/(2\pi) \neq \pi/2$.

The lists below contain only the more important variables or instances of ambiguous notation, in quasi-alphabetical order, first of Roman characters and then of mainly Greek characters and operators. Distinct meanings are separated with a semi-colon.

Variable	Description
a	Radius of Earth.
b	Buoyancy, $-g\delta\rho/\rho_0$ or $g\delta\theta/\tilde{\theta}$.
B	Planck function, often σT^4.
$\boldsymbol{c}_g$	Group velocity, (c_g^x, c_g^y, c_g^z).
c_p	Phase speed; heat capacity at constant pressure.
c_v	Heat capacity at constant volume.
c_s	Sound speed.
f, f_0	Coriolis parameter, and its reference value.
$\boldsymbol{g}$, g	Vector acceleration due to gravity, magnitude of $\boldsymbol{g}$.
g	Gibbs function.
$\mathbf{i}, \mathbf{j}, \mathbf{k}$	Unit vectors in (x, y, z) directions.
i; i	An integer index; square root of minus one.
I	Internal energy.
$\boldsymbol{k}$	Wave vector, with components (k, l, m) or (k^x, k^y, k^z).
k_d	Wave number corresponding to deformation radius.
L_d	Deformation radius.
L, H	Horizontal length scale, vertical (height) scale.
m	Angular momentum about the Earth's axis of rotation.
N	Buoyancy, or Brunt–Väisälä, frequency.
p, p_R	Pressure, and a reference value of pressure.
Pr	Prandtl ratio, f_0/N.
q	Quasi-geostrophic potential vorticity; water vapour specific humidity.
Q	Potential vorticity (in particular Ertel PV).
$\dot{Q}$	Rate of heating.
Ra	Rayleigh number.
Re ; Re	Real part of expression; Reynolds number, UL/ν.
Ro	Rossby number, U/fL.
S	Salinity; source term on right-hand side of an evolution equation.
$S_o, \mathbf{S}_o$	Solenoidal term, solenoidal vector.
T	Temperature; scaling value for time.
t	Time.
$\boldsymbol{u}$	Two-dimensional (horizontal) velocity, (u, v).
$\boldsymbol{v}$	Three-dimensional velocity, (u, v, w).
w	Vertical velocity; water vapour mixing ratio.
x, y, z	Cartesian coordinates, usually in zonal, meridional and vertical directions.
Z	Log-pressure, $-H \log p/p_R$; scaling for z.

Variable	Description
$\mathcal{A}$	Wave activity.
α	Inverse density, or specific volume; aspect ratio.
β; β^*	Rate of change of f with latitude, $\partial f/\partial y$; $\beta^* = \beta - u_{yy}$
$\beta_T, \beta_S, \beta_p$	Coefficient of expansion with respect to temperature, salinity and pressure, respectively.
ϵ	Generic small parameter (epsilon).
ε	Cascade or dissipation rate of energy (varepsilon).
η	Specific entropy; perturbation height; enstrophy cascade or dissipation rate.
$\boldsymbol{\mathcal{F}}$	Eliassen Palm flux, $(\mathcal{F}^y, \mathcal{F}^z)$.
γ	The ratio c_p/c_v; Vorticity gradient, e.g., $\beta - u_{yy}$.
Γ	Lapse rate (sometimes subscripted, e.g., Γ_z, but here this does not denote a differential).
κ	Diffusivity; the ratio R/c_p.
$\mathcal{K}$	Kolmogorov or Kolmogorov-like constant.
Λ	Shear, e.g., $\partial U/\partial z$.
μ	Viscosity; chemical potential.
ν	Kinematic viscosity, μ/ρ.
υ	Meridional component of velocity.
$\mathcal{P}$	Pseudomomentum.
ϕ	Pressure divided by density, p/ρ.
φ	Passive tracer.
Φ	Geopotential, usually gz; scaling value of ϕ.
Π	Exner function, $\Pi = c_p T/\theta = c_p(p/p_R)^{R/c_p}$; an enthalpy-like quantity.
$\boldsymbol{\omega}$	Vorticity.
$\Omega, \boldsymbol{\Omega}$	Rotation rate of Earth and associated vector.
ψ	Streamfunction.
ρ	Density.
ρ_θ	Potential density.
σ	Layer thickness, $\partial z/\partial\theta$; Prandtl number ν/κ; measure of density, $\rho - 1000$.
$\boldsymbol{\tau}$	Stress vector, often wind stress.
$\tilde{\boldsymbol{\tau}}$	Kinematic stress, $\boldsymbol{\tau}/\rho$.
τ	Zonal component or magnitude of wind stress; eddy turnover time; optical depth.
θ; Θ	Potential temperature; generic thermodynamic variable, often conservative temperature.
ϑ, λ	Latitude, longitude.
ζ	Vertical component of vorticity.
$\left(\frac{\partial a}{\partial b}\right)_c$	Derivative of a with respect to b at constant c.
$\left.\frac{\partial a}{\partial b}\right\|_c$	Derivative of a with respect to b evaluated at $b = c$.
∇_a	Gradient operator at constant value of coordinate a. Thus, $\nabla_z = \mathbf{i}\partial_x + \mathbf{j}\partial_y$.
$\nabla_a\cdot$	Divergence operator at constant value of coordinate a. Thus, $\nabla_z\cdot = (\mathbf{i}\partial_x + \mathbf{j}\partial_y)\cdot$.
$\nabla^\perp$	Perpendicular gradient, $\nabla^\perp\phi \equiv \mathbf{k}\times\nabla\phi$.
curl_z	Vertical component of $\nabla\times$ operator, $\mathrm{curl}_z\boldsymbol{A} = \mathbf{k}\cdot\nabla\times\boldsymbol{A} = \partial_x A^y - \partial_y A^x$.
$\frac{\mathrm{D}}{\mathrm{D}t}$	Material derivative (generic).
$\frac{\mathrm{D}_g}{\mathrm{D}t}$	Material derivative using geostrophic velocity, for example $\partial/\partial t + \boldsymbol{u}_g\cdot\nabla$.

Part I

FUNDAMENTALS OF GEOPHYSICAL FLUID DYNAMICS

To begin at the beginning:
'It is spring, moonless night in the small town,
starless and bible-black, the cobblestreets silent
and the hunched, courters'-and-rabbits' wood limping invisible down
to the sloeblack, slow, black, crowblack, fishingboat-bobbing sea.
Dylan Thomas, *Under Milk Wood*, 1954.

CHAPTER 1

Equations of Motion

HAVING NOTHING BUT A BLANK SLATE, we begin by establishing the governing equations of motion for a fluid, with particular attention to the fluids of Earth's atmosphere and ocean. These equations determine how a fluid flows and evolves when forces are applied to it, or when it is heated or cooled, and so involve both dynamics and thermodynamics. And because the equations of motion are nonlinear the two become intertwined and at times inseparable.

1.1 TIME DERIVATIVES FOR FLUIDS

The equations of motion of fluid mechanics differ from those of rigid-body mechanics because fluids form a continuum, and because fluids flow and deform. Thus, even though the same relatively simple physical laws (Newton's laws and the laws of thermodynamics) govern both solid and fluid media, the expression of these laws differs between the two. To determine the equations of motion for fluids we must clearly establish what the time derivative of some property of a fluid actually means, and that is the subject of this section.

1.1.1 Field and Material Viewpoints

In solid-body mechanics one is normally concerned with the position and momentum of identifiable objects — the angular velocity of a spinning top or the motions of the planets around the Sun are two well-worn examples. The position and velocity of a particular object are then computed as a function of time by formulating equations of the form

$$\frac{\mathrm{d}x_i}{\mathrm{d}t} = F(\{x_i\}, t), \tag{1.1}$$

where $\{x_i\}$ is the set of positions and velocities of all the interacting objects and the operator F on the right-hand side is formulated using Newton's laws of motion. For example, two massive point objects interacting via their gravitational field obey

$$\frac{\mathrm{d}\boldsymbol{r}_i}{\mathrm{d}t} = \boldsymbol{v}_i, \quad \frac{\mathrm{d}\boldsymbol{v}_i}{\mathrm{d}t} = \frac{Gm_j}{(\boldsymbol{r}_i - \boldsymbol{r}_j)^2}\hat{\boldsymbol{r}}_{i,j}, \qquad i = 1, 2;\ j = 3 - i. \tag{1.2}$$

We thereby predict the positions, $\boldsymbol{r}_i$, and velocities, $\boldsymbol{v}_i$, of the objects given their masses, m_i, and the gravitational constant G, and where $\hat{\boldsymbol{r}}_{i,j}$ is a unit vector directed from $\boldsymbol{r}_i$ to $\boldsymbol{r}_j$.

In fluid dynamics such a procedure would lead to an analysis of fluid motions in terms of the positions and momenta of different fluid parcels, each identified by some label, which might simply be their position at an initial time. We call this a *material* point of view, because we are concerned with identifiable pieces of material; it is also sometimes called a *Lagrangian* view, after J.-L. Lagrange. The procedure is perfectly acceptable in principle, and if followed would provide a complete description of the fluid dynamical system. However, from a practical point of view it is much more than we need, and it would be extremely complicated to implement. Instead, for most problems we would like to know what the values of velocity, density and so on are at *fixed points* in space as time passes. (A weather forecast we might care about tells us how warm it will be where we live and, if we are given that, we do not particularly care where a fluid parcel comes from, or where it subsequently goes.) Since the fluid is a continuum, this knowledge is equivalent to knowing how the fields of the dynamical variables evolve in space and time, and this is often known as the *field* or *Eulerian* viewpoint, after L. Euler.[1] Thus, whereas in the material view we consider the time evolution of identifiable fluid elements, in the field view we consider the time evolution of the fluid field from a particular frame of reference. That is, we seek evolution equations of the general form

$$\frac{\partial}{\partial t}\varphi(x, y, z, t) = \mathcal{G}(\varphi, x, y, z, t), \tag{1.3}$$

where the field $\varphi(x, y, z, t)$ represents all the dynamical variables (velocity, density, temperature, etc.) and $\mathcal{G}$ is some operator to be determined from Newton's laws of motion and appropriate thermodynamic laws.

Although the field viewpoint will often turn out to be the most practically useful, the material description is invaluable both in deriving the equations and in the subsequent insight it frequently provides. This is because the important quantities from a fundamental point of view are often those which are associated with a given fluid element: it is these which directly enter Newton's laws of motion and the thermodynamic equations. It is thus important to have a relationship between the rate of change of quantities associated with a given fluid element and the local rate of change of a field. The material or advective derivative provides this relationship.

1.1.2 The Material Derivative of a Fluid Property

A *fluid element* is an infinitesimal, indivisible, piece of fluid — effectively a very small fluid parcel of fixed mass. The *material derivative* is the rate of change of a property (such as temperature or momentum) of a particular fluid element or finite mass of fluid; that is, it is the total time derivative of a property of a piece of fluid. It is also known as the 'substantive derivative' (the derivative associated with a parcel of fluid substance), the 'advective derivative' (because the fluid property is being advected), the 'convective derivative' (convection is a slightly old-fashioned name for advection, still used in some fields), or the 'Lagrangian derivative' (after Lagrange).

Let us suppose that a fluid is characterized by a given velocity field $\boldsymbol{v}(\boldsymbol{x}, t)$, which determines its velocity throughout. Let us also suppose that the fluid has another property φ, and let us seek an expression for the rate of change of φ of a fluid element. Since φ is changing in time and in space we use the chain rule,

$$\delta\varphi = \frac{\partial\varphi}{\partial t}\delta t + \frac{\partial\varphi}{\partial x}\delta x + \frac{\partial\varphi}{\partial y}\delta y + \frac{\partial\varphi}{\partial z}\delta z = \frac{\partial\varphi}{\partial t}\delta t + \delta\boldsymbol{x}\cdot\nabla\varphi. \tag{1.4}$$

This is true in general for any δt, δx, etc. The total time derivative is then

$$\frac{\mathrm{d}\varphi}{\mathrm{d}t} = \frac{\partial\varphi}{\partial t} + \frac{\mathrm{d}\boldsymbol{x}}{\mathrm{d}t}\cdot\nabla\varphi. \tag{1.5}$$

If this equation is to represent a material derivative we must identify the time derivative in the second term on the right-hand side with the rate of change of position of a fluid element, namely

its velocity. Hence, the material derivative of the property φ is

$$\frac{\mathrm{d}\varphi}{\mathrm{d}t} = \frac{\partial\varphi}{\partial t} + \boldsymbol{v}\cdot\nabla\varphi. \tag{1.6}$$

The right-hand side expresses the material derivative in terms of the local rate of change of φ plus a contribution arising from the spatial variation of φ, experienced only as the fluid parcel moves. Because the material derivative is so common, and to distinguish it from other derivatives, we denote it by the operator $\mathrm{D}/\mathrm{D}t$. Thus, the material derivative of the field φ is

$$\frac{\mathrm{D}\varphi}{\mathrm{D}t} = \frac{\partial\varphi}{\partial t} + (\boldsymbol{v}\cdot\nabla)\varphi. \tag{1.7}$$

The brackets in the last term of this equation are helpful in reminding us that $(\boldsymbol{v}\cdot\nabla)$ is an operator acting on φ. The operator $\partial/\partial t + (\boldsymbol{v}\cdot\nabla)$ is the *Eulerian representation of the Lagrangian derivative as applied to a field.* We use the notation $\mathrm{D}/\mathrm{D}t$ rather generally for Lagrangian derivatives, but the operator may take a different form when applied to other objects, such as a fluid volume.

Material derivative of vector field

The material derivative may act on a vector field $\boldsymbol{b}$, in which case

$$\frac{\mathrm{D}\boldsymbol{b}}{\mathrm{D}t} = \frac{\partial\boldsymbol{b}}{\partial t} + (\boldsymbol{v}\cdot\nabla)\boldsymbol{b}. \tag{1.8}$$

In Cartesian coordinates this is

$$\frac{\mathrm{D}\boldsymbol{b}}{\mathrm{D}t} = \frac{\partial\boldsymbol{b}}{\partial t} + u\frac{\partial\boldsymbol{b}}{\partial x} + v\frac{\partial\boldsymbol{b}}{\partial y} + w\frac{\partial\boldsymbol{b}}{\partial z}, \tag{1.9}$$

and for a particular component of $\boldsymbol{b}$, b^x say,

$$\frac{\mathrm{D}b^x}{\mathrm{D}t} = \frac{\partial b^x}{\partial t} + u\frac{\partial b^x}{\partial x} + v\frac{\partial b^x}{\partial y} + w\frac{\partial b^x}{\partial z}, \tag{1.10}$$

and similarly for b^y and b^z. In Cartesian tensor notation the expression becomes

$$\frac{\mathrm{D}b_i}{\mathrm{D}t} = \frac{\partial b_i}{\partial t} + v_j\frac{\partial b_i}{\partial x_j} = \frac{\partial b_i}{\partial t} + v_j\partial_j b_i, \tag{1.11}$$

where the subscripts denote the Cartesian components, repeated indices are summed, and $\partial_j b_i \equiv \partial b_i/\partial x_j$. In coordinate systems other than Cartesian the advective derivative of a vector is not simply the sum of the advective derivative of its components, because the coordinate vectors themselves change direction with position; this will be important when we deal with spherical coordinates. Finally, we remark that the advective derivative of the position of a fluid element, $\boldsymbol{r}$ say, is its velocity, and this may easily be checked by explicitly evaluating $\mathrm{D}\boldsymbol{r}/\mathrm{D}t$.

1.1.3 Material Derivative of a Volume

The volume that a given, unchanging, mass of fluid occupies is deformed and advected by the fluid motion, and there is no reason why it should remain constant. Rather, the volume will change as a result of the movement of each element of its bounding material surface, and in particular will change if there is a non-zero normal component of the velocity at the fluid surface. That is, if the volume of some fluid is $\int \mathrm{d}V$, then

$$\frac{\mathrm{D}}{\mathrm{D}t}\int_V \mathrm{d}V = \int_S \boldsymbol{v}\cdot\mathrm{d}\boldsymbol{S}, \tag{1.12}$$

where the subscript V indicates that the integral is a definite integral over some finite volume V, although the limits of the integral will be functions of time if the volume is changing. The integral on the right-hand side is over the closed surface, S, bounding the volume. Although intuitively apparent (to some), this expression may be derived more formally using Leibniz's formula for the rate of change of an integral whose limits are changing. Using the divergence theorem on the right-hand side, (1.12) becomes

$$\frac{\mathrm{D}}{\mathrm{D}t}\int_V \mathrm{d}V = \int_V \nabla\cdot\boldsymbol{v}\,\mathrm{d}V. \tag{1.13}$$

The rate of change of the volume of an infinitesimal fluid element of volume ΔV is obtained by taking the limit of this expression as the volume tends to zero, giving

$$\lim_{\Delta V\to 0}\frac{1}{\Delta V}\frac{\mathrm{D}\Delta V}{\mathrm{D}t} = \nabla\cdot\boldsymbol{v}. \tag{1.14}$$

We will often write such expressions informally as

$$\frac{\mathrm{D}\Delta V}{\mathrm{D}t} = \Delta V\nabla\cdot\boldsymbol{v}, \tag{1.15}$$

with the limit implied.

Consider now the material derivative of some fluid property, ξ say, multiplied by the volume of a fluid element, ΔV. Such a derivative arises when ξ is the amount per unit volume of ξ-substance — the mass density or the amount of a dye per unit volume, for example. Then we have

$$\frac{\mathrm{D}}{\mathrm{D}t}(\xi\Delta V) = \xi\frac{\mathrm{D}\Delta V}{\mathrm{D}t} + \Delta V\frac{\mathrm{D}\xi}{\mathrm{D}t}. \tag{1.16}$$

Using (1.15) this becomes

$$\frac{\mathrm{D}}{\mathrm{D}t}(\xi\Delta V) = \Delta V\left(\xi\nabla\cdot\boldsymbol{v} + \frac{\mathrm{D}\xi}{\mathrm{D}t}\right), \tag{1.17}$$

and the analogous result for a finite fluid volume is just

$$\frac{\mathrm{D}}{\mathrm{D}t}\int_V \xi\,\mathrm{d}V = \int_V\left(\xi\nabla\cdot\boldsymbol{v} + \frac{\mathrm{D}\xi}{\mathrm{D}t}\right)\mathrm{d}V. \tag{1.18}$$

This expression is to be contrasted with the Eulerian derivative for which the volume, and so the limits of integration, are fixed and we have

$$\frac{\mathrm{d}}{\mathrm{d}t}\int_V \xi\,\mathrm{d}V = \int_V \frac{\partial\xi}{\partial t}\,\mathrm{d}V. \tag{1.19}$$

Now consider the material derivative of a fluid property φ multiplied by the mass of a fluid element, $\rho\Delta V$, where ρ is the fluid density. Such a derivative arises when φ is the amount of φ-substance per unit mass (note, for example, that the momentum of a fluid element is $\rho\boldsymbol{v}\Delta V$). The material derivative of $\varphi\rho\Delta V$ is given by

$$\frac{\mathrm{D}}{\mathrm{D}t}(\varphi\rho\Delta V) = \rho\Delta V\frac{\mathrm{D}\varphi}{\mathrm{D}t} + \varphi\frac{\mathrm{D}}{\mathrm{D}t}(\rho\Delta V). \tag{1.20}$$

But $\rho\Delta V$ is just the mass of the fluid element, and that is constant — that is how a fluid element is defined. Thus the second term on the right-hand side vanishes and

$$\frac{\mathrm{D}}{\mathrm{D}t}(\varphi\rho\Delta V) = \rho\Delta V\frac{\mathrm{D}\varphi}{\mathrm{D}t} \qquad \text{and} \qquad \frac{\mathrm{D}}{\mathrm{D}t}\int_V \varphi\rho\,\mathrm{d}V = \int_V \rho\frac{\mathrm{D}\varphi}{\mathrm{D}t}\,\mathrm{d}V, \tag{1.21a,b}$$

Material and Eulerian Derivatives

The material derivatives of a scalar (φ) and a vector ($\boldsymbol{b}$) field are given by:

$$\frac{\mathrm{D}\varphi}{\mathrm{D}t} = \frac{\partial\varphi}{\partial t} + \boldsymbol{v}\cdot\nabla\varphi, \qquad \frac{\mathrm{D}\boldsymbol{b}}{\mathrm{D}t} = \frac{\partial\boldsymbol{b}}{\partial t} + (\boldsymbol{v}\cdot\nabla)\boldsymbol{b}. \tag{D.1}$$

Various material derivatives of integrals are:

$$\frac{\mathrm{D}}{\mathrm{D}t}\int_V \varphi\,\mathrm{d}V = \int_V \left(\frac{\mathrm{D}\varphi}{\mathrm{D}t} + \varphi\nabla\cdot\boldsymbol{v}\right)\mathrm{d}V = \int_V \left(\frac{\partial\varphi}{\partial t} + \nabla\cdot(\varphi\boldsymbol{v})\right)\mathrm{d}V, \tag{D.2}$$

$$\frac{\mathrm{D}}{\mathrm{D}t}\int_V \mathrm{d}V = \int_V \nabla\cdot\boldsymbol{v}\,\mathrm{d}V, \tag{D.3}$$

$$\frac{\mathrm{D}}{\mathrm{D}t}\int_V \rho\varphi\,\mathrm{d}V = \int_V \rho\frac{\mathrm{D}\varphi}{\mathrm{D}t}\,\mathrm{d}V. \tag{D.4}$$

These formulae also hold if φ is a vector. The Eulerian derivative of an integral is:

$$\frac{\mathrm{d}}{\mathrm{d}t}\int_V \varphi\,\mathrm{d}V = \int_V \frac{\partial\varphi}{\partial t}\,\mathrm{d}V, \tag{D.5}$$

so that

$$\frac{\mathrm{d}}{\mathrm{d}t}\int_V \mathrm{d}V = 0 \quad \text{and} \quad \frac{\mathrm{d}}{\mathrm{d}t}\int_V \rho\varphi\,\mathrm{d}V = \int_V \frac{\partial\rho\varphi}{\partial t}\,\mathrm{d}V. \tag{D.6}$$

where (1.21b) applies to a finite volume. That expression may also be derived more formally using Leibniz's formula for the material derivative of an integral, and the result also holds when φ is a vector. The result is quite different from the corresponding Eulerian derivative, in which the volume is kept fixed; in that case we have:

$$\frac{\mathrm{d}}{\mathrm{d}t}\int_V \varphi\rho\,\mathrm{d}V = \int_V \frac{\partial}{\partial t}(\varphi\rho)\,\mathrm{d}V. \tag{1.22}$$

Various material and Eulerian derivatives are summarized in the shaded box above.

1.2 THE MASS CONTINUITY EQUATION

In classical mechanics mass is absolutely conserved and in solid-body mechanics we normally do not need an explicit equation of mass conservation. However, in fluid mechanics fluid flows into and away from regions, and fluid density may change, and an equation that explicitly accounts for the flow of mass is one of the equations of motion of the fluid.

1.2.1 An Eulerian Derivation

We will first derive the mass conservation equation from an Eulerian point of view; that is to say, our reference frame is fixed in space and the fluid flows through it.

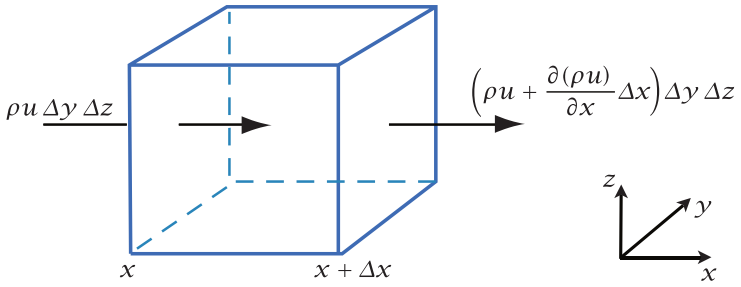

Fig. 1.1 Mass conservation in an Eulerian cuboid control volume. The mass convergence, $-\partial(\rho u)/\partial x$ (plus contributions from the y and z directions), must be balanced by a density increase, $\partial\rho/\partial t$.

Cartesian derivation

Consider an infinitesimal, rectangular cuboid, control volume, $\Delta V = \Delta x\Delta y\Delta z$ that is fixed in space, as in Fig. 1.1. Fluid moves into or out of the volume through its surface, including through its faces in the y–z plane of area $\Delta A = \Delta y\Delta z$ at coordinates x and $x+\Delta x$. The accumulation of fluid within the control volume due to motion in the x-direction is evidently

$$\Delta y\Delta z[(\rho u)(x,y,z) - (\rho u)(x+\Delta x,y,z)] = -\left.\frac{\partial(\rho u)}{\partial x}\right|_{x,y,z}\Delta x\,\Delta y\,\Delta z. \tag{1.23}$$

To this must be added the effects of motion in the y- and z-directions, namely

$$-\left[\frac{\partial(\rho v)}{\partial y} + \frac{\partial(\rho w)}{\partial z}\right]\Delta x\,\Delta y\,\Delta z. \tag{1.24}$$

This net accumulation of fluid must be accompanied by a corresponding increase of fluid mass within the control volume. This is

$$\frac{\partial}{\partial t}\,(\text{density}\times\text{volume}) = \Delta x\,\Delta y\,\Delta z\frac{\partial\rho}{\partial t}, \tag{1.25}$$

because the volume is constant. Thus, because mass is conserved, (1.23), (1.24) and (1.25) give

$$\Delta x\,\Delta y\,\Delta z\left[\frac{\partial\rho}{\partial t} + \frac{\partial(\rho u)}{\partial x} + \frac{\partial(\rho v)}{\partial y} + \frac{\partial(\rho w)}{\partial z}\right] = 0. \tag{1.26}$$

The quantity in square brackets must be zero and we therefore have

$$\frac{\partial\rho}{\partial t} + \nabla\cdot(\rho\boldsymbol{v}) = 0. \tag{1.27}$$

This is called the *mass continuity equation* for it recognizes the continuous nature of the mass field in a fluid. There is no diffusion term in (1.27), no term like $\kappa\nabla^2\rho$. This is because mass is transported by the macroscopic movement of molecules; even if this motion appears diffusion-like any net macroscopic molecular motion constitutes, by definition, a velocity field.

Vector derivation

Consider an arbitrary control volume V bounded by a surface S, fixed in space, with by convention the direction of $\boldsymbol{S}$ being toward the outside of V, as in Fig. 1.2. The rate of fluid loss due to flow through the closed surface S is then given by

$$\text{fluid loss} = \int_S \rho\boldsymbol{v}\cdot\mathrm{d}\boldsymbol{S} = \int_V \nabla\cdot(\rho\boldsymbol{v})\,\mathrm{d}V, \tag{1.28}$$

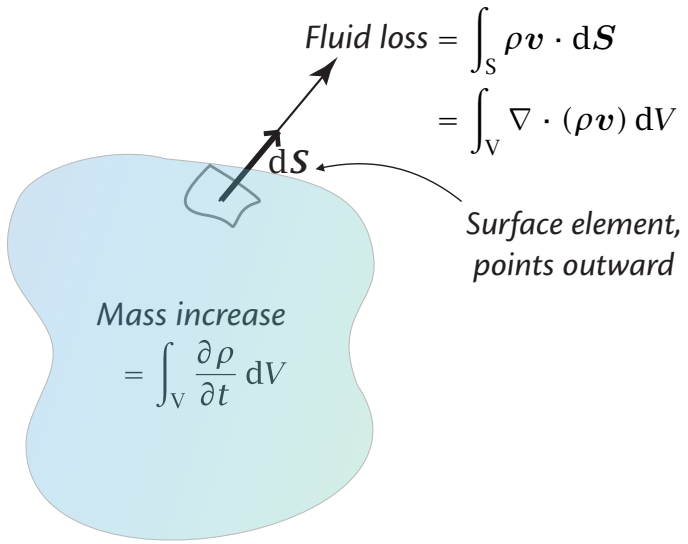

Fig. 1.2 Mass conservation in an arbitrary Eulerian control volume V bounded by a surface S. The mass increase, $\int_V (\partial\rho/\partial t)\, \mathrm{d}V$ is equal to the mass flowing into the volume, $-\int_S (\rho\boldsymbol{v}) \cdot \mathrm{d}\boldsymbol{S} = -\int_V \nabla \cdot (\rho\boldsymbol{v})\, \mathrm{d}V$.

using the divergence theorem.

This must be balanced by a change in the mass M of the fluid within the control volume, which, since its volume is fixed, implies a density change. That is

$$\text{fluid loss} = -\frac{\mathrm{d}M}{\mathrm{d}t} = -\frac{\mathrm{d}}{\mathrm{d}t}\int_V \rho\, \mathrm{d}V = -\int_V \frac{\partial \rho}{\partial t}\, \mathrm{d}V. \tag{1.29}$$

Equating (1.28) and (1.29) yields

$$\int_V \left[\frac{\partial \rho}{\partial t} + \nabla \cdot (\rho \boldsymbol{v})\right] \mathrm{d}V = 0. \tag{1.30}$$

Because the volume is arbitrary, the integrand must vanish and we recover (1.27).

1.2.2 Mass Continuity via the Material Derivative

We now derive the mass continuity equation (1.27) from a material perspective. This is the most fundamental approach of all since the principle of mass conservation states simply that the mass of a given element of fluid is, by definition of the element, constant. Thus, consider a small mass of fluid of density ρ and volume ΔV. Then conservation of mass may be represented by

$$\frac{\mathrm{D}}{\mathrm{D}t}(\rho \Delta V) = 0. \tag{1.31}$$

Both the density and the volume of the parcel may change, so

$$\Delta V \frac{\mathrm{D}\rho}{\mathrm{D}t} + \rho \frac{\mathrm{D}\Delta V}{\mathrm{D}t} = \Delta V \left(\frac{\mathrm{D}\rho}{\mathrm{D}t} + \rho \nabla \cdot \boldsymbol{v}\right) = 0, \tag{1.32}$$

where the second expression follows using (1.15). Since the volume element is arbitrary, the term in brackets must vanish and

$$\frac{\mathrm{D}\rho}{\mathrm{D}t} + \rho \nabla \cdot \boldsymbol{v} = 0. \tag{1.33}$$

After expansion of the first term this becomes identical to (1.27). This result may be derived more formally by rewriting (1.31) as the integral expression

$$\frac{\mathrm{D}}{\mathrm{D}t}\int_V \rho\, \mathrm{d}V = 0. \tag{1.34}$$

Expanding the derivative using (1.18) gives

$$\frac{\mathrm{D}}{\mathrm{D}t}\int_V \rho\,\mathrm{d}V = \int_V \left(\frac{\mathrm{D}\rho}{\mathrm{D}t} + \rho\nabla\cdot\boldsymbol{v}\right)\mathrm{d}V = 0. \tag{1.35}$$

Because the volume over which the integral is taken is arbitrary the integrand itself must vanish and we recover (1.33). Summarizing, equivalent partial differential equations representing conservation of mass are:

$$\frac{\mathrm{D}\rho}{\mathrm{D}t} + \rho\nabla\cdot\boldsymbol{v} = 0, \qquad \frac{\partial\rho}{\partial t} + \nabla\cdot(\rho\boldsymbol{v}) = 0. \tag{1.36a,b}$$

1.2.3 A General Continuity Equation

The derivation of a continuity equation for a general scalar property of a fluid is similar to that for density, except that there may be an external source or sink, and potentially a means of transferring the property from one location to another differently than by fluid motion, for example by diffusion. If ξ is the amount of some property of the fluid per unit volume (the volume concentration, sometimes simply called the concentration), and if the net effect per unit volume of all non-conservative processes is denoted by $Q_{[v,\xi]}$, then the continuity equation for concentration may be written:

$$\frac{\mathrm{D}}{\mathrm{D}t}(\xi\Delta V) = Q_{[v,\xi]}\Delta V. \tag{1.37}$$

Expanding the left-hand side and using (1.15) we obtain

$$\frac{\mathrm{D}\xi}{\mathrm{D}t} + \xi\nabla\cdot\boldsymbol{v} = Q_{[v,\xi]}, \qquad \text{or} \qquad \frac{\partial\xi}{\partial t} + \nabla\cdot(\xi\boldsymbol{v}) = Q_{[v,\xi]}. \tag{1.38}$$

If we are interested in a tracer that is normally measured per unit mass of fluid (which is typical when considering thermodynamic quantities) then the conservation equation would be written

$$\frac{\mathrm{D}}{\mathrm{D}t}(\varphi\rho\Delta V) = Q_{[m,\varphi]}\rho\Delta V, \tag{1.39}$$

where φ is the tracer mixing ratio or mass concentration — that is, the amount of tracer per unit fluid mass — and $Q_{[m,\varphi]}$ represents non-conservative sources of φ per unit mass. Then, since $\rho\Delta V$ is constant we obtain

$$\frac{\mathrm{D}\varphi}{\mathrm{D}t} = Q_{[m,\varphi]} \qquad \text{or} \qquad \frac{\partial(\rho\varphi)}{\partial t} + \nabla\cdot(\rho\varphi\boldsymbol{v}) = \rho Q_{[m,\varphi]}, \tag{1.40}$$

using the mass continuity equation, (1.36), to obtain the equation on the right. The source term $Q_{[m,\varphi]}$ is evidently equal to the rate of change of φ of a fluid element. When this is so, we often write it simply as $\dot{\varphi}$, so that

$$\frac{\mathrm{D}\varphi}{\mathrm{D}t} = \dot{\varphi}. \tag{1.41}$$

A tracer obeying (1.41) with $\dot{\varphi} = 0$ is said to be *materially conserved*. If a tracer is materially conserved except for the effects of sources or sinks, or diffusion terms, then it is sometimes (if rather loosely) said to be an 'adiabatically conserved' variable, although adiabatic properly means with no heat exchange. If those sources and sinks are in the form of the divergence of a flux with φ satisfying $\rho\mathrm{D}\varphi/\mathrm{D}t = \nabla\cdot\boldsymbol{F}_\varphi$ or equivalently, using the mass continuity equation, $\partial(\rho\varphi)/\partial t + \nabla\cdot(\rho\boldsymbol{v}\varphi) = \nabla\cdot\boldsymbol{F}_\varphi$, then φ is said to be a *conservative* variable because, with no flux boundary conditions, $\int\rho\varphi\,\mathrm{d}V$ = constant. Although momentum as a whole is conserved, momentum is not a materially conserved variable, as we are about to see.

The heavens themselves, the planets, and this centre
Observe degree, priority, and place,
Insisture, course, proportion, season, form,
Office, and custom, in all line of order.
And therefore is the glorious planet Sol
In noble eminence enthroned and sphered.
William Shakespeare, *Troilus and Cressida*, c. 1602.

Eppur si muove. (And yet it does move.)
Galileo Galilei, apocryphal, 1633.

CHAPTER 2

Effects of Rotation and Stratification

THE ATMOSPHERE AND OCEAN are shallow layers of fluid on a sphere, 'shallow' because their thickness is much less than their horizontal extent. Their motion is strongly influenced by two effects: rotation and stratification, the latter meaning that there is a mean vertical gradient of (potential) density that is often large compared with the horizontal gradient. Here we consider how the equations of motion are affected by these effects. First, we consider some elementary effects of rotation on a fluid and derive the Coriolis and centrifugal forces, and write down the equations of motion appropriate for motion on a sphere. Then we discuss some approximations to the equations of motion that are appropriate for large-scale flow in the ocean and atmosphere, in particular the hydrostatic and geostrophic approximations, and finally we look at the possible static instability of stratified flows.

2.1 EQUATIONS OF MOTION IN A ROTATING FRAME

Newton's second law of motion, that the acceleration of a body is proportional to the imposed force divided by the body's mass, applies in so-called inertial frames of reference; that is, frames that are stationary or moving only with a constant rectilinear velocity relative to the distant galaxies. Now Earth spins round its own axis with a period of almost 24 hours (23h 56m, the difference due to Earth's rotation around the Sun) and so the surface of the Earth manifestly is not an inertial frame. Nevertheless, it is very convenient to describe the flow relative to Earth's surface (which in fact is moving at speeds of up to a few hundreds of metres per second), rather than in some inertial frame.[2] This necessitates recasting the equations into a form appropriate in a rotating frame of reference, and that is the subject of this section.

2.1.1 Rate of Change of a Vector

Consider first a vector $\boldsymbol{C}$ of constant length rotating relative to an inertial frame at a constant angular velocity $\boldsymbol{\Omega}$. Then, in a frame rotating with that same angular velocity it appears stationary and constant. If in a small interval of time δt the vector $\boldsymbol{C}$ rotates through a small angle $\delta\lambda$ then the change in $\boldsymbol{C}$, as perceived in the inertial frame, is given by (see Fig. 2.1)

$$\delta\boldsymbol{C} = |\boldsymbol{C}| \cos\vartheta \, \delta\lambda \, \boldsymbol{m}, \tag{2.1}$$

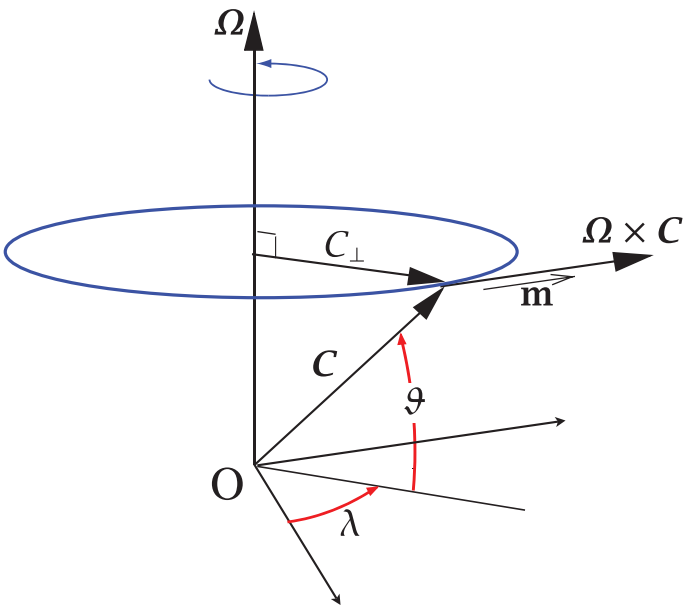

Fig. 2.1 A vector $\boldsymbol{C}$ rotating at an angular velocity $\boldsymbol{\Omega}$. It appears to be a constant vector in the rotating frame, whereas in the inertial frame it evolves according to $(\mathrm{d}\boldsymbol{C}/\mathrm{d}t)_I = \boldsymbol{\Omega} \times \boldsymbol{C}$.

where the vector $\boldsymbol{m}$ is the unit vector in the direction of change of $\boldsymbol{C}$, which is perpendicular to both $\boldsymbol{C}$ and $\boldsymbol{\Omega}$. But the rate of change of the angle λ is just, by definition, the angular velocity so that $\delta\lambda = |\boldsymbol{\Omega}|\delta t$ and

$$\delta \boldsymbol{C} = |\boldsymbol{C}||\boldsymbol{\Omega}| \sin\widehat{\vartheta}\, \boldsymbol{m}\, \delta t = \boldsymbol{\Omega} \times \boldsymbol{C}\, \delta t, \tag{2.2}$$

using the definition of the vector cross product, where $\widehat{\vartheta} = (\pi/2 - \vartheta)$ is the angle between $\boldsymbol{\Omega}$ and $\boldsymbol{C}$. Thus

$$\left(\frac{\mathrm{d}\boldsymbol{C}}{\mathrm{d}t}\right)_I = \boldsymbol{\Omega} \times \boldsymbol{C}, \tag{2.3}$$

where the left-hand side is the rate of change of $\boldsymbol{C}$ as perceived in the inertial frame.

Now consider a vector $\boldsymbol{B}$ that changes in the inertial frame. In a small time δt the change in $\boldsymbol{B}$ as seen in the rotating frame is related to the change seen in the inertial frame by

$$(\delta \boldsymbol{B})_I = (\delta \boldsymbol{B})_R + (\delta \boldsymbol{B})_{rot}, \tag{2.4}$$

where the terms are, respectively, the change seen in the inertial frame, the change due to the vector itself changing as measured in the rotating frame, and the change due to the rotation. Using (2.2) $(\delta \boldsymbol{B})_{rot} = \boldsymbol{\Omega} \times \boldsymbol{B}\, \delta t$, and so the rates of change of the vector $\boldsymbol{B}$ in the inertial and rotating frames are related by

$$\left(\frac{\mathrm{d}\boldsymbol{B}}{\mathrm{d}t}\right)_I = \left(\frac{\mathrm{d}\boldsymbol{B}}{\mathrm{d}t}\right)_R + \boldsymbol{\Omega} \times \boldsymbol{B}. \tag{2.5}$$

This relation applies to a vector $\boldsymbol{B}$ that, as measured at any one time, is the same in both inertial and rotating frames.

2.1.2 Velocity and Acceleration in a Rotating Frame

The velocity of a body is not measured to be the same in the inertial and rotating frames, so care must be taken when applying (2.5) to velocity. First apply (2.5) to $\boldsymbol{r}$, the position of a particle to obtain

$$\left(\frac{\mathrm{d}\boldsymbol{r}}{\mathrm{d}t}\right)_I = \left(\frac{\mathrm{d}\boldsymbol{r}}{\mathrm{d}t}\right)_R + \boldsymbol{\Omega} \times \boldsymbol{r} \tag{2.6}$$

or

$$\boldsymbol{v}_I = \boldsymbol{v}_R + \boldsymbol{\Omega} \times \boldsymbol{r}. \tag{2.7}$$

We refer to $\boldsymbol{v}_R$ and $\boldsymbol{v}_I$ as the relative and inertial velocity, respectively, and (2.7) relates the two. Apply (2.5) again, this time to the velocity $\boldsymbol{v}_R$ to give

$$\left(\frac{\mathrm{d}\boldsymbol{v}_R}{\mathrm{d}t}\right)_I = \left(\frac{\mathrm{d}\boldsymbol{v}_R}{\mathrm{d}t}\right)_R + \boldsymbol{\Omega} \times \boldsymbol{v}_R, \tag{2.8}$$

or, using (2.7)

$$\left(\frac{\mathrm{d}}{\mathrm{d}t}(\boldsymbol{v}_I - \boldsymbol{\Omega} \times \boldsymbol{r})\right)_I = \left(\frac{\mathrm{d}\boldsymbol{v}_R}{\mathrm{d}t}\right)_R + \boldsymbol{\Omega} \times \boldsymbol{v}_R, \tag{2.9}$$

or

$$\left(\frac{\mathrm{d}\boldsymbol{v}_I}{\mathrm{d}t}\right)_I = \left(\frac{\mathrm{d}\boldsymbol{v}_R}{\mathrm{d}t}\right)_R + \boldsymbol{\Omega} \times \boldsymbol{v}_R + \frac{\mathrm{d}\boldsymbol{\Omega}}{\mathrm{d}t} \times \boldsymbol{r} + \boldsymbol{\Omega} \times \left(\frac{\mathrm{d}\boldsymbol{r}}{\mathrm{d}t}\right)_I. \tag{2.10}$$

Then, noting that

$$\left(\frac{\mathrm{d}\boldsymbol{r}}{\mathrm{d}t}\right)_I = \left(\frac{\mathrm{d}\boldsymbol{r}}{\mathrm{d}t}\right)_R + \boldsymbol{\Omega} \times \boldsymbol{r} = (\boldsymbol{v}_R + \boldsymbol{\Omega} \times \boldsymbol{r}), \tag{2.11}$$

and assuming that the rate of rotation is constant, (2.10) becomes

$$\left(\frac{\mathrm{d}\boldsymbol{v}_R}{\mathrm{d}t}\right)_R = \left(\frac{\mathrm{d}\boldsymbol{v}_I}{\mathrm{d}t}\right)_I - 2\boldsymbol{\Omega} \times \boldsymbol{v}_R - \boldsymbol{\Omega} \times (\boldsymbol{\Omega} \times \boldsymbol{r}). \tag{2.12}$$

This equation may be interpreted as follows. The term on the left-hand side is the rate of change of the relative velocity as measured in the rotating frame. The first term on the right-hand side is the rate of change of the inertial velocity as measured in the inertial frame (the inertial acceleration, which is, by Newton's second law, equal to the force on a fluid parcel divided by its mass). The second and third terms on the right-hand side (including the minus signs) are the *Coriolis force* and the *centrifugal force* per unit mass. Neither of these is a true force — they may be thought of as quasi-forces (i.e., 'as if' forces); that is, when a body is observed from a rotating frame it behaves as if unseen forces are present that affect its motion. If (2.12) is written, as is common, with the terms $+2\boldsymbol{\Omega} \times \boldsymbol{v}_r$ and $+\boldsymbol{\Omega} \times (\boldsymbol{\Omega} \times \boldsymbol{r})$ on the left-hand side then these terms should be referred to as the Coriolis and centrifugal *accelerations.*[3]

Centrifugal force

If $\boldsymbol{r}_\perp$ is the perpendicular distance from the axis of rotation (see Fig. 2.1 and substitute $\boldsymbol{r}$ for $\boldsymbol{C}$), then, because $\boldsymbol{\Omega}$ is perpendicular to $\boldsymbol{r}_\perp$, $\boldsymbol{\Omega} \times \boldsymbol{r} = \boldsymbol{\Omega} \times \boldsymbol{r}_\perp$. Then, using the vector identity $\boldsymbol{\Omega} \times (\boldsymbol{\Omega} \times \boldsymbol{r}_\perp) = (\boldsymbol{\Omega} \cdot \boldsymbol{r}_\perp)\boldsymbol{\Omega} - (\boldsymbol{\Omega} \cdot \boldsymbol{\Omega})\boldsymbol{r}_\perp$ and noting that the first term is zero, we see that the centrifugal force per unit mass is just given by

$$\boldsymbol{F}_{ce} = -\boldsymbol{\Omega} \times (\boldsymbol{\Omega} \times \boldsymbol{r}) = \Omega^2 \boldsymbol{r}_\perp. \tag{2.13}$$

This may usefully be written as the gradient of a scalar potential,

$$\boldsymbol{F}_{ce} = -\nabla \Phi_{ce}\,, \tag{2.14}$$

where $\Phi_{ce} = -(\Omega^2 r_\perp^2)/2 = -(\boldsymbol{\Omega} \times \boldsymbol{r}_\perp)^2/2$.

Coriolis force

The Coriolis force per unit mass is given by

$$\boldsymbol{F}_{Co} = -2\boldsymbol{\Omega} \times \boldsymbol{v}_R. \tag{2.15}$$

It plays a central role in much of geophysical fluid dynamics and will be considered extensively later on. For now, we just note three basic properties:

(i) There is no Coriolis force on bodies that are stationary in the rotating frame.
(ii) The Coriolis force acts to deflect moving bodies at right angles to their direction of travel.
(iii) The Coriolis force does no work on a body because it is perpendicular to the velocity, and so $\boldsymbol{v}_R \cdot (\boldsymbol{\Omega} \times \boldsymbol{v}_R) = 0$.

2.1.3 Momentum Equation in a Rotating Frame

Since (2.12) simply relates the accelerations of a particle in the inertial and rotating frames, then in the rotating frame of reference the momentum equation may be written

$$\frac{\mathrm{D}\boldsymbol{v}}{\mathrm{D}t} + 2\boldsymbol{\Omega} \times \boldsymbol{v} = -\frac{1}{\rho}\nabla p - \nabla\Phi, \tag{2.16}$$

incorporating the centrifugal term into the potential, Φ. We have dropped the subscript R; henceforth, unless we need to be explicit (as in the next section), all velocities without a subscript will be considered to be relative to the rotating frame.

2.1.4 Mass and Tracer Conservation in a Rotating frame

Let φ be a scalar field that, in the inertial frame, obeys

$$\frac{\mathrm{D}\varphi}{\mathrm{D}t} + \varphi\nabla \cdot \boldsymbol{v}_I = 0. \tag{2.17}$$

Now, observers in both the rotating and inertial frame measure the same value of φ. Further, $\mathrm{D}\varphi/\mathrm{D}t$ is simply the rate of change of φ associated with a material parcel, and therefore is reference frame invariant. Thus, without further ado, we write

$$\left(\frac{\mathrm{D}\varphi}{\mathrm{D}t}\right)_R = \left(\frac{\mathrm{D}\varphi}{\mathrm{D}t}\right)_I, \tag{2.18}$$

where $(\mathrm{D}\varphi/\mathrm{D}t)_R = (\partial\varphi/\partial t)_R + \boldsymbol{v}_R \cdot \nabla\varphi$ and $(\mathrm{D}\varphi/\mathrm{D}t)_I = (\partial\varphi/\partial t)_I + \boldsymbol{v}_I \cdot \nabla\varphi$, and the local temporal derivatives $(\partial\varphi/\partial t)_R$ and $(\partial\varphi/\partial t)_I$ are evaluated at fixed locations in the rotating and inertial frames, respectively.

Further, using (2.7), we have that

$$\nabla \cdot \boldsymbol{v}_I = \nabla \cdot (\boldsymbol{v}_R + \boldsymbol{\Omega} \times \boldsymbol{r}) = \nabla \cdot \boldsymbol{v}_R, \tag{2.19}$$

since $\nabla \cdot (\boldsymbol{\Omega} \times \boldsymbol{r}) = 0$. Thus, using (2.18) and (2.19), (2.17) is equivalent to

$$\frac{\mathrm{D}\varphi}{\mathrm{D}t} + \varphi\nabla \cdot \boldsymbol{v}_R = 0, \tag{2.20}$$

where all observables are measured in the *rotating* frame. Thus, the equation for the evolution of a scalar whose measured value is the same in rotating and inertial frames is unaltered by the presence of rotation. In particular, the mass conservation equation is unaltered by the presence of rotation.

Although we have taken (2.18) as true a priori, the individual components of the material derivative differ in the rotating and inertial frames. In particular

$$\left(\frac{\partial \varphi}{\partial t}\right)_I = \left(\frac{\partial \varphi}{\partial t}\right)_R - (\boldsymbol{\Omega} \times \boldsymbol{r}) \cdot \nabla \varphi, \tag{2.21}$$

because $\boldsymbol{\Omega} \times \boldsymbol{r}$ is the velocity, in the inertial frame, of a uniformly rotating body. Similarly,

$$\boldsymbol{v}_I \cdot \nabla \varphi = (\boldsymbol{v}_R + \boldsymbol{\Omega} \times \boldsymbol{r}) \cdot \nabla \varphi. \tag{2.22}$$

Adding the last two equations reprises and confirms (2.18).

2.2 EQUATIONS OF MOTION IN SPHERICAL COORDINATES

The Earth is very nearly spherical and it might appear obvious that we should cast our equations in spherical coordinates. Although this does turn out to be true, the presence of a centrifugal force causes some complications that we should first discuss. The reader who is willing ab initio to treat the Earth as a perfect sphere and to neglect the horizontal component of the centrifugal force may skip the next section.

2.2.1 ✦ The Centrifugal Force and Spherical Coordinates

The centrifugal force is a potential force, like gravity, and so we may therefore define an 'effective gravity' equal to the sum of the true, or Newtonian, gravity and the centrifugal force. The Newtonian gravitational force is directed approximately toward the centre of the Earth, with small deviations due mainly to the Earth's oblateness. The line of action of the effective gravity will in general differ slightly from this, and therefore have a component in the 'horizontal' plane, that is the plane perpendicular to the radial direction. The magnitude of the centrifugal force is $\Omega^2 r_\perp$, and so the effective gravity is given by

$$\boldsymbol{g} \equiv \boldsymbol{g}_{eff} = \boldsymbol{g}_{grav} + \Omega^2 \boldsymbol{r}_\perp, \tag{2.23}$$

where $\boldsymbol{g}_{grav}$ is the Newtonian gravitational force due to the gravitational attraction of the Earth and $\boldsymbol{r}_\perp$ is normal to the rotation vector (in the direction $\boldsymbol{C}$ in Fig. 2.2), with $r_\perp = r \cos\vartheta$. Both gravity and centrifugal force are potential forces and therefore we may define the *geopotential*, Φ, such that

$$\boldsymbol{g} = -\nabla \Phi. \tag{2.24}$$

Surfaces of constant Φ are not quite spherical because $r_\perp$, and hence the centrifugal force, vary with latitude (Fig. 2.2); this has certain ramifications, as we now discuss.

The components of the centrifugal force parallel and perpendicular to the radial direction are $\Omega^2 r \cos^2\vartheta$ and $\Omega^2 r \cos\vartheta \sin\vartheta$. Newtonian gravity is much larger than either of these, and at the Earth's surface the ratio of centrifugal to gravitational terms is approximately, and no more than,

$$\alpha \approx \frac{\Omega^2 a}{g} \approx \frac{(7.27 \times 10^{-5})^2 \times 6.4 \times 10^6}{9.8} \approx 3 \times 10^{-3}. \tag{2.25}$$

(At the equator and pole the horizontal component of the centrifugal force is zero and the effective gravity is aligned with Newtonian gravity.) The angle between $\boldsymbol{g}$ and the line to the centre of the Earth is given by a similar expression and so is also small, typically around $3{\times}10^{-3}$ radians. However, the horizontal component of the centrifugal force is still large compared to the Coriolis force, the ratio of their magnitudes in mid-latitudes being given by

$$\frac{\text{horizontal centrifugal force}}{\text{Coriolis force}} \approx \frac{\Omega^2 a \cos\vartheta \sin\vartheta}{2\Omega|u|} \approx \frac{\Omega a}{4|u|} \approx 10, \tag{2.26}$$

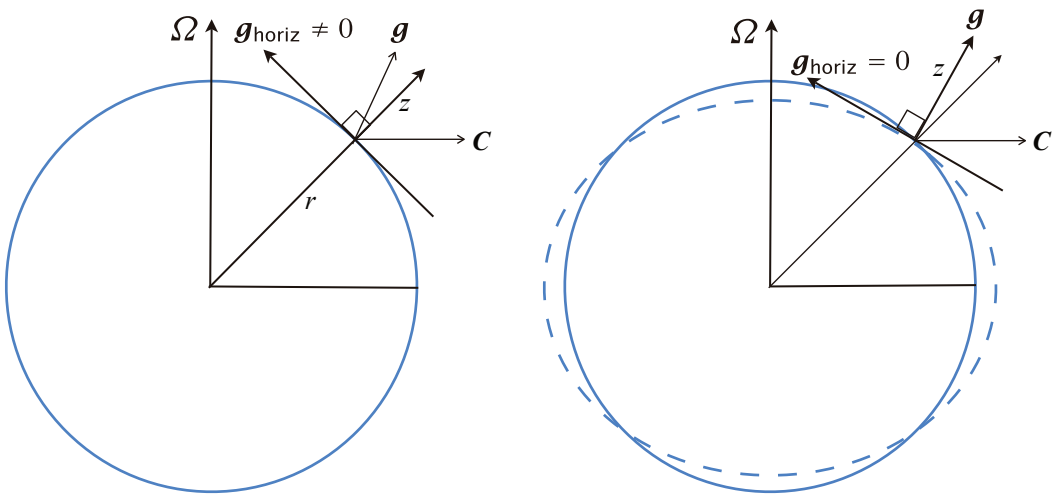

Fig. 2.2 Left: directions of forces and coordinates in true spherical geometry. $\boldsymbol{g}$ is the effective gravity (including the centrifugal force, $\boldsymbol{C}$) and its horizontal component is evidently non-zero. Right: a modified coordinate system, in which the vertical direction is defined by the direction of $\boldsymbol{g}$, and so the horizontal component of $\boldsymbol{g}$ is identically zero. The dashed line schematically indicates a surface of constant geopotential. The differences between the direction of $\boldsymbol{g}$ and the direction of the radial coordinate, and between the sphere and the geopotential surface, are much exaggerated and in reality are similar to the thickness of the lines themselves.

using $u = 10\ \text{m s}^{-1}$. The centrifugal term therefore dominates over the Coriolis term, and is largely balanced by a pressure gradient force. Thus, if we adhered to true spherical coordinates, both the horizontal and radial components of the momentum equation would be dominated by a static balance between a pressure gradient and gravity or centrifugal terms. Although in principle there is nothing wrong with writing the equations this way, it obscures the dynamical balances involving the Coriolis force and pressure that determine the large-scale horizontal flow.

A way around this problem is to use the direction of the geopotential force to *define* the vertical direction, and then for all geometric purposes to regard the surfaces of constant Φ as if they were true spheres.[4] The horizontal component of effective gravity is then identically zero, and we have traded a potentially large dynamical error for a very small geometric error. In fact, over time, the Earth has developed an equatorial bulge to compensate for and neutralize the centrifugal force, so that the effective gravity does act in a direction virtually normal to the Earth's surface; that is, the surface of the Earth is an oblate spheroid of nearly constant geopotential. The geopotential Φ is then a function of the vertical coordinate alone, and for many purposes we can just take $\Phi = gz$; that is, the direction normal to geopotential surfaces, the local vertical, is, in this approximation, taken to be the direction of increasing r in spherical coordinates. It is because the oblateness is very small (the polar diameter is about 12 714 km, whereas the equatorial diameter is about 12 756 km) that using spherical coordinates is a very accurate way to map the spheroid. If the angle between effective gravity and a natural direction of the coordinate system were not small then more heroic measures would be called for.

If the solid Earth did not bulge at the equator, the *behaviour* of the atmosphere and ocean would differ significantly from that of the present system. For example, the surface of the ocean is, necessarily, very nearly a geopotential surface; if the solid Earth were exactly spherical then the ocean would perforce become much deeper at low latitudes and the ocean basins would dry out completely at high latitudes. We could still choose to use the spherical coordinate system discussed above to describe the dynamics, but the shape of the surface of the solid Earth would have to

be represented by a topography, with the topographic height increasing monotonically polewards nearly everywhere.

2.2.2 Some Identities in Spherical Coordinates

The location of a point is given by the coordinates (λ, ϑ, r) where λ is the angular distance eastwards (i.e., longitude), ϑ is angular distance polewards (i.e., latitude) and r is the radial distance from the centre of the Earth — see Fig. 2.3. (In some other fields of study co-latitude is used as a spherical coordinate.) If a is the radius of the Earth, then we also define $z = r - a$. At a given location we may also define the Cartesian increments $(\delta x, \delta y, \delta z) = (r\cos\vartheta\delta\lambda, r\delta\vartheta, \delta r)$.

For a scalar quantity ϕ the material derivative in spherical coordinates is

$$\frac{\mathrm{D}\phi}{\mathrm{D}t} = \frac{\partial\phi}{\partial t} + \frac{u}{r\cos\vartheta}\frac{\partial\phi}{\partial\lambda} + \frac{v}{r}\frac{\partial\phi}{\partial\vartheta} + w\frac{\partial\phi}{\partial r}, \tag{2.27}$$

where the velocity components corresponding to the coordinates (λ, ϑ, r) are

$$(u, v, w) \equiv \left(r\cos\vartheta\frac{\mathrm{D}\lambda}{\mathrm{D}t}, r\frac{\mathrm{D}\vartheta}{\mathrm{D}t}, \frac{\mathrm{D}r}{\mathrm{D}t}\right). \tag{2.28}$$

That is, u is the zonal velocity, v is the meridional velocity and w is the vertical velocity. If we define $(\mathbf{i}, \mathbf{j}, \mathbf{k})$ to be the unit vectors in the direction of increasing (λ, ϑ, r) then

$$\boldsymbol{v} = \mathbf{i}u + \mathbf{j}v + \mathbf{k}w. \tag{2.29}$$

Note also that $\mathrm{D}r/\mathrm{D}t = \mathrm{D}z/\mathrm{D}t$.

The divergence of a vector $\boldsymbol{B} = \mathbf{i}\,B^\lambda + \mathbf{j}\,B^\vartheta + \mathbf{k}\,B^r$ is

$$\nabla\cdot\boldsymbol{B} = \frac{1}{\cos\vartheta}\left[\frac{1}{r}\frac{\partial B^\lambda}{\partial\lambda} + \frac{1}{r}\frac{\partial}{\partial\vartheta}(B^\vartheta\cos\vartheta) + \frac{\cos\vartheta}{r^2}\frac{\partial}{\partial r}(r^2B^r)\right]. \tag{2.30}$$

The vector gradient of a scalar is:

$$\nabla\phi = \mathbf{i}\frac{1}{r\cos\vartheta}\frac{\partial\phi}{\partial\lambda} + \mathbf{j}\frac{1}{r}\frac{\partial\phi}{\partial\vartheta} + \mathbf{k}\frac{\partial\phi}{\partial r}. \tag{2.31}$$

The Laplacian of a scalar is:

$$\nabla^2\phi \equiv \nabla\cdot\nabla\phi = \frac{1}{r^2\cos\vartheta}\left[\frac{1}{\cos\vartheta}\frac{\partial^2\phi}{\partial\lambda^2} + \frac{\partial}{\partial\vartheta}\left(\cos\vartheta\frac{\partial\phi}{\partial\vartheta}\right) + \cos\vartheta\frac{\partial}{\partial r}\left(r^2\frac{\partial\phi}{\partial r}\right)\right]. \tag{2.32}$$

The curl of a vector is:

$$\mathrm{curl}\,\boldsymbol{B} = \nabla\times\boldsymbol{B} = \frac{1}{r^2\cos\vartheta}\begin{vmatrix} \mathbf{i}\,r\cos\vartheta & \mathbf{j}\,r & \mathbf{k} \\ \partial/\partial\lambda & \partial/\partial\vartheta & \partial/\partial r \\ B^\lambda r\cos\vartheta & B^\vartheta r & B^r \end{vmatrix}. \tag{2.33}$$

The vector Laplacian $\nabla^2\boldsymbol{B}$ (used for example when calculating viscous terms in the momentum equation) may be obtained from the vector identity:

$$\nabla^2\boldsymbol{B} = \nabla(\nabla\cdot\boldsymbol{B}) - \nabla\times(\nabla\times\boldsymbol{B}). \tag{2.34}$$

Only in Cartesian coordinates does this take the simple form:

$$\nabla^2\boldsymbol{B} = \frac{\partial^2\boldsymbol{B}}{\partial x^2} + \frac{\partial^2\boldsymbol{B}}{\partial y^2} + \frac{\partial^2\boldsymbol{B}}{\partial z^2}. \tag{2.35}$$

The expansion in spherical coordinates is of itself, to most eyes, rather uninformative.

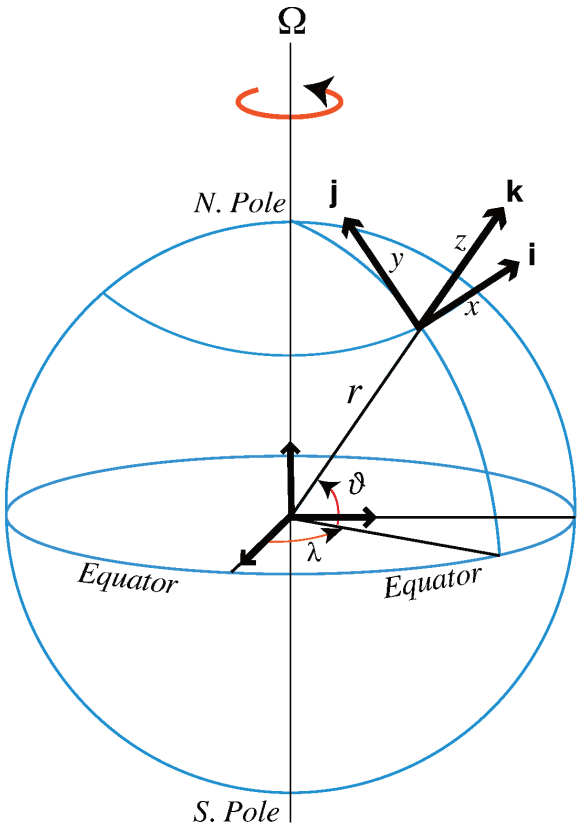

Fig. 2.3 The spherical coordinate system. The orthogonal unit vectors **i**, **j** and **k** point in the direction of increasing longitude λ, latitude ϑ, and altitude z. Locally, one may apply a Cartesian system with variables x, y and z measuring distances along **i**, **j** and **k**.

Rate of change of unit vectors

In spherical coordinates the defining unit vectors are **i**, the unit vector pointing eastwards, parallel to a line of latitude; **j** is the unit vector pointing polewards, parallel to a meridian; and **k**, the unit vector pointing radially outward. The directions of these vectors change with location, and in fact this is the case in nearly all coordinate systems, with the notable exception of the Cartesian one, and thus their material derivative is not zero. One way to evaluate this is to consider geometrically how the coordinate axes change with position. Another way, and the way that we shall proceed, is to first obtain the effective rotation rate $\boldsymbol{\Omega}_{flow}$, relative to the Earth, of a unit vector as it moves with the flow, and then apply (2.3). Specifically, let the fluid velocity be $\boldsymbol{v} = (u, v, w)$. The meridional component, v, produces a displacement $r\delta\vartheta = v\delta t$, and this gives rise to a local effective vector rotation rate around the local zonal axis of $-(v/r)\mathbf{i}$, the minus sign arising because a displacement in the direction of the north pole is produced by negative rotational displacement around the **i** axis. Similarly, the zonal component, u, produces a displacement $\delta\lambda r\cos\vartheta = u\delta t$ and so an effective rotation rate, about the Earth's rotation axis, of $u/(r\cos\vartheta)$. Now, a rotation around the Earth's rotation axis may be written as (see Fig. 2.4)

$$\boldsymbol{\Omega} = \Omega(\mathbf{j}\cos\vartheta + \mathbf{k}\sin\vartheta). \tag{2.36}$$

If the scalar rotation rate is not Ω but is $u/(r\cos\vartheta)$, then the vector rotation rate is

$$\frac{u}{r\cos\vartheta}(\mathbf{j}\cos\vartheta + \mathbf{k}\sin\vartheta) = \mathbf{j}\frac{u}{r} + \mathbf{k}\frac{u\tan\vartheta}{r}. \tag{2.37}$$

Thus, the total rotation rate of a vector that moves with the flow is

$$\boldsymbol{\Omega}_{flow} = -\mathbf{i}\frac{v}{r} + \mathbf{j}\frac{u}{r} + \mathbf{k}\frac{u\tan\vartheta}{r}. \tag{2.38}$$

Applying (2.3) to (2.38), we find

$$\frac{\mathrm{D}\mathbf{i}}{\mathrm{D}t} = \boldsymbol{\Omega}_{flow}\times\mathbf{i} = \frac{u}{r\cos\vartheta}(\mathbf{j}\sin\vartheta - \mathbf{k}\cos\vartheta), \tag{2.39a}$$

$$\frac{\mathrm{D}\mathbf{j}}{\mathrm{D}t} = \boldsymbol{\Omega}_{flow}\times\mathbf{j} = -\mathbf{i}\frac{u}{r}\tan\vartheta - \mathbf{k}\frac{v}{r}, \tag{2.39b}$$

$$\frac{\mathrm{D}\mathbf{k}}{\mathrm{D}t} = \boldsymbol{\Omega}_{flow}\times\mathbf{k} = \mathbf{i}\frac{u}{r} + \mathbf{j}\frac{v}{r}. \tag{2.39c}$$

2.2.3 Equations of Motion

Mass conservation and thermodynamic equation

The mass conservation equation, (1.36a), expanded in spherical co-ordinates, is

$$\frac{\partial\rho}{\partial t} + \frac{u}{r\cos\vartheta}\frac{\partial\rho}{\partial\lambda} + \frac{v}{r}\frac{\partial\rho}{\partial\vartheta} + w\frac{\partial\rho}{\partial r} + \frac{\rho}{r\cos\vartheta}\left[\frac{\partial u}{\partial\lambda} + \frac{\partial}{\partial\vartheta}(v\cos\vartheta) + \frac{1}{r}\frac{\partial}{\partial r}(wr^2\cos\vartheta)\right] = 0. \tag{2.40}$$

Equivalently, using the form (1.36b), this is

$$\frac{\partial\rho}{\partial t} + \frac{1}{r\cos\vartheta}\frac{\partial(u\rho)}{\partial\lambda} + \frac{1}{r\cos\vartheta}\frac{\partial}{\partial\vartheta}(v\rho\cos\vartheta) + \frac{1}{r^2}\frac{\partial}{\partial r}(r^2w\rho) = 0. \tag{2.41}$$

The thermodynamic equation, (1.108), is a tracer advection equation. Thus, using (2.27), its (adiabatic) spherical coordinate form is

$$\frac{\mathrm{D}\theta}{\mathrm{D}t} = \frac{\partial\theta}{\partial t} + \frac{u}{r\cos\vartheta}\frac{\partial\theta}{\partial\lambda} + \frac{v}{r}\frac{\partial\theta}{\partial\vartheta} + w\frac{\partial\theta}{\partial r} = 0, \tag{2.42}$$

and similarly for tracers such as water vapour or salt.

Momentum equation

Recall that the inviscid momentum equation is:

$$\frac{\mathrm{D}\boldsymbol{v}}{\mathrm{D}t} + 2\boldsymbol{\Omega}\times\boldsymbol{v} = -\frac{1}{\rho}\nabla p - \nabla\Phi, \tag{2.43}$$

where Φ is the geopotential. In spherical coordinates the directions of the coordinate axes change with position and so the component expansion of (2.43) is

$$\frac{\mathrm{D}\boldsymbol{v}}{\mathrm{D}t} = \frac{\mathrm{D}u}{\mathrm{D}t}\mathbf{i} + \frac{\mathrm{D}v}{\mathrm{D}t}\mathbf{j} + \frac{\mathrm{D}w}{\mathrm{D}t}\mathbf{k} + u\frac{\mathrm{D}\mathbf{i}}{\mathrm{D}t} + v\frac{\mathrm{D}\mathbf{j}}{\mathrm{D}t} + w\frac{\mathrm{D}\mathbf{k}}{\mathrm{D}t} \tag{2.44a}$$

$$= \frac{\mathrm{D}u}{\mathrm{D}t}\mathbf{i} + \frac{\mathrm{D}v}{\mathrm{D}t}\mathbf{j} + \frac{\mathrm{D}w}{\mathrm{D}t}\mathbf{k} + \boldsymbol{\Omega}_{flow}\times\boldsymbol{v}, \tag{2.44b}$$

using (2.39). Using either (2.44a) and the expressions for the rates of change of the unit vectors given in (2.39), or (2.44b) and the expression for $\boldsymbol{\Omega}_{flow}$ given in (2.38), (2.44) becomes

$$\frac{\mathrm{D}\boldsymbol{v}}{\mathrm{D}t} = \mathbf{i}\left(\frac{\mathrm{D}u}{\mathrm{D}t} - \frac{uv\tan\vartheta}{r} + \frac{uw}{r}\right) + \mathbf{j}\left(\frac{\mathrm{D}v}{\mathrm{D}t} + \frac{u^2\tan\vartheta}{r} + \frac{vw}{r}\right) + \mathbf{k}\left(\frac{\mathrm{D}w}{\mathrm{D}t} - \frac{u^2+v^2}{r}\right). \tag{2.45}$$

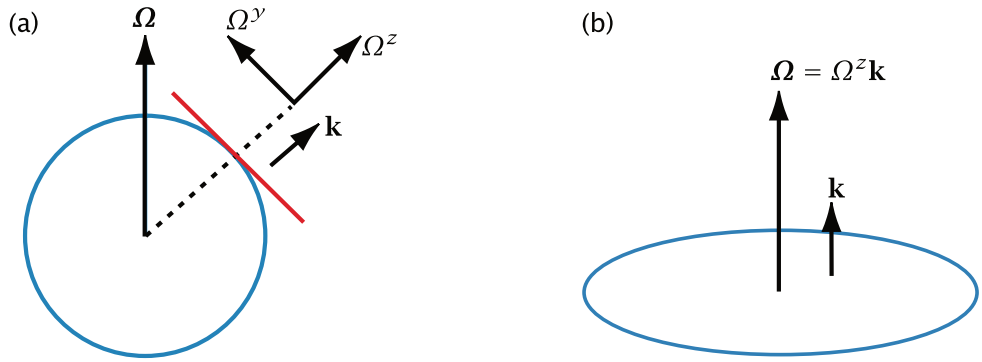

Fig. 2.4 (a) On the sphere the rotation vector $\boldsymbol{\Omega}$ can be decomposed into two components, one in the local vertical and one in the local horizontal, pointing toward the pole. That is, $\boldsymbol{\Omega} = \Omega_y \mathbf{j} + \Omega_z \mathbf{k}$ where $\Omega_y = \Omega \cos\vartheta$ and $\Omega_z = \Omega \sin\vartheta$. In geophysical fluid dynamics, the rotation vector in the local vertical is often the more important component in the horizontal momentum equations. On a rotating disk, (b), the rotation vector $\boldsymbol{\Omega}$ is parallel to the local vertical $\mathbf{k}$.

Using the definition of a vector cross product the Coriolis term is:

$$2\boldsymbol{\Omega} \times \boldsymbol{v} = \begin{vmatrix} \mathbf{i} & \mathbf{j} & \mathbf{k} \\ 0 & 2\Omega\cos\vartheta & 2\Omega\sin\vartheta \\ u & v & w \end{vmatrix}$$
$$= \mathbf{i}\,(2\Omega w\cos\vartheta - 2\Omega v\sin\vartheta) + \mathbf{j}\,2\Omega u\sin\vartheta - \mathbf{k}\,2\Omega u\cos\vartheta. \tag{2.46}$$

Using (2.45) and (2.46), and the gradient operator given by (2.31), the momentum equation (2.43) becomes:

$$\frac{\mathrm{D}u}{\mathrm{D}t} - \left(2\Omega + \frac{u}{r\cos\vartheta}\right)(v\sin\vartheta - w\cos\vartheta) = -\frac{1}{\rho r\cos\vartheta}\frac{\partial p}{\partial\lambda}, \tag{2.47a}$$

$$\frac{\mathrm{D}v}{\mathrm{D}t} + \frac{wv}{r} + \left(2\Omega + \frac{u}{r\cos\vartheta}\right)u\sin\vartheta = -\frac{1}{\rho r}\frac{\partial p}{\partial\vartheta}, \tag{2.47b}$$

$$\frac{\mathrm{D}w}{\mathrm{D}t} - \frac{u^2+v^2}{r} - 2\Omega u\cos\vartheta = -\frac{1}{\rho}\frac{\partial p}{\partial r} - g. \tag{2.47c}$$

The terms involving Ω are called Coriolis terms, and the quadratic terms on the left-hand sides involving $1/r$ are often called metric terms.

2.2.4 The Primitive Equations

The so-called *primitive equations* of motion are simplifications of the above equations frequently used in atmospheric and oceanic modelling.[5] Three related approximations are involved:

(*i*) *The hydrostatic approximation.* In the vertical momentum equation the gravitational term is assumed to be balanced by the pressure gradient term, so that

$$\frac{\partial p}{\partial z} = -\rho g. \tag{2.48}$$

The advection of vertical velocity, the Coriolis terms, and the metric term $(u^2 + v^2)/r$ are all neglected.

(ii) *The shallow-fluid approximation.* We write $r = a + z$ where the constant a is the radius of the Earth and z increases in the radial direction. The coordinate r is then replaced by a except where it is used as the differentiating argument. Thus, for example,

$$\frac{1}{r^2}\frac{\partial(r^2 w)}{\partial r} \to \frac{\partial w}{\partial z}. \tag{2.49}$$

(iii) *The traditional approximation.* Coriolis terms in the horizontal momentum equations involving the vertical velocity, and the still smaller metric terms uw/r and vw/r, are neglected.

The second and third of these approximations should be taken, or not, together, the underlying reason being that they both relate to the presumed small aspect ratio of the motion, so the approximations succeed or fail together. If we make one approximation but not the other then we are being asymptotically inconsistent, and angular momentum and energy conservation are not assured.[6] The hydrostatic approximation also depends on the small aspect ratio of the flow, but in a slightly different way. For large-scale flow in the terrestrial atmosphere and ocean all three approximations are in fact very accurate approximations. We defer a more complete treatment until Section 2.7, in part because a treatment of the hydrostatic approximation is done most easily in the context of the Boussinesq equations, derived in Section 2.4.

Making these approximations, the momentum equations for a shallow layer are

$$\frac{\mathrm{D}u}{\mathrm{D}t} - 2\Omega\sin\vartheta v - \frac{uv}{a}\tan\vartheta = -\frac{1}{a\rho\cos\vartheta}\frac{\partial p}{\partial\lambda}, \tag{2.50a}$$

$$\frac{\mathrm{D}v}{\mathrm{D}t} + 2\Omega\sin\vartheta u + \frac{u^2\tan\vartheta}{a} = -\frac{1}{\rho a}\frac{\partial p}{\partial\vartheta}, \tag{2.50b}$$

$$0 = -\frac{1}{\rho}\frac{\partial p}{\partial z} - g, \tag{2.50c}$$

where

$$\frac{\mathrm{D}}{\mathrm{D}t} = \left(\frac{\partial}{\partial t} + \frac{u}{a\cos\vartheta}\frac{\partial}{\partial\lambda} + \frac{v}{a}\frac{\partial}{\partial\vartheta} + w\frac{\partial}{\partial z}\right). \tag{2.51}$$

We note the ubiquity of the factor $2\Omega\sin\vartheta$, and take the opportunity to define the *Coriolis parameter*, $f \equiv 2\Omega\sin\vartheta$. The associated mass conservation equation for a shallow fluid layer is:

$$\frac{\partial\rho}{\partial t} + \frac{u}{a\cos\vartheta}\frac{\partial\rho}{\partial\lambda} + \frac{v}{a}\frac{\partial\rho}{\partial\vartheta} + w\frac{\partial\rho}{\partial z} + \rho\left[\frac{1}{a\cos\vartheta}\frac{\partial u}{\partial\lambda} + \frac{1}{a\cos\vartheta}\frac{\partial}{\partial\vartheta}(v\cos\vartheta) + \frac{\partial w}{\partial z}\right] = 0, \tag{2.52}$$

or equivalently,

$$\frac{\partial\rho}{\partial t} + \frac{1}{a\cos\vartheta}\frac{\partial(u\rho)}{\partial\lambda} + \frac{1}{a\cos\vartheta}\frac{\partial}{\partial\vartheta}(v\rho\cos\vartheta) + \frac{\partial(w\rho)}{\partial z} = 0. \tag{2.53}$$

2.2.5 Primitive Equations in Vector Form

The primitive equations on a sphere may be written in a compact vector form provided we make a slight reinterpretation of the material derivative of the coordinate axes. Instead of (2.39) we take the material derivative of the unit vectors to be

$$\frac{\mathrm{D}\mathbf{i}}{\mathrm{D}t} = \tilde{\boldsymbol{\Omega}}_{flow}\times\mathbf{i} = \mathbf{j}\frac{u\tan\vartheta}{a}, \tag{2.54a}$$

$$\frac{\mathrm{D}\mathbf{j}}{\mathrm{D}t} = \tilde{\boldsymbol{\Omega}}_{flow}\times\mathbf{j} = -\mathbf{i}\frac{u\tan\vartheta}{a}, \tag{2.54b}$$

where $\widetilde{\boldsymbol{\Omega}}_{flow} = \mathbf{k}u\tan\vartheta/a$, which is the vertical component of (2.38) with r replaced by a. Given (2.54), the primitive equations (2.50a) and (2.50b) may be written as

$$\frac{\mathrm{D}\boldsymbol{u}}{\mathrm{D}t} + \boldsymbol{f}\times\boldsymbol{u} = -\frac{1}{\rho}\nabla_z p, \tag{2.55}$$

where $\boldsymbol{u} = u\mathbf{i} + v\mathbf{j} + 0\,\mathbf{k}$ is the horizontal velocity, $\nabla_z p = [(a\cos\vartheta)^{-1}\partial p/\partial\lambda,\ a^{-1}\partial p/\partial\vartheta]$ is the gradient operator at constant z, and $\boldsymbol{f} = f\mathbf{k} = 2\Omega\sin\vartheta\mathbf{k}$. In (2.55) the material derivative of the horizontal velocity is given by

$$\frac{\mathrm{D}\boldsymbol{u}}{\mathrm{D}t} = \mathbf{i}\frac{\mathrm{D}u}{\mathrm{D}t} + \mathbf{j}\frac{\mathrm{D}v}{\mathrm{D}t} + u\frac{\mathrm{D}\mathbf{i}}{\mathrm{D}t} + v\frac{\mathrm{D}\mathbf{j}}{\mathrm{D}t}. \tag{2.56}$$

The advection of the horizontal wind $\boldsymbol{u}$ is still by the three-dimensional velocity $\boldsymbol{v}$.

The vertical momentum equation is the hydrostatic equation, (2.50c), and the mass conservation equation is

$$\frac{\mathrm{D}\rho}{\mathrm{D}t} + \rho\nabla\cdot\boldsymbol{v} = 0 \qquad \text{or} \qquad \frac{\partial\rho}{\partial t} + \nabla\cdot(\rho\boldsymbol{v}) = 0, \tag{2.57}$$

where $\mathrm{D}/\mathrm{D}t$ is given by (2.51), and the second expression is written out in full in (2.53).

2.2.6 The Vector Invariant Form of the Momentum Equation

The 'vector invariant' form of the momentum equation is so-called because it appears to take the same form in all coordinate systems — there is no advective derivative of the coordinate system to worry about. With the aid of the identity $(\boldsymbol{v}\cdot\nabla)\boldsymbol{v} = -\boldsymbol{v}\times\boldsymbol{\omega} + \nabla(\boldsymbol{v}^2/2)$, where $\boldsymbol{\omega} \equiv \nabla\times\boldsymbol{v}$ is the relative vorticity (which we explore at greater length in Chapter 4) the three-dimensional momentum equation, (2.16), may be written:

$$\frac{\partial\boldsymbol{v}}{\partial t} + (2\boldsymbol{\Omega} + \boldsymbol{\omega})\times\boldsymbol{v} = -\frac{1}{\rho}\nabla p - \frac{1}{2}\nabla\boldsymbol{v}^2 + \boldsymbol{g}, \tag{2.58}$$

and this is the vector invariant momentum equation. In spherical coordinates the relative vorticity is given by:

$$\begin{aligned}\boldsymbol{\omega} = \nabla\times\boldsymbol{v} &= \frac{1}{r^2\cos\vartheta}\begin{vmatrix} \mathbf{i}\,r\cos\vartheta & \mathbf{j}\,r & \mathbf{k} \\ \partial/\partial\lambda & \partial/\partial\vartheta & \partial/\partial r \\ ur\cos\vartheta & rv & w \end{vmatrix} \\ &= \mathbf{i}\,\frac{1}{r}\left(\frac{\partial w}{\partial\vartheta} - \frac{\partial(rv)}{\partial r}\right) - \mathbf{j}\,\frac{1}{r\cos\vartheta}\left(\frac{\partial w}{\partial\lambda} - \frac{\partial}{\partial r}(ur\cos\vartheta)\right) + \mathbf{k}\,\frac{1}{r\cos\vartheta}\left(\frac{\partial v}{\partial\lambda} - \frac{\partial}{\partial\vartheta}(u\cos\vartheta)\right).\end{aligned} \tag{2.59}$$

We can write the horizontal momentum equations of the primitive equations in a similar way. Making the traditional and shallow fluid approximations, the horizontal components of (2.58) become

$$\frac{\partial\boldsymbol{u}}{\partial t} + (\boldsymbol{f} + \mathbf{k}\zeta)\times\boldsymbol{u} + w\frac{\partial\boldsymbol{u}}{\partial z} = -\frac{1}{\rho}\nabla_z p - \frac{1}{2}\nabla\boldsymbol{u}^2, \tag{2.60}$$

where $\boldsymbol{u} = (u, v, 0)$, $\boldsymbol{f} = \mathbf{k}\,2\Omega\sin\vartheta$ and ∇_z is the horizontal gradient operator (the gradient at a constant value of z). Using (2.59), ζ is given by

$$\zeta = \frac{1}{a\cos\vartheta}\frac{\partial v}{\partial\lambda} - \frac{1}{a\cos\vartheta}\frac{\partial}{\partial\vartheta}(u\cos\vartheta) = \frac{1}{a\cos\vartheta}\frac{\partial v}{\partial\lambda} - \frac{1}{a}\frac{\partial u}{\partial\vartheta} + \frac{u}{a}\tan\vartheta. \tag{2.61}$$

The separate components of the momentum equation are given by:

$$\frac{\partial u}{\partial t} - (f+\zeta)v + w\frac{\partial u}{\partial z} = -\frac{1}{a\cos\vartheta}\left(\frac{1}{\rho}\frac{\partial p}{\partial\lambda} + \frac{1}{2}\frac{\partial\boldsymbol{u}^2}{\partial\lambda}\right), \tag{2.62}$$

and

$$\frac{\partial v}{\partial t} + (f + \zeta)u + w\frac{\partial v}{\partial z} = -\frac{1}{a}\left(\frac{1}{\rho}\frac{\partial p}{\partial \vartheta} + \frac{1}{2}\frac{\partial \boldsymbol{u}^2}{\partial \vartheta}\right). \tag{2.63}$$

2.2.7 Angular Momentum

The zonal momentum equation can be usefully expressed as a statement about axial angular momentum; that is, angular momentum about the rotation axis. The zonal angular momentum per unit mass is the component of angular momentum in the direction of the axis of rotation and it is given by, without making any shallow atmosphere approximation,

$$m = (u + \Omega r\cos\vartheta)r\cos\vartheta. \tag{2.64}$$

The evolution equation for this quantity follows from the zonal momentum equation and has the simple form

$$\frac{\mathrm{D}m}{\mathrm{D}t} = -\frac{1}{\rho}\frac{\partial p}{\partial \lambda}, \tag{2.65}$$

where the material derivative is

$$\frac{\mathrm{D}}{\mathrm{D}t} = \frac{\partial}{\partial t} + \frac{u}{r\cos\vartheta}\frac{\partial}{\partial \lambda} + \frac{v}{r}\frac{\partial}{\partial \vartheta} + w\frac{\partial}{\partial r}. \tag{2.66}$$

Using the mass continuity equation, (2.65) can be written as

$$\frac{\mathrm{D}\rho m}{\mathrm{D}t} + \rho m\nabla\cdot\boldsymbol{v} = -\frac{\partial p}{\partial \lambda} \tag{2.67}$$

or

$$\frac{\partial \rho m}{\partial t} + \frac{1}{r\cos\vartheta}\frac{\partial(\rho u m)}{\partial \lambda} + \frac{1}{r\cos\vartheta}\frac{\partial}{\partial \vartheta}(\rho v m\cos\vartheta) + \frac{1}{r^2}\frac{\partial}{\partial r}(\rho m w r^2) = -\frac{\partial p}{\partial \lambda}. \tag{2.68}$$

This is an angular momentum conservation equation.

If the fluid is confined to a shallow layer near the surface of a sphere, then we may replace r, the radial coordinate, by a, the radius of the sphere, in the definition of m, and we define $\widetilde{m} \equiv (u + \Omega a\cos\vartheta)a\cos\vartheta$. Then (2.65) is replaced by

$$\frac{\mathrm{D}\widetilde{m}}{\mathrm{D}t} = -\frac{1}{\rho}\frac{\partial p}{\partial \lambda}, \tag{2.69}$$

where now

$$\frac{\mathrm{D}}{\mathrm{D}t} = \frac{\partial}{\partial t} + \frac{u}{a\cos\vartheta}\frac{\partial}{\partial \lambda} + \frac{v}{a}\frac{\partial}{\partial \vartheta} + w\frac{\partial}{\partial z}. \tag{2.70}$$

In the shallow fluid approximation (2.68) becomes

$$\frac{\partial \rho m}{\partial t} + \frac{1}{a\cos\vartheta}\frac{\partial(\rho u m)}{\partial \lambda} + \frac{1}{a\cos\vartheta}\frac{\partial}{\partial \vartheta}(\rho v m\cos\vartheta) + \frac{\partial}{\partial z}(\rho m w) = -\frac{\partial p}{\partial \lambda}, \tag{2.71}$$

which is an angular momentum conservation equation for a shallow atmosphere.

✦ *From angular momentum to the spherical component equations*

An alternative way of deriving the three components of the momentum equation in spherical polar coordinates is to *begin* with (2.65) and the principle of conservation of energy. That is, we take the equations for conservation of angular momentum and energy as true a priori and demand that the forms of the momentum equation be constructed to satisfy these. Expanding the material

derivative in (2.65), noting that $\mathrm{D}r/\mathrm{D}t = w$ and $\mathrm{D}\cos\vartheta/\mathrm{D}t = -(v/r)\sin\vartheta$, immediately gives (2.47a). Multiplication by u then yields

$$u\frac{\mathrm{D}u}{\mathrm{D}t} - 2\Omega uv\sin\vartheta + 2\Omega uw\cos\vartheta - \frac{u^2v\tan\vartheta}{r} + \frac{u^2w}{r} = -\frac{u}{\rho r\cos\vartheta}\frac{\partial p}{\partial\lambda}. \tag{2.72}$$

Now suppose that the meridional and vertical momentum equations are of the form

$$\frac{\mathrm{D}v}{\mathrm{D}t} + \text{Coriolis and metric terms} = -\frac{1}{\rho r}\frac{\partial p}{\partial\vartheta}, \tag{2.73a}$$

$$\frac{\mathrm{D}w}{\mathrm{D}t} + \text{Coriolis and metric terms} = -\frac{1}{\rho}\frac{\partial p}{\partial r}, \tag{2.73b}$$

but that we do not know what form the Coriolis and metric terms take. To determine that form, construct the kinetic energy equation by multiplying (2.73) by v and w, respectively. Now, the metric terms must vanish when we sum the resulting equations along with (2.72), so that (2.73a) must contain the Coriolis term $2\Omega u\sin\vartheta$ as well as the metric term $u^2\tan\vartheta/r$, and (2.73b) must contain the term $-2\Omega u\cos\phi$ as well as the metric term u^2/r. But if (2.73b) contains the term u^2/r it must also contain the term v^2/r by isotropy, and therefore (2.73a) must also contain the term vw/r. In this way, (2.47) is precisely reproduced, although the sceptic might argue that the uniqueness of the form has not been demonstrated.

A particular advantage of this approach arises in determining the appropriate momentum equations that conserve angular momentum and energy in the shallow-fluid approximation. We begin with (2.69) and expand to obtain (2.50a). Multiplying by u gives

$$u\frac{\mathrm{D}u}{\mathrm{D}t} - 2\Omega uv\sin\vartheta - \frac{u^2v\tan\vartheta}{a} = -\frac{u}{\rho a\cos\vartheta}\frac{\partial p}{\partial\lambda}. \tag{2.74}$$

To ensure energy conservation, the meridional momentum equation must contain the Coriolis term $2\Omega u\sin\vartheta$ and the metric term $u^2\tan\vartheta/a$, but the vertical momentum equation must have neither of the metric terms appearing in (2.47c). Thus we deduce the following equations:

$$\frac{\mathrm{D}u}{\mathrm{D}t} - \left(2\Omega\sin\vartheta + \frac{u\tan\vartheta}{a}\right)v = -\frac{1}{\rho a\cos\vartheta}\frac{\partial p}{\partial\lambda}, \tag{2.75a}$$

$$\frac{\mathrm{D}v}{\mathrm{D}t} + \left(2\Omega\sin\vartheta + \frac{u\tan\vartheta}{a}\right)u = -\frac{1}{\rho a}\frac{\partial p}{\partial\vartheta}, \tag{2.75b}$$

$$\frac{\mathrm{D}w}{\mathrm{D}t} = -\frac{1}{\rho}\frac{\partial\rho}{\partial r} - g. \tag{2.75c}$$

This equation set, when used in conjunction with the thermodynamic and mass continuity equations, conserves appropriate forms of angular momentum and energy. In the hydrostatic approximation the material derivative of w in (2.75c) is *additionally* neglected. Thus, the hydrostatic approximation is mathematically and physically consistent with the shallow-fluid approximation, but it is an additional approximation with slightly different requirements that one may choose, rather than being required, to make. From an asymptotic perspective, the difference lies in the small parameter necessary for either approximation to hold, namely:

$$\text{shallow fluid and traditional approximations:} \qquad \gamma \equiv \frac{H}{a} \ll 1, \tag{2.76a}$$

$$\text{small aspect ratio for hydrostatic approximation:} \qquad \alpha \equiv \frac{H}{L} \ll 1, \tag{2.76b}$$

where L is the horizontal scale of the motion and a is the radius of the Earth. For hemispheric or global scale phenomena $L \sim a$ and the two approximations coincide. (Requirement (2.76b) for the hydrostatic approximation will be derived in Section 2.7.)

Since all models are wrong the scientist cannot obtain a 'correct' one by excessive elaboration … he should seek an economical description of natural phenomena.
George E. Box, *Science and Statistics*, 1976.

The sciences do not try to explain … they mainly make models … a mathematical construct the justification [of which] is that it is expected to work.
John von Neumann, *Methods in the Physical Sciences*, 1955.

CHAPTER 3

Shallow Water Systems

CONVENTIONALLY, 'THE' SHALLOW WATER EQUATIONS describe a thin layer of constant density fluid in hydrostatic balance, rotating or not, bounded from below by a rigid surface and from above by a free surface, above which we suppose is another fluid of negligible inertia. Such a configuration can be generalized to multiple layers of immiscible fluids of different densities lying one on top of another, forming a stably-stratified 'stacked shallow water' system, which in many ways behaves like a continuously stratified fluid. These types of systems are the main subject of this chapter. We also introduce the notion of available potential energy, which involves thinking about a continuously stratified system as if it were a stacked shallow water system.

The single-layer model is one of the simplest useful models in geophysical fluid dynamics because it allows for a consideration of the effects of rotation in a simple framework without the complicating effects of stratification. A model with just two layers is not only a simple model of a stratified fluid, it is a surprisingly good model of many phenomena in the ocean and atmosphere. Such models are more than just pedagogical tools — we will find that there is a close physical and mathematical analogy between the shallow water equations and a description of the continuously stratified ocean or atmosphere written in isopycnal or isentropic coordinates, with a meaning beyond a coincidental similarity in the equations. Let us begin with the single-layer case.

3.1 DYNAMICS OF A SINGLE SHALLOW LAYER OF FLUID

Shallow water dynamics apply, by definition, to a fluid layer of constant density in which the horizontal scale of the flow is much greater than the layer depth. The fluid motion is fully determined by the momentum and mass continuity equations, and because of the assumed small aspect ratio the hydrostatic approximation is well satisfied, and we invoke this from the outset. Consider, then, fluid in a container above which is another fluid of negligible density (and therefore negligible inertia) relative to the fluid of interest, as illustrated in Fig. 3.1. Our notation is that $\boldsymbol{v} = u\mathbf{i} + v\mathbf{j} + w\mathbf{k}$ is the three-dimensional velocity and $\boldsymbol{u} = u\mathbf{i} + v\mathbf{j}$ is the horizontal velocity. $h(x, y)$ is the thickness of the liquid column, H is its mean height, and η is the height of the free surface. In a flat-bottomed container $\eta = h$, whereas in general $h = \eta - \eta_b$, where η_b is the height of the floor of the container.

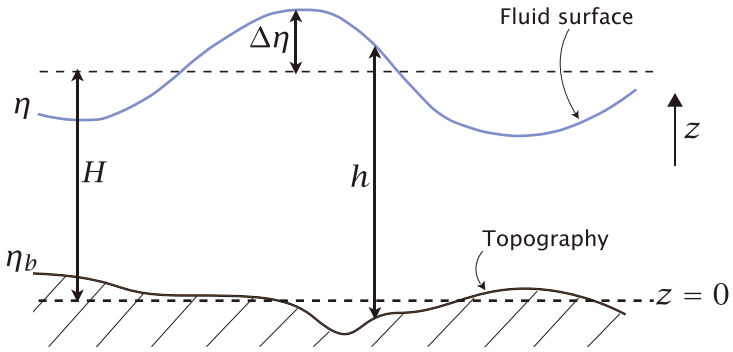

Fig. 3.1 A shallow water system. h is the thickness of a water column, H its mean thickness, η the height of the free surface and η_b is the height of the lower, rigid, surface above some arbitrary origin, typically chosen such that the average of η_b is zero. $\Delta\eta$ is the deviation free surface height, so we have $\eta = \eta_b + h = H + \Delta\eta$.

3.1.1 Momentum Equations

The vertical momentum equation is just the hydrostatic equation,

$$\frac{\partial p}{\partial z} = -\rho_0 g, \tag{3.1}$$

and, because density is assumed constant, we may integrate this to

$$p(x, y, z, t) = -\rho_0 g z + p_o. \tag{3.2}$$

At the top of the fluid, $z = \eta$, the pressure is determined by the weight of the overlying fluid and this is assumed to be negligible. Thus, $p = 0$ at $z = \eta$, giving

$$p(x, y, z, t) = \rho_0 g(\eta(x, y, t) - z). \tag{3.3}$$

The consequence of this is that the horizontal gradient of pressure is independent of height. That is

$$\nabla_z p = \rho_0 g \nabla_z \eta, \tag{3.4}$$

where

$$\nabla_z = \mathbf{i}\frac{\partial}{\partial x} + \mathbf{j}\frac{\partial}{\partial y} \tag{3.5}$$

is the gradient operator at constant z. (In the rest of this chapter we will drop the subscript z unless that causes ambiguity. The three-dimensional gradient operator will be denoted by ∇_3. We will also mostly use Cartesian coordinates, but the shallow water equations may certainly be applied over a spherical planet — 'Laplace's tidal equations' are essentially the shallow water equations on a sphere.) The horizontal momentum equations therefore become

$$\frac{\mathrm{D}\boldsymbol{u}}{\mathrm{D}t} = -\frac{1}{\rho_0}\nabla p = -g\nabla\eta. \tag{3.6}$$

The right-hand side of this equation is independent of the vertical coordinate z. Thus, if the flow is initially independent of z, it must stay so. (This z-independence is unrelated to that arising from the rapid rotation necessary for the Taylor–Proudman effect.) The velocities u and v are functions of x, y and t only, and the horizontal momentum equation is therefore

$$\frac{\mathrm{D}\boldsymbol{u}}{\mathrm{D}t} = \frac{\partial \boldsymbol{u}}{\partial t} + u\frac{\partial \boldsymbol{u}}{\partial x} + v\frac{\partial \boldsymbol{u}}{\partial y} = -g\nabla\eta. \tag{3.7}$$

That the horizontal velocity is independent of z is a consequence of the hydrostatic equation, which ensures that the horizontal pressure gradient is independent of height. (Another starting point

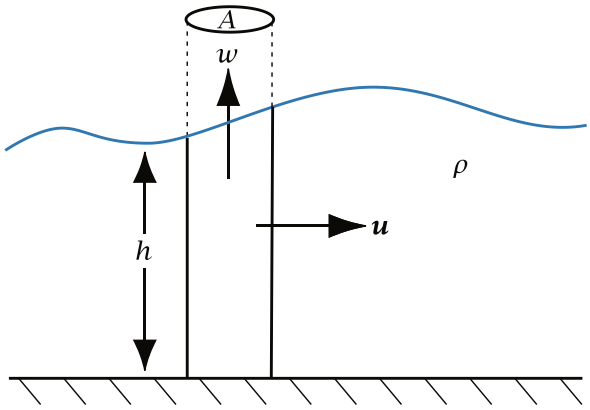

Fig. 3.2 The mass budget for a column of area A in a shallow water system. The fluid leaving the column is $\oint \rho_0 h\boldsymbol{u} \cdot \boldsymbol{n}\,\mathrm{d}l$ where $\boldsymbol{n}$ is the unit vector normal to the boundary of the fluid column. There is a non-zero vertical velocity at the top of the column if the mass convergence into the column is non-zero.

would be to take this independence of the horizontal motion with height as the *definition* of shallow water flow. In real physical situations such independence does not hold exactly — for example, friction at the bottom may induce a vertical dependence of the flow in a boundary layer.) In the presence of rotation, (3.7) easily generalizes to

$$\frac{\mathrm{D}\boldsymbol{u}}{\mathrm{D}t} + \boldsymbol{f} \times \boldsymbol{u} = -g\nabla\eta, \tag{3.8}$$

where $\boldsymbol{f} = f\mathbf{k}$. Just as with the primitive equations, f may be constant or may vary with latitude, so that on a spherical planet $f = 2\Omega \sin\vartheta$ and on the β-plane $f = f_0 + \beta y$.

3.1.2 Mass Continuity Equation

From first principles

The mass contained in a fluid column of height h and cross-sectional area A is given by $\int_A \rho_0 h\,\mathrm{d}\boldsymbol{A}$ (see Fig. 3.2). If there is a net flux of fluid across the column boundary (by advection) then this must be balanced by a net increase in the mass in A, and therefore a net increase in the height of the water column. The mass convergence into the column is given by

$$F_m = \text{mass flux in} = -\int_S \rho_0 \boldsymbol{u} \cdot \mathrm{d}\boldsymbol{S}, \tag{3.9}$$

where S is the area of the vertical boundary of the column. The surface area of the column is composed of elements of area $h\boldsymbol{n}\,\delta l$, where δl is a line element circumscribing the column and $\boldsymbol{n}$ is a unit vector perpendicular to the boundary, pointing outwards. Thus (3.9) becomes

$$F_m = -\oint \rho_0 h\boldsymbol{u} \cdot \boldsymbol{n}\,\mathrm{d}l. \tag{3.10}$$

Using the divergence theorem in two dimensions, (3.10) simplifies to

$$F_m = -\int_A \nabla \cdot (\rho_0 \boldsymbol{u} h)\,\mathrm{d}A, \tag{3.11}$$

where the integral is over the cross-sectional area of the fluid column (looking down from above). This is balanced by the local increase in height of the water column, given by

$$F_m = \frac{\mathrm{d}}{\mathrm{d}t}\int \rho_0\,\mathrm{d}V = \frac{\mathrm{d}}{\mathrm{d}t}\int_A \rho_0 h\,\mathrm{d}A = \int_A \rho_0 \frac{\partial h}{\partial t}\,\mathrm{d}A. \tag{3.12}$$

Because ρ_0 is constant, the balance between (3.11) and (3.12) leads to

$$\int_A \left[\frac{\partial h}{\partial t} + \nabla \cdot (\boldsymbol{u}h) \right] \mathrm{d}A = 0, \tag{3.13}$$

and because the area is arbitrary the integrand itself must vanish, whence,

$$\frac{\partial h}{\partial t} + \nabla \cdot (\boldsymbol{u}h) = 0 \qquad \text{or} \qquad \frac{\mathrm{D}h}{\mathrm{D}t} + h\nabla \cdot \boldsymbol{u} = 0. \tag{3.14a,b}$$

This derivation holds whether or not the lower surface is flat. If it is, then $h = \eta$, and if not $h = \eta - \eta_b$. Equations (3.8) and (3.14) form a complete set, summarized in the shaded box on page 109.

From the 3D mass conservation equation

Since the fluid is incompressible, the three-dimensional mass continuity equation is just $\nabla \cdot \boldsymbol{v} = 0$. Writing this out in component form

$$\frac{\partial w}{\partial z} = -\left(\frac{\partial u}{\partial x} + \frac{\partial v}{\partial y} \right) = -\nabla \cdot \boldsymbol{u}. \tag{3.15}$$

Integrate this from the bottom of the fluid ($z = \eta_b$) to the top ($z = \eta$), noting that the right-hand side is independent of z, to give

$$w(\eta) - w(\eta_b) = -h\nabla \cdot \boldsymbol{u}. \tag{3.16}$$

At the top the vertical velocity is the material derivative of the position of a particular fluid element. But the position of the fluid at the top is just η, and therefore (see Fig. 3.2)

$$w(\eta) = \frac{\mathrm{D}\eta}{\mathrm{D}t}. \tag{3.17a}$$

At the bottom of the fluid we have similarly

$$w(\eta_b) = \frac{\mathrm{D}\eta_b}{\mathrm{D}t}, \tag{3.17b}$$

where, apart from earthquakes and the like, $\partial\eta_b/\partial t = 0$. Using (3.17a,b), (3.16) becomes

$$\frac{\mathrm{D}}{\mathrm{D}t}(\eta - \eta_b) + h\nabla \cdot \boldsymbol{u} = 0 \tag{3.18}$$

or, as in (3.14b),

$$\frac{\mathrm{D}h}{\mathrm{D}t} + h\nabla \cdot \boldsymbol{u} = 0. \tag{3.19}$$

3.1.3 A Rigid Lid

The case where the *upper* surface is held flat by the imposition of a rigid lid is sometimes of interest. The ocean suggests one such example, since the bathymetry at the bottom of the ocean provides much larger variations in fluid thickness than do the small variations in the height of the ocean surface. If we suppose that the upper surface is at a constant height H, then from (3.14a) with $\partial h/\partial t = 0$ the mass conservation equation is

$$\nabla_h \cdot (\boldsymbol{u}h_b) = 0, \tag{3.20}$$

The Shallow Water Equations

For a single-layer fluid, and including the Coriolis term, the inviscid shallow water equations are

$$\text{momentum:} \quad \frac{\mathrm{D}\boldsymbol{u}}{\mathrm{D}t} + \boldsymbol{f} \times \boldsymbol{u} = -g\nabla\eta. \tag{SW.1}$$

$$\text{mass continuity:} \quad \frac{\mathrm{D}h}{\mathrm{D}t} + h\nabla \cdot \boldsymbol{u} = 0 \quad \text{or} \quad \frac{\partial h}{\partial t} + \nabla \cdot (h\boldsymbol{u}) = 0, \tag{SW.2}$$

where $\boldsymbol{u}$ is the horizontal velocity, h is the total fluid thickness, η is the height of the upper free surface and η_b is the height of the lower surface (the bottom topography). Thus,

$$h(x, y, t) = \eta(x, y, t) - \eta_b(x, y) \tag{SW.3}$$

The material derivative is

$$\frac{\mathrm{D}}{\mathrm{D}t} = \frac{\partial}{\partial t} + \boldsymbol{u} \cdot \nabla = \frac{\partial}{\partial t} + u\frac{\partial}{\partial x} + v\frac{\partial}{\partial y}, \tag{SW.4}$$

with the rightmost expression holding in Cartesian coordinates.

where $h_b = H - \eta_b$. Note that (3.20) allows us to define an incompressible *mass-transport velocity,* $\boldsymbol{U} \equiv h_b\boldsymbol{u}$.

Although the upper surface is flat, the pressure there is no longer constant because a force must be provided by the rigid lid to keep the surface flat. The horizontal momentum equation is

$$\frac{\mathrm{D}\boldsymbol{u}}{\mathrm{D}t} = -\frac{1}{\rho_0}\nabla p_{lid}, \tag{3.21}$$

where p_{lid} is the pressure at the lid, and the complete equations of motion are then (3.20) and (3.21).[7] If the lower surface is flat, the two-dimensional flow itself is divergence-free, and the equations reduce to the two-dimensional incompressible Euler equations.

3.1.4 Stretching and the Vertical Velocity

Because the horizontal velocity is depth independent, the vertical velocity plays no role in advection. However, w is certainly not zero for then the free surface would be unable to move up or down, but because of the vertical independence of the horizontal flow w does have a simple vertical structure; to determine this we write the mass conservation equation as

$$\frac{\partial w}{\partial z} = -\nabla \cdot \boldsymbol{u}, \tag{3.22}$$

and integrate upwards from the bottom to give

$$w = w_b - (\nabla \cdot \boldsymbol{u})(z - \eta_b). \tag{3.23}$$

Thus, the vertical velocity is a linear function of height. Equation (3.23) can be written as

$$\frac{\mathrm{D}z}{\mathrm{D}t} = \frac{\mathrm{D}\eta_b}{\mathrm{D}t} - (\nabla \cdot \boldsymbol{u})(z - \eta_b), \tag{3.24}$$

and at the upper surface $w = \mathrm{D}\eta/\mathrm{D}t$ so that here we have

$$\frac{\mathrm{D}\eta}{\mathrm{D}t} = \frac{\mathrm{D}\eta_b}{\mathrm{D}t} - (\nabla \cdot \boldsymbol{u})(\eta - \eta_b). \tag{3.25}$$

Eliminating the divergence term from the last two equations gives

$$\frac{\mathrm{D}}{\mathrm{D}t}(z - \eta_b) = \frac{z - \eta_b}{\eta - \eta_b}\frac{\mathrm{D}}{\mathrm{D}t}(\eta - \eta_b), \tag{3.26}$$

which in turn gives

$$\frac{\mathrm{D}}{\mathrm{D}t}\left(\frac{z - \eta_b}{\eta - \eta_b}\right) = \frac{\mathrm{D}}{\mathrm{D}t}\left(\frac{z - \eta_b}{h}\right) = 0. \tag{3.27}$$

This means that the ratio of the height of a fluid parcel above the floor to the total depth of the column is fixed; that is, the fluid stretches uniformly in a column, and this is a kinematic property of the shallow water system.

3.1.5 Analogy with Compressible Flow

The shallow water equations (3.8) and (3.14) are analogous to the compressible gas dynamic equations in two dimensions, namely

$$\frac{\mathrm{D}\boldsymbol{u}}{\mathrm{D}t} = -\frac{1}{\rho}\nabla p \tag{3.28}$$

and

$$\frac{\partial \rho}{\partial t} + \nabla \cdot (\boldsymbol{u}\rho) = 0, \tag{3.29}$$

along with an equation of state which we take to be $p = f(\rho)$. The mass conservation equations (3.14) and (3.29) are identical, with the replacement $\rho \leftrightarrow h$. If $p = C\rho^\gamma$, then (3.28) becomes

$$\frac{\mathrm{D}\boldsymbol{u}}{\mathrm{D}t} = -\frac{1}{\rho}\frac{\mathrm{d}p}{\mathrm{d}\rho}\nabla\rho = -C\gamma\rho^{\gamma-2}\nabla\rho. \tag{3.30}$$

If $\gamma = 2$ then the momentum equations (3.8) and (3.30) become equivalent, with $\rho \leftrightarrow h$ and $C\gamma \leftrightarrow g$. In an ideal gas $\gamma = c_p/c_v$ and values typically are in fact less than 2 (in air $\gamma \approx 7/5$); however, if the equations are linearized, then the analogy is exact for all values of γ, for then (3.30) becomes $\partial \boldsymbol{v}'/\partial t = -\rho_0^{-1}c_s^2\nabla\rho'$ where $c_s^2 = \mathrm{d}p/\mathrm{d}\rho$, and the linearized shallow water momentum equation is $\partial \boldsymbol{u}'/\partial t = -H^{-1}(gH)\nabla h'$, so that $\rho_0 \leftrightarrow H$ and $c_s^2 \leftrightarrow gH$. The sound waves of a compressible fluid are then analogous to shallow water waves, which are considered in Section 3.8.

A little inaccuracy sometimes saves a ton of explanation.
H. M. Munro (Saki), *The Square Egg,* 1924.

Every decoding is another encoding.
David Lodge, in the voice of Morris Zapp, *Small World,* 1984.

CHAPTER 4

Geostrophic Theory

LARGE-SCALE FLOW IN THE OCEAN AND THE ATMOSPHERE is characterized by an approximate balance in the vertical direction between the pressure gradient and gravity (hydrostatic balance), and in the horizontal direction between the pressure gradient and the Coriolis force (geostrophic balance). In this chapter we exploit these balances to simplify the Navier–Stokes equations and thereby obtain various sets of simplified 'geostrophic equations'. Depending on the precise nature of the assumptions we make, we are led to the *quasi-geostrophic* (QG) system for horizontal scales similar to that on which most synoptic activity takes place and, for very large-scale motion, to the *planetary-geostrophic* (PG) set of equations. By eliminating unwanted or unimportant modes of motion, in particular sound waves and gravity waves, and by building in the important balances between flow fields, these filtered equation sets allow the investigator to better focus on a particular class of phenomena and to potentially achieve a deeper understanding than might otherwise be possible.[8]

Simplifying the equations in this way relies first on scaling the equations. The idea is that we *choose* the scales we wish to describe, typically either on some a-priori basis or by using observations as a guide. We then attempt to derive a set of equations that is simpler than the original set but that consistently describes motion of the chosen scale. An asymptotic method is one way to achieve this, for it systematically tells us which terms we can drop and which we should keep. The combined approach — scaling plus asymptotics — has proven enormously useful, but we should always remember two things: (i) that scaling is a choice; (ii) that the approach does not explain the existence of particular scales of motion, it just describes the motion that might occur on such scales. We have already employed this general approach in deriving the hydrostatic primitive equations, but now we go further.

4.1 GEOSTROPHIC SCALING

4.1.1 Scaling in the Shallow Water Equations

Postponing the complications that come with stratification, we begin with the shallow water equations. With the odd exception, we will denote the scales of variables by capital letters; thus, if L is a typical length scale of the motion we wish to describe, and U is a typical velocity scale, and

assuming the scales are horizontally isotropic, we write

$$\begin{aligned} (x, y) &\sim L \qquad \text{or} \qquad (x, y) = \mathcal{O}(L) \\ (u, v) &\sim U \qquad \text{or} \qquad (u, v) = \mathcal{O}(U), \end{aligned} \tag{4.1}$$

and similarly for other variables. We may then nondimensionalize the variables by writing

$$(x, y) = L(\hat{x}, \hat{y}), \qquad (u, v) = U(\hat{u}, \hat{v}), \tag{4.2}$$

where the hatted variables are nondimensional and, by supposition, are $\mathcal{O}(1)$. The various terms in the momentum equation then scale as:

$$\frac{\partial \boldsymbol{u}}{\partial t} + \boldsymbol{u} \cdot \nabla \boldsymbol{u} + \boldsymbol{f} \times \boldsymbol{u} = -g \nabla \eta, \tag{4.3a}$$

$$\frac{U}{T} \qquad \frac{U^2}{L} \qquad fU \quad \sim \quad g\frac{\mathcal{H}}{L}, \tag{4.3b}$$

where the ∇ operator acts in the x–y plane and $\mathcal{H}$ is the amplitude of the variations in the surface displacement. (We use η to denote the height of the free surface above some arbitrary reference level, as in Fig. 3.1. Thus, $\eta = H + \Delta\eta$, where $\Delta\eta$ denotes the variation of η about its mean position.)

The ratio of the advective term to the rotational term in the momentum equation (5.3) is $(U^2/L)/(fU) = U/fL$; this is the Rossby number,[9] first encountered in Chapter 2. Using values typical of the large-scale circulation (e.g., from Table 2.1) we find that $Ro \approx 0.1$ for the atmosphere and $Ro \approx 0.01$ for the ocean: small in both cases. If we are interested in motion that has the advective time scale $T = L/U$ then we scale time by L/U so that

$$t = \frac{L}{U}\hat{t}, \tag{4.4}$$

and the local time derivative and the advective term then both scale as U^2/L, and both are smaller than the rotation term by a factor of the order of the Rossby number. Then, either the Coriolis term is the dominant term in the equation, in which case we have a state of no motion with $-fv = 0$, or else the Coriolis force is balanced by the pressure force, and the dominant balance is

$$-fv = -g\frac{\partial \eta}{\partial x}, \tag{4.5}$$

namely *geostrophic balance*, as encountered in Chapter 2. If we make this non-trivial choice, then the equation informs us that variations in η (i.e., $\Delta\eta$) scale according to

$$\Delta\eta \sim \mathcal{H} = \frac{fUL}{g}. \tag{4.6}$$

We can also write $\mathcal{H}$ as

$$\mathcal{H} = Ro\,\frac{f^2L^2}{g} = Ro\;H\frac{L^2}{L_d^2}, \tag{4.7}$$

where $L_d = \sqrt{gH}/f$ is the deformation radius and H is the mean depth of the fluid. The variations in fluid height thus scale as

$$\frac{\Delta\eta}{H} \sim Ro\,\frac{L^2}{L_d^2}, \tag{4.8}$$

and the height of the fluid may be written as

$$\eta = H\left(1 + Ro\,\frac{L^2}{L_d^2}\hat{\eta}\right) \qquad \text{and} \qquad \Delta\eta = Ro\,\frac{L^2}{L_d^2}H\hat{\eta}, \tag{4.9}$$

where $\hat{\eta}$ is the $\mathcal{O}(1)$ nondimensional value of the surface height deviation.

Nondimensional momentum equation

If we use (5.9) to scale height variations, (5.2) to scale lengths and velocities, and (5.4) to scale time, then the momentum equation (5.3) becomes

$$Ro\left[\frac{\partial \widehat{\boldsymbol{u}}}{\partial \hat{t}} + (\widehat{\boldsymbol{u}}\cdot\nabla)\widehat{\boldsymbol{u}}\right] + \widehat{\boldsymbol{f}}\times\widehat{\boldsymbol{u}} = -\nabla\hat{\eta}, \tag{4.10}$$

where $\widehat{\boldsymbol{f}} = \mathbf{k}\hat{f} = \mathbf{k}f/f_0$, where f_0 is a representative value of the Coriolis parameter. (If f is a constant, then $\hat{f} = 1$, but it is informative to explicitly write $\hat{f}$ in the equations. Also, where the operator ∇ operates on a nondimensional variable then the differentials are taken with respect to the nondimensional variables $\hat{x}$, $\hat{y}$.) All the variables in (5.10) will be assumed to be of order unity, and the Rossby number multiplying the local time derivative and the advective terms indicates the smallness of those terms. By construction, the dominant balance in this equation is the geostrophic balance between the last two terms.

Nondimensional mass continuity (height) equation

The (dimensional) mass continuity equation can be written as

$$\frac{1}{H}\frac{\mathrm{D}\eta}{\mathrm{D}t} + \left(1 + \frac{\Delta\eta}{H}\right)\nabla\cdot\boldsymbol{u} = 0. \tag{4.11}$$

Using (5.2), (5.4) and (5.9) this equation may be written

$$Ro\left(\frac{L}{L_d}\right)^2\frac{\mathrm{D}\hat{\eta}}{\mathrm{D}\hat{t}} + \left[1 + Ro\left(\frac{L}{L_d}\right)^2\hat{\eta}\right]\nabla\cdot\widehat{\boldsymbol{u}} = 0. \tag{4.12}$$

Equations (5.10) and (5.12) are the nondimensional versions of the full shallow water equations of motion. Evidently, some terms in the equations of motion are small and may be eliminated with little loss of accuracy, and the way this is done will depend on the size of the second nondimensional parameter, $(L/L_d)^2$, which we come to shortly.

Froude and Burger numbers

The Froude number may be generally defined as the ratio of a fluid particle speed to a wave speed. In a shallow water system this gives

$$Fr \equiv \frac{U}{\sqrt{gH}} = \frac{U}{f_0 L_d} = Ro\,\frac{L}{L_d}\,. \tag{4.13}$$

The Burger number[10] is a useful measure of the scale of motion of the fluid, relative to the deformation radius, and may be defined by

$$Bu \equiv \left(\frac{L_d}{L}\right)^2 = \frac{gH}{f_0^2 L^2} = \left(\frac{Ro}{Fr}\right)^2. \tag{4.14}$$

It is also useful to define the parameter $F \equiv Bu^{-1}$, which is like the square of a Froude number but uses the rotational speed fL instead of U in the numerator.

4.1.2 Geostrophic Scaling in the Stratified Equations

We now apply the same scaling ideas, *mutatis mutandis,* to the stratified primitive equations. We use the hydrostatic anelastic equations, which we write as

$$\frac{\mathrm{D}\boldsymbol{u}}{\mathrm{D}t} + \boldsymbol{f} \times \boldsymbol{u} = -\nabla_z \phi, \tag{4.15a}$$

$$\frac{\partial \phi}{\partial z} = b, \tag{4.15b}$$

$$\frac{\mathrm{D}b}{\mathrm{D}t} = 0, \tag{4.15c}$$

$$\nabla \cdot (\tilde{\rho}\boldsymbol{v}) = 0, \tag{4.15d}$$

where b is the buoyancy and $\tilde{\rho}$ is a reference density profile. Anticipating that the average stratification may not scale in the same way as the deviation from it, let us separate out the contribution of the advection of a reference stratification in (5.15c) by writing

$$b = \tilde{b}(z) + b'(x, y, z, t). \tag{4.16}$$

The thermodynamic equation then becomes

$$\frac{\mathrm{D}b'}{\mathrm{D}t} + N^2 w = 0, \tag{4.17}$$

where $N^2 \equiv \partial \tilde{b}/\partial z$ (and the advective derivative is still three-dimensional). We then let $\phi = \bar{\phi}(z) + \phi'$, where $\bar{\phi}$ is hydrostatically balanced by $\tilde{b}$, and the hydrostatic equation becomes

$$\frac{\partial \phi'}{\partial z} = b'. \tag{4.18}$$

Equations (5.17) and (5.18) replace (5.15c) and (5.15b), and ϕ' is used in (5.15a).

Nondimensional equations

We scale the basic variables by supposing that

$$(x, y) \sim L, \quad (u, v) \sim U, \quad t \sim \frac{L}{U}, \quad z \sim H, \quad f \sim f_0, \tag{4.19}$$

where the scaling variables (capitalized, except for f_0) are chosen to be such that the nondimensional variables have magnitudes of the order of unity. We presume that the scales chosen are such that the Rossby number is small; that is $Ro = U/(f_0 L) \ll 1$. In the momentum equation the pressure term then balances the Coriolis force,

$$|\boldsymbol{f} \times \boldsymbol{u}| \sim |\nabla \phi'|, \tag{4.20}$$

and so the pressure scales as

$$\phi' \sim \Phi = f_o U L. \tag{4.21}$$

Using the hydrostatic relation, (5.21) implies that the buoyancy scales as

$$b' \sim B = \frac{f_0 U L}{H}, \tag{4.22}$$

and from this we obtain

$$\frac{(\partial b'/\partial z)}{N^2} \sim Ro \, \frac{L^2}{L_d^2}, \tag{4.23}$$

where $L_d = NH/f_0$ is the deformation radius in the continuously stratified fluid, analogous to the quantity $\sqrt{gH}/f_0$ in the shallow water system, and we use the same symbol, L_d, for both. In the continuously stratified system, *if the scale of motion is the same as or smaller than the deformation radius, and the Rossby number is small, then the variations in stratification are small.* The choice of scale is the key difference between the planetary-geostrophic and quasi-geostrophic equations.

Finally, we will nondimensionalize the vertical velocity by using the mass conservation equation,

$$\frac{1}{\tilde{\rho}}\frac{\partial \tilde{\rho} w}{\partial z} = -\left(\frac{\partial u}{\partial x} + \frac{\partial v}{\partial y}\right), \tag{4.24}$$

and we suppose that this implies

$$w \sim W = \frac{UH}{L}\,. \tag{4.25}$$

This is a naïve scaling for rotating flow: if the Coriolis parameter is nearly constant the geostrophic velocity is nearly horizontally non-divergent and the right-hand side of (5.24) is small, and $W \ll UH/L$. We might then estimate w by cross-differentiating geostrophic balance (with $\tilde{\rho}$ constant for simplicity) to obtain the linear geostrophic vorticity equation and corresponding scaling:

$$\beta v \approx f\frac{\partial w}{\partial z}, \qquad w \sim W = \frac{\beta UH}{f_0}. \tag{4.26a,b}$$

However, rather than using (5.26b) from the outset, we will use (5.25) and let the asymptotics guide us to a proper scaling in the fullness of time. Note that if variations in the Coriolis parameter are large and $\beta \sim f_0/L$, then (5.26b) is the same as (5.25).

Given the scalings above (using (5.25) for w) we nondimensionalize by setting

$$\begin{gathered}(\hat{x}, \hat{y}) = L^{-1}(x, y), \qquad \hat{z} = H^{-1}z, \quad (\hat{u}, \hat{v}) = U^{-1}(u, v), \quad \hat{t} = \frac{U}{L}t, \\ \hat{w} = \frac{L}{UH}w, \quad \hat{f} = f_0^{-1}f, \quad \hat{\phi} = \frac{\phi'}{f_0 UL}, \quad \hat{b} = \frac{H}{f_0 UL}b',\end{gathered} \tag{4.27}$$

where the hatted variables are nondimensional. The horizontal momentum and hydrostatic equations then become

$$Ro\,\frac{\mathrm{D}\hat{\boldsymbol{u}}}{\mathrm{D}\hat{t}} + \hat{\boldsymbol{f}} \times \hat{\boldsymbol{u}} = -\nabla\hat{\phi}, \tag{4.28}$$

and

$$\frac{\partial \hat{\phi}}{\partial \hat{z}} = \hat{b}. \tag{4.29}$$

The nondimensional mass conservation equation is simply

$$\frac{1}{\tilde{\rho}}\nabla\cdot(\tilde{\rho}\hat{\boldsymbol{v}}) = \left(\frac{\partial \hat{u}}{\partial \hat{x}} + \frac{\partial \hat{v}}{\partial \hat{y}} + \frac{1}{\tilde{\rho}}\frac{\partial \tilde{\rho}\hat{w}}{\partial \hat{z}}\right) = 0, \tag{4.30}$$

and the nondimensional thermodynamic equation is

$$\frac{f_0 UL}{H}\frac{U}{L}\frac{\mathrm{D}\hat{b}}{\mathrm{D}\hat{t}} + N^2\frac{HU}{L}\hat{w} = 0, \tag{4.31}$$

or

$$Ro\,\frac{\mathrm{D}\hat{b}}{\mathrm{D}\hat{t}} + \left(\frac{L_d}{L}\right)^2\hat{w} = 0. \tag{4.32}$$

The nondimensional primitive equations are summarized in the box on page 176.

Nondimensional Primitive Equations

$$Ro\,\frac{\mathrm{D}\widehat{\boldsymbol{u}}}{\mathrm{D}\hat{t}} + \widehat{\boldsymbol{f}}\times\widehat{\boldsymbol{u}} = -\nabla\hat{\phi} \qquad \text{Horizontal momentum:} \qquad \text{(PE.1)}$$

$$\frac{\partial\hat{\phi}}{\partial\hat{z}} = \hat{b} \qquad \text{Hydrostatic:} \qquad \text{(PE.2)}$$

$$\left(\frac{\partial\widehat{u}}{\partial\hat{x}} + \frac{\partial\widehat{v}}{\partial\hat{y}} + \frac{1}{\widetilde{\rho}}\frac{\partial\widetilde{\rho}\widehat{w}}{\partial\hat{z}}\right) = 0 \qquad \text{Mass continuity:} \qquad \text{(PE.3)}$$

$$Ro\,\frac{\mathrm{D}\hat{b}}{\mathrm{D}\hat{t}} + \left(\frac{L_d}{L}\right)^2\widehat{w} = 0 \qquad \text{Thermodynamic:} \qquad \text{(PE.4)}$$

These equations are written for the anelastic equations in a rotating frame of reference. The Boussinesq equations result if we take $\widetilde{\rho} = 1$. The equations in pressure coordinates also have a similar form — see Section 2.6.2.

4.2 THE PLANETARY-GEOSTROPHIC EQUATIONS

We now use the low Rossby number scalings above to derive equation sets that are simpler than the original, 'primitive', ones. The planetary-geostrophic equations are probably the simplest such set of equations, and we derive these equations first for the shallow water equations, and then for the stratified primitive equations.

4.2.1 Using the Shallow Water Equations

Informal derivation

The advection and time derivative terms in the momentum equation (5.10) are order Rossby number smaller than the Coriolis and pressure terms (the term in square brackets is multiplied by Ro), and therefore let us neglect them. The momentum equation straightforwardly becomes

$$\widehat{\boldsymbol{f}}\times\widehat{\boldsymbol{u}} = -\nabla\hat{\eta}. \tag{4.33}$$

The mass conservation equation (5.12), contains two nondimensional parameters, $Ro = U/(f_0 L)$ (the Rossby number), and $F = (L/L_d)^2$ (the ratio of the length scale of the motion to the deformation scale; $F = Bu^{-1}$) and we must make a choice as to the relationship between these two numbers. We will choose

$$F\,Ro = \mathcal{O}(1), \tag{4.34}$$

which implies

$$L^2 \gg L_d^2 \qquad \text{or equivalently} \qquad F \gg 1, \quad Bu \ll 1. \tag{4.35}$$

That is to say, we suppose that the scales of motion are much larger than the deformation scale. Given this choice, all the terms in the mass conservation equation, (5.12), are of roughly the same size, and we retain them all. Thus, the shallow water planetary geostrophic equations are the full mass continuity equation along with geostrophic balance and a geometric relationship between the height field and the fluid thickness, and in dimensional form these are:

$$\frac{\mathrm{D}h}{\mathrm{D}t} + h\nabla\cdot\boldsymbol{u} = 0,$$
$$\boldsymbol{f}\times\boldsymbol{u} = -g\nabla\eta, \qquad \eta = h + \eta_b\,. \tag{4.36a,b,c}$$

We emphasize that *the planetary-geostrophic equations are only valid for scales of motion much larger than the deformation radius.* The height variations are then as large as the mean height field itself; that is, using (5.8), $\Delta\eta/H = \mathcal{O}(1)$.

Formal derivation

We make the following assumptions:

(i) The Rossby number is small. $Ro = U/f_0 L \ll 1$.

(ii) The scale of the motion is significantly larger than the deformation scale. That is, (5.34) holds or equivalently

$$F = Bu^{-1} = \left(\frac{L}{L_d}\right)^2 \gg 1 \tag{4.37}$$

and in particular

$$F\,Ro = \mathcal{O}(1). \tag{4.38}$$

(iii) Time scales advectively, so that $T = L/U$.

The idea is now to expand the nondimensional velocity and height fields in an asymptotic series with the Rossby number as the small parameter, substitute into the equations of motion and derive a simpler set of equations. It is a nearly trivial exercise in this instance, and so illustrates the methodology well. The expansions are

$$\widehat{\boldsymbol{u}} = \widehat{\boldsymbol{u}}_0 + Ro\ \widehat{\boldsymbol{u}}_1 + Ro^2\,\widehat{\boldsymbol{u}}_2 + \ldots \qquad \text{and} \qquad \widehat{\eta} = \widehat{\eta}_0 + Ro\ \widehat{\eta}_1 + Ro^2\,\widehat{\eta}_2 + \ldots . \tag{4.39a,b}$$

Substituting (5.39) into the momentum equation then gives

$$Ro\left[\frac{\partial \widehat{\boldsymbol{u}}_0}{\partial \hat{t}} + \widehat{\boldsymbol{u}}_0 \cdot \nabla \widehat{\boldsymbol{u}}_0 + \widehat{\boldsymbol{f}} \times \widehat{\boldsymbol{u}}_1\right] + \widehat{\boldsymbol{f}} \times \widehat{\boldsymbol{u}}_0 = -\nabla \widehat{\eta}_0 - Ro\left[\nabla \widehat{\eta}_1\right] + \mathcal{O}(Ro^2). \tag{4.40}$$

The Rossby number is an asymptotic ordering parameter; thus, the sum of all the terms at any particular order in Rossby number must vanish. At lowest order we obtain the simple expression

$$\widehat{\boldsymbol{f}} \times \widehat{\boldsymbol{u}}_0 = -\nabla \widehat{\eta}_0. \tag{4.41}$$

Note that although f_0 is a representative value of f, we have made no assumptions about the constancy of f. In particular, f is allowed to vary by an order one amount, provided that it does not become so small that the Rossby number $U/(fL)$ is not small.

The appropriate height (mass conservation) equation is similarly obtained by substituting (5.39) into the shallow water mass conservation equation. Because $F\,Ro = \mathcal{O}(1)$ at lowest order we simply retain all the terms in the equation to give

$$F\,Ro\left[\frac{\partial \widehat{\eta}_0}{\partial t} + \widehat{\boldsymbol{u}}_0 \cdot \nabla \widehat{\eta}_0\right] + \left[1 + F\,Ro\ \widehat{\eta}\right] \nabla \cdot \widehat{\boldsymbol{u}}_0 = 0. \tag{4.42}$$

Equations (5.41) and (5.42) are a closed set, namely the nondimensional planetary-geostrophic equations. The dimensional forms of these equations are just (5.36).

Variation of the Coriolis parameter

Suppose then that f is a constant (f_0). Then, from the curl of (5.41), $\nabla \cdot \boldsymbol{u}_0 = 0$. This means that we can define a streamfunction for the flow and, from geostrophic balance, the height field is just that streamfunction. That is, in dimensional form,

$$\psi = \frac{g}{f_0}\eta, \qquad \boldsymbol{u} = \mathbf{k} \times \nabla\psi, \tag{4.43a,b}$$

and (5.42) becomes, in dimensional form,

$$\frac{\partial \eta}{\partial t} + \boldsymbol{u} \cdot \nabla \eta = 0 \qquad \text{or} \qquad \frac{\partial \eta}{\partial t} + J(\psi, \eta) = 0, \tag{4.44}$$

where $J(a,b) \equiv a_x b_y - a_y b_x$. But since $\eta \propto \psi$ the advective term is proportional to $J(\psi,\psi)$, which is zero. Thus, the flow does not evolve at this order. The planetary-geostrophic equations are *uninteresting* if the scale of the motion is such that the Coriolis parameter is not variable. On Earth, the scale of motion on which this parameter regime exists is rather limited, since the planetary-geostrophic equations require that the scale of motion also be larger than the deformation radius. In the Earth's atmosphere, any scale that is larger than the deformation radius will be such that the Coriolis parameter varies significantly over it, and we do not encounter this parameter regime. On the other hand, in the Earth's ocean the deformation radius is relatively small and there exists a small parameter regime (called the frontal geostrophic regime) that has scales larger than the deformation radius but smaller than that on which the Coriolis parameter varies.

Potential vorticity

The shallow water PG equations may be written as an evolution equation for an appropriate potential vorticity. A little manipulation reveals that (5.36) are equivalent to:

$$\begin{aligned} \frac{DQ}{Dt} &= 0, \\ Q = \frac{f}{h}, \quad \boldsymbol{f} \times \boldsymbol{u} &= -g\nabla\eta, \quad \eta = h + \eta_b \,. \end{aligned} \tag{4.45}$$

Thus, potential vorticity is a material invariant in the approximate equation set, just as it is in the full equations. The other variables — the free surface height and the velocity — are diagnosed from it, a process known as *potential vorticity inversion*. In the planetary geostrophic approximation, the inversion proceeds using the approximate form f/h rather than the full potential vorticity, $(f+\zeta)/h$. Thus, in a strict sense, we do not approximate potential vorticity, because this is the evolving variable. Rather, we approximate the inversion relations from which we derive the height and velocity fields. The simplest way of all to derive the shallow water PG equations is to *begin* with the conservation of potential vorticity, and to note that at small Rossby number the expression $(\zeta + f)/h$ may be approximated by f/h. Then, noting in addition that the flow is geostrophic, (5.45) immediately emerges. *Every* approximate set of equations that we derive in this chapter may be expressed as the evolution of potential vorticity, with the other fields being obtained diagnostically from it.

4.2.2 Planetary-Geostrophic Equations for Stratified Flow

To explore the stratified system we will use the inviscid and adiabatic Boussinesq equations of motion with the hydrostatic approximation. The derivation carries through easily enough using the anelastic or pressure-coordinate equations, but as the PG equations have more oceanographic than atmospheric importance, using the incompressible equations is quite appropriate.

Simplifying the equations

The nondimensional equations we begin with are (5.28)–(5.32). As in the shallow water case we expand these in a series in the Rossby number, so that:

$$\widehat{u} = \widehat{u}_0 + Ro\ \widehat{u}_1 + Ro^2\, \widehat{u}_2 + \ldots, \qquad \hat{b} = \hat{b}_0 + Ro\ \hat{b}_1 + Ro^2\, \hat{b}_2 + \ldots, \tag{4.46}$$

and similarly for $\widehat{v}$, $\widehat{w}$ and $\widehat{\phi}$. Substituting into the nondimensional equations of motion (on page 176) and equating powers of Ro gives the lowest-order momentum, hydrostatic, and mass conservation equations:

$$\widehat{\boldsymbol{f}} \times \widehat{\boldsymbol{u}}_0 = -\nabla\widehat{\phi}_0, \qquad \frac{\partial\widehat{\phi}_0}{\partial\widehat{z}} = \hat{b}_0, \qquad \nabla \cdot \widehat{\boldsymbol{v}}_0 = 0. \tag{4.47a,b,c}$$

If we also assume that $L_d/L = \mathcal{O}(1)$, then the thermodynamic equation (5.32) becomes

$$\left(\frac{L_d}{L}\right)^2 \widehat{w}_0 = 0. \tag{4.48}$$

Of course we have neglected any diabatic terms in this equation, which would in general provide a non-zero right-hand side. Nevertheless, this is not a useful equation, because the set of the equations we have derived, (5.47) and (5.48), can no longer evolve: all the time derivatives have been scaled away! Thus, although instructive, these equations are not very useful. If instead we assume that the scale of motion is much larger than the deformation scale then the other terms in the thermodynamic equation will become equally important. Thus, we suppose that $L_d^2 \ll L^2$ or, more formally, that $L^2 = \mathcal{O}(Ro^{-1})L_d^2$, and then all the terms in the thermodynamic equation are retained. A closed set of equations is then given by (5.47) and the thermodynamic equation (5.32).

Dimensional equations

Restoring the dimensions, dropping the asymptotic subscripts, and allowing for the possibility of a source term, denoted by $S_{[b']}$, in the thermodynamic equation, the *planetary-geostrophic* equations of motion are:

$$\begin{aligned} \frac{\mathrm{D}b'}{\mathrm{D}t} + wN^2 &= S_{[b']}, \\ \boldsymbol{f} \times \boldsymbol{u} = -\nabla\phi', \qquad \frac{\partial\phi'}{\partial z} &= b', \qquad \nabla \cdot \boldsymbol{v} = 0. \end{aligned} \tag{4.49}$$

The thermodynamic equation may also be written simply as

$$\frac{\mathrm{D}b}{\mathrm{D}t} = \dot{b}, \tag{4.50}$$

where b now represents the total stratification. The relevant pressure, ϕ, is then the pressure that is in hydrostatic balance with b, so that geostrophic and hydrostatic balance are most usefully written as

$$\boldsymbol{f} \times \boldsymbol{u} = -\nabla\phi, \qquad \frac{\partial\phi}{\partial z} = b. \tag{4.51a,b}$$

Potential vorticity

Manipulation of (5.49) reveals that we can equivalently write the equations as an evolution equation for potential vorticity. Thus, the evolution equations may be written as

$$\frac{\mathrm{D}Q}{\mathrm{D}t} = \dot{Q}, \qquad Q = f\frac{\partial b}{\partial z}, \tag{4.52}$$

where $\dot{Q} = f\partial\dot{b}/\partial z$, and the inversion — i.e., the diagnosis of velocity, pressure and buoyancy — is carried out using the hydrostatic, geostrophic and mass conservation equations.

Applicability to the ocean and atmosphere

In the atmosphere a typical deformation radius NH/f is about 1000 km. The constraint that the scale of motion be significantly larger than the deformation radius is thus hard to satisfy, since one quickly runs out of room on a planet whose equator-to-pole distance is 10 000 km. Only the largest planetary waves can satisfy the planetary-geostrophic scaling in the atmosphere and we should then also write the equations in spherical coordinates. In the ocean the deformation radius is about 100 km, so there is lots of room for the planetary-geostrophic equations to hold, and much of the theory of the large-scale structure of the ocean involves these equations.

Part II

WAVES, INSTABILITIES AND TURBULENCE

The waves broke and spread their waters swiftly over the shore. One after another they massed themselves and fell; the spray tossed itself back with the energy of their fall. The waves were steeped deep-blue save for a pattern of diamond-pointed light on their backs which rippled as the backs of great horses ripple with muscles as they move. The waves fell; withdrew and fell again.

Virginia Woolf, *The Waves*, 1931.

CHAPTER 5

Wave Fundamentals

WAVES ARE EVERYWHERE: on the sea-shore, on piano wires, in football stadiums, and filling the space between the distant stars and Earth. This chapter provides an introduction to their properties, paying particular attention to a wave that is especially important to the large scale flow in both ocean and atmosphere — the Rossby wave. We start with an elementary introduction to wave kinematics, discussing such basic concepts as phase speed and group velocity. Then, beginning with Section 6.4, we discuss the dynamics of Rossby waves, and this part may be considered to be the natural follow-on from the geostrophic theory of the previous chapter. Finally, in Section 6.7, we return to group velocity in a more general way and illustrate the results using Poincaré waves, with more applications to gravity and Rossby waves in later chapters.

The reason for such an ordering of topics is that wave kinematics without a dynamical example is jejune and dry, yet understanding wave dynamics of any sort is hardly possible without appreciating at least some of its formal structure, and readers should flip pages back and forth through the chapter as needed. Those readers who wish to cut to the chase may skip the first few sections and begin at Section 6.4, referring back as needed. (Many of the key elementary results are summarized in the shaded box on page 218.) Other readers may wish to skip the sections on Rossby waves altogether and, after absorbing the sections on the wave theory move on to Chapter 7 on gravity waves, returning to Rossby waves (or not) later on. The Rossby wave and gravity wave discussions are largely independent of each other, although they both require that the reader is familiar with such ideas as group velocity and phase speed. Rossby waves and gravity waves can co-exist and close to the equator the two kinds of waves become more intertwined; we deal with the ensuing waves in Chapter 8. We also extend our discussion of Rossby waves in a global atmospheric context in Chapter 16.

5.1 FUNDAMENTALS AND FORMALITIES

5.1.1 Definitions and Kinematics

A wave may be more easily recognized than defined. Loosely speaking, a wave is a propagating disturbance that has a characteristic relationship between its frequency and size, and a linear wave may be defined as a disturbance that satisfies a *dispersion relation.* (Nonlinear waves exist, but the curious reader must look elsewhere to learn about them.[11]) In order to see what all this means, and what a dispersion relation is, suppose that a disturbance, $\psi(\boldsymbol{x}, t)$ (where ψ might be velocity,

streamfunction, pressure, etc.), satisfies the equation

$$L(\psi) = 0, \tag{5.1}$$

where L is a linear operator, typically a polynomial in time and space derivatives; one example is $L(\psi) = \partial\nabla^2\psi/\partial t + \beta\partial\psi/\partial x$. If (6.1) has constant coefficients (if β is constant in this example) then harmonic solutions may often be found that are a superposition of *plane waves,* each of which satisfy

$$\psi = \mathrm{Re}\,\tilde{\psi}e^{i\theta(\boldsymbol{x},t)} = \mathrm{Re}\,\tilde{\psi}e^{i(\boldsymbol{k}\cdot\boldsymbol{x}-\omega t)}, \tag{5.2}$$

where $\tilde{\psi}$ is a complex constant, θ is the phase, ω is the wave frequency and $\boldsymbol{k}$ is the vector wavenumber (k, l, m) (also written as (k^x, k^y, k^z) or, in subscript notation, k_i). The prefix Re denotes the real part of the expression, but we will drop it if there is no ambiguity.

Earlier, we said that waves are characterized by having a particular relationship between the frequency and wavevector known as the *dispersion relation*. This is an equation of the form

$$\omega = \Omega(\boldsymbol{k}), \tag{5.3}$$

where $\Omega(\boldsymbol{k})$, or $\Omega(k_i)$, and meaning $\Omega(k, l, m)$, is some function determined by the form of L in (6.1) and which thus depends on the particular type of wave — the function is different for sound waves, light waves and the Rossby waves and gravity waves we will encounter in this book (peek ahead to (6.60) and (7.56), and there is more discussion in Section 6.1.3). Unless it is necessary to explicitly distinguish the function Ω from the frequency ω, we will often write $\omega = \omega(\boldsymbol{k})$.

If the medium in which the waves are propagating is inhomogeneous then (6.1) will probably not have constant coefficients (for example, β may vary with y). Nevertheless, if the medium is varying sufficiently slowly, wave solutions may often still be found with the general form

$$\psi(\boldsymbol{x}, t) = a(\boldsymbol{x}, t)e^{i\theta(\boldsymbol{x},t)}, \tag{5.4}$$

where the amplitude $a(\boldsymbol{x}, t)$ varies slowly compared to the phase, θ. The frequency and wavenumber are then defined by

$$\boldsymbol{k} \equiv \nabla\theta, \qquad \omega \equiv -\frac{\partial\theta}{\partial t}. \tag{5.5}$$

The example of (6.2) is clearly just a special case of this. Equation (6.5) implies the formal relation between $\boldsymbol{k}$ and ω:

$$\frac{\partial\boldsymbol{k}}{\partial t} + \nabla\omega = 0. \tag{5.6}$$

The WKB method, described in Appendix A at the end of this chapter, is one way of finding such solutions.

5.1.2 Wave Propagation and Phase Speed

A common property of waves is that they propagate through space with some velocity, which in special cases might be zero. Waves in fluids may carry energy and momentum but not normally, at least to a first approximation, fluid parcels themselves. Further, it turns out that the speed at which properties like energy are transported (the group speed) may be different from the speed at which the wave crests themselves move (the phase speed). Let's try to understand this statement, beginning with the phase speed. A summary of key results is given on page 218.

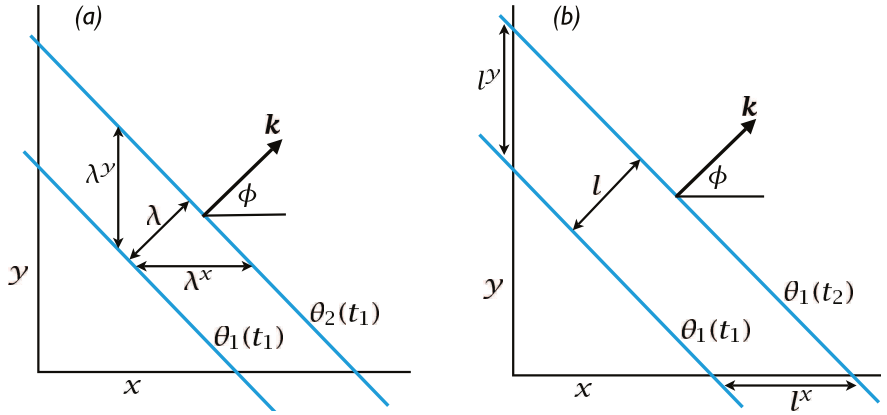

Fig. 5.1 The propagation of a two-dimensional wave. (a) Two lines of constant phase (e.g., two wavecrests) at a time t_1. The wave is propagating in the direction $\boldsymbol{k}$ with wavelength λ. (b) The same line of constant phase at two successive times. The phase speed is the speed of advancement of the wavecrest in the direction of travel, and so $c_p = l/(t_2 - t_1)$. The phase speed in the x-direction is the speed of propagation of the wavecrest along the x-axis, and $c_p^x = l^x/(t_2 - t_1) = c_p/\cos\phi$.

Phase speed

Consider the propagation of monochromatic plane waves, for that is all that is needed to introduce the phase speed. Given (6.2) a wave will propagate in the direction of $\boldsymbol{k}$ (Fig. 6.1). At a given instant and location we can align our coordinate axis along this direction, and we write $\boldsymbol{k}\cdot\boldsymbol{x} = Kx^*$, where x^* increases in the direction of $\boldsymbol{k}$ and $K^2 = |\boldsymbol{k}|^2$ is the magnitude of the wavenumber. With this, we can write (6.2) as

$$\psi = \mathrm{Re}\,\tilde{\psi}\mathrm{e}^{\mathrm{i}(Kx^*-\omega t)} = \mathrm{Re}\,\tilde{\psi}\mathrm{e}^{\mathrm{i}K(x^*-ct)}, \tag{5.7}$$

where $c = \omega/K$. From this equation it is evident that the phase of the wave propagates at the speed c in the direction of $\boldsymbol{k}$, and we define the *phase speed* by

$$c_p \equiv \frac{\omega}{K}. \tag{5.8}$$

The wavelength of the wave, λ, is the distance between two wavecrests — that is, the distance between two locations along the line of travel whose phase differs by 2π — and evidently this is given by

$$\lambda = \frac{2\pi}{K}. \tag{5.9}$$

In (for simplicity) a two-dimensional wave, and referring to Fig. 6.1, the wavelength and wave vectors in the x- and y-directions are given by,

$$\lambda^x = \frac{\lambda}{\cos\phi}, \quad \lambda^y = \frac{\lambda}{\sin\phi}, \qquad k^x = K\cos\phi, \quad k^y = K\sin\phi. \tag{5.10}$$

In general, lines of constant phase intersect both the coordinate axes and propagate along them. The speed of propagation along these axes is given by

$$c_p^x = c_p\frac{l^x}{l} = \frac{c_p}{\cos\phi} = c_p\frac{K}{k^x} = \frac{\omega}{k^x}, \qquad c_p^y = c_p\frac{l^y}{l} = \frac{c_p}{\sin\phi} = c_p\frac{K}{k^y} = \frac{\omega}{k^y}, \tag{5.11}$$

using (6.8) and (6.10), and again referring to Fig. 6.1 for notation. The speed of phase propagation along any one of the axes is in general *larger* than the phase speed in the primary direction of

Wave Fundamentals

- A wave is a propagating disturbance that has a characteristic relationship between its frequency and size, known as the dispersion relation. Waves typically arise as solutions to a linear problem of the form

$$L(\psi) = 0, \tag{WF.1}$$

where L is, commonly, a linear operator in space and time. Two examples are

$$\frac{\partial^2 \psi}{\partial t^2} - c^2 \nabla^2 \psi = 0 \qquad \text{and} \qquad \frac{\partial}{\partial t} \nabla^2 \psi + \beta \frac{\partial \psi}{\partial x} = 0. \tag{WF.2}$$

The first example is so common in all areas of physics it is sometimes called 'the' wave equation. The second example gives rise to Rossby waves.

- Solutions to the governing equation are often sought in the form of plane waves that have the form

$$\psi = \mathrm{Re}\, A \mathrm{e}^{\mathrm{i}(\boldsymbol{k}\cdot\boldsymbol{x} - \omega t)}, \tag{WF.3}$$

where A is the wave amplitude, $\boldsymbol{k} = (k, l, m)$ is the wavevector, and ω is the frequency.

- The dispersion relation connects the frequency and wavevector through an equation of the form $\omega = \Omega(\boldsymbol{k})$ where Ω is some function. The relation is normally derived by substituting a trial solution like (WF.3) into the governing equation (WF.1). For the examples of (WF.2) we obtain $\omega = c^2 K^2$ and $\omega = -\beta k / K^2$ where $K^2 = k^2 + l^2 + m^2$ or, in two dimensions, $K^2 = k^2 + l^2$.

- The phase speed is the speed at which the wave crests move. In the direction of propagation and in the x, y and z directions the phase speeds are given by, respectively,

$$c_p = \frac{\omega}{K}, \qquad c_p^x = \frac{\omega}{k}, \quad c_p^y = \frac{\omega}{l}, \quad c_p^z = \frac{\omega}{m}, \tag{WF.4}$$

where $K = 2\pi/\lambda$ and λ is the wavelength. The wave crests have both a speed (c_p) and a direction of propagation (the direction of $\boldsymbol{k}$), like a vector, but the components defined in (WF.4) are not the components of that vector.

- The group velocity is the velocity at which a wave packet or wave group moves. It is a vector and is given by

$$\boldsymbol{c}_g = \frac{\partial \omega}{\partial \boldsymbol{k}} \quad \text{with components} \quad c_g^x = \frac{\partial \omega}{\partial k}, \quad c_g^y = \frac{\partial \omega}{\partial l}, \quad c_g^z = \frac{\partial \omega}{\partial m}. \tag{WF.5}$$

Many physical quantities of interest are transported at the group velocity.

- If the coefficients of the wave equation are not constant (for example if the medium is inhomogeneous) then, if the coefficients are only slowly varying, approximate solutions may sometimes be found in the form

$$\psi = \mathrm{Re}\, A(\boldsymbol{x}, t) \mathrm{e}^{\mathrm{i}\theta(\boldsymbol{x}, t)}, \tag{WF.6}$$

where the amplitude A is also slowly varying and the local wavenumber and frequency are related to the phase, θ, by $\boldsymbol{k} = \nabla\theta$ and $\omega = -\partial\theta/\partial t$. The dispersion relation is then a *local* one of the form $\omega = \Omega(\boldsymbol{k}; x, t)$.

the wave. The phase speeds are clearly *not* components of a vector: for example, $c_p^x \neq c_p \cos\phi$. Analogously, the wavevector $\boldsymbol{k}$ is a true vector, whereas the wavelength λ is not.

To summarize, the phase speed and its components are given by

$$c_p = \frac{\omega}{K}, \qquad c_p^x = \frac{\omega}{k^x}, \quad c_p^y = \frac{\omega}{k^y}. \tag{5.12}$$

Phase velocity

Although it is not particularly useful, there is a way of defining a phase speed so that it is a true vector, and which might then be called phase velocity. We define the phase velocity to be the velocity that has the magnitude of the phase speed and the direction in which wave crests are propagating; that is

$$\boldsymbol{c}_p \equiv \frac{\omega}{K}\frac{\boldsymbol{k}}{|K|} = c_p \frac{\boldsymbol{k}}{|K|}, \tag{5.13}$$

where $\boldsymbol{k}/|K|$ is the unit vector in the direction of wave-crest propagation. The components of the phase velocity in the x- and y-directions are then given by

$$c_p^x = c_p \cos\phi, \qquad c_p^y = c_p \sin\phi. \tag{5.14}$$

Defined this way, the quantity given by (6.13) is a vector velocity. However, the components in the x- and y-directions are manifestly not the speed at which wave crests propagate in those directions, and it is a misnomer to call these quantities phase speeds. Still, it can be helpful to ascribe a direction to the phase speed and the quantity given by (6.13) may then be useful.

5.1.3 The Dispersion Relation

The above description is kinematic, in that it applies to almost any disturbance that has a wavevector and a frequency. The particular *dynamics* of a wave are determined by the relationship between the wavevector and the frequency; that is, by the *dispersion relation*. Once the dispersion relation is known a great many of the properties of the wave follow in a more-or-less straightforward manner. Picking up from (6.3), the dispersion relation is a functional relationship between the frequency and the wavevector of the general form

$$\omega = \Omega(\boldsymbol{k}). \tag{5.15}$$

Perhaps the simplest example of a linear operator that gives rise to waves is the one-dimensional equation

$$\frac{\partial \psi}{\partial t} + c\frac{\partial \psi}{\partial x} = 0. \tag{5.16}$$

Substituting a trial solution of the form $\psi = \mathrm{Re}\, A e^{\mathrm{i}(kx-\omega t)}$ we obtain $(-\mathrm{i}\omega + c\mathrm{i}k)A = 0$, giving the dispersion relation

$$\omega = ck. \tag{5.17}$$

The phase speed of this wave is $c_p = \omega/k = c$. A few other examples of governing equations, dispersion relations and phase speeds are:

$$\frac{\partial \psi}{\partial t} + \boldsymbol{c}\cdot\nabla\psi = 0, \qquad \omega = \boldsymbol{c}\cdot\boldsymbol{k}, \qquad c_p = |\boldsymbol{c}|\cos\theta, \qquad c_p^x = \frac{\boldsymbol{c}\cdot\boldsymbol{k}}{k}, \qquad c_p^y = \frac{\boldsymbol{c}\cdot\boldsymbol{k}}{l}, \tag{5.18a}$$

$$\frac{\partial^2 \psi}{\partial t^2} - c^2\nabla^2\psi = 0, \qquad \omega^2 = c^2K^2, \qquad c_p = \pm c, \qquad c_p^x = \pm\frac{cK}{k}, \qquad c_p^y = \pm\frac{cK}{l}, \tag{5.18b}$$

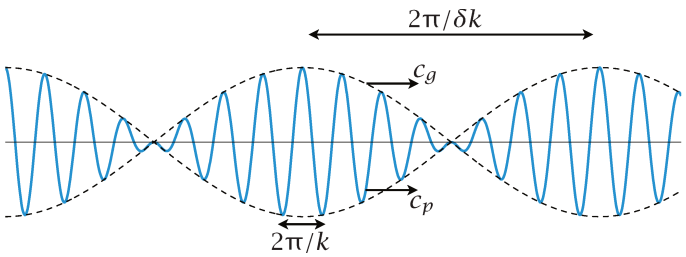

Fig. 5.2 Superposition of two sinusoidal waves with wavenumbers k and $k + \delta k$, producing a wave (solid line) that is modulated by a slowly varying wave envelope or packet (dashed).

The envelope moves at the group velocity, $c_g = \partial\omega/\partial k$, and the phase moves at the group speed, $c_p = \omega/k$.

$$\frac{\partial}{\partial t}\nabla^2\psi + \beta\frac{\partial\psi}{\partial x} = 0, \qquad \omega = \frac{-\beta k}{K^2}, \qquad c_p = \frac{\omega}{K}, \qquad c_p^x = -\frac{\beta}{K^2}, \qquad c_p^y = -\frac{\beta k/l}{K^2}, \tag{5.18c}$$

where $K^2 = k^2 + l^2$ and θ is the angle between $\boldsymbol{c}$ and $\boldsymbol{k}$, and the examples are all two-dimensional, with variation in x and y only.

A wave is said to be *nondispersive* if the phase speed is independent of the wavelength. This condition is satisfied for the simple example (6.16) but is manifestly not satisfied for (6.18c), and these waves (Rossby waves, in fact) are *dispersive*. Waves of different wavelengths then travel at different speeds so that a group of waves will spread out — disperse — even if the medium is homogeneous. When a wave is dispersive there is another characteristic speed at which the waves propagate, the group velocity, and we come to this shortly.

Most media are inhomogeneous, but if the medium varies sufficiently slowly in space and time — and in particular if the variations are slow compared to the wavelength and period — we may still have a *local* dispersion relation between frequency and wavevector,

$$\omega = \Omega(\boldsymbol{k}; \boldsymbol{x}, t), \tag{5.19}$$

where x and t are slowly varying parameters. We'll resume our discussion of this topic in Section 6.3, but before that we must introduce the group velocity.

5.2 GROUP VELOCITY

Information and energy do not, in general, propagate at the phase speed. Rather, most quantities of interest propagate at the *group velocity,* a quantity of enormous importance in wave theory.[12] Roughly speaking, group velocity is the velocity at which a packet or a group of waves will travel, whereas the individual wave crests travel at the phase speed. To introduce the idea we will consider the superposition of plane waves, noting that a truly monochromatic plane wave already fills all space uniformly so that there can be no propagation of energy from place to place.

5.2.1 Superposition of Two Waves

Consider the linear superposition of two waves. Limiting attention to the one-dimensional case for simplicity, consider a disturbance represented by

$$\psi = \mathrm{Re}\,\tilde{\psi}(\mathrm{e}^{\mathrm{i}(k_1 x - \omega_1 t)} + \mathrm{e}^{\mathrm{i}(k_2 x - \omega_2 t)}). \tag{5.20}$$

Let us further suppose that the two waves have similar wavenumbers and frequency, and, in particular, that $k_1 = k + \Delta k$ and $k_2 = k - \Delta k$, and $\omega_1 = \omega + \Delta\omega$ and $\omega_2 = \omega - \Delta\omega$. With this, (6.20) becomes

$$\begin{aligned}\psi &= \mathrm{Re}\,\tilde{\psi}\mathrm{e}^{\mathrm{i}(kx-\omega t)}[\mathrm{e}^{\mathrm{i}(\Delta k x - \Delta\omega t)} + \mathrm{e}^{-\mathrm{i}(\Delta k x - \Delta\omega t)}] \\ &= 2\,\mathrm{Re}\,\tilde{\psi}\mathrm{e}^{\mathrm{i}(kx-\omega t)}\cos(\Delta k\, x - \Delta\omega\, t).\end{aligned} \tag{5.21}$$

The resulting disturbance, illustrated in Fig. 6.2 has two aspects: a rapidly varying component, with wavenumber k and frequency ω, and a more slowly varying envelope, with wavenumber Δk and frequency $\Delta\omega$. The envelope modulates the fast oscillation, and moves with velocity $\Delta\omega/\Delta k$; in the limit $\Delta k \to 0$ and $\Delta\omega \to 0$ this is the *group velocity*, $c_g = \partial\omega/\partial k$. Group velocity is equal to the phase speed, ω/k, only when the frequency is a linear function of wavenumber. The energy in the disturbance must move at the group velocity — note that the node of the envelope moves at the speed of the envelope and no energy can cross the node. These concepts generalize to more than one dimension, and if the wavenumber is the three-dimensional vector $\boldsymbol{k} = (k, l, m)$ then the three-dimensional envelope propagates at the group velocity given by

$$\boldsymbol{c}_g = \frac{\partial\omega}{\partial\boldsymbol{k}} \equiv \left(\frac{\partial\omega}{\partial k}, \frac{\partial\omega}{\partial l}, \frac{\partial\omega}{\partial m}\right). \tag{5.22}$$

The group velocity is also written as $\boldsymbol{c}_g = \nabla_{\boldsymbol{k}}\omega$ or, in subscript notation, $c_{gi} = \partial\Omega/\partial k_i$, with the subscript i denoting the component of a vector.

5.2.2 Superposition of Many Waves

Now consider a slight extension of the above arguments to the case in which many waves are excited. The essential assumption of this derivation is that the wavenumber distribution is sufficiently narrow so that the dispersion relation can be approximated as

$$\omega(k) \approx \omega(k_0) + \left.\frac{\mathrm{d}\omega}{\mathrm{d}k}\right|_{k_0} (k - k_0). \tag{5.23}$$

We treat only the one-dimensional case but the three-dimensional generalization is possible.

A superposition of plane waves, each satisfying some dispersion relation, can be represented by the Fourier integral

$$\psi(x,t) = \int_{-\infty}^{\infty} \tilde{A}(k)\mathrm{e}^{\mathrm{i}(kx-\omega t)}\,\mathrm{d}k. \tag{5.24a}$$

The function $\tilde{A}(k)$ is given by the initial conditions:

$$\tilde{A}(k) = \frac{1}{2\pi}\int_{-\infty}^{\infty} \psi(x,0)\mathrm{e}^{-\mathrm{i}kx}\,\mathrm{d}x. \tag{5.24b}$$

Note that if the waves are dispersionless and $\omega = ck$ where c is a constant, then

$$\psi(x,t) = \int_{-\infty}^{+\infty} \tilde{A}(k)\mathrm{e}^{\mathrm{i}k(x-ct)}\,\mathrm{d}k = \psi(x-ct,0), \tag{5.25}$$

by comparison with (6.24a) at $t = 0$. That is, the initial condition simply translates at a speed c, with no change in structure.

Now consider the case for which the disturbance is a *wave packet* — essentially a nearly plane wave or superposition of waves that is confined to a finite region of space. We will consider a case with the initial condition

$$\psi(x,0) = a(x)\mathrm{e}^{\mathrm{i}k_0 x}, \tag{5.26}$$

where $a(x,t)$, rather like the envelope in Fig. 6.3, modulates the amplitude of the wave on a scale much longer than that of the wavelength $2\pi/k_0$, and more slowly than the wave period. That is,

$$\frac{1}{a}\frac{\partial a}{\partial x} \ll k_0, \qquad \frac{1}{a}\frac{\partial a}{\partial t} \ll k_0 c, \tag{5.27a,b}$$

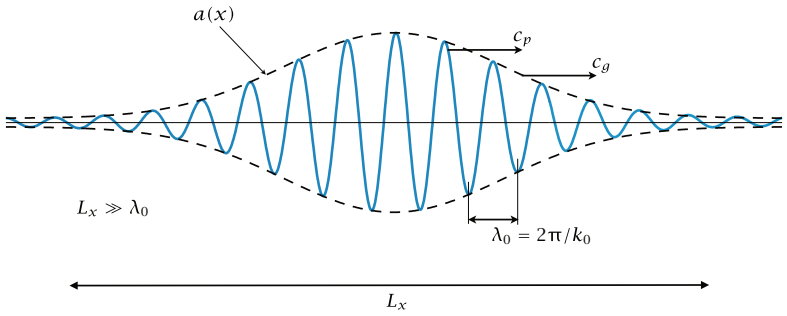

Fig. 5.3 A wave packet. The envelope, $a(x)$, has a scale, L_x, much larger than the wavelength, λ_0, of the wave embedded inside. The envelope moves at the group velocity, c_g, and the phase of the waves at the phase speed, c_p.

and the disturbance is essentially a slowly modulated plane wave. We suppose that $a(x,0)$ is peaked around some value x_0 and is very small if $|x-x_0| \gg k_0^{-1}$; that is, $a(x,0)$ is small if we are sufficiently many wavelengths of the plane wave away from the peak, as is the case in Fig. 6.3. We would like to know how such a packet evolves.

We can express the envelope as a Fourier integral by first writing the initial conditions as a Fourier integral,

$$\psi(x,0) = \int_{-\infty}^{\infty} \tilde{A}(k) \mathrm{e}^{\mathrm{i}kx}\,\mathrm{d}k \quad \text{where} \quad \tilde{A}(k) = \frac{1}{2\pi}\int_{-\infty}^{+\infty} \psi(x,0)\mathrm{e}^{-ikx}\,\mathrm{d}x, \tag{5.28a,b}$$

so that, using (6.26),

$$\tilde{A}(k) = \frac{1}{2\pi}\int_{-\infty}^{+\infty} a(x,0)\mathrm{e}^{\mathrm{i}(k_0-k)x}\,\mathrm{d}x \quad \text{and} \quad a(x) = \int_{-\infty}^{\infty} \tilde{A}(k)\mathrm{e}^{\mathrm{i}(k-k_0)x}\,\mathrm{d}k. \tag{5.29a,b}$$

We still haven't made much progress beyond (6.24). To do so, we note first that $a(x)$ is confined in space, so that to a good approximation the limits of the integral in (6.29a) can be made finite, $\pm L$ say, provided $L \gg k_0^{-1}$. We then note that when $(k_0 - k)$ is large the integrand in (6.29a) oscillates rapidly; successive intervals in x therefore cancel each other and make a small net contribution to the integral. Thus, the integral is dominated by values of k near k_0, and $\tilde{A}(k)$ is peaked near k_0. (The finite spatial extent of $a(x,0)$ is needed for this argument.)

We can now evaluate how the wave packet evolves. Beginning with (6.24a) we have

$$\psi(x,t) = \int_{-\infty}^{\infty} \tilde{A}(k)\exp\{\mathrm{i}(kx-\omega(k)t)\}\,\mathrm{d}k \tag{5.30a}$$

$$\approx \int_{-\infty}^{\infty} \tilde{A}(k)\exp\left\{\mathrm{i}[k_0x-\omega(k_0)t] + \mathrm{i}(k-k_0)x - \mathrm{i}(k-k_0)\left.\frac{\partial\omega}{\partial k}\right|_{k=k_0} t\right\}\,\mathrm{d}k, \tag{5.30b}$$

having expanded $\omega(k)$ in a Taylor series about k_0, using (6.23). We thus have

$$\begin{aligned}\psi(x,t) &= \exp\{\mathrm{i}[k_0x-\omega(k_0)t]\}\int\int_{-\infty}^{\infty}\tilde{A}(k)\exp\left\{\mathrm{i}(k-k_0)\left[x-\left.\frac{\partial\omega}{\partial k}\right|_{k=k_0}t\right]\right\}\,\mathrm{d}k \\ &= \exp\{\mathrm{i}[k_0x-\omega(k_0)t]\}\,a(x-c_gt),\end{aligned} \tag{5.31}$$

using (6.29b) and where $c_g = \partial\omega/\partial k$ evaluated at $k = k_0$. That is to say, the envelope $a(x,t)$ moves at the group velocity, keeping its initial shape.

The group velocity has a meaning beyond that implied by the derivation above: it turns out to be a quite general property of waves that energy (and certain other quadratic properties) propagate at the group velocity. This is to be expected, at least in the presence of coherent wave packets, because there is no energy outside the wave envelope so the energy must propagate with the envelope.

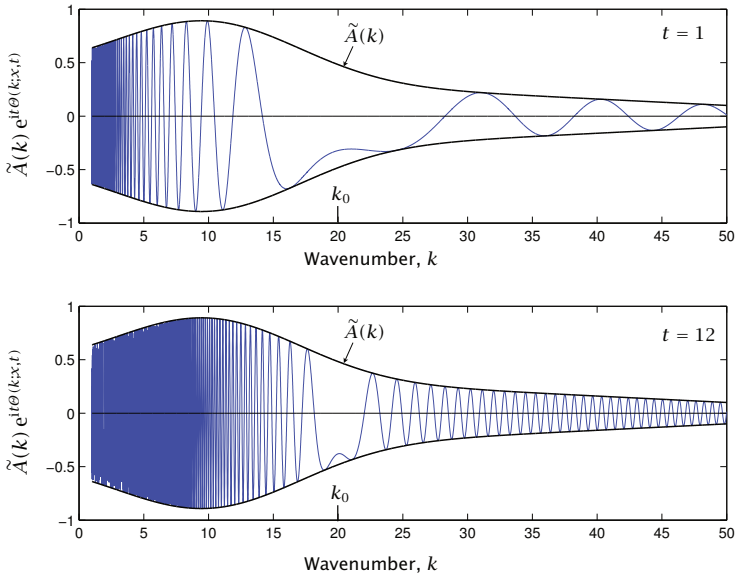

Fig. 5.4 The integrand of (6.32), namely the function that when integrated over wavenumber gives the wave amplitude at a particular x and t.

The example shown is for a Rossby wave with $\omega = -\beta/k$, with $\beta = 400$ and $x/t = 1$, and hence $k_0 = 20$, for two times $t = 1$ and $t = 12$. (The amplitude of the envelope, $\tilde{A}(k)$ is arbitrary.) At the later time the oscillations are much more rapid in k, so that the contribution is more peaked from wavenumbers near to k_0.

5.2.3 ✦ The Method of Stationary Phase

We will now relax the assumption that wavenumbers are confined to a narrow band but (since there is no free lunch) we confine ourselves to seeking solutions at large t; that is, we will be seeking a description of waves far from their source. Consider a disturbance of the general form

$$\psi(x,t) = \int_{-\infty}^{\infty} \tilde{A}(k)\,\mathrm{e}^{\mathrm{i}[kx-\omega(k)t]}\,\mathrm{d}k = \int_{-\infty}^{\infty} \tilde{A}(k)\,\mathrm{e}^{\mathrm{i}\Theta(k;x,t)t}\,\mathrm{d}k, \tag{5.32}$$

where $\Theta(k;x,t) \equiv kx/t - \omega(k)$. (Here we regard Θ as a function of k with parameters x and t; we will sometimes just write $\Theta(k)$ with $\Theta'(k) = \partial\Theta/\partial k$.) Now, a standard result in mathematics (known as the 'Riemann–Lebesgue lemma') states that

$$I = \lim_{t\to\infty} \int_{-\infty}^{\infty} f(k)\,\mathrm{e}^{\mathrm{i}kt}\,\mathrm{d}k = 0, \tag{5.33}$$

provided that $f(k)$ is integrable and $\int_{-\infty}^{\infty} f(k)\,\mathrm{d}k$ is finite. Intuitively, as t increases the oscillations in the integral increase and become much faster than any variation in $f(k)$; successive oscillations thus cancel and the integral becomes very small.

Looking at (6.32), with $\tilde{A}$ playing the role of $f(k)$, the integral will be small if Θ is everywhere varying with k. However, if there is a region where Θ does not vary with k — that is, if there is a region where the phase is stationary and $\partial\Theta/\partial k = 0$ — then there will be a contribution to the integral from that region. Thus, for large t, an observer will predominantly see waves for which $\Theta'(k) = 0$ and so, using the definition of Θ, for which

$$\frac{x}{t} = \frac{\partial\omega}{\partial k}. \tag{5.34}$$

In other words, at some space-time location (x,t) the waves that dominate are those whose group velocity $\partial\omega/\partial k$ is x/t. An example is plotted in Fig. 6.4 with a dispersion relation $\omega = -\beta/k$; the wavenumber that dominates, k_0 say, is thus given by solving $\beta/k_0^2 = x/t$, which for $x/t = 1$ and $\beta = 400$ gives $k_0 = 20$.

We may actually approximately calculate the contribution to $\psi(x,t)$ from waves moving with the group velocity. Let us expand $\Theta(k)$ around the point, k_0, where $\Theta'(k_0) = 0$. We obtain

$$\psi(x,t) = \int_{-\infty}^{\infty} \tilde{A}(k) \exp\left\{ \mathrm{i}t \left[\Theta(k_0) + (k-k_0)\Theta'(k_0) + \tfrac{1}{2}(k-k_0)^2\Theta''(k_0) \ldots \right] \right\} \mathrm{d}k \tag{5.35}$$

The higher order terms are small because $k - k_0$ is presumed small (for if it is large the integral vanishes), and the term involving $\Theta'(k_0)$ is zero. The integral becomes

$$\psi(x,t) = \tilde{A}(k_0)\mathrm{e}^{\mathrm{i}\Theta(k_0)} \int_{-\infty}^{\infty} \exp\left\{ \mathrm{i}t\tfrac{1}{2}(k-k_0)^2\Theta''(k_0) \right\} \mathrm{d}k. \tag{5.36}$$

We thus have to evaluate a Gaussian, and because $\int_{-\infty}^{\infty} \mathrm{e}^{-cx^2}\,\mathrm{d}x = \sqrt{\pi/c}$ we obtain

$$\psi(x,t) \approx \tilde{A}(k_0)\mathrm{e}^{\mathrm{i}\Theta(k_0)t} \left[\frac{-2\pi}{(\mathrm{i}t\theta''(k_0))} \right]^{1/2} = \tilde{A}(k_0) \left[\frac{2\mathrm{i}\pi}{(t\theta''(k_0))} \right]^{1/2} \mathrm{e}^{\mathrm{i}(k_0 x - \omega(k_0)t)}. \tag{5.37}$$

The solution is therefore a plane wave, with wavenumber k_0 and frequency $\omega(k_0)$, slowly modulated by an envelope determined by the form of $\Theta(k_0; x, t)$, where k_0 is the wavenumber such that $x/t = c_g = \partial\omega/\partial k|_{k=k_0}$.

5.3 RAY THEORY

Most waves propagate in a medium that is inhomogeneous; for example, in the Earth's atmosphere and ocean the stratification varies with altitude and the Coriolis parameter varies with latitude. In these cases it can be hard to obtain the solution of a wave problem by Fourier methods, even approximately. Nonetheless, the idea of signals propagating at the group velocity is a robust one, and we can often obtain some of the information we want — and in particular the trajectory of a wave — using a recipe known as *ray theory*.[13]

Come with rain, O loud Southwester!
Bring the singer, bring the nester;
Give the buried flower a dream;
Make the settled snowbank steam.
Robert Frost, *To the Thawing Wind*, 1915.

CHAPTER 6

Barotropic and Baroclinic Instability

WHAT HYDRODYNAMIC STATES OCCUR IN NATURE? If we take as given the applicability of the Navier–Stokes equations, any flow must be a solution of these equations, subject to the relevant initial and boundary conditions. Most of the flows we experience are of course *time-dependent* solutions, not steady solutions. Why should this be? There are many steady solutions to the equations of motion — certain purely zonal flows, for example. However, steady solutions do not abound in nature because, in order to persist, they must be stable to those small perturbations that inevitably arise. Indeed, all the steady solutions that are known for the large-scale flow in the Earth's atmosphere and ocean have been found to be unstable. It is such instability that makes the subject an interesting one.

There are a myriad forms of hydrodynamic instability, but our focus in this chapter is on barotropic and baroclinic instability. *Baroclinic instability* (and we will define the term more precisely later on) is an instability that arises in rotating, stratified fluids that are subject to a horizontal temperature gradient. It is the instability that gives rise to the large- and mesoscale motion in the atmosphere and ocean — it produces atmospheric weather systems, for example — and so is, perhaps, the form of hydrodynamic instability that most affects the human condition. *Barotropic instability* is an instability that arises because of the shear in a flow, and may occur in fluids of constant density. It is important to us for two reasons: first, it is important in its own right as an instability mechanisms for jets and vortices, and as an important process in both two- and three-dimensional turbulence; second, many problems in barotropic and baroclinic instability are formally and dynamically similar, so that the solutions and insight we obtain in the often simpler problems in barotropic instability may be useful in the baroclinic problem.

6.1 KELVIN–HELMHOLTZ INSTABILITY

To introduce the issue, we first consider, rather informally, perhaps the simplest physically interesting instance of a fluid-dynamical instability — that of a constant-density flow with a shear perpendicular to the fluid's mean velocity, this being an example of a *Kelvin–Helmholtz instability,*[14] and of a barotropic instability. (More generally, Kelvin–Helmholtz instability involves fluid with varying density.) Let us consider two fluid masses of equal density, with a common interface at $y = 0$, moving with velocities $-U$ and $+U$ in the x-direction, respectively (Fig. 9.1). There is no variation in the basic flow in the z-direction (normal to the page), and we will assume this is also true for the instability (these restrictions are not essential). This flow is clearly a solution of

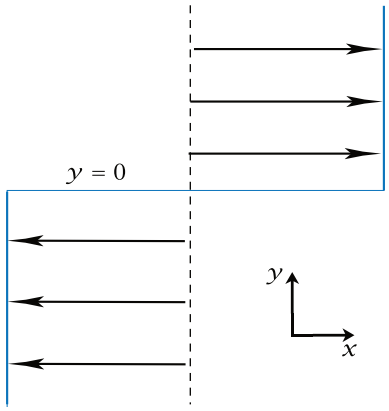

Fig. 6.1 A simple basic state giving rise to shear-flow instability. The velocity profile is discontinuous and the density is uniform.

the Euler equations. What happens if the flow is perturbed slightly? If the perturbation is initially small then even if it grows we can, for small times after the onset of instability, neglect the nonlinear interactions in the governing equations because these are the squares of small quantities. The equations determining the evolution of the initial perturbation are then the Euler equations linearized about the steady solution. Thus, denoting perturbation quantities with a prime and basic state variables with capital letters, for $y > 0$ the perturbation satisfies

$$\frac{\partial \boldsymbol{u}'}{\partial t} + U\frac{\partial \boldsymbol{u}'}{\partial x} = -\nabla p', \qquad \nabla \cdot \boldsymbol{u}' = 0, \tag{6.1a,b}$$

and a similar equation holds for $y < 0$, but with U replaced by $-U$. Given periodic boundary conditions in the x-direction, we may seek solutions of the form

$$\phi'(x, y, t) = \mathrm{Re} \sum_k \tilde{\phi}_k(y) \exp[\mathrm{i}k(x - ct)], \tag{6.2}$$

where ϕ is any field variable (e.g., pressure or velocity), and Re denotes that only the real part should be taken. (Typically we use tildes over variables to denote Fourier-like modes, and we will often omit the marker 'Re'.) Because (9.1a) is linear, the Fourier modes do not interact and we may confine attention to just one. Taking the divergence of (9.1a), the left-hand side vanishes and the pressure satisfies Laplace's equation

$$\nabla^2 p' = 0. \tag{6.3}$$

This has solutions in the form

$$p' = \begin{cases} \mathrm{Re}\, \tilde{p}_1 \mathrm{e}^{\mathrm{i}kx - ky} \mathrm{e}^{\sigma t} & y > 0, \\ \mathrm{Re}\, \tilde{p}_2 \mathrm{e}^{\mathrm{i}kx + ky} \mathrm{e}^{\sigma t} & y < 0, \end{cases} \tag{6.4}$$

where, anticipating the possibility of growing solutions, we have written the time variation in terms of a growth rate, $\sigma = -\mathrm{i}kc$. In general σ is complex: if it has a positive real component, the amplitude of the perturbation will grow and there is an instability; if σ has a non-zero imaginary component, then there will be oscillatory motion, and there may be both oscillatory motion *and* an instability. To obtain the dispersion relationship, we consider the y-component of (9.1a), namely (for $y > 0$)

$$\frac{\partial v_1'}{\partial t} + U\frac{\partial v_1'}{\partial x} = -\frac{\partial p_1'}{\partial y}. \tag{6.5}$$

Substituting a solution of the form $v_1' = \tilde{v}_1 \exp(\mathrm{i}kx + \sigma t)$ yields, with (9.4),

$$(\sigma + \mathrm{i}kU)\tilde{v}_1 = k\tilde{p}_1. \tag{6.6}$$

But the velocity normal to the interface is, at the interface, nothing but the rate of change of the position of the interface itself; that is, at $y = +0$

$$v_1 = \frac{\partial \eta'}{\partial t} + U\frac{\partial \eta'}{\partial x}, \tag{6.7}$$

or

$$\tilde{v}_1 = (\sigma + \mathrm{i}kU)\tilde{\eta}, \tag{6.8}$$

where η' is the displacement of the interface from its equilibrium position. Using this in (9.6) gives

$$(\sigma + \mathrm{i}kU)^2\tilde{\eta} = k\tilde{p}_1. \tag{6.9}$$

The above few equations pertain to motion on the $y > 0$ side of the interface. Similar reasoning on the other side gives (at $y = -0$)

$$(\sigma - \mathrm{i}kU)^2\tilde{\eta} = -k\tilde{p}_2. \tag{6.10}$$

But at the interface $p_1 = p_2$, because pressure must be continuous. The dispersion relationship then emerges from (9.9) and (9.10), giving

$$\sigma^2 = k^2U^2. \tag{6.11}$$

This equation has two roots, one of which is positive. Thus, the amplitude of the perturbation grows exponentially, like $\mathrm{e}^{\sigma t}$, and the flow is *unstable*. The instability itself can be seen in the natural world when billow clouds appear wrapped up into spirals: the clouds are acting as tracers of fluid flow, and are a manifestation of the instability at finite amplitude, as seen later in Fig. 9.6.

'Below, a myriad, myriad waves hastening, lifting up their necks,
Tending in ceaseless flow toward the track of the ship,
'Waves of the ocean bubbling and gurgling, blithely prying,
'Waves, undulating waves, liquid, uneven, emulous waves,
Toward that whirling current, laughing and buoyant.
Walt Whitman, *After the Sea-Ship*, in *Leaves of Grass*, 1881.

CHAPTER 7

Waves, Mean-Flows, and their Interaction

WAVE–MEAN-FLOW INTERACTION is concerned with how some mean-flow, perhaps a time or zonal average, interacts with a wave-like departure from that mean, and this chapter provides an elementary introduction to this topic. It is 'elementary' because our derivations and discussion are obtained by straightforward manipulations of the equations of motion in the simplest case that illustrates the relevant principle. It is implicit in what we do that it is a sensible thing to decompose the fields into a mean plus some departure, and one case when this is so is when the departure is of small amplitude. Departures from the mean — generically called *eddies* — are in reality not always small; for example, in the mid-latitude troposphere the eddies are often of similar amplitude to the mean-flow, and Chapters 12 and 13 explore this from the standpoint of turbulence. However, in this chapter we will assume that eddies are indeed of small amplitude, and, in particular, that eddy–mean-flow interaction is larger than eddy–eddy interaction.

A *wave* is an eddy that satisfies, at least approximately, a dispersion relation. It is the presence of such a dispersion relation that enables a number of results to be obtained that would otherwise be out of our reach. It is implicit in defining waves this way that they are generally of small amplitude, for it is this that allows the equations of motion to be sensibly linearized and a dispersion relation to be obtained (although some waves have finite amplitude and still satisfy a dispersion relation), and the interaction with the mean-flow calculated. The qualitative nature of such interaction can then provide insights into the finite-amplitude problem, and one goal of wave–mean-flow theory is to provide a way of qualitatively understanding more realistic situations, and to suggest diagnostics that might be used to analyze both observations and numerical solutions of the nonlinear problem. In this chapter we will largely concern ourselves with a *zonal* mean, since this is the simplest and often most useful case because of the presence of simple boundary conditions. We will also be mainly concerned with quasi-geostrophic dynamics on a β-plane (and hence Rossby waves), using Boussinesq dynamics, since here the concepts are most clearly illustrated. Thus, in this chapter the reader will find an introduction to such matters as the 'transformed Eulerian mean', the 'Eliassen–Palm flux' and the 'non-acceleration result', and later in the chapter we look at how some related ideas can be used to prove stability of a flow without invoking normal modes. Impatient readers who are anxious for real examples may wish to first look at Chapters 15 and 17 and then come back to this chapter as needed.

7.1 QUASI-GEOSTROPHIC WAVE–MEAN-FLOW INTERACTION

7.1.1 Preliminaries

To fix our dynamical system and notation, we write down the Boussinesq quasi-geostrophic potential vorticity equation

$$\frac{\partial q}{\partial t} + J(\psi, q) = D, \tag{7.1}$$

where D represents any non-conservative terms and the potential vorticity in a Boussinesq system is

$$q = \beta y + \zeta + \frac{\partial}{\partial z}\left(\frac{f_0}{N^2} b\right), \tag{7.2}$$

where ζ is the relative vorticity and b is the buoyancy perturbation from the background state characterized by N^2. (In an ideal gas $q = \beta y + \zeta + (f_0/\rho_R)\partial_z\left(\rho_R b/N^2\right)$, where ρ_R is a specified density profile, and most of our derivations can be extended to that case.) We will refer to lines of constant b as isentropes. In terms of the streamfunction, the variables are

$$\zeta = \nabla^2\psi, \qquad b = f_0\frac{\partial \psi}{\partial z}, \qquad q = \beta y + \left[\nabla^2 + \frac{\partial}{\partial z}\left(\frac{f_0^2}{N^2}\frac{\partial}{\partial z}\right)\right]\psi. \tag{7.3}$$

where $\nabla^2 \equiv (\partial_x^2 + \partial_y^2)$. The potential vorticity equation holds in the fluid interior; the boundary conditions on (10.3) are provided by the thermodynamic equation

$$\frac{\partial b}{\partial t} + J(\psi, b) + wN^2 = H, \tag{7.4}$$

where H represents heating terms. The vertical velocity at the boundary, w, is zero in the absence of topography and Ekman friction, and if H is also zero the boundary condition is just

$$\frac{\partial b}{\partial t} + J(\psi, b) = 0. \tag{7.5}$$

Equations (10.1) and (10.5) are the evolution equations for the system and if both D and H are zero they conserve both the total energy, $\widehat{E}$ and the total enstrophy, $\widehat{Z}$:

$$\begin{aligned} \frac{\mathrm{d}\widehat{E}}{\mathrm{d}t} &= 0, \qquad \widehat{E} = \frac{1}{2}\int_V (\nabla\psi)^2 + \frac{f_0^2}{N^2}\left(\frac{\partial\psi}{\partial z}\right)^2 \mathrm{d}V, \\ \frac{\mathrm{d}\widehat{Z}}{\mathrm{d}t} &= 0, \qquad \widehat{Z} = \frac{1}{2}\int_V q^2\,\mathrm{d}V, \end{aligned} \tag{7.6}$$

where V is a volume bounded by surfaces at which the normal velocity is zero, or that has periodic boundary conditions. The enstrophy is also conserved layerwise; that is, the horizontal integral of q^2 is conserved at every level.

7.1.2 Potential Vorticity Flux in the Linear Equations

Let us decompose the fields into a mean (to be denoted with an overbar) plus a perturbation (denoted with a prime), and let us suppose the perturbation fields are of small amplitude. (In linear problems, such as those considered in Chapter 9, we decomposed the flow into a 'basic state' plus a perturbation, with the basic state fixed in time. Our approach here is similar, but soon we will allow the mean state to evolve.) The linearized quasi-geostrophic potential vorticity equation is then

$$\frac{\partial q'}{\partial t} + \overline{u}\frac{\partial q'}{\partial x} + u'\frac{\partial \overline{q}}{\partial x} + \overline{v}\frac{\partial q'}{\partial y} + v'\frac{\partial \overline{q}}{\partial y} = D', \tag{7.7}$$

where D' represents eddy forcing and dissipation and, in terms of streamfunction,

$$(u'(x,y,z,t), v'(x,y,z,t)) = \left(-\frac{\partial \psi'}{\partial y}, \frac{\partial \psi'}{\partial x}\right), \tag{7.8a}$$

$$q'(x,y,z,t) = \nabla^2 \psi' + \frac{\partial}{\partial z}\left(\frac{f_0^2}{N^2}\frac{\partial \psi'}{\partial z}\right). \tag{7.8b}$$

If the mean is a zonal mean then $\partial \overline{q}/\partial x = 0$ and $\overline{v} = 0$ (because v is purely geostrophic) and (10.7) simplifies to

$$\frac{\partial q'}{\partial t} + \overline{u}\frac{\partial q'}{\partial x} + v'\frac{\partial \overline{q}}{\partial y} = D', \tag{7.9}$$

where

$$\overline{q} = \beta y - \frac{\partial \overline{u}}{\partial y} + \frac{\partial}{\partial z}\left(\frac{f_0}{N^2}\overline{b}\right), \quad \text{and} \quad \frac{\partial \overline{q}}{\partial y} = \beta - \frac{\partial^2 \overline{u}}{\partial y^2} - \frac{\partial}{\partial z}\left(\frac{f_0^2}{N^2}\frac{\partial \overline{u}}{\partial z}\right). \tag{7.10a,b}$$

using thermal wind, $f_0 \partial \overline{u}/\partial z = -\partial b/\partial y$.

Multiplying by q' and zonally averaging gives the enstrophy equation:

$$\frac{1}{2}\frac{\partial}{\partial t}\overline{q'^2} = -\overline{v'q'}\frac{\partial \overline{q}}{\partial y} + \overline{D'q'}. \tag{7.11}$$

The quantity $\overline{v'q'}$ is the meridional flux of potential vorticity; this is downgradient (by definition) when the first term on the right-hand side is positive (i.e., $\overline{v'q'}\partial \overline{q}/\partial y < 0$), and it then acts to increase the variance of the perturbation. (This occurs, for example, when the flux is diffusive so that $\overline{v'q'} = -\kappa \partial \overline{q}/\partial y$, where κ may vary but is everywhere positive.) This argument may be inverted: for inviscid flow ($D = 0$), if the waves are growing, as for example in the canonical models of baroclinic instability discussed in Chapter 9, then *the potential vorticity flux is downgradient*.

If the second term on the right-hand side of (10.11) is negative, as it will be if D' is a dissipative process (e.g., if $D' = A\nabla^2 q'$ or if $D' = -rq'$, where A and r are positive) then a statistical balance can be achieved between enstrophy production via downgradient transport, and dissipation. If the waves are steady (by which we mean statistically steady, neither growing nor decaying in amplitude) and conservative (i.e., $D' = 0$) then we must have

$$\overline{v'q'} = 0. \tag{7.12}$$

Similar results follow for the buoyancy at the boundary; we start by linearizing the thermodynamic equation (10.5) to give

$$\frac{\partial b'}{\partial t} + \overline{u}\frac{\partial b'}{\partial x} + v'\frac{\partial \overline{b}}{\partial y} = H', \tag{7.13}$$

where H' is a diabatic source term. Multiplying (10.13) by b' and averaging gives

$$\frac{1}{2}\frac{\partial}{\partial t}\overline{b'^2} = -\overline{v'b'}\frac{\partial \overline{b}}{\partial y} + \overline{H'b'}. \tag{7.14}$$

Thus growing adiabatic waves have a downgradient flux of buoyancy at the boundary. In the Eady problem there is no interior gradient of basic-state potential vorticity and all the terms in (10.11) are zero, but the perturbation grows at the boundary. If the waves are steady and adiabatic then, analogously to (10.12),

$$\overline{v'b'} = 0. \tag{7.15}$$

The boundary conditions and fluxes may be absorbed into the interior definition of potential vorticity and its fluxes by way of the delta-function boundary layer construction, described in Section 5.4.3. In models with discrete vertical layers or a finite number of levels it is common practice to absorb the boundary conditions into the definition of potential vorticity at top and bottom.

7.1.3 Wave–Mean-Flow Interaction

In linear problems we usually suppose that the mean-flow is fixed and that the zonal mean terms, $\overline{u}$ and $\overline{q}$ in (10.9), are functions only of y and z. However, in reality we might expect that the mean-flow would change because of momentum and heat flux convergences arising from the eddy–eddy interactions. To calculate these changes we begin with the potential vorticity equation (10.1) and, in the usual way, express the variables as a zonal mean plus an eddy term and obtain

$$\frac{\partial \overline{q}}{\partial t} + \nabla \cdot (\overline{\boldsymbol{u}}\,\overline{q}) + \nabla \cdot (\overline{\boldsymbol{u}'q'}) = \overline{D}. \tag{7.16}$$

Now, since the mean-flow is a zonal mean, and $\overline{v} = 0$, the first term is zero and the mean-flow evolves according to

$$\frac{\partial \overline{q}}{\partial t} + \frac{\partial}{\partial y}\overline{v'q'} = \overline{D}. \tag{7.17}$$

Similarly, at the boundary the mean buoyancy evolution equation is

$$\frac{\partial \overline{b}}{\partial t} + \frac{\partial}{\partial y}\overline{v'b'} = \overline{H}. \tag{7.18}$$

To obtain $\overline{u}$ from $\overline{q}$ and $\overline{b}$ we use thermal wind balance to define a streamfunction Ψ. That is, since

$$f_0 \frac{\partial \overline{u}}{\partial z} = -\frac{\partial \overline{b}}{\partial y}, \quad \text{then} \quad \left(\overline{u}, \frac{1}{f_0}\overline{b}\right) = \left(-\frac{\partial \Psi}{\partial y}, \frac{\partial \Psi}{\partial z}\right) \tag{7.19a,b}$$

whence, using (10.10a), the potential vorticity is

$$\overline{q}(y,z,t) - \beta y = \frac{\partial}{\partial z}\left(\frac{f_0^2}{N^2}\frac{\partial \Psi}{\partial z}\right) + \frac{\partial^2 \Psi}{\partial y^2}. \tag{7.20}$$

If $\overline{q}$ is known in the interior from (10.18), and $\overline{b}$ (i.e., $f_0 \partial\Psi/\partial z$) is known at the boundaries, then $\overline{u}$ and $\overline{b}$ in the interior may be obtained using (10.20) and (10.19b). The equations are also summarized in the grey box on page 390.

To close the system we suppose that the eddy terms themselves evolve according to (10.9) and (10.13). If in those equations we were to include the eddy–eddy interaction terms we would simply recover the full system, so in neglecting those terms we have constructed an eddy–mean-flow system, commonly called a *wave–mean-flow* system because by eliminating the nonlinear terms in the perturbation equation the eddies will often be wavelike. Non quasi-geostrophic wave–mean-flow systems may be constructed in a similar fashion: for example, we could construct a system using the primitive equations with separate equations for eddy and zonal-mean temperature and velocity fields, and an example involving gravity waves is given in Chapter 17.

It is important to realise that such systems do differ from linear ones. In constructing linear systems we posit that the eddy terms are small compared to the mean-flow and thus neglect the eddy–eddy interaction terms and keep the mean-flow fixed. In a wave–mean-flow problem we similarly suppose the eddy terms are small, and we neglect eddy–eddy interaction terms where they produce another eddy, because the terms involving the mean-flow are larger. However, in the mean-flow equation, (10.16), there are no mean-flow terms that are larger, so we keep the eddy–eddy terms and allow the mean-flow to evolve. Such a justification is hardly a rigorous one, since if the eddy terms are small then the effects on the mean-flow will be small, and so one might suppose that the mean-flow should be held fixed. The wave–mean-flow equations really can only be justified on a case-by-case basis with a detailed examination of the size of the terms and the rate at which they evolve, and that is the subject of weakly nonlinear theory. Another justification for wave–mean-flow problems is that they lead to insight into the behaviour of the full system.

We now consider some more properties of the waves themselves — how they propagate and what they conserve — beginning with a discussion of the potential vorticity flux and its relative, the Eliassen–Palm flux

Shootings of water thread down the slope
of the huge green stone —
The white eddy-rose that blossom'd up
against the stream in the scollop,
by fits and starts, obstinate in resurrection —
'It is the life *that we live.*
Samuel Taylor Coleridge, *The Eddy-Rose,* adapted from notebook, 1799.

CHAPTER 8

Basics of Incompressible Turbulence

TURBULENCE IS HIGH REYNOLDS NUMBER FLUID FLOW, dominated by nonlinearity, containing both spatial and temporal disorder. No definition is perfect, and it is hard to disentangle a definition from a property, but this statement captures the essential aspects. A turbulent flow has eddies with a spectrum of sizes between some upper and lower bounds, the former often determined by the forcing scale or the domain scale, and the latter usually by viscosity. The individual eddies come and go, and are inherently unpredictable. Rather like life, turbulent flows are endlessly fascinating and not a little frustrating.[15]

The circulation of the atmosphere and ocean is, *inter alia,* the motion of a forced-dissipative fluid subject to various constraints such as rotation and stratification. The larger scales are orders of magnitude larger than the dissipation scale (the scale at which molecular viscosity becomes important) and at many if not all scales the motion is highly nonlinear and quite unpredictable. Thus, we can justifiably say that the atmosphere and ocean are turbulent fluids. We are not simply talking about the small-scale flows traditionally regarded as turbulent; rather, our main focus will be the large-scale flows associated with baroclinic instability and greatly influenced by rotation and stratification, a kind of turbulence known as *geostrophic turbulence*. However, before discussing turbulence in the atmosphere and ocean, in this chapter we consider from a fairly elementary standpoint the basic theory of two- and three-dimensional turbulence, and in particular the theory of inertial ranges. We do not provide a comprehensive discussion of turbulence; rather, we provide an introduction to those aspects of most interest or relevance to the dynamical oceanographer or meteorologist. In the next chapter we consider the effects of rotation and stratification, and after that we look at turbulent diffusion.

8.1 THE FUNDAMENTAL PROBLEM OF TURBULENCE

Turbulence is a difficult subject because it is nonlinear, and because, and relatedly, there are interactions between scales of motion. Let us first see what difficulties these bring, beginning with the closure problem itself.

8.1.1 The Closure Problem

Although in a turbulent flow it may be virtually impossible to predict the detailed motion of each eddy, the statistical properties — time averages for example — are not necessarily changing and we

might like to predict such averages. Effectively, we accept that we cannot predict the weather, but we can try to predict the climate. Even though we know the equations that determine the system, this task proves to be very difficult because the equations are nonlinear, and we come up against the *closure problem*. To see what this is, let us decompose the velocity field into mean and fluctuating components,

$$\boldsymbol{v} = \overline{\boldsymbol{v}} + \boldsymbol{v}'. \tag{8.1}$$

Here $\overline{\boldsymbol{v}}$ is the mean velocity field, and $\boldsymbol{v}'$ is the deviation from that mean. The mean might be a time average, in which case $\overline{\boldsymbol{v}}$ is a function only of space and not of time, or it might be a time mean over a finite period (e.g., a season if we are dealing with the weather), or it might be some form of ensemble mean. The average of the deviation is, by definition, zero; that is $\overline{\boldsymbol{v}'} = 0$. The idea is to substitute (11.1) into the momentum equation and try to obtain a closed equation for the mean quantity $\overline{\boldsymbol{v}}$. Rather than dealing with the full Navier–Stokes equations, let us carry out this program for a model nonlinear system that obeys

$$\frac{\mathrm{d}u}{\mathrm{d}t} + uu + ru = 0, \tag{8.2}$$

where r is a constant. The average of this equation is:

$$\frac{\mathrm{d}\overline{u}}{\mathrm{d}t} + \overline{uu} + r\overline{u} = 0. \tag{8.3}$$

The value of the term $\overline{uu}$ (i.e., $\overline{u^2}$) is not deducible simply by knowing $\overline{u}$, since it involves correlations between eddy quantities, namely $\overline{u'u'}$. That is, $\overline{uu} = \overline{u}\,\overline{u} + \overline{u'u'} \neq \overline{u}\,\overline{u}$. We can go to the next order to try (vainly!) to obtain an equation for $\overline{u}\,\overline{u}$. First multiply (11.2) by u to obtain an equation for u^2, and then average it to yield

$$\frac{1}{2}\frac{\mathrm{d}\overline{u^2}}{\mathrm{d}t} + \overline{uuu} + r\overline{u^2} = 0. \tag{8.4}$$

This equation contains the undetermined cubic term $\overline{uuu}$. An equation determining this would contain a quartic term, and so on in an unclosed hierarchy. Many methods of closing the hierarchy make assumptions about the relationship of $(n+1)$th order terms to nth order terms, for example by supposing that

$$\overline{uuuu} = \alpha\overline{uu}\,\overline{uu} + \beta\overline{uuu}, \tag{8.5}$$

where α and β are some parameters, and closures set in physical space or in spectral space (i.e., acting on the Fourier transformed variables) have both been proposed. If we know that the variables are distributed normally then such closures can sometimes be made exact, but this is not generally the case in turbulence and all closures that have been proposed so far are, at best, approximations.

This same closure problem arises in the Navier–Stokes equations. If density is constant (say $\rho = 1$) the x-momentum equation for an averaged flow is

$$\frac{\partial\overline{u}}{\partial t} + (\overline{\boldsymbol{v}}\cdot\nabla)\overline{u} = -\frac{\partial\overline{p}}{\partial x} - \nabla\cdot\overline{\boldsymbol{v}'u'}. \tag{8.6}$$

Written out in full in Cartesian coordinates, the last term is

$$\nabla\cdot\overline{\boldsymbol{v}'u'} = \frac{\partial}{\partial x}\overline{u'u'} + \frac{\partial}{\partial y}\overline{u'v'} + \frac{\partial}{\partial z}\overline{u'w'}. \tag{8.7}$$

These terms, and the similar ones in the y- and z-momentum equations, represent the effects of eddies on the mean flow and are known as *Reynolds stress* terms. The 'closure problem' of turbulence may be thought of as finding a representation of such Reynolds stress terms in terms of mean

flow quantities. Nobody has been able to close the system, in any useful way, without introducing physical assumptions not directly deducible from the equations of motion themselves. Indeed, not only has the problem not been solved, it is not clear that in general a useful closed-form solution actually exists.

8.1.2 Triad Interactions in Turbulence

The nonlinear term in the equations of motion not only leads to difficulties in closing the equations, but it leads to interactions among different length scales, and in this section we write the equations of motion in a form that makes this explicit. For algebraic simplicity we will restrict our attention to two-dimensional flows, but very similar considerations also apply in three dimensions, and the details of the algebra following are not of themselves important to subsequent sections.[16]

The equation of motion for an incompressible fluid in two dimensions — see for example (4.67) or (5.119) — may be written as

$$\frac{\partial \zeta}{\partial t} + J(\psi, \zeta) = F + \nu \nabla^2 \zeta, \qquad \zeta = \nabla^2 \psi. \tag{8.8}$$

We include a forcing and viscous term but no Coriolis term. Let us suppose that the fluid is contained in a square, doubly-periodic domain of side L, and let us expand the streamfunction and vorticity in Fourier series so that, with a tilde denoting a Fourier coefficient,

$$\psi(x, y, t) = \sum_{\boldsymbol{k}} \tilde{\psi}(\boldsymbol{k}, t) \mathrm{e}^{\mathrm{i}\boldsymbol{k}\cdot\boldsymbol{x}}, \qquad \zeta(x, y, t) = \sum_{\boldsymbol{k}} \tilde{\zeta}(\boldsymbol{k}, t) \mathrm{e}^{\mathrm{i}\boldsymbol{k}\cdot\boldsymbol{x}}, \tag{8.9}$$

where $\boldsymbol{k} = \mathbf{i}k^x + \mathbf{j}k^y$, $\tilde{\zeta} = -k^2\tilde{\psi}$ where $k^2 = k^{x2} + k^{y2}$ and, to ensure that ψ is real, $\tilde{\psi}(k^x, k^y, t) = \tilde{\psi}^*(-k^x, -k^y, t)$, where * denotes the complex conjugate, and this property is known as conjugate symmetry. The summations are over all positive and negative x- and y-wavenumbers, and $\tilde{\psi}(\boldsymbol{k}, t)$ is shorthand for $\tilde{\psi}(k^x, k^y, t)$. Substituting (11.9) in (11.8) gives, with (for the moment) F and ν both zero,

$$\begin{aligned} \frac{\partial}{\partial t} \sum_{\boldsymbol{k}} \tilde{\zeta}(\boldsymbol{k}, t) \mathrm{e}^{\mathrm{i}\boldsymbol{k}\cdot\boldsymbol{x}} = &\sum_{\boldsymbol{p}} p^x \tilde{\psi}(\boldsymbol{p}, t) \mathrm{e}^{\mathrm{i}\boldsymbol{p}\cdot\boldsymbol{x}} \times \sum_{\boldsymbol{q}} q^y \tilde{\zeta}(\boldsymbol{q}, t) \mathrm{e}^{\mathrm{i}\boldsymbol{q}\cdot\boldsymbol{x}} \\ &- \sum_{\boldsymbol{p}} p^y \tilde{\psi}(\boldsymbol{p}, t) \mathrm{e}^{\mathrm{i}\boldsymbol{p}\cdot\boldsymbol{x}} \times \sum_{\boldsymbol{q}} q^x \tilde{\zeta}(\boldsymbol{q}, t) \mathrm{e}^{\mathrm{i}\boldsymbol{q}\cdot\boldsymbol{x}}, \end{aligned} \tag{8.10}$$

where $\boldsymbol{p}$ and $\boldsymbol{q}$ are, like $\boldsymbol{k}$, horizontal wave vectors. We may obtain an evolution equation for the wavevector $\boldsymbol{k}$ by multiplying (11.10) by $\exp(-\mathrm{i}\boldsymbol{k}\cdot\boldsymbol{x})$ and integrating over the domain, and using the fact that the Fourier modes are orthogonal; that is

$$\int \mathrm{e}^{\mathrm{i}\boldsymbol{p}\cdot\boldsymbol{x}} \mathrm{e}^{\mathrm{i}\boldsymbol{q}\cdot\boldsymbol{x}} \, \mathrm{d}A = L^2 \delta(\boldsymbol{p} + \boldsymbol{q}), \tag{8.11}$$

where $\delta(\boldsymbol{p}+\boldsymbol{q})$ equals unity if $\boldsymbol{p} = -\boldsymbol{q}$ and is zero otherwise. Using this, (11.10) becomes, restoring the forcing and dissipation terms,

$$\frac{\partial}{\partial t} \tilde{\psi}(\boldsymbol{k}, t) = \sum_{\boldsymbol{p},\boldsymbol{q}} A(\boldsymbol{k}, \boldsymbol{p}, \boldsymbol{q}) \tilde{\psi}(\boldsymbol{p}, t) \tilde{\psi}(\boldsymbol{q}, t) + \tilde{F}(\boldsymbol{k}) - \nu k^2 \tilde{\psi}(\mathbf{k}, t), \tag{8.12}$$

where $A(\boldsymbol{k}, \boldsymbol{p}, \boldsymbol{q}) = (q^2/k^2)(p^x q^y - p^y q^x)\delta(\boldsymbol{p} + \boldsymbol{q} - \mathbf{k})$ is an 'interaction coefficient', and the summation is over all $\boldsymbol{p}$ and $\boldsymbol{q}$; however, only those wavevector triads with $\boldsymbol{p} + \boldsymbol{q} = \mathbf{k}$ make a non-zero contribution, because of the presence of the delta function.

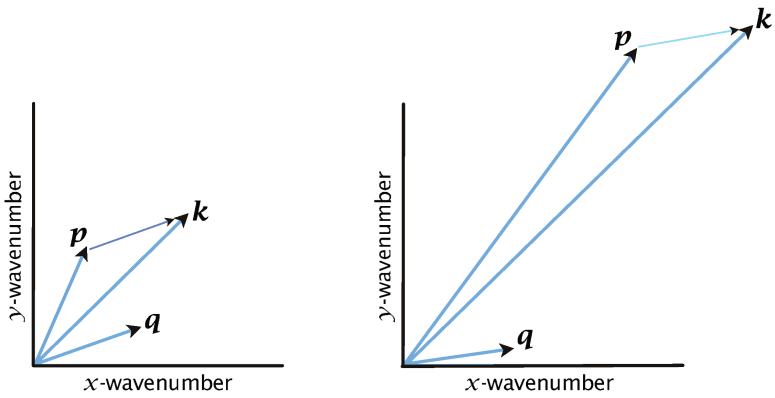

Fig. 8.1 Two interacting triads, each with $\boldsymbol{k} = \boldsymbol{p} + \boldsymbol{q}$. On the left, a local triad with $k \sim p \sim q$. On the right, a non-locpwal triad with $k \sim p \gg q$.

Consider, then, a fluid in which just two Fourier modes are initially excited, with wavevectors $\boldsymbol{p}$ and $\boldsymbol{q}$, along with their conjugate-symmetric partners at $-\boldsymbol{p}$ and $-\boldsymbol{q}$. These modes interact, obeying (11.12), to generate third and fourth wavenumbers, $\boldsymbol{k} = \boldsymbol{p} + \boldsymbol{q}$ and $\boldsymbol{m} = \boldsymbol{p} - \boldsymbol{q}$ (along with their conjugate-symmetric partners). These four wavenumbers can interact among themselves to generate several additional wavenumbers, $\boldsymbol{k} + \boldsymbol{p}$, $\boldsymbol{k} + \boldsymbol{m}$ and so on, so potentially filling out the entire spectrum of wavenumbers. The individual interactions are called *triad interactions,* and it is by way of such interactions that energy is transferred between scales in turbulent flows, in both two and three dimensions. The dissipation term does not lead to interactions between modes with different wavevectors; rather, it acts like a drag on each Fourier mode, with a coefficient that increases with wavenumber and therefore that preferentially affects small scales.

The selection rule for triad interactions — that $\boldsymbol{k} = \boldsymbol{p} + \boldsymbol{q}$ — does not restrict the scales of these interacting wavevectors, and the types of triad interactions fall between two extremes:

(i) local interactions, in which $k \sim p \sim q$;

(ii) non-local interactions, in which $k \sim p \gg q$.

These two kinds of triads are schematically illustrated in Fig. 11.1. Without a detailed analysis of the solutions of the equations of motion — an analysis that is in general impossible for fully-developed turbulence — we cannot say with certainty whether one kind of triad interaction dominates. The theory of Kolmogorov considered below, and its two-dimensional analogue, assume that it is the *local* triads that are most important in transferring energy; this is a reasonable assumption because, from the perspective of a small eddy, large eddies appear as a nearly-uniform flow and so translate the small eddies around without distortion and thus without transferring energy between scales.

8.2 THE KOLMOGOROV THEORY

The foundation of many theories of turbulence is the spectral theory of Kolmogorov.[17] This theory does not close the equations as explicit a manner as (11.5), but it does provide a prediction for the energy spectrum of a turbulent flow (i.e., how much energy is present at a particular spatial scale) and it does this by suggesting a relationship between the energy spectrum (a second-order quantity in velocity) and the spectral energy flux (a third-order quantity).

8.2.1 The Physical Picture

Consider high Reynolds number (Re) incompressible flow that is being maintained by some external force. Then the evolution of a system that has $\rho = 1$ is governed by

$$\frac{\partial \boldsymbol{v}}{\partial t} + (\boldsymbol{v} \cdot \nabla)\boldsymbol{v} = -\nabla p + \boldsymbol{F} + \nu \nabla^2 \boldsymbol{v} \tag{8.13}$$

and

$$\nabla \cdot \boldsymbol{v} = 0. \tag{8.14}$$

Here, $\boldsymbol{F}$ is some force we apply to maintain fluid motion — for example, we stir the fluid with a spoon. (One might argue that such stirring is not a force, like gravity, but a continuous changing of the boundary conditions. Having noted this, we treat it as a force.) A simple scale analysis of these equations seems to indicate that the ratio of the size of the inertial terms on the left-hand side to the viscous term is the Reynolds number VL/ν, where V and L are velocity and length scales. To be explicit let us consider the ocean, and take $V = 0.1\,\mathrm{m\,s^{-1}}$, $L = 1000\,\mathrm{km}$ and $\nu = 10^{-6}\,\mathrm{m^2\,s^{-1}}$. Then $Re = VL/\nu \approx 10^{11}$, and it seems that we can neglect the viscous term on the right-hand side of (11.13). But this can lead to a paradox, as if the fluid is being forced this forcing is likely to put energy into the fluid. To see this, we obtain the energy budget for (11.13) by multiplying by $\boldsymbol{v}$ and integrating over a domain. If there is no flow into or out of our domain, the inertial terms in the momentum equation conserve energy and, recalling Section 1.10, the energy equation is

$$\frac{\mathrm{d}\widehat{E}}{\mathrm{d}t} = \frac{\mathrm{d}}{\mathrm{d}t}\int \frac{1}{2}\boldsymbol{v}^2\,\mathrm{d}V = \int \left(\boldsymbol{F}\cdot\boldsymbol{v} + \nu\boldsymbol{v}\cdot\nabla^2\boldsymbol{v}\right)\,\mathrm{d}V = \int \left(\boldsymbol{F}\cdot\boldsymbol{v} - \nu\boldsymbol{\omega}^2\right)\,\mathrm{d}V, \tag{8.15}$$

where $\widehat{E}$ is the total energy. If we neglect the viscous term we are led to an inconsistency, since the forcing term is a source of energy ($\overline{\boldsymbol{F}\cdot\boldsymbol{v}} > 0$), because a force will normally, on average, produce a velocity that is correlated with the force itself. Without viscosity, energy keeps on increasing.

What is amiss? It is true that for motion with a 1000 km length scale and a velocity of a few centimetres per second we can neglect viscosity when considering the balance of forces in the momentum equation. But this does not mean that there is no motion at much smaller length scales — indeed we seem to be led to the inescapable conclusion that there must be some motion at smaller scales in order to remove energy. Scale analysis of the momentum equation suggests that viscous terms will be comparable with the inertial terms at a scale L_ν where the Reynolds number based on that scale is of order unity, giving

$$L_\nu \sim \frac{\nu}{V}. \tag{8.16}$$

This is a very small scale for geophysical flows, of order millimetres or less. Where and how are such small scales generated? Boundaries are one important region; if there is high Reynolds number flow above a solid boundary, for example the wind above the ground, then viscosity *must* become important in bringing the velocity to zero in order that it can satisfy the no-slip condition at the surface, as illustrated in Fig. 5.4.

Motion on very small scales may also be generated in the fluid interior. How might this happen? Suppose the forcing acts only at large scales, and its direct action is to set up some correspondingly large-scale flow, composed of eddies and shear flows and such-like. Then typically there will be an instability in the flow, and a smaller eddy will grow: initially, the large-scale flow may be treated as an unchanging shear flow, and the disturbance while small will obey linear equations of motion similar to those applicable in an idealized Kelvin–Helmholtz instability. This instability clearly must draw from the large scale quasi-stationary flow, and it will eventually saturate at some finite amplitude. Although it has grown in intensity, it is still typically smaller than the large scale flow that fostered it (remember how the growth rate of the shear instability gets larger as the wavelength of the perturbation decreased). As it reaches finite amplitude, the perturbation itself may become unstable, and smaller eddies will feed off its energy and grow, and so on.[18] Vortex stretching plays an important role in all this, stretching line elements and creating eddies, and energy, at small scales. The general picture that emerges is of a large-scale flow that is unstable to eddies somewhat smaller in scale. These eddies grow, and develop still smaller eddies, and energy is transferred to smaller and smaller scales in a cascade-like process, sketched in Fig. 11.2. Finally, eddies are generated that are sufficiently small that they feel the effects of viscosity, and energy is drained away. Thus, there is a flux of kinetic energy from the large to the small scales, where it is dissipated into heat.

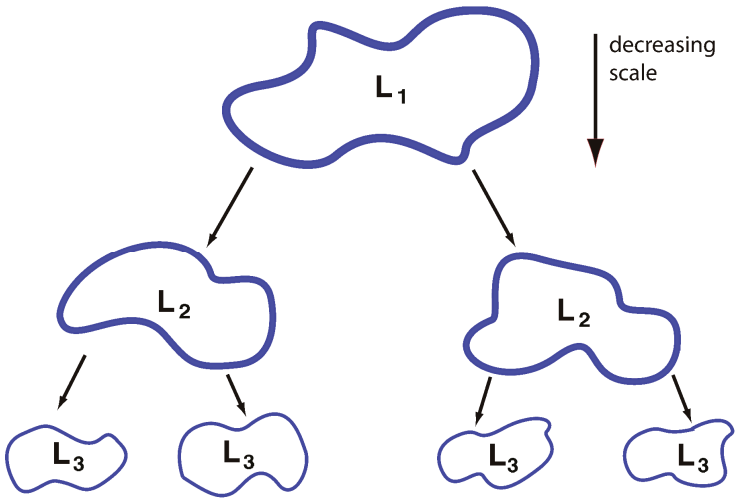

Fig. 8.2 The passage of energy to smaller scales: eddies at large scale break up into ones at smaller scale, thereby transferring energy to smaller scales. (The eddies in reality are embedded within each other.)

If the passage occurs between eddies of similar sizes (i.e., if it is spectrally local) the transfer is said to be a cascade.

8.2.2 Inertial-range Theory

Given the above picture it becomes possible to predict what the energy spectrum is. Let us suppose that the flow is statistically isotropic (i.e., the same in all directions) and homogeneous (i.e., the same everywhere; all isotropic flows are homogeneous, but not vice versa). Homogeneity precludes the presence of solid boundaries but can be achieved in a periodic domain, and the finite domain puts an upper limit, sometimes called the outer scale, on the size of eddies.

If we decompose the velocity field into Fourier components, then in a finite domain we may write

$$u(x,y,z,t) = \sum_{\boldsymbol{k}} \widetilde{u}(\boldsymbol{k},t)\mathrm{e}^{\mathrm{i}(k^x x + k^y y + k^z z)}, \tag{8.17}$$

where $\widetilde{u}$ is the Fourier transformed field of u, with similar identities for v and w, and $\boldsymbol{k} = (k^x, k^y, k^z)$. The sum is a triple sum over all wavenumbers (k^x, k^y, k^z), and in a finite domain these wavenumbers are quantized. Finally, to ensure that u is real we require that $\widetilde{u}(-\boldsymbol{k}) = \widetilde{u}^*(\boldsymbol{k})$, where the asterisk denotes the complex conjugate. Using Parseval's theorem (and assuming density is unity, as we shall throughout this chapter) the energy in the fluid is given by

$$\frac{1}{V}\int_V E\,\mathrm{d}V = \frac{1}{2V}\int_V \left(u^2 + v^2 + w^2\right)\,\mathrm{d}V = \frac{1}{2}\sum_{\boldsymbol{k}}\left(|\widetilde{u}|^2 + |\widetilde{v}|^2 + |\widetilde{w}|^2\right) \equiv \sum_{\boldsymbol{k}} \mathcal{E}_{\boldsymbol{k}}, \tag{8.18}$$

where E is the energy density per unit mass, V is the volume of the domain, and the last equality serves to define the discrete energy spectrum $\mathcal{E}_{\boldsymbol{k}}$. We will now assume that the turbulence is isotropic, and that the domain is sufficiently large that the sums in the above equations may be replaced by integrals. We may then write

$$\overline{E} = \frac{1}{V}\widehat{E} = \frac{1}{2V}\int_V \boldsymbol{v}^2\,\mathrm{d}V = \int \mathcal{E}(k)\,\mathrm{d}k, \tag{8.19}$$

where $\overline{E}$ is the average energy, $\widehat{E}$ is the total energy and $\mathcal{E}(k)$ is the energy spectral density, or the energy spectrum, so that $\mathcal{E}(k)\delta k$ is the energy in the small wavenumber interval δk. Because of the assumed isotropy, the energy is a function only of the scalar wavenumber k, where $k^2 = k^{x2} + k^{y2} + k^{z2}$. The units of $\mathcal{E}(k)$ are L^3/T^2 and the units of $\overline{E}$ are L^2/T^2.

We now suppose that the fluid is stirred at large scales and, via the nonlinear terms in the momentum equation, that this energy is transferred to small scales where it is dissipated by viscosity. The key assumption is to suppose that, if the forcing scale is sufficiently larger than the dissipation

Dimensions and the Kolmogorov Spectrum

Quantity	Dimension
Wavenumber, k	1/L
Energy per unit mass, E	$U^2 = L^2/T^2$
Energy spectrum, $\mathcal{E}(k)$	$EL = L^3/T^2$
Energy flux, ε	$E/T = L^2/T^3$

If $\mathcal{E} = f(\varepsilon, k)$ then the only dimensionally consistent relation for the energy spectrum is

$$\mathcal{E} = \mathcal{K}\varepsilon^{2/3}k^{-5/3},$$

where $\mathcal{K}$ is a dimensionless constant.

scale, there exists a range of scales that is intermediate between the large scale and the dissipation scale and where neither forcing nor dissipation are explicitly important to the dynamics. This assumption, known as the *locality hypothesis,* depends on the nonlinear transfer of energy being sufficiently local (in spectral space). This intermediate range is known as the *inertial range,* because the inertial terms and not forcing or dissipation must dominate in the momentum balance. If the rate of energy input per unit volume by stirring is equal to ε, then if we are in a steady state there must be a flux of energy from large to small scales that is also equal to ε, and an energy dissipation rate, also ε.

Now, we have no general theory for the energy spectrum of a turbulent fluid, but we might suppose it takes the general form

$$\mathcal{E}(k) = g(\varepsilon, k, k_0, k_\nu), \tag{8.20}$$

where the right-hand side denotes a function of the spectral energy flux or cascade rate ε, the wavenumber k, the forcing wavenumber k_0 and the wavenumber at which dissipation acts, k_ν (and $k_\nu \sim L_\nu^{-1}$). The function g will of course depend on the particular nature of the forcing. Now, the locality hypothesis essentially says that at some scale within the inertial range the flux of energy to smaller scales depends only on processes occurring at or near that scale. That is to say, the energy flux is only a function of $\mathcal{E}$ and k, or equivalently that the energy spectrum can be a function *only* of the energy flux ε and the wavenumber itself. From a physical point of view, as energy cascades to smaller scales the details of the forcing are forgotten but the effects of viscosity are not yet apparent, and the energy spectrum takes the form,

$$\mathcal{E}(k) = g(\varepsilon, k). \tag{8.21}$$

The function g is assumed to be *universal,* the same for every turbulent flow.

Let us now use dimensional analysis to give us the form of the function $g(\varepsilon, k)$ (see the shaded box on page 419). In (11.21), the left-hand side has dimensions L^3/T^2; the factor T^{-2} can only be balanced by $\varepsilon^{2/3}$ because k has no time dependence; that is, (11.21), and its dimensions, must take the form

$$\mathcal{E}(k) = \varepsilon^{2/3} g(k), \tag{8.22a}$$

$$\frac{L^3}{T^2} \sim \frac{L^{4/3}}{T^2} g(k), \tag{8.22b}$$

where $g(k)$ is some function. Evidently $g(k)$ must have dimensions $L^{5/3}$, and the functional rela-

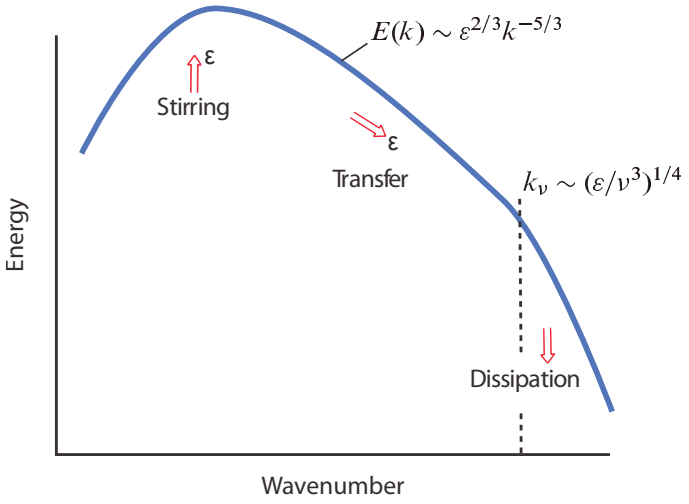

Fig. 8.3 The energy spectrum in three-dimensional turbulence, in the theory of Kolmogorov. Energy is supplied at some rate ε; it is cascaded to small scales, where it is ultimately dissipated by viscosity. There is no systematic energy transfer to scales larger than the forcing scale, so here the energy falls off.

tionship we must have, if the physical assumptions are right, is

$$\mathcal{E}(k) = \mathcal{K}\varepsilon^{2/3}k^{-5/3}. \tag{8.23}$$

This is the famous 'Kolmogorov -5/3 spectrum', enshrined as one of the cornerstones of turbulence theory. It is sketched in Fig. 11.3, and some experimental results are shown in Fig. 11.4. The parameter $\mathcal{K}$ is a dimensionless constant, undetermined by this theory; it is known as Kolmogorov's constant and experimentally its value is found to be about 1.5.[19]

An equivalent, and revealing, way to derive this result is to first define an eddy turnover time τ_k, which is the time taken for a parcel with velocity v_k to move a distance $1/k$, v_k being the velocity associated with the (inverse) scale k. On dimensional considerations $v_k = [\mathcal{E}(k)k]^{1/2}$ so that

$$\tau_k = \left[k^3\mathcal{E}(k)\right]^{-1/2}. \tag{8.24}$$

Kolmogorov's assumptions are then equivalent to setting

$$\varepsilon \sim \frac{v_k^2}{\tau_k} = \frac{k\mathcal{E}(k)}{\tau_k}. \tag{8.25}$$

If we demand that ε be a constant then (11.24) and (11.25) yield (11.23).

The viscous scale and energy dissipation

At some small length scale we should expect viscosity to become important and the scaling theory we have just set up will fail. What is that scale? In the inertial range friction is unimportant because the time scales on which it acts are too long for it be important and dynamical effects dominate. In the momentum equation the viscous term is $\nu\nabla^2 u$ so that a viscous or dissipation time scale at a scale k^{-1}, τ_k^ν, is

$$\tau_k^\nu \sim \frac{1}{k^2\nu}, \tag{8.26}$$

so that the viscous time scale decreases with scale. The eddy turnover time, τ_k — that is, the inertial time scale — in the Kolmogorov spectrum is

$$\tau_k = \varepsilon^{-1/3}k^{-2/3}. \tag{8.27}$$

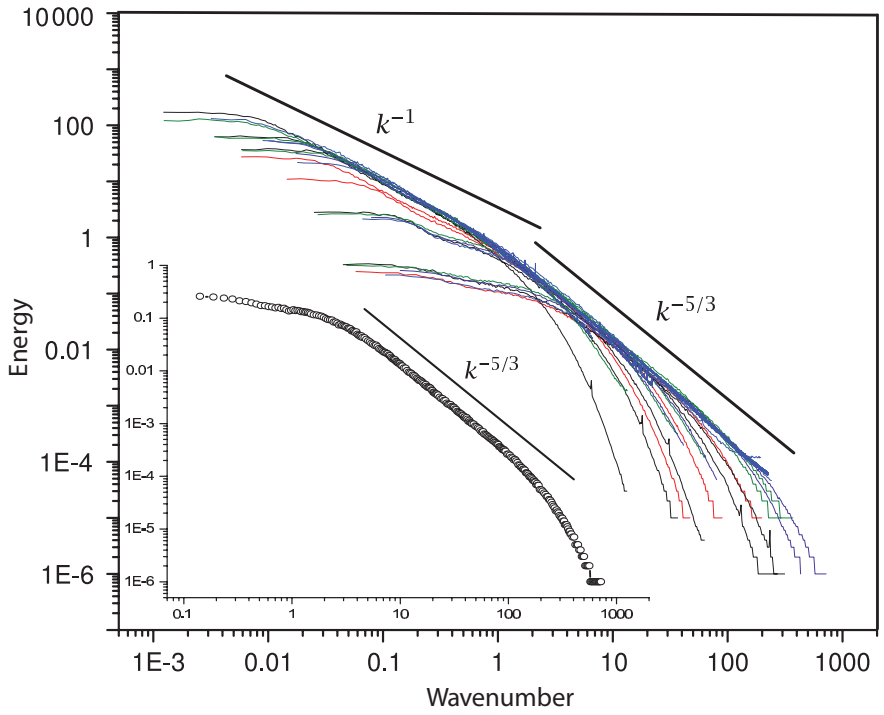

Fig. 8.4 The energy spectrum of 3D turbulence measured in some experiments at the Princeton Superpipe facility.[20] The outer plot shows the spectra from a large number of experiments at different Reynolds numbers up to 10^6, with the magnitude of their spectra appropriately rescaled. Smaller scales show a good $-5/3$ spectrum, whereas at larger scales the eddies feel the effects of the pipe wall and the spectra are a little shallower. The inner plot shows the spectrum in the centre of the pipe in a single experiment at $Re \approx 10^6$.

The wavenumber at which dissipation becomes important is then given by equating the above two time scales, yielding the dissipation wavenumber, k_ν and the associated length scale, L_ν,

$$k_\nu \sim \left(\frac{\varepsilon}{\nu^3}\right)^{1/4}, \qquad L_\nu \sim \left(\frac{\nu^3}{\varepsilon}\right)^{1/4}. \tag{8.28a,b}$$

L_ν is called the *Kolmogorov scale*. It is the *only* quantity which can be created from the quantities ν and ε that has the dimensions of length. (It is the same as the scale given by (11.16) provided that in that expression V is the velocity magnitude at the Kolmogorov scale.) Thus, for $L \gg L_\nu$, $\tau_k \ll \tau_k^\nu$ and inertial effects dominate. For $L \ll L_\nu$, $\tau_k^\nu \ll \tau_k$ and frictional effects dominate. In fact for length scales smaller than the dissipation scale, (11.27) is inaccurate; the energy spectrum falls off more rapidly than $k^{-5/3}$ and the inertial time scale falls off less rapidly than (11.27) implies, and dissipation dominates even more.

Given the dissipation scale, let us estimate the average energy dissipation rate, $\mathrm{d}/\mathrm{d}T\overline{E}$. This is given by

$$\frac{\mathrm{d}}{\mathrm{d}t}\overline{E} = \frac{1}{V}\int \nu \boldsymbol{v}\cdot\nabla^2\boldsymbol{v}\,\mathrm{d}V. \tag{8.29}$$

The length at which dissipation acts is the Kolmogorov scale and, noting that $v_k^2 \sim \varepsilon^{2/3}k^{-2/3}$ and

using (11.28a), the average energy dissipation rate scales as

$$\mathrm{d}/\mathrm{d}t\,\overline{E} \sim \nu k_\nu^2 v_{k_\nu}^2 \sim \nu k_\nu^2 \frac{\varepsilon^{2/3}}{k_\nu^{2/3}} \sim \varepsilon. \tag{8.30}$$

That is, the energy dissipation rate is equal to the energy cascade rate. On the one hand this seems sensible, but on the other hand it is *independent of the viscosity*. In particular, in the limit of viscosity tending to zero the energy dissipation remains finite! Surely the energy dissipation rate must go to zero if viscosity goes to zero? To see that this is not the case, consider that energy is input at some large scales, and the magnitude of the stirring largely determines the energy input and cascade rate. The scale at which viscous effects then become important is determined by the viscous scale, L_ν, given by (11.28b). *As viscosity tends to zero L_ν becomes smaller in just such a way as to preserve the constancy of the energy dissipation.* This is one of the most important results in three-dimensional turbulence. Now, we established in Section 1.10 that the Euler equations (i.e., the fluid equations with the viscous term omitted from the outset) do conserve energy. This means that the Euler equations are a *singular limit* of the Navier–Stokes equations: the behaviour of the Navier–Stokes equations as viscosity tends to zero is different from the behaviour resulting from simply omitting the viscous term from the equations ab initio.

How big is L_ν in the atmosphere? A crude estimate, perhaps wrong by an order of magnitude, comes from noting that ε has units of U^3/L, and that at length scales of the order of 100 m in the atmospheric boundary layer (where there might be a three-dimensional energy cascade to small scales) velocity fluctuations are of the order of 1 cm s^{-1}, giving $\varepsilon \approx 10^{-8}$ m^2 s^{-3}. Using (11.28b) we then find the dissipation scale to be of the order of a millimetre or so. In the ocean the dissipation scale is also of the order of millimetres. Various inertial range properties, in both three and two dimensions, are summarized in the shaded box on page 423.

Degrees of freedom

How many degrees of freedom does a turbulent fluid like the atmosphere potentially have? We might estimate this number, N say, by the expression

$$N \sim \left(\frac{L}{L_\nu}\right)^3, \tag{8.31}$$

where L is the length scale of the energy-containing eddies at the large scale. If we take $L = 1000$ km and $L_\nu = 1$ mm this gives about 10^{27}! On a rather more general basis, we can obtain an expression for N using (11.28b), to give

$$N \sim L^3 \left(\frac{\varepsilon}{\nu^3}\right)^{3/4}, \tag{8.32}$$

or, using $\varepsilon \sim U^3/L$,

$$N \sim \left(\frac{UL}{\nu}\right)^{9/4} = Re^{\,9/4}, \tag{8.33}$$

where Re is the Reynolds number based on the large-scale flow. For typical large-scale atmospheric flows with $U \sim 10$ m s^{-1}, $L \sim 10^6$ m and $\nu = 10^5$ m^2 s^{-1}, $Re \sim 10^{12}$ and again $N \sim 10^{27}$. Obviously, this number is very approximate, but nevertheless the number of potential degrees of freedom in the atmosphere is truly enormous, greater than Avogadro's number. Thus trying to model the turbulent atmosphere explicitly is akin to trying to model the gas in a room by following the motion of each individual molecule, and it seems unnecessary. How *should* we model it? That, in a nutshell, is the (unsolved) problem of turbulence.

Inertial Range Properties in 3D and 2D Turbulence

For reference, a few inertial range properties are listed below, omitting non-dimensional constants.

	3D energy range	2D enstrophy range	
Energy spectrum	$\varepsilon^{2/3}k^{-5/3}$	$\eta^{2/3}k^{-3}$	(T.1)
Turnover time	$\varepsilon^{-1/3}k^{-2/3}$	$\eta^{-1/3}$	(T.2)
Viscous scale, L_ν	$(\nu^3/\varepsilon)^{1/4}$	$(\nu^3/\eta)^{1/6}$	(T.3)
Passive tracer spectrum	$\chi\varepsilon^{-1/3}k^{-5/3}$	$\chi\eta^{-1/3}k^{-1}$	(T.4)

In these expressions:

ν = viscosity, k = wavenumber, ε = energy cascade rate,
η = enstrophy cascade rate, χ = tracer variance cascade rate.

8.2.3 A Final Note on our Assumptions

The assumptions of homogeneity and isotropy that are made in the Kolmogorov theory are ansatzes, in that we make them because we want to have a tractable model of turbulence (and certainly we can conceive of an experiment in which turbulence is for most practical purposes homogeneous and isotropic). The essential *physical* assumptions are: (i) that there exists an inertial range in which the energy flux is constant; and (ii) that the energy is cascaded from large to small scales in a series of small steps, as the energy spectra will then be determined by spectrally local quantities. The second assumption is the locality assumption and without it we could have, instead of (11.23),

$$\mathcal{E}(k) = C\varepsilon^{2/3}k^{-5/3}g(k/k_0)h(k/k_\nu), \tag{8.34}$$

where g and h are unknown functions. We essentially postulate that there exists a range of intermediate wavenumbers over which $g(k/k_0) = h(k/k_\nu) = 1$.

The first, and less obvious, assumption might be called the *non-intermittency* assumption, and it demands that rare events (in time or space) with large amplitudes do not dominate the energy flux or the dissipation rate. If they were to do so, then the flux would fluctuate strongly, the turbulent statistics would not be completely characterized by ε and Kolmogorov's theory would not be exactly right. Note that in the theory ε is the mean energy cascade rate, and $\varepsilon^{2/3}$ is the two-thirds power of the mean, which is not equal to the mean of the two-thirds power. In fact, in high Reynolds turbulence the $-5/3$ spectra is often observed to a fairly high degree of accuracy (e.g., as in Fig. 11.4), although the higher-order statistics (e.g., higher-order structure functions) predicted by the theory are often found to be in error, and it is generally believed that Kolmogorov's theory is not exact.[21]

8.3 TWO-DIMENSIONAL TURBULENCE

Two-dimensional turbulence behaves in a profoundly different way from three-dimensional turbulence, largely because of the presence of another quadratic invariant, the enstrophy (defined below;

see also Section 5.6.3). In two dimensions, the vorticity equation for incompressible flow is:

$$\frac{\partial \zeta}{\partial t} + \boldsymbol{u} \cdot \nabla \zeta = F + \nu \nabla^2 \zeta, \tag{8.35}$$

where $\boldsymbol{u} = u\boldsymbol{i} + v\boldsymbol{j}$ and $\zeta = \boldsymbol{k} \cdot \nabla \times \boldsymbol{u}$ and F is a stirring term. In terms of a streamfunction, $u = -\partial\psi/\partial y$, $v = \partial\psi/\partial x$, and $\zeta = \nabla^2\psi$, and (11.35) may be written as

$$\frac{\partial \nabla^2 \psi}{\partial t} + J(\psi, \nabla^2\psi) = F + \nu \nabla^4 \psi. \tag{8.36}$$

We obtain an energy equation by multiplying by $-\psi$ and integrating over the domain, and an enstrophy equation by multiplying by ζ and integrating. When $F = \nu = 0$ we find

$$\widehat{E} = \frac{1}{2}\int_A (u^2 + v^2)\,\mathrm{d}A = \frac{1}{2}\int_A (\nabla\psi)^2\,\mathrm{d}A, \qquad \frac{\mathrm{d}\widehat{E}}{\mathrm{d}t} = 0, \tag{8.37a}$$

$$\widehat{Z} = \frac{1}{2}\int_A \zeta^2\,\mathrm{d}A = \frac{1}{2}\int_A (\nabla^2\psi)^2\,\mathrm{d}A, \qquad \frac{\mathrm{d}\widehat{Z}}{\mathrm{d}t} = 0, \tag{8.37b}$$

where the integral is over a finite area with either no-normal flow or periodic boundary conditions. The quantity $\widehat{E}$ is the energy, and $\widehat{Z}$ is known as the *enstrophy*. The enstrophy invariant arises because the vortex stretching term, so important in three-dimensional turbulence, vanishes identically in two dimensions. In fact, because vorticity is conserved on parcels it is clear that the integral of *any* function of vorticity is zero when integrated over A; that is, from (11.35)

$$\frac{\mathrm{D}g(\zeta)}{\mathrm{D}t} = 0 \qquad \text{and} \qquad \frac{\mathrm{d}}{\mathrm{d}t}\int_A g(\zeta)\,\mathrm{d}A = 0, \tag{8.38}$$

where $g(\zeta)$ is an arbitrary function. Of this infinity of conservation properties, enstrophy conservation (with $g(\zeta) = \zeta^2$) in particular has been found to have enormous consequences to the flow of energy between scales, as we will soon discover.[22]

Part III

LARGE-SCALE ATMOSPHERIC CIRCULATION

'Blow the wind southerly, southerly, southerly,
'Blow the wind south o'er the bonny blue sea;
'Blow the wind southerly, southerly, southerly,
'Blow bonnie breeze, my lover to me.

Traditional English folk song, *Blow the Wind Southerly*, c. 1834.

CHAPTER 9

The Overturning Circulation: Hadley and Ferrel Cells

THE LARGE-SCALE CIRCULATION OF THE ATMOSPHERE is normally taken to mean the flow on scales of the weather — several hundred or a thousand kilometres, say — to the global scale. The *general circulation* is virtually synonymous with the large-scale circulation, although the former is sometimes taken to be the time- or ensemble-averaged flow. Our goal in this and the next few chapters is understand this circulation and other properties of the atmosphere that accompany it — the temperature and moisture fields, for example. We might hope to answer the simple question, why do the winds blow as they do? In this chapter we focus on the dynamics of the Hadley Cell and, rather descriptively, on the mid-latitude overturning cell or the Ferrel Cell, moving to a more dynamical view of the extratropical zonally averaged circulation in Chapter 15.

The atmosphere is a terribly complex system, and we cannot hope to fully explain its motion as the analytic solution to a small set of equations. Rather, a full understanding of the atmosphere requires describing it in a consistent way on many levels simultaneously. One of these levels involves simulating the flow by numerically solving the governing equations of motion as completely as possible by using a comprehensive General Circulation Model (GCM). Such a simulation brings problems sof its own, for example understanding the simulation itself and discerning whether it is a good representation of reality, and so we shall concentrate on simpler, more conceptual models and the basic theory of the circulation. We begin this chapter with a brief observational overview of some of the large-scale features of the atmosphere, concentrating on the zonally-averaged fields.[23]

9.1 BASIC FEATURES OF THE ATMOSPHERE

9.1.1 The Radiative Equilibrium Distribution

A gross but informative measure characterizing the atmosphere, and the effects that dynamics have on it, is the pole-to-equator temperature distribution. The *radiative equilibrium* temperature is the hypothetical, three-dimensional, temperature field that would obtain if there were no atmospheric or oceanic motion, given the composition and radiative properties of the atmosphere and surface. The field is a function of the incoming solar radiation and the atmospheric composition, and its determination entails a complicated calculation, especially as the radiative properties of the atmosphere depend heavily on the amount of water vapour and cloudiness it contains. (The distribution

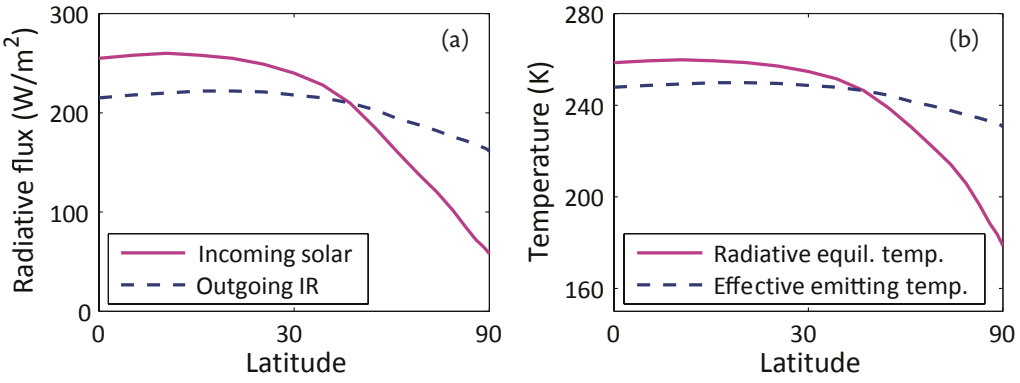

Fig. 9.1 (a) The (approximate) observed net average incoming solar radiation and outgoing infrared radiation at the top of the atmosphere, as a function of latitude (plotted on a sine scale). (b) The temperatures associated with these fluxes, calculated using $T = (R/\sigma)^{1/4}$, where R is the solar flux for the radiative equilibrium temperature and where R is the infrared flux for the effective emitting temperature. Thus, the solid line is an approximate radiative equilibrium temperature

of absorbers is usually taken to be that which obtains in the observed, moving, atmosphere, in order that the differences between the calculated radiative equilibrium temperature and the observed temperature are due to fluid motion.)

A much simpler calculation that illustrates the essence of the situation is to first note that at the top of the atmosphere the globally averaged incoming solar radiation is balanced by the outgoing infrared radiation. If there is no lateral transport of energy in the atmosphere or ocean then *at each latitude* the incoming solar radiation will be balanced by the outgoing infrared radiation, and if we parameterize the latter using a single latitudinally-dependent temperature we will obtain a crude radiative-equilibrium temperature (the 'radiative emitting temperature') for the atmospheric column at each latitude. Specifically, a black body subject to a net incoming radiation of S (watts per square metre) has a radiative-equilibrium temperature T_{rad} given by $\sigma T_{rad}^4 = S$, this being Stefan's law with Stefan–Boltzmann constant $\sigma = 5.67 \times 10^{-8}\,\mathrm{W\,m^{-2}\,K^{-4}}$. Thus, for the Earth, we have, at each latitude,

$$\sigma T_{rad}^4 = S(\vartheta)(1 - \alpha), \tag{9.1}$$

where α is the albedo of the Earth and $S(\vartheta)$ is the incoming solar radiation at the top of the atmosphere, and its solution is shown in Fig. 14.1. The solid lines in the two panels show the net solar radiation and the solution to (14.1), T_{rad}; the dashed lines show the observed outgoing infrared radiative flux, I, and the effective emitting temperature associated with it, $(I/\sigma)^{1/4}$. The emitting temperature does not quantitatively characterize that temperature at the Earth's surface, nor at any single level in the atmosphere, because the atmosphere is not a black body and the outgoing radiation originates from multiple levels. Nevertheless, the qualitative point is evident: the radiative equilibrium temperature has a much stronger pole-to-equator gradient than does the effective emitting temperature, indicating that there is a poleward transport of heat in the atmosphere–ocean system. More detailed calculations indicate that the atmosphere is further from its radiative equilibrium in winter than summer, indicating a larger heat transport. The transport occurs because poleward moving air tends to have a higher static energy ($c_pT + gz$ for dry air; in addition there is some energy transport associated with water vapour evaporation and condensation) than the equatorward moving air, most of this movement being associated with the large-scale circulation. The radiative forcing thus seeks to maintain a pole-to-equator temperature gradient, and the ensuing circulation seeks to reduce this gradient.

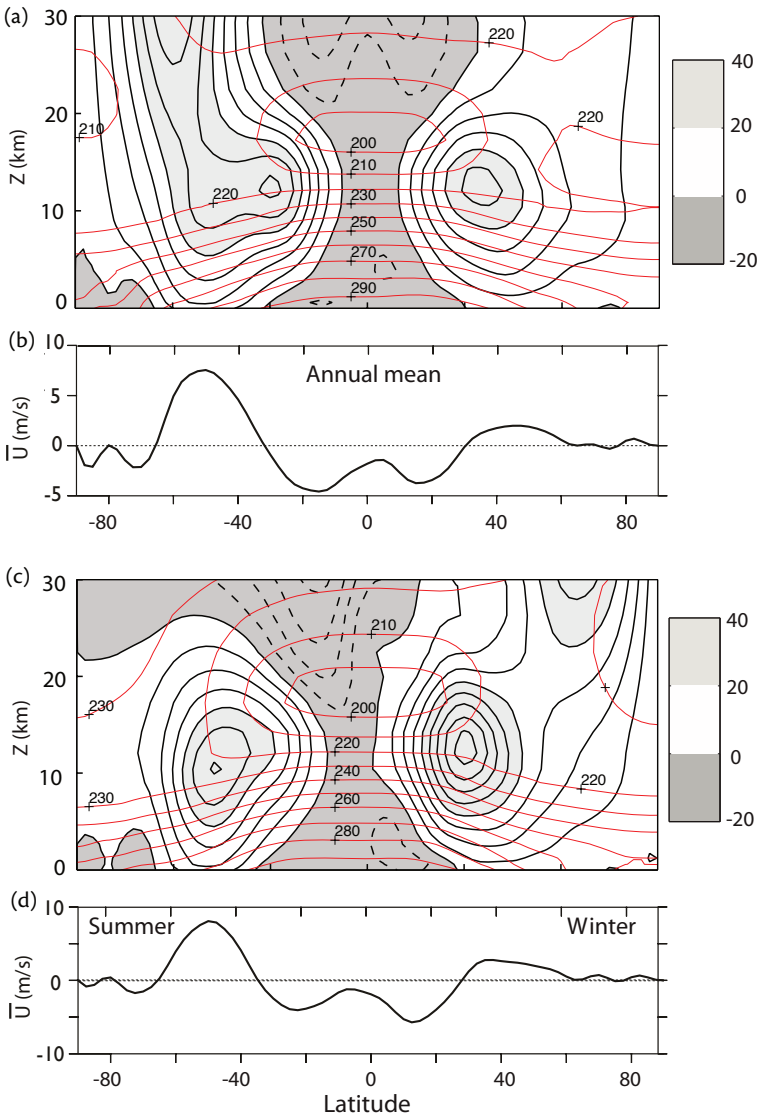

Fig. 9.2 (a) Annual mean, zonally-averaged zonal wind (heavy contours and shading) and the zonally-averaged temperature (red, thinner contours).

(b) Annual mean, zonally averaged zonal winds at the surface.

(c) and (d) Same as (a) and (b), except for northern hemisphere winter (December–January–February, or DJF).

The wind contours are at intervals of 5 m s^{-1} with shading for eastward winds above 20 m s^{-1} and for all westward winds, and the temperature contours are labelled. The ordinate of (a) and (c) is $Z = -H \log(p/p_R)$, where H = 7.5 km and p_R =100 hPa.

9.1.2 Observed Wind and Temperature Fields

The observed zonally-averaged temperature and zonal wind fields are illustrated in Fig. 14.2. The vertical coordinate is log pressure, multiplied by a constant factor $H = RT_0/g = 7.5\,\text{km}$, so that the ordinate is similar to height in kilometres. (In an isothermal hydrostatic atmosphere $(RT_0/g)\mathrm{d}\ln p = -\mathrm{d}z$, and the value of H chosen corresponds to $T_0 = 256\,\text{K}$.) To a good approximation temperature and zonal wind are related by thermal wind balance, which in pressure coordinates is

$$f\frac{\partial u}{\partial p} = \frac{R}{p}\frac{\partial T}{\partial y}. \tag{9.2}$$

In the lowest several kilometres of the atmosphere temperature falls almost monotonically with latitude and height, and this region is called the *troposphere* (look ahead to Fig. 15.25). The temperature in the lower troposphere in fact varies more rapidly with latitude than does the effective emitting temperature, T_E, the latter being more characteristic of the temperature in the mid-to-

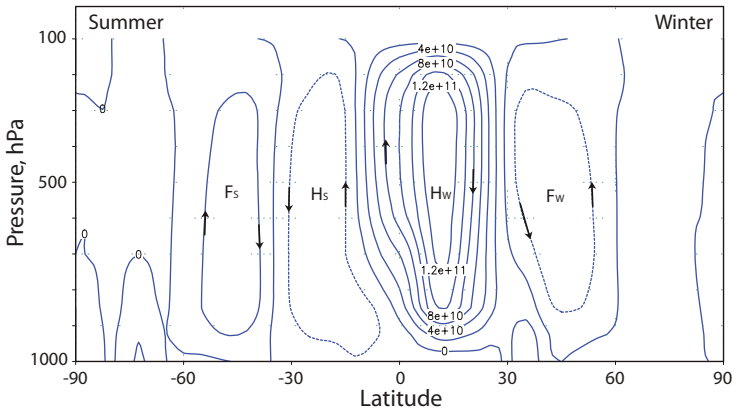

Fig. 9.3 The observed meridional overturning circulation (MOC) of the atmosphere ($kg\,s^{-1}$) averaged over December–January–February. Note the direct *Hadley Cells,* particularly strong in winter (H_W and H_S, in winter and summer respectively) with rising motion near the equator, descending motion in the subtropics, and the weaker, indirect, *Ferrel Cells* (F_W and F_S) at mid-latitudes.

upper troposphere. The meridional temperature gradient is much larger in winter than summer, because in winter high latitudes receive virtually no direct heating from the Sun. The gradient is also strongest at the edge of the subtropics, and here it is associated with a zonal jet, particularly strong in winter. There is no need to 'drive' this wind with any kind of convergent momentum fluxes: given the temperature, the flow is a consequence of thermal wind balance, and to the extent that the upper troposphere is relatively frictionless there is no need to maintain it against dissipation. Of course just as the radiative-equilibrium temperature gradient is much larger than that observed, so the zonal wind shear associated with it is much larger than that observed. Thus, the overall effect of the atmospheric and oceanic circulation, and in particular of the turbulent circulation of the mid-latitude atmosphere, is to *reduce* the amplitude of the vertical shear of the eastward flow by way of a poleward heat transport. Observations indicate that about two-thirds of this transport is effected by the atmosphere, and about a third by the ocean, rather more in low latitudes.[24]

Above the troposphere is the *stratosphere,* and here temperature typically increases with height. The boundary between the two regions is called the *tropopause,* and this varies in height from about 16 km in the tropics to about 8 km in polar regions. We consider the maintenance of this stratification in Section 15.5.

The surface winds typically have, going from the equator to the pole, an E–W–E (easterly–westerly–easterly) pattern, although the polar easterlies are weak and barely present in the Northern Hemisphere. (Meteorologists use 'westerly' to denote winds from the west, that is eastward winds; similarly 'easterlies' are westward winds.) In a given hemisphere, the surface winds are stronger in winter than summer, and they are also consistently stronger in the Southern Hemisphere than in the Northern Hemisphere, because in the former the surface drag is weaker because of the relative lack of continental land masses and topography. The surface winds are *not* explained by thermal wind balance. Indeed, unlike the upper level winds, they must be maintained against the dissipating effects of friction, and this implies a momentum convergence into regions of surface westerlies and a divergence into regions of surface easterlies. Typically, the maxima in the eastward surface winds are in mid-latitudes and somewhat poleward of the subtropical maxima in the upper-level westerlies and at latitudes where the zonal flow is a little more constant with height. The mechanisms of the momentum transport in the mid-latitudes and the maintenance of the surface westerly winds are the topics of section 15.1.

9.1.3 Meridional Overturning Circulation

The observed (Eulerian) zonally-averaged meridional overturning circulation (MOC) is shown in Fig. 14.3. The figure shows a streamfunction, Ψ for the vertical and meridional velocities such that,

Some Features of the Large-scale Atmospheric Circulation

From Figures 14.1–14.3 we see or infer the following:

1. A pole–equator temperature gradient that is much smaller than the radiative equilibrium gradient.
2. A troposphere, in which temperature generally falls with height, above which lies the stratosphere, in which temperature increases with height. The two regions are separated by a tropopause, which varies in height from about 16 km at the equator to about 6 km at the pole.
3. A monotonically decreasing temperature from equator to pole in the troposphere, but a weakening and sometimes reversal of this above the tropopause.
4. A westerly (i.e., eastward) tropospheric jet. The time and zonally-averaged jet is a maximum at the edge or just poleward of the subtropics, where it is associated with a strong meridional temperature gradient. In mid-latitudes the jet has a stronger barotropic component.
5. An E–W–E (easterlies–westerlies–easterlies) surface wind distribution. The latitude of the maximum in the surface westerlies is in mid-latitudes, where the zonally-averaged flow is more barotropic. The surface easterlies at high latitudes are very weak and seasonal, barely showing on an annual average.

in the pressure coordinates used in the figure,

$$\frac{\partial \Psi}{\partial y} = -\overline{\omega}, \qquad \frac{\partial \Psi}{\partial p} = \overline{v}, \tag{9.3}$$

where the overbar indicates a zonal average. In each hemisphere there is rising motion near the equator and sinking in the subtropics, and this circulation is known as the *Hadley Cell.*[25] The Hadley Cell is a thermally direct cell (i.e., the warmer fluid rises, the colder fluid sinks), much stronger in the winter hemisphere, and extends to about 25–30°. In mid-latitudes the sense of the overturning circulation is apparently reversed, with rising motion in the high-mid-latitudes, at around 60° and sinking in the subtropics, and this is known as the *Ferrel Cell.* However, as with most pictures of averaged streamlines in unsteady flow, this gives a misleading impression as to the actual material flow of parcels of air because of the presence of eddying motion, and we discuss this in the next chapter. At low latitudes the circulation is more nearly zonally symmetric and the picture does give a qualitatively correct representation of the actual flow. At high latitudes there is again a thermally direct cell (although it is weak and not always present), and thus the atmosphere is often referred to as having a three-celled structure.

9.1.4 Summary

Some of the main features of the zonally-averaged circulation are summarized in the shaded box on page 515. We emphasize that the zonally-averaged circulation is not synonymous with a zonally symmetric circulation, and the mid-latitude circulation is highly asymmetric. Any model of the mid-latitudes that did not take into account the zonal asymmetries in the circulation — of which the weather is the main manifestation — would be seriously in error. This was first explicitly realized in the 1920s, and taking into account such asymmetries is the main task of the dynamical

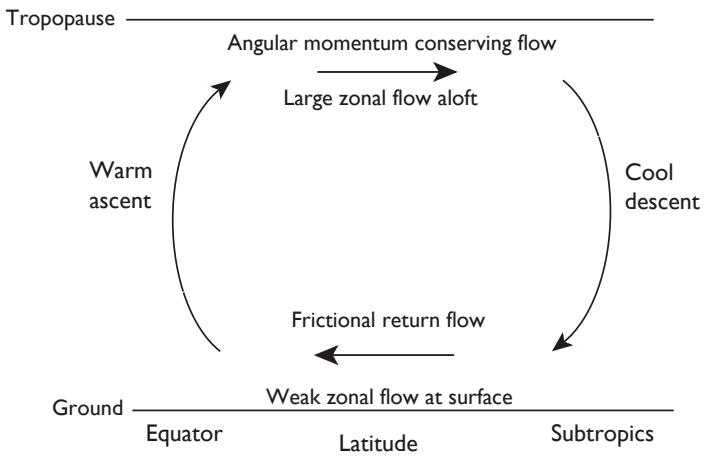

Fig. 9.4 A simple model of the Hadley Cell. Rising air near the equator moves poleward near the tropopause, descending in the subtropics and returning.

The poleward moving air conserves its angular momentum, leading to a shear of the zonal wind that increases away from the equator. By thermal wind the temperature of the air falls as it moves poleward, and to satisfy the thermodynamic budget it sinks in the subtropics.

meteorology of the mid-latitudes, and is the subject of the next chapter. The large-scale tropical circulation of the atmosphere is to a much larger degree zonally symmetric, and although monsoonal circulations and the Walker circulation (a cell with rising air in the Eastern Pacific and descending motion in the Western Pacific) are zonally asymmetric, they are relatively weaker than typical mid-latitude weather systems. Indeed the boundary between the tropics and mid-latitude may be usefully defined by the latitude at which such zonal asymmetries become dynamically important on the large scale and this boundary, at about 25°–30° on average, roughly coinciding with edge Hadley Cell. We begin our dynamical description with a study of the low-latitude zonally symmetric atmospheric circulation.

9.2 A STEADY MODEL OF THE HADLEY CELL

Ceci n'est pas une pipe.
René Magritte. Title of painting, 1929.

9.2.1 Assumptions

Let us try to construct a zonally symmetric model of the Hadley Cell, recognizing that such a model is likely applicable mainly to the tropical atmosphere, this being more zonally symmetric than the mid-latitudes.[26] We suppose that heating is maximum at the equator, and our intuitive picture, drawing on the observed flow of Fig. 14.3, is of air rising at the equator and moving poleward at some height H, descending at some latitude ϑ_H, and returning equatorward near the surface. We will make three major assumptions:

(i) that the circulation is steady;

(ii) that the poleward moving air conserves its axial angular momentum, whereas the zonal flow associated with the near-surface, equatorward moving flow is frictionally retarded and weak;

(iii) that the circulation is in thermal wind balance.

We also assume the model is symmetric about the equator (an assumption we relax in Section 14.4). These are all reasonable assumptions, but they cannot be rigorously justified; in other words, we are constructing a *model* of the Hadley Cell, schematically illustrated in Fig. 14.4. The model defines a limiting case — steady, inviscid, zonally-symmetric flow — that cannot be expected to describe the atmosphere quantitatively, but that can be analysed fairly completely. Another limiting case, in which eddies play a significant role, is described in Section 14.5. The real atmosphere may defy such simple characterizations, but the two limiting cases provide useful benchmarks of understanding.

9.2.2 Dynamics

We now try to determine the strength and poleward extent of the Hadley circulation in our steady model. For simplicity we work with a Boussinesq atmosphere, but this is not an essential aspect. We first derive the conditions under which conservation of angular momentum will hold, and then determine the consequences of that.

The zonally-averaged zonal momentum equation may be easily derived from (2.50a) and/or (2.62) and in the absence of friction it is

$$\frac{\partial \overline{u}}{\partial t} - (f + \overline{\zeta})\overline{v} + \overline{w}\frac{\partial \overline{u}}{\partial z} = -\frac{1}{a\cos^2\vartheta}\frac{\partial}{\partial \vartheta}(\cos^2\vartheta \overline{u'v'}) - \frac{\partial \overline{u'w'}}{\partial z}, \tag{9.4}$$

where $\overline{\zeta} = -(a\cos\vartheta)^{-1}\partial_\vartheta(\overline{u}\cos\vartheta)$ and the overbars represent zonal averages. If we neglect the vertical advection and the eddy terms on the right-hand side, then a steady solution, if it exists, obeys

$$(f + \overline{\zeta})\overline{v} = 0. \tag{9.5}$$

Presuming that the meridional flow $\overline{v}$ is non-zero (an issue we address in Section 14.2.8) then $f + \overline{\zeta} = 0$, or equivalently

$$2\Omega\sin\vartheta = \frac{1}{a}\frac{\partial \overline{u}}{\partial \vartheta} - \frac{\overline{u}\tan\vartheta}{a}. \tag{9.6}$$

At the equator we shall assume that $\overline{u} = 0$, because here parcels have risen from the surface where, by assumption, the flow is weak. Equation (14.6) then has a solution of

$$\overline{u} = \Omega a\frac{\sin^2\vartheta}{\cos\vartheta} \equiv U_M\,. \tag{9.7}$$

This gives the zonal velocity of the poleward moving air in the upper branch of the (model) Hadley Cell, above the frictional boundary layer. We can derive (14.7) directly from the conservation of axial angular momentum, m, of a parcel of air at a latitude ϑ. In the shallow atmosphere approximation we have (cf. (2.64) and equations following)

$$\overline{m} = (\overline{u} + \Omega a\cos\vartheta)a\cos\vartheta, \tag{9.8}$$

and if $\overline{u} = 0$ at $\vartheta = 0$ and if $\overline{m}$ is conserved on a poleward moving parcel, then (14.8) leads to (14.7). It also may be directly checked that

$$f + \overline{\zeta} = -\frac{1}{a^2\cos\vartheta}\frac{\partial \overline{m}}{\partial \vartheta}. \tag{9.9}$$

We have thus shown that, if eddy fluxes and frictional effects are negligible, the poleward flow will conserve its angular momentum, the result of which, by (14.7), is that the magnitude of the zonal flow in the Earth's rotating frame will increase with latitude (see Fig. 14.5). (Also, given the absence of eddies our model is zonally symmetric and we shall drop the overbars over the variables.)

If (14.7) gives the zonal velocity in the upper branch of the Hadley Cell, and that in the lower branch is close to zero, then the thermal wind equation can be used to infer the vertically averaged temperature. Although the geostrophic wind relation is not valid at the equator (a more accurate balance is the gradient wind balance, $fu + u^2\tan\vartheta/a = -a^{-1}\partial\phi/\partial\vartheta$) the zonal wind is in fact geostrophically balanced until very close to the equator, and at the equator itself the horizontal temperature gradient in our model vanishes, because of the assumed interhemispheric symmetry. Thus, conventional thermal wind balance suffices for our purposes, and this is

$$2\Omega\sin\vartheta\frac{\partial u}{\partial z} = -\frac{1}{a}\frac{\partial b}{\partial \vartheta}, \tag{9.10}$$

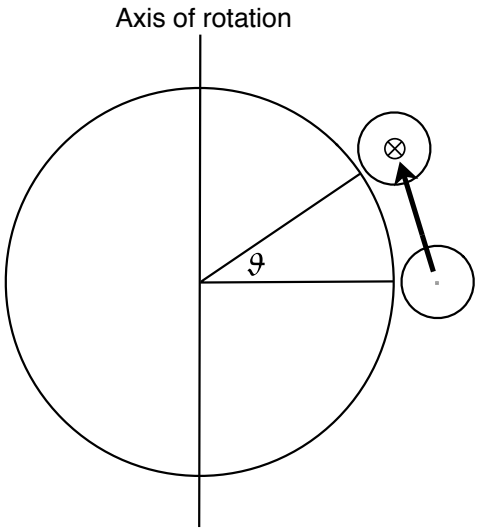

Fig. 9.5 If a ring of air at the equator moves poleward it moves closer to the axis of rotation. If the parcels in the ring conserve their angular momentum their zonal velocity must increase; thus, if $m = (\overline{u} + \Omega a \cos\vartheta) a \cos\vartheta$ is preserved and $\overline{u} = 0$ at $\vartheta = 0$ we recover (14.7).

where $b = g\,\delta\theta/\theta_0$ is the buoyancy and $\delta\theta$ is the deviation of potential temperature from a constant reference value θ_0. (Be reminded that θ is potential temperature, whereas ϑ is latitude.) Vertically integrating from the ground to the height H where the outflow occurs and substituting (14.7) for u yields

$$\frac{1}{a\theta_0}\frac{\partial\theta}{\partial\vartheta} = -\frac{2\Omega^2 a}{gH}\frac{\sin^3\vartheta}{\cos\vartheta}, \tag{9.11}$$

where $\theta = H^{-1}\int_0^H \delta\theta\,\mathrm{d}z$ is the vertically averaged potential temperature. If the latitudinal extent of the Hadley Cell is not too great we can make the small-angle approximation, and replace $\sin\vartheta$ by ϑ and $\cos\vartheta$ by one, then integrating (14.11) gives

$$\theta = \theta(0) - \frac{\theta_0\Omega^2 y^4}{2gHa^2}, \tag{9.12}$$

where $y = a\vartheta$ and $\theta(0)$ is the potential temperature at the equator, as yet unknown. Away from the equator, the zonal velocity given by (14.7) increases rapidly poleward and the temperature correspondingly drops. How far poleward is this solution valid? And what determines the value of the integration constant $\theta(0)$? To answer these questions we turn to thermodynamics.

9.2.3 Thermodynamics

In the above discussion, the temperature field is slaved to the momentum field in that it seems to follow passively from the dynamics of the momentum equation. Nevertheless, the thermodynamic equation must still be satisfied. Let us assume that the thermodynamic forcing can be represented by a Newtonian cooling to some specified radiative equilibrium temperature, θ_E; this is a severe simplification, especially in equatorial regions where the release of heat by condensation is important. The thermodynamic equation is then

$$\frac{\mathrm{D}\theta}{\mathrm{D}t} = \frac{\theta_E - \theta}{\tau}, \tag{9.13}$$

where τ is a relaxation time scale, perhaps a few weeks. Let us suppose that θ_E falls monotonically from the equator to the pole, and that it increases linearly with height, and a simple representation

of this is

$$\frac{\theta_E(\vartheta, z)}{\theta_0} = 1 - \frac{2}{3}\Delta_H P_2(\sin\vartheta) + \Delta_V\left(\frac{z}{H} - \frac{1}{2}\right), \tag{9.14}$$

where Δ_H and Δ_V are nondimensional constants that determine the fractional temperature difference between the equator and the pole, and the ground and the top of the fluid, respectively. P_2 is the second Legendre polynomial, and it is usually the leading term in the Taylor expansion of symmetric functions (symmetric around the equator) that decrease from pole to equator; it also integrates to zero over the sphere. $P_2(y) = (3y^2 - 1)/2$, so that in the small-angle approximation and at $z = H/2$, or for the vertically averaged field, we have

$$\frac{\theta_E}{\theta_0} = 1 + \frac{1}{3}\Delta_H - \Delta_H\left(\frac{y}{a}\right)^2 \qquad \text{or} \qquad \theta_E = \theta_{E0} - \Delta\theta\left(\frac{y}{a}\right)^2, \tag{9.15a,b}$$

where θ_{E0} is the equilibrium temperature at the equator, $\Delta\theta$ determines the equator–pole radiative-equilibrium temperature difference, and

$$\theta_{E0} = \theta_0(1 + \Delta_H/3), \qquad \Delta\theta = \theta_0\Delta_H. \tag{9.16}$$

Now, let us suppose that the solution (14.12) is valid between the equator and a latitude ϑ_H where $v = 0$, so that within this region the system is essentially closed. Conservation of potential temperature then requires that the solution (14.12) must satisfy

$$\int_0^{Y_H} \theta\,\mathrm{d}y = \int_0^{Y_H} \theta_E\,\mathrm{d}y, \tag{9.17}$$

where $Y_H = a\vartheta_H$ is as yet undetermined. Poleward of this, the solution is just $\theta = \theta_E$. Now, we may demand that the solution be continuous at $y = Y_H$ (without temperature continuity the thermal wind would be infinite) and so

$$\theta(Y_H) = \theta_E(Y_H). \tag{9.18}$$

The constraints (14.17) and (14.18) determine the values of the unknowns $\theta(0)$ and Y_H. A little algebra gives

$$Y_H = \left(\frac{5\Delta\theta g H}{3\Omega^2\theta_0}\right)^{1/2}, \tag{9.19}$$

and

$$\theta(0) = \theta_{E0} - \left(\frac{5\Delta\theta^2 g H}{18a^2\Omega^2\theta_0}\right). \tag{9.20}$$

A useful nondimensional number that parameterizes these solutions is

$$R \equiv \frac{gH\Delta\theta}{\theta_0\Omega^2a^2} = \frac{gH\Delta_H}{\Omega^2a^2}, \tag{9.21}$$

which is the square of the ratio of the speed of shallow water waves to the rotational velocity of the Earth, multiplied by the fractional temperature difference from equator to pole. Typical values for the Earth's atmosphere are a little less than 0.1. In terms of R we have

$$Y_H = a\left(\frac{5}{3}R\right)^{1/2}, \qquad \theta(0) = \theta_{E0} - \left(\frac{5}{18}R\right)\Delta\theta. \tag{9.22a,b}$$

The solution, (14.12) with $\theta(0)$ given by (14.22b) is plotted in Fig. 14.6. Perhaps the single most important aspect of the model is that it predicts that the Hadley Cell has a *finite* meridional extent, *even for an atmosphere that is completely zonally symmetric.* The baroclinic instability that does occur in mid-latitudes is not necessary for the Hadley Cell to terminate in the subtropics, although it may be an important factor, or even the determining factor, in the real world.

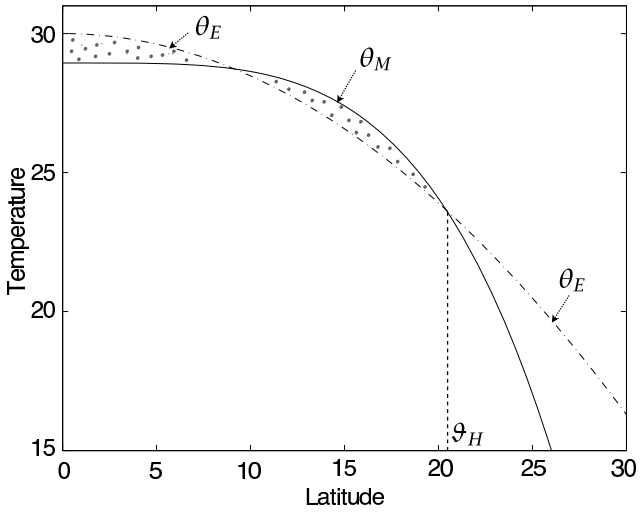

Fig. 9.6 The radiative equilibrium temperature (θ_E, dashed line) and the angular-momentum-conserving solution (θ_M, solid line) as a function of latitude. The two dotted regions have equal areas. The parameters are: $\theta_{E0} = 303\,\mathrm{K}$, $\Delta\theta = 50\,\mathrm{K}$, $\theta_0 = 300\,\mathrm{K}$, $\Omega = 7.272 \times 10^{-5}\,\mathrm{s}^{-1}$, $g = 9.81\,\mathrm{m\,s}^{-2}$, $H = 10\,\mathrm{km}$. These give $R = 0.076$ and $Y_H/a = 0.356$, corresponding to $\vartheta_H = 20.4°$.

9.2.4 Zonal Wind

The angular-momentum-conserving zonal wind is given by (14.7), which in the small-angle approximation becomes

$$U_M = \Omega \frac{y^2}{a}. \tag{9.23}$$

This relation holds for $y < Y_H$. The zonal wind corresponding to the radiative-equilibrium solution is given using thermal wind balance and (14.15b), which leads to

$$U_E = \Omega a R. \tag{9.24}$$

That the radiative-equilibrium zonal wind is a constant follows from our choice of the second Legendre function for the radiative equilibrium temperature and is not a fundamental result; nonetheless, for most reasonable choices of θ_E the corresponding zonal wind will vary much less than the angular-momentum-conserving wind (14.23). The winds are illustrated in Fig. 14.7. There is a discontinuity in the zonal wind at the edge of the Hadley Cell, and of the meridional temperature gradient, but not of the temperature itself.

9.2.5 Properties of the Solution

From (14.22) we can see that the model predicts that the latitudinal extent of the Hadley Cell is:

- proportional to the square root of the meridional radiative equilibrium temperature gradient: the stronger the gradient, the farther the circulation must extend to achieve thermodynamic balance via the equal-area construction in Fig. 14.6;
- proportional to the square root of the height of the outward flowing branch: the higher the outward flowing branch, the weaker the ensuing temperature gradient of the solution (via thermal wind balance), and so the further poleward the circulation must go;
- inversely proportional to the rotation rate Ω: the stronger the rotation rate, the stronger the angular-momentum-conserving wind, the stronger the ensuing temperature gradient and so the more compact the circulation.

These precise dependencies on particular powers of parameters are not especially significant in themselves, nor are they robust to changes in parameters. For example, were we to choose a meridional distribution of radiative equilibrium temperature different from (14.14) we might find different exponents in some of the solutions, although we would expect the same qualitative dependen-

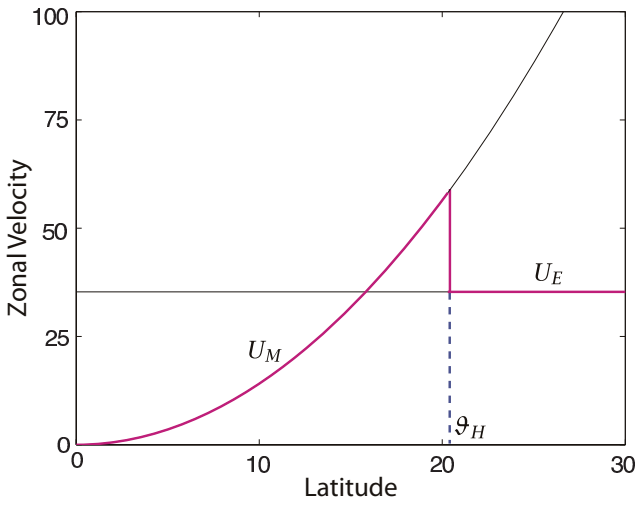

Fig. 9.7 The zonal wind corresponding to the radiative equilibrium temperature (U_E,) and the angular-momentum-conserving solution (U_M) as a function of latitude, given (14.23) and (14.24) respectively.

The parameters are the same as those of Fig. 14.6, and the radiative equilibrium wind, U_E is a constant, ΩaR. The actual zonal wind (in the model) follows the thick solid line: $u = U_m$ for $\vartheta < \vartheta_H$ ($y < Y_H$), and $u = U_E$ for $\vartheta > \vartheta_H$ ($y > Y_H$).

cies. However, the dependencies do provide predictions that may be tested with a numerical model. Also, as we have already noted, a key property of the model is that it predicts that the Hadley Cell has a finite meridional extent, even in the absence of mid-latitude baroclinic instability.

Another interesting property of the solutions is a discontinuity in the zonal wind. For tropical latitudes (i.e., $y < Y_H$), then $\overline{u} = U_M$ (the constant angular momentum solution), whereas for $y > Y_H$, $\overline{u} = U_E$ (the thermal wind associated with radiative equilibrium temperature θ_E). There is therefore a discontinuity of $\overline{u}$ at $y = Y_H$, because u is related to the meridional gradient of θ which changes discontinuously, even though θ itself is continuous. No such discontinuity is observed in the real world, although one may observe a baroclinic jet at the edge of the Hadley Cell.

9.2.6 Strength of the Circulation

We can make an estimate of the strength of the Hadley Cell by consideration of the thermodynamic equation at the equator, namely

$$w\frac{\partial\theta}{\partial z} \approx \frac{\theta_{E0} - \theta}{\tau}, \tag{9.25}$$

this being a balance between adiabatic cooling and radiative heating. If the static stability is determined largely by the forcing, and not by the meridional circulation itself, then $\theta_0^{-1}\partial\theta/\partial z \approx \Delta_V/H$, and (14.25) gives

$$w \approx \frac{H}{\theta_0\Delta_V}\frac{\theta_{E0} - \theta}{\tau}. \tag{9.26}$$

Thus, the strength of the circulation is proportional to the distance of the solution from the radiative equilibrium temperature. The right-hand side of (14.25) can be evaluated from the solution itself, and from (14.22b) we have

$$\frac{\theta_{E0} - \theta}{\tau} = \frac{5R\Delta\theta}{18\tau}. \tag{9.27}$$

The vertical velocity is then given by

$$w \approx \frac{5R\Delta\theta H}{18\tau\Delta_V\theta_0} = \frac{5R\Delta_H H}{18\tau\Delta_V}. \tag{9.28}$$

Using mass continuity we can transform this into an estimate for the meridional velocity. Thus, if we let $(v/Y_H) \sim (w/H)$ and use (14.22), we obtain

$$v \sim \frac{R^{3/2} a \Delta_H}{\tau \Delta_V} \propto \frac{\Delta_H^{5/2}}{\Delta_V} \qquad \text{and} \qquad \Psi \sim vH \sim \frac{R^{3/2} a H \Delta_H}{\tau \Delta_V} \propto (\Delta\theta)^{5/2}, \tag{9.29}$$

where Ψ is the meridional overturning stream function Ψ, which evidently increases fairly rapidly as the gradient of the radiative equilibrium temperature increases. The characteristic overturning time of the circulation, τ_d is then

$$\tau_d = \frac{H}{w} \sim \frac{\tau \Delta_V}{R \Delta_H}. \tag{9.30}$$

We require $\tau_d/\tau \gg 1$ for the effects of the circulation on the static stability to be small and therefore $\Delta_V/(R\Delta_H) \gg 1$, or equivalently, using (14.16),

$$\theta_0 \Delta_V \gg R(\theta_{E0} - \theta_0). \tag{9.31}$$

If instead $\tau \gg \tau_d$, then the potential temperature would be nearly conserved as a parcel ascended in the rising branch of the Hadley Cell, and the static stability would be nearly neutral.

9.2.7 † Effects of Moisture

Suppose now that moisture is present, but that the Hadley Cell remains a self-contained system; that is, it neither imports nor exports moisture. We envision that water vapour joins the circulation by way of evaporation from a saturated surface into the equatorward, lower branch of the Hadley Cell, and that this water vapour then condenses in and near the upward branch of the cell. The latent heat released by condensation is exactly equal to the heat required to evaporate moisture from the surface, and no heat is lost or gained to the system. However, the heating *distribution* is changed from the dry case, becoming a strong function of the solution itself and likely to have a sharp maximum near the equator. Even if we were to try to parameterize the latent heat release by simply choosing a flow dependent radiative equilibrium temperature, the resulting problem would still be quite nonlinear and a general analytic solution seems out of our reach.[27]

Nevertheless, we may see quite easily the qualitative features of moisture, at least within the context of this model. The meridional distribution of temperature is still given by way of thermal wind balance with an angular-momentum-conserving zonal wind, and so is still given by (14.12). We may also assume that the meridional extent of the Hadley Cell is unaltered; that is, a solution exists with circulation confined to $\vartheta < \vartheta_H$ (although it may not be the unique solution). Then, if θ_E^* is the effective radiative equilibrium temperature of the moist solution, we have that $\theta_E^*(Y_H) = \theta_E(Y_H)$ and, in the small-angle approximation,

$$\int_0^{Y_H} \theta \, \mathrm{d}y = \int_0^{Y_H} \theta_E^* \, \mathrm{d}y = \int_0^{Y_H} \theta_E \, \mathrm{d}y, \tag{9.32}$$

where the first equality holds because it defines the solution, and the second equality holds because moisture provides no net energy source. Because condensation will occur mainly in the upward branch of the Hadley Cell, θ_E^* will be peaked near the equator, as sketched in Fig. 14.8. This construction makes it clear that the main difference between the dry and moist solutions is that the latter has a more intense overturning circulation, because, from (14.25), the circulation increases with the temperature difference between the solution and the forcing temperature. Concomitantly, our intuition suggests that the upward branch of the moist Hadley circulation will become much narrower and more intense than the downward branch because of the enhanced efficiency of moist convection, and these expectations are generally confirmed by numerical integrations of the moist equations of motion.

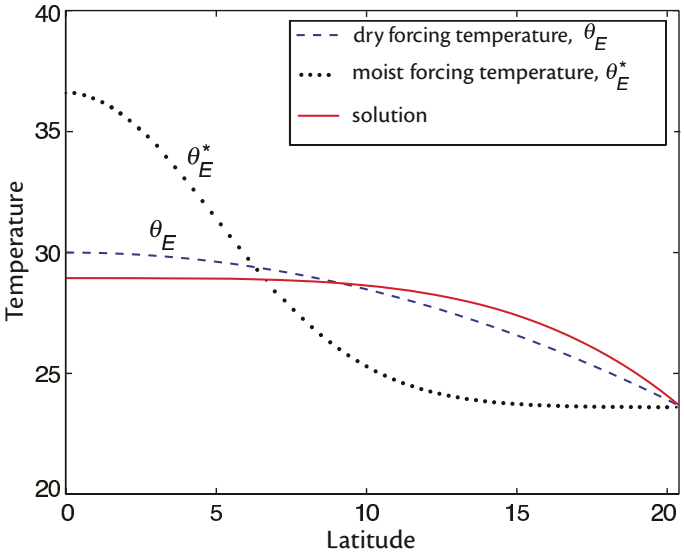

Fig. 9.8 Schematic of the effects of moisture on a model of the Hadley Cell. The temperature of the solution (solid line) is the same as that of a dry model, because this is determined from the angular-momentum-conserving wind. The heating distribution (as parameterized by a forcing temperature) is peaked near the equator in the moist case, leading to a more vigorous overturning circulation.

9.2.8 The Radiative Equilibrium Solution

Instead of a solution given by (14.12), could the temperature not simply be in radiative equilibrium everywhere? Such a state would have no meridional overturning circulation and the zonal velocity would be determined by thermal wind balance; that is,

$$v = 0, \qquad \theta = \theta_E, \qquad f\frac{u}{H} = -g\frac{\partial}{\partial y}\left(\frac{\theta_E}{\theta_0}\right). \tag{9.33}$$

To answer this question we consider the steady zonally symmetric zonal angular momentum equation with viscosity; that is, the zonally-averaged, viscous, steady, shallow atmosphere version of (2.68), namely

$$\frac{1}{a\cos\vartheta}\frac{\partial}{\partial\vartheta}(vm\cos\vartheta) + \frac{\partial(mw)}{\partial z} = \frac{\nu}{a\cos\vartheta}\frac{\partial}{\partial\vartheta}\left(\cos^2\vartheta\frac{\partial}{\partial\vartheta}\frac{u}{\cos\vartheta}\right) + \nu a\cos\vartheta\frac{\partial^2 u}{\partial z^2}, \tag{9.34}$$

where the variables vary only in the ϑ–z plane. The viscous term on the right-hand side arises from the expansion in spherical coordinates of the Laplacian. Note that it is angular *velocity*, not the angular momentum, that is diffused, because there is no diffusion of the angular momentum due to the Earth's rotation. However, to a very good approximation, the viscous term will be dominated by vertical derivatives and we may then write (14.34) as

$$\nabla_x\cdot(\boldsymbol{v}m) = \nu\frac{\partial^2 m}{\partial z^2}. \tag{9.35}$$

where $\nabla_x\cdot$ is the divergence in the meridional plane. The right-hand side now has a diffusive form, and in Section 13.5.1 we showed that variables obeying equations like this can have no extrema within the fluid. Thus, there can be no maximum or minimum of angular momentum in the interior of the fluid, a result known as Hide's theorem.[28] In effect, diffusion always acts to smooth away an isolated extremum, and this cannot be counterbalanced by advection. The result also implies that there can be no interior extrema in a statistically steady state if there is any zonally asymmetric eddy motion that transports angular momentum downgradient.

If the viscosity were so large that the viscous term was dominant in (14.34), and so with the horizontal term now important, then the fluid would evolve toward a state of solid body rotation,

this being the fluid state with no internal stresses. In that case, there would be a maximum of angular momentum at the equator — a state of 'super-rotation'. (Related mechanisms have been proposed for the maintenance of super-rotation on Venus.[29])

Returning now to the question posed at the head of this section, suppose that the radiative equilibrium solution does hold. Then a radiative equilibrium temperature decreasing away from the equator more rapidly than the angular-momentum-conserving solution θ_M implies, using thermal wind balance, a maximum of m at the equator and above the surface, in violation of the no-extremum principle. Of course, we have derived the angular-momentum-conserving solution in the inviscid limit, in which the no-extrema principle does not apply. But any small viscosity will make the radiative equilibrium solution completely invalid, but potentially have only a small effect on the angular-momentum-conserving solution; that is, in the *limit* of small viscosity the angular-momentum-conserving solution can conceivably hold approximately, at least in the absence of boundary layers, whereas the radiative equilibrium solution cannot.

However, if the radiative equilibrium temperature varies more slowly with latitude than the temperature corresponding to the angular momentum conserving solution then a radiative equilibrium solution *can* obtain, without violating Hide's theorem. In particular, this is the case if $\theta_E \propto P_4(\sin\vartheta)$, where P_4 is the fourth Legendre polynomial, and so the possibility exists of two equilibrium solutions for the same forcing; however, P_4 is an unrealistically flat radiative equilibrium temperature for the Earth's atmosphere.

9.3 A SHALLOW WATER MODEL OF THE HADLEY CELL

Although expressed in the notation of the primitive equations, the model described above takes no account of any vertical structure in its stratification and is, *de facto,* a shallow water model. (We discuss how the primitive equations reduce to the shallow water equations in Sections 3.4 and 18.7.) Furthermore, the geometric aspects of sphericity play no essential role. Thus, we may transparently express the essence of the model by:

(i) explicitly using the shallow water equations instead of the stratified equations;

(ii) using the equatorial β-plane, with $f = f_0 + \beta y$ and $f_0 = 0$.

Let us therefore, if only as an exercise, construct a reduced-gravity model with an active upper layer overlying a stationary lower layer.

9.3.1 Momentum Balance

The inviscid zonal momentum equation of the upper layer is

$$\frac{\mathrm{D}u}{\mathrm{D}t} - \beta y v = 0 \tag{9.36}$$

or

$$\frac{\mathrm{D}}{\mathrm{D}t}\left(u - \frac{\beta y^2}{2}\right) = 0, \tag{9.37}$$

which is the β-plane analogue of the conservation of axial angular momentum. (In this section, all variables are zonally averaged, but we omit any notation denoting that.) From (14.37) we obtain the zonal wind as a function of latitude,

$$u = \frac{1}{2}\beta y^2 + A, \tag{9.38}$$

where A is a constant, which is zero if $u = 0$ at the equator, $y = 0$. The flow given by (14.38) is then analogous to the angular momentum conserving flow in the spherical model, (14.7). Because

the lower layer is stationary, the analogue of thermal wind balance in the stratified model is just geostrophic balance, namely

$$fu = -g' \frac{\partial h}{\partial y}, \tag{9.39}$$

where h is the thickness of the active upper layer. Using (14.39) and $f = \beta y$ we obtain

$$g' \frac{\partial h}{\partial y} = -\frac{1}{2}\beta^2 y^3, \qquad \text{whence} \qquad h = -\frac{1}{8g'}\beta^2 y^4 + h(0), \tag{9.40a,b}$$

where $h(0)$ is the value of h at $y = 0$.

9.3.2 Thermodynamic Balance

The thermodynamic equation in the shallow water equations is just the mass conservation equation, which we write as

$$\frac{\mathrm{D}h}{\mathrm{D}t} = -\frac{1}{\tau}(h - h^*), \tag{9.41}$$

where the right-hand side represents heating — h^* is the field to which the height relaxes on a time scale τ. For illustrative purposes we will choose

$$h^* = h_0(1 - \alpha|y|). \tag{9.42}$$

(If we chose the more realistic quadratic dependence on y, the model would be more similar to that of the previous section.) To be in thermodynamic equilibrium we require that the right-hand side integrates to zero over the Hadley Cell; that is

$$\int_0^Y (h - h^*)\,\mathrm{d}y = 0, \tag{9.43}$$

where Y is the latitude of the poleward extent of the Hadley Cell, thus far unknown. Poleward of this, the height field is simply in equilibrium with the forcing — there is no meridional motion and $h = h^*$. Since the height field must be continuous, we require that

$$h(Y) = h^*(Y). \tag{9.44}$$

The two constraints (14.43) and (14.44) provide values of the unknowns $h(0)$ and Y, and give

$$Y = \left(\frac{5h_0\alpha g'}{\beta^2}\right)^{1/3}, \tag{9.45}$$

which is analogous to (14.19), as well as an expression for $h(0)$ that we leave as a problem for the reader. The qualitative dependence on the parameters is similar to that of the full model, although the latitudinal extent of the Hadley Cell is proportional to the cube root of the meridional thickness gradient α.

9.4 † ASYMMETRY AROUND THE EQUATOR

The Sun is overhead at the equator but two days out of the year, and in this section we investigate the effects that asymmetric heating has on the Hadley circulation. Observations indicate that except for the brief periods around the equinoxes, the circulation is dominated by a single cell with rising motion centred in the summer hemisphere, but extending well into the winter hemisphere. That is, as seen in Fig. 14.3, the 'winter cell' is broader and stronger than the 'summer cell', and it behoves us to try to explain this. We will stay in the framework of the inviscid angular-momentum model

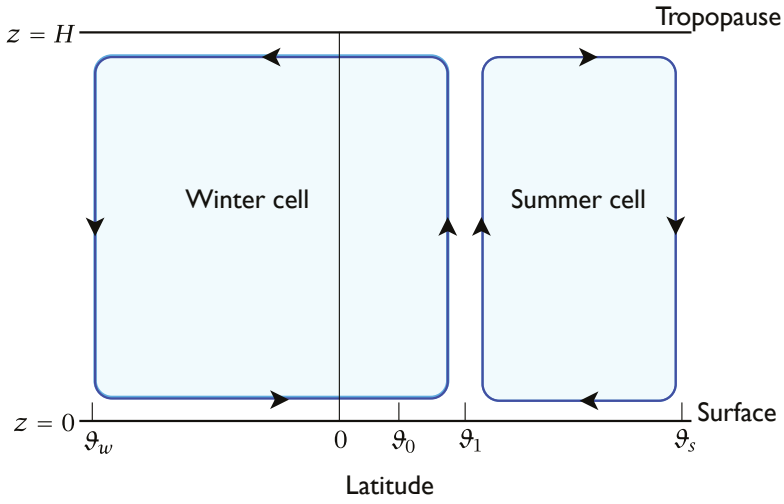

Fig. 9.9 A Hadley circulation model in which the heating is centred off the equator, at a latitude ϑ_0. The lower level convergence occurs at a latitude ϑ_1 that is not in general equal to ϑ_0. The resulting winter Hadley Cell is stronger and wider than the summer cell.

of Section 14.2, changing only the forcing field to represent the asymmetry and being a little more attentive to the details of spherical geometry.[30]

To represent an asymmetric heating we may choose a radiative equilibrium temperature of the form

$$\begin{aligned}\frac{\theta_E(\vartheta,z)}{\theta_0} &= 1-\frac{2}{3}\Delta_H P_2(\sin\vartheta-\sin\vartheta_0)+\Delta_V\left(\frac{z}{H}-\frac{1}{2}\right)\\ &= 1+\frac{\Delta_H}{3}\left[1-3(\sin\vartheta-\sin\vartheta_0)^2\right]+\Delta_V\left(\frac{z}{H}-\frac{1}{2}\right).\end{aligned} \tag{9.46}$$

This is similar to (14.14), but now the forcing temperature falls monotonically from a specified latitude ϑ_0. If $\vartheta_0 = 0$ the model is identical to the earlier one, but if not we envision a circulation as qualitatively sketched in Fig. 14.9, with rising motion off the equator at some latitude ϑ_1, extending into the winter hemisphere to a latitude ϑ_w, and into the summer hemisphere to ϑ_s. We will discover that, in general, $\vartheta_1 \neq \vartheta_0$ except when $\vartheta_0 = 0$. Following our procedure we used in the symmetric case as closely as possible, we then make the following assumptions:

(i) The flow is quasi-steady. That is, at any time of year the flow adjusts to a steady circulation on a time scale more rapid than that on which the solar zenith angle appreciably changes.

(ii) The flows in the upper branches conserve angular momentum, m. Further assuming that $u = 0$ at $\vartheta = \vartheta_1$ so that $m = \Omega a^2 \cos^2\vartheta_1$ we obtain

$$u(\vartheta) = \frac{\Omega a(\cos^2\vartheta_1 - \cos^2\vartheta)}{\cos\vartheta}\,. \tag{9.47}$$

Thus, we expect to see westward (negative) winds aloft at the equator. In the lower branches the zonal flow is assumed to be approximately zero, i.e., $u(0) \approx 0$.

(iii) The flow satisfies hydrostatic and gradient wind balance. The meridional momentum equation is then

$$fu + \frac{u^2\tan\vartheta}{a} = -\frac{1}{a}\frac{\partial\phi}{\partial\vartheta}\,, \tag{9.48}$$

and because the flow crosses the equator we cannot neglect the second term on the left-hand side. Combining this with hydrostatic balance ($\partial\phi/\partial z = g\theta/\theta_0$) leads to a generalized

thermal wind balance, which may be written as

$$m\frac{\partial m}{\partial z} = -\frac{ga^2\cos^2\vartheta}{2\theta_0\tan\vartheta}\frac{\partial\theta}{\partial\vartheta}. \tag{9.49}$$

If the undifferentiated m is approximated by $\Omega a^2\cos^2\vartheta$, this reduces to conventional thermal wind balance, (14.10).

(iv) Potential temperature in each cell is conserved when integrated over the extent of the cell. Thus,

$$\int_{\vartheta_1}^{\vartheta_s}(\theta-\theta_E)\cos\vartheta\,\mathrm{d}\vartheta = 0, \qquad \int_{\vartheta_1}^{\vartheta_w}(\theta-\theta_E)\cos\vartheta\,\mathrm{d}\vartheta = 0, \tag{9.50}$$

for the summer and winter cells, respectively, where θ is the vertically averaged potential temperature.

(v) Potential temperature is continuous at the edge of each cell, so that

$$\theta(\vartheta_s) = \theta_E(\vartheta_s), \qquad \theta(\vartheta_w) = \theta_E(\vartheta_w), \tag{9.51}$$

and is also continuous at ϑ_1. This last condition must be explicitly imposed in the asymmetric model, whereas in the symmetric model it holds by symmetry. Now, recall from the symmetric model that the value of the temperature at the equator was determined by the integral constraint (14.17) and the continuity constraint (14.18). We have analogues of these in each hemisphere, namely (14.50) and (14.51), and thus, if ϑ_1 is set equal to ϑ_0 we cannot expect that they each would give the same temperature at ϑ_0. Thus, ϑ_1 must be a free parameter to be determined.

Given these assumptions, the solution may be calculated. Using thermal wind balance, (14.49), with $m(H) = \Omega a^2\cos^2\vartheta_1$ and $m(0) = \Omega a^2\cos^2\vartheta$ we find

$$-\frac{1}{\theta_0}\frac{\partial\theta}{\partial\vartheta} = \frac{\Omega^2a^2}{gH}\left(\frac{\sin\vartheta}{\cos^3\vartheta}\cos^4\vartheta_1 - \sin\vartheta\cos\vartheta\right), \tag{9.52}$$

which integrates to

$$\theta(\vartheta) - \theta(\vartheta_1) = -\frac{\theta_0\Omega^2a^2}{2gH}\frac{(\sin^2\vartheta-\sin^2\vartheta_1)^2}{\cos^2\vartheta}. \tag{9.53}$$

The value of ϑ_1, and the value of $\theta(\vartheta_1)$, are determined by the constraints (14.50) and (14.51). It is not in general possible to obtain a solution analytically, but one may be found numerically by an iterative procedure and one such is illustrated in Fig. 14.10. The zonal wind of the solution is always symmetric around the equator, because it is determined solely by angular momentum conservation. The temperature is therefore also symmetric, as (14.53) explicitly shows. However, the width of the solution in each hemisphere will, in general, be different.

Furthermore, because the strength of the circulation increases with difference between the temperature of the solution and the radiative equilibrium temperature, the circulation in the winter hemisphere will also be much stronger than that in the summer, a prediction that is consistent with the observations (see Fig. 14.3). More detailed calculations show that, because the strength of the model Hadley Cell increases nonlinearly with ϑ_0, the time-average strength of the Hadley Cell with seasonal forcing is stronger that that produced by annually averaged forcing. However, this does not appear to be a feature of either the observations or more complete numerical simulations, suggesting that an angular-momentum-conserving model has some deficiencies.[31]

The lack of consideration of zonal asymmetries and the lack of angular momentum conservation because of the effects of baroclinic eddies are issues that are shared with the steady model with

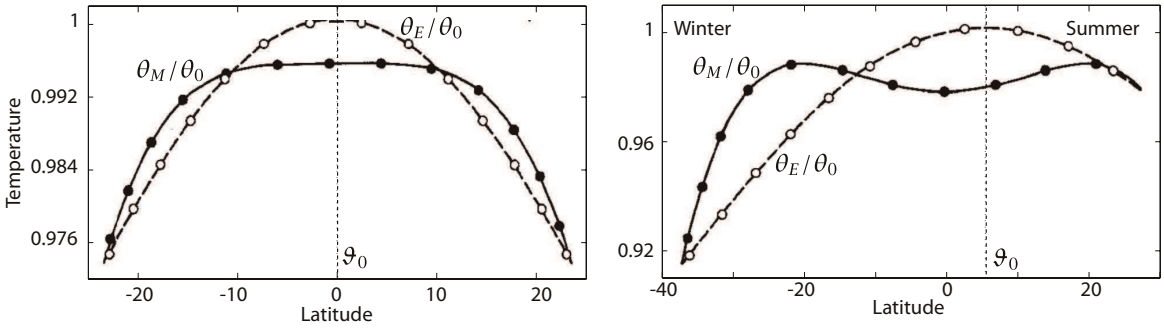

Fig. 9.10 Solutions of the Hadley Cell model with heating centred at the equator ($\vartheta_0 = 0°$, left) and off the equator ($\vartheta_0 = +6°$ N, right), with $\Delta_H = 1/6$. The dashed line is the radiative equilibrium temperature and the solid line is the angular-momentum-conserving solution. In the right-hand panel, $\vartheta_1 \approx +18°$, and the circulation is dominated by the cell extending from $+18°$ to $-36°$.[8]

hemispheric symmetry. A problem that is unique to the asymmetric model is the quasi-steady assumption, given the presence of a temporally progressing seasonal cycle. Because the latitude of the upward branch of the Hadley Cell varies with season, the value of the angular momentum entering the system also varies with time, and so a homogenized value of angular momentum is hard to achieve. Nonetheless, the overall picture that the model paints, with its qualitative explanation of the strengthened and extended winter Hadley Cell, is very useful, even if quantitatively flawed.

'Place me on Sunium's marbled steep,
'Where nothing, save the waves and I,
May hear our mutual murmurs sweep.
George Gordon Byron (Lord Byron), *The Isles of Greece,* 1820.

CHAPTER 10

Planetary Waves and Zonal Asymmetries

Planetary waves are large-scale Rossby waves in which the potential vorticity gradient is provided by differential rotation (i.e., the beta-effect). They are ubiquitous in Earth's atmosphere and almost certainly in other planetary atmospheres. They propagate horizontally over the two Poles, and they propagate vertically into the stratosphere and beyond. In the previous chapter we saw that it is the propagation of Rossby waves away from their mid-latitude source that gives rise to the mean eastward eddy-driven jet. In this chapter we will see that the dynamics of such waves also largely determines the large-scale *zonally asymmetric* circulation of the mid-latitude atmosphere. In the first few sections we discuss the properties and propagation of planetary waves themselves, and in many ways these sections are a continuation of Chapter 6. We then look more specifically at planetary waves forced by surface variations in topography and thermal properties, for it is these waves that give rise to the zonally asymmetric circulation.

In proceeding this way we are dividing our task of constructing a theory of the general circulation of the extratropical atmosphere into two. The first task (Chapters 14 and 15) was to understand the zonally averaged circulation and the transient zonal asymmetries by supposing that, to a first approximation, this circulation is qualitatively the same as it would be if the boundary conditions were zonally symmetric, with no mountains or land–sea contrasts. Given the statistically zonally symmetric circulation, the second task is to understand the zonally asymmetric circulation. We may do this by supposing that the latter is a perturbation on the former, and using a theory linearized about the zonally symmetric state. It is by no means obvious that such a procedure will be successful, for it depends on the nonlinear interactions among the zonal asymmetries being weak. We might make some a priori estimates that suggest that this might be the case, but the ultimate justification for the approach lies in its a posteriori success. In our discussion of stationary waves we will focus first on the response to orography at the lower boundary, and then consider thermodynamic forcing — arising, for example, from an inhomogeneous surface temperature field. Our focus throughout this chapter is the mid-latitudes.

10.1 ROSSBY WAVE PROPAGATION IN A SLOWLY VARYING MEDIUM

In Chapters 6 and 7 we looked at wave propagation using linearized equations of motion. We now focus and extend this discussion by looking at Rossby wave propagation in a medium in which the parameters (such as the zonal wind and the stratification) vary spatially — as occurs in the real

atmosphere. If the parameters do vary then waves may propagate into a region in which they amplify, perhaps violating the initial assumption of linearity, so let us first look at what the conditions for linearity are.[32]

10.1.1 Linear Dynamics

If the linear equations are to be an accurate representation of the dynamics then the perturbation quantities need to be small compared to the background state, or at least the nonlinear terms must be small. In reality this is not always the case and indeed it may be that in course of propagation the waves amplify and may even *break*. Wave breaking is familiar to anyone who has been to the beach and watched water waves move toward the shore and crash in the 'surf zone' as the mean depth becomes too shallow to support laminar surface waves. Manifestly, the linear approximation breaks down at this point. More generally, wave breaking simply refers to an irreversible deformation of material surfaces, generally leading to dissipation. Since Rossby waves generally grow in amplitude as they propagate up (because density falls) we can expect Rossby wave breaking to occur somewhere in the atmosphere, but waves can also break as they propagate laterally, if and when they grow in size to such an extent that the nonlinear terms in the equations of motion become important.

To examine this consider the quasi-geostrophic potential vorticity equation,

$$\left(\frac{\partial}{\partial t} + \boldsymbol{u}\cdot\nabla\right) q = 0, \qquad q = \beta y + \nabla^2\psi' + \frac{f_0^2}{\rho_R}\frac{\partial}{\partial z}\left(\frac{\rho_R}{N^2}\frac{\partial \psi}{\partial z}\right). \tag{10.1a,b}$$

The derivation of this equation was given in Chapter 5 and all the terms are defined there. In brief, q is the quasi-geostrophic potential vorticity and ψ the streamfunction, f_0 is the Coriolis parameter and ρ_R is a density profile, a function of z only. Breaking the above equation up into mean and perturbation quantities in the usual way we obtain

$$\left(\frac{\partial}{\partial t} + \overline{u}(y,z)\frac{\partial}{\partial x}\right) q' + v'\frac{\partial \overline{q}}{\partial y} = -\left(\frac{\partial u'q'}{\partial x} + \frac{\partial v'q'}{\partial y}\right). \tag{10.2}$$

In the linear approximation we neglect the terms on the right-hand side and, seeking wave-like solutions of the form $\psi = F(x - ct)$, we obtain

$$(\overline{u} - c)\frac{\partial q'}{\partial x} + v'\frac{\partial \overline{q}}{\partial y} = 0. \tag{10.3}$$

For the linear approximation to be valid the terms in this equation must be larger than the nonlinear terms in (16.2), and this will be the case if

$$|\overline{u} - c| \gg |u'| \qquad \text{and} \qquad \left|\frac{\partial \overline{q}}{\partial y}\right| \gg \left|\frac{\partial q'}{\partial y}\right|. \tag{10.4a,b}$$

Although it is common to only treat the case in which $\overline{u}$ is a constant, we may also consider the case in which $\overline{u}$ varies slowly, either in latitude or height or both, and (16.3) then approximately holds locally. But if a wave propagates into a region in which $\overline{u} = c$ then the linear criterion *must* break down. Regions where $\overline{u} = c$ are called *critical lines, critical surfaces, critical heights* or *critical latitudes,* depending on context, and in many circumstances a *critical layer* of finite width will surround the critical line, in which frictional and/or nonlinear effects are important. The location of a critical surface does not depend on the frame of reference used to measure the velocities.

For reference we first write down a few results for the simplest case when $\partial\overline{q}/\partial y$, $\overline{u}$, N^2 and ρ_R are all constant, referring to Section 6.5 as needed. We look for solutions of the form

$$\psi' = \mathrm{Re}\,\widetilde{\psi}\mathrm{e}^{\mathrm{i}(kx+ly+mz-\omega t)}, \tag{10.5}$$

and obtain the dispersion relation

$$\omega = \overline{u}k - \frac{k\beta}{k^2 + l^2 + Pr^2m^2}, \tag{10.6}$$

where $Pr = f_0/N$ is the Prandtl ratio. The components of the group velocity are given by

$$c_g^x = \overline{u} + \frac{(k^2 - l^2 - Pr^2m^2)\beta}{(k^2 + l^2 + Pr^2m^2)^2}, \qquad c_g^y = \frac{2kl\beta}{(k^2 + l^2 + Pr^2m^2)^2}, \qquad c_g^z = \frac{2kmPr^2\beta}{(k^2 + l^2 + Pr^2m^2)^2}. \tag{10.7a,b,c}$$

10.1.2 Conditions for Wave Propagation

Suppose that the zonal wind varies slowly with latitude and height, but that, for simplicity, the density, ρ_R, is a constant. The equation of motion is

$$\left(\frac{\partial}{\partial t} + \overline{u}(y,z)\frac{\partial}{\partial x}\right)q' + v'\frac{\partial \overline{q}}{\partial y} = 0. \tag{10.8}$$

Because the coefficients of the equation are not constant we cannot assume harmonic solutions in the y and z directions; rather, we seek solutions of the form

$$\psi' = \widetilde{\psi}(y,z)e^{ik(x-ct)}. \tag{10.9}$$

If the parameters in (16.8) are varying slowly compared to the wavelength of the waves then a dispersion relation still exists (as discussed in Section 6.3), but the relation will be of the form $\omega = \Omega(\boldsymbol{k}; \boldsymbol{x}, t)$; where the function Ω varies slowly in space. Now, if the medium is not an explicit function of x or of time the x-wavenumber and the frequency will be a constant, and hence c is constant too, and we can use the dispersion relation to find what are effectively the other wavenumbers in the problem. Using (16.9) in (16.8) we find (with N^2 constant)

$$\frac{\partial^2\widetilde{\psi}}{\partial y^2} + \frac{f_0^2}{N^2}\frac{\partial^2\widetilde{\psi}}{\partial z^2} + n^2(y,z)\widetilde{\psi} = 0, \qquad \text{where} \qquad n^2(y,z) = \frac{\partial \overline{q}/\partial y}{\overline{u} - c} - k^2. \tag{10.10a,b}$$

Equation (16.10a) is similar to the Rayleigh or Rayleigh–Kuo equation encountered in Chapter 9, but now c is given and is not an eigenvalue; rather, the frequency is known and the dispersion relation gives the quantity n. The quantity n is the *refractive index* and it greatly affects how the waves propagate: solutions are wavelike when n^2 is positive and evanescent when n^2 is negative. To see this in a simple case, suppose there is no z-variation so that $\partial^2\widetilde{\psi}/\partial y^2 + n^2\widetilde{\psi} = 0$, whereas if n is constant and real we have harmonic solutions in the y-direction of the form $\exp(iny)$. If $n^2 < 0$ the solutions will evanesce. Waves tend to propagate toward regions of large n^2 and turn away from regions of negative n^2, as we will see in the examples to follow.

The value of n^2 will become very large if and as $\overline{u}$ approaches c from above and the waves, being very short, will tend to break. If $\overline{u}$ continues to diminish and becomes smaller than c then n^2 switches from being large and positive to large and negative. If n^2 diminishes because $\partial\overline{q}/\partial y$ diminishes then it will transition smoothly to a negative value. The location where $\overline{u} = c$ is called a critical surface (or line). The location where n^2 passes through zero is called a turning surface (or line).

The bounds on n^2 can be translated into bounds on the zonal phase speed c. Given a zonal wind $\overline{u}$, wave propagation requires that c is bounded by

$$\overline{u} - \frac{\partial \overline{q}/\partial y}{k^2 + \gamma^2} < c < \overline{u}. \tag{10.11}$$

At the upper bound (a critical surface) the wavelength is small and wave breaking is likely to occur. At the lower bound (a turning surface) the refractive index tends to zero and the wavelength tends to infinity. Waves will tend to propagate away from regions with a small n and be refracted toward regions of large n. The bounds can also be expressed in terms of the zonal velocity:

$$0 < \overline{u} - c < \frac{\partial \overline{q}/\partial y}{k^2 + \gamma^2}. \tag{10.12}$$

This form is useful when considering a situation in which the wave speed is given, for example by boundary conditions; Equation (16.12) then tells us under what configurations of zonal velocity wave propagation can occur. The lower bound corresponds to a critical surface and the upper bound to a turning surface.

It is algebraically complicated to continue our analysis in the three-dimensional case, so let us consider the cases in which the inhomogeneities in the medium occur separately in the horizontal and vertical. A summary of some key concepts is provided on page 590.

And beyond it, the deep blue air, that shows
Nothing, and is nowhere, and is endless.
Philip Larkin, *High Windows*, 1974.

CHAPTER 11

The Stratosphere

THE *STRATOSPHERE* IS THE REGION OF THE ATMOSPHERE above the troposphere and below the mesosphere; thus, it extends from the tropopause at a height of about 8–15 km, or a pressure of around 200–300 hPa, to the stratopause at about 50 km or about 1 hPa (see Fig. 15.24 on page 574). The *middle atmosphere* is the somewhat larger region that also includes the mesosphere, and so that extends up to the mesopause at about 90 km or 2×10^{-3} hPa, but we won't consider the mesosphere here. Our goal in this chapter is to provide an introduction to the dynamics giving rise to the structure and variability of the stratosphere.[33]

The outline of this chapter is roughly as follows. We begin with a rather descriptive overview of the stratosphere as a whole. Then, starting in Section 17.2, we discuss the Rossby and gravity waves that in many ways serve to drive the circulation. We come back to the circulation itself in Section 17.4, focusing mainly on the generation of zonal flows and the meridional residual overturning circulation. We round out the chapter with discussions of two striking examples of stratospheric variability, namely the quasi-biennial oscillation in Section 17.6, and extratropical variability and sudden warmings in Section 17.7, with these terms to be defined in the sections ahead.

11.1 A DESCRIPTIVE OVERVIEW

In the troposphere the stratification is determined by dynamical processes — largely by convection at low latitudes and additionally by baroclinic instability at high latitudes — and the tropopause is the height to which the dynamical activity reaches, as discussed in Chapter 15. In contrast, in the stratosphere the temperature is determined to a much greater degree by radiative processes and the dynamics are, compared to those in the tropopause, slow. Over much of the stratosphere the temperature actually increases with height, and this is due to a layer of ozone that absorbs solar radiation in the mid-stratosphere between about 20 and 30 km. If there were no ozone we would certainly have a tropopause and a stratosphere, but the temperature in the stratosphere would increase much less with height than it in fact does.

The radiative-equilibrium temperature for January is illustrated in Fig. 17.1. This temperature is that which would putatively ensue without any stratospheric fluid motion, although we take the distribution of absorbers (such as ozone) to be those present in the actual, moving, atmosphere, and the calculation involves a linearization around the observed temperature.[34] There is quite a strong lateral gradient in the winter hemisphere and a weaker reversed temperature in the summer hemisphere, and in fact the part of the stratosphere with the highest radiative equilibrium

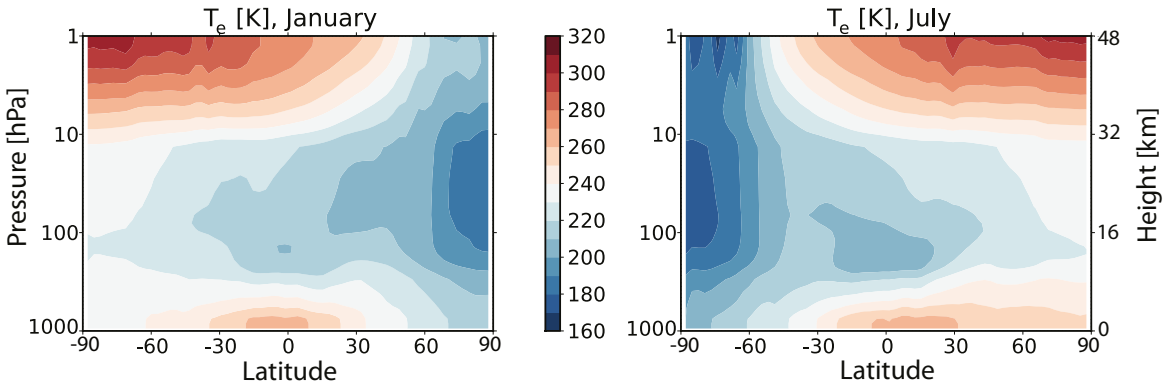

Fig. 11.1 The zonally averaged radiative-equilibrium temperature in January and July; that is, the temperature that would nominally arise in the absence of fluid motion in the stratosphere, but with the actual distribution of radiative absorbers. Above about 50 km the equilibrium temperature generally diminishes with height. The ordinate is pressure, and the height values are approximate.

temperature is the upper-stratosphere summer pole, at around 1 hPa. The actual observed zonally averaged temperature and zonal-wind structure are plotted in Fig. 17.2. From these figures we infer the following:

- The stratosphere is very stably stratified, with a typical lapse rate corresponding to $N \approx 2\times10^{-2}$ s, about twice that of the troposphere on average. This is in part due to the absorption of solar radiation by ozone between 20 and 50 km.
- In the summer the solar absorption at high latitudes leads to a reversed temperature gradient (warmer pole than equator) and, by thermal wind balance, a negative vertical shear of the zonal wind. The temperature distribution is not far from the radiative equilibrium distribution, and over much of the summer stratosphere the mean winds are negative (westward).
- In winter high latitudes receive very little solar radiation and there is a strong meridional temperature gradient and consequently a strong vertical shear in the zonal wind. Nevertheless, this temperature gradient is significantly weaker than the radiative equilibrium temperature gradient, implying a poleward heat transfer by the fluid motions.

How do the dynamics of the stratosphere differ from the troposphere? One way is that there is little, if any, baroclinic instability in the stratosphere — for various reasons. Suppose we first think of the stratosphere in isolation. There is no clear reversal of the potential vorticity gradient and no real opportunity for counter-propagating edge waves or Rossby waves to interact in the stratosphere, and hence stratosphere alone may simply be baroclinically stable. If the stratosphere were baroclinically unstable the instability would be much weaker, because of its higher stratification. A typical value of the static stability in the stratosphere is $N \approx 2\times10^{-2}\,\mathrm{s}^{-1}$, and using a height scale of 20 km gives a value of the deformation radius NH/f of about 4000 km, as opposed to the canonical value of 1000 km in the troposphere. (The stratospheric estimate is very approximate because the scale height, H_s is much less than 20 km, and a relevant deformation radius is then $N\sqrt{HH_s}/f$. But on the other hand one could also take $H > 20$ km, so 4000 km may be a fair estimate.) Thus, even with the same horizontal temperature gradient as the troposphere, a typical instability scale (of the stratosphere in isolation) would be large, perhaps at wavenumber 2 rather than wavenumber 8. The stratospheric growth rate would then be much less than in the troposphere: the Eady growth rate is given by $\sigma_E \equiv 0.31\Lambda H/L_d = 0.31U/L_d$, where Λ is the shear, giving the growth rate that is several times smaller than its tropospheric counterpart. Of course, if baroclinic instability has a modal form then the instability has the same horizontal scale and grows at the same rate in

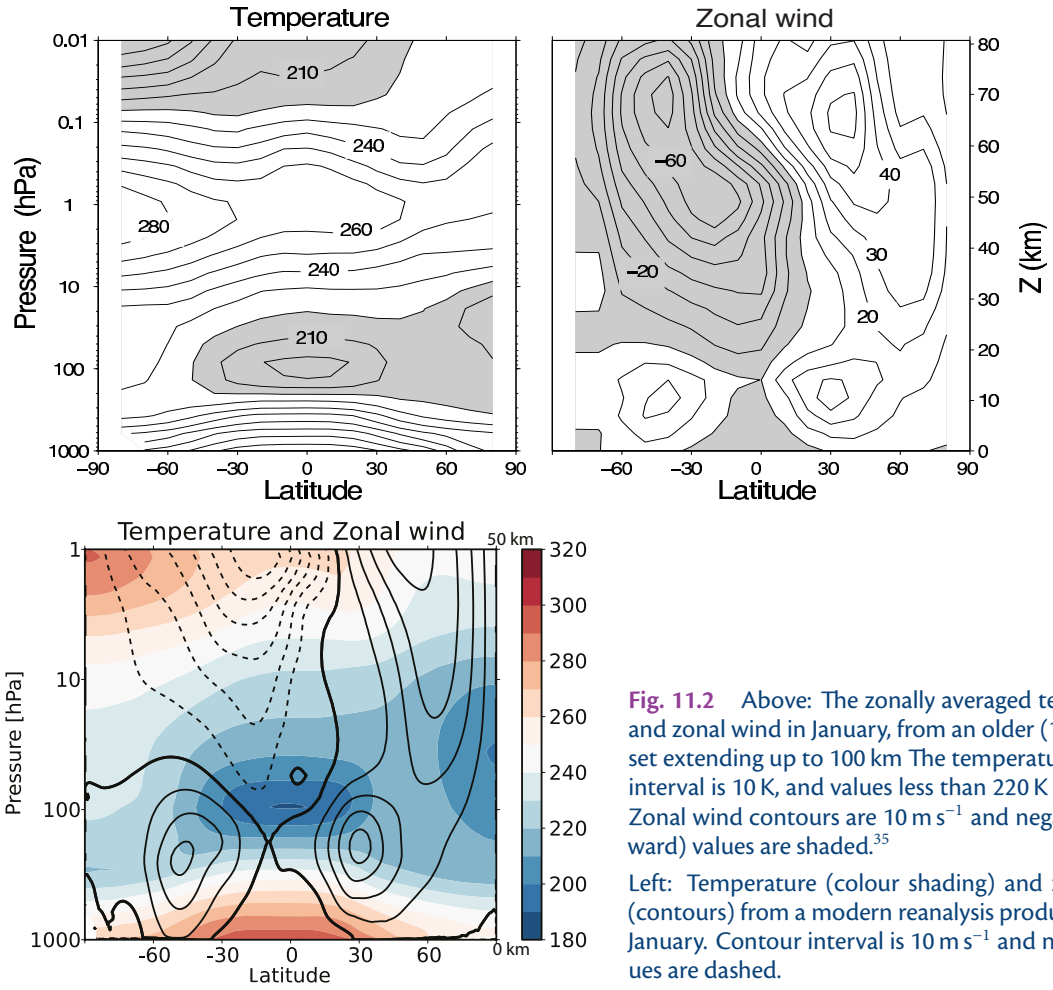

Fig. 11.2 Above: The zonally averaged temperature and zonal wind in January, from an older (1980s) data set extending up to 100 km The temperature contour interval is 10 K, and values less than 220 K are shaded. Zonal wind contours are 10 m s^{-1} and negative (westward) values are shaded.[35]

Left: Temperature (colour shading) and zonal wind (contours) from a modern reanalysis product, also for January. Contour interval is 10 m s^{-1} and negative values are dashed.

the stratosphere as the tropospheric one — it is the same mode! But in this case the higher lapse rate suppresses the amplitude of the stratospheric instability, as shown in Fig. 9.21.

For all these reasons, baroclinic instability is not the main process leading to a circulation in the stratosphere — the main process is the propagation and subsequent breaking and dissipation of gravity and Rossby waves from the troposphere to the stratosphere. This breaking will produce an acceleration of the zonal flow, and/or a meridional overturning circulation, and a good fraction of this chapter will be devoted to describing that process. But first we'll provide a little more description about the circulation itself, and it is convenient to divide that into two parts:

(i) a quasi-horizontal circulation;

(ii) a meridional overturning circulation (MOC) that is most usefully described as a residual circulation (the residual meridional circulation, or RMOC) using the TEM formalism.

11.1.1 The Quasi-Horizontal Circulation

In the extra-tropics the stratification is high and the Rossby number small and, at least to the extent that the scales of motion are not truly hemispheric the circulation is well described by the quasi-geostrophic equations. Now, not only does any stratospheric baroclinic instability tend to occur on a large scale, but so does any wave activity that arises from the propagation of Rossby waves up from

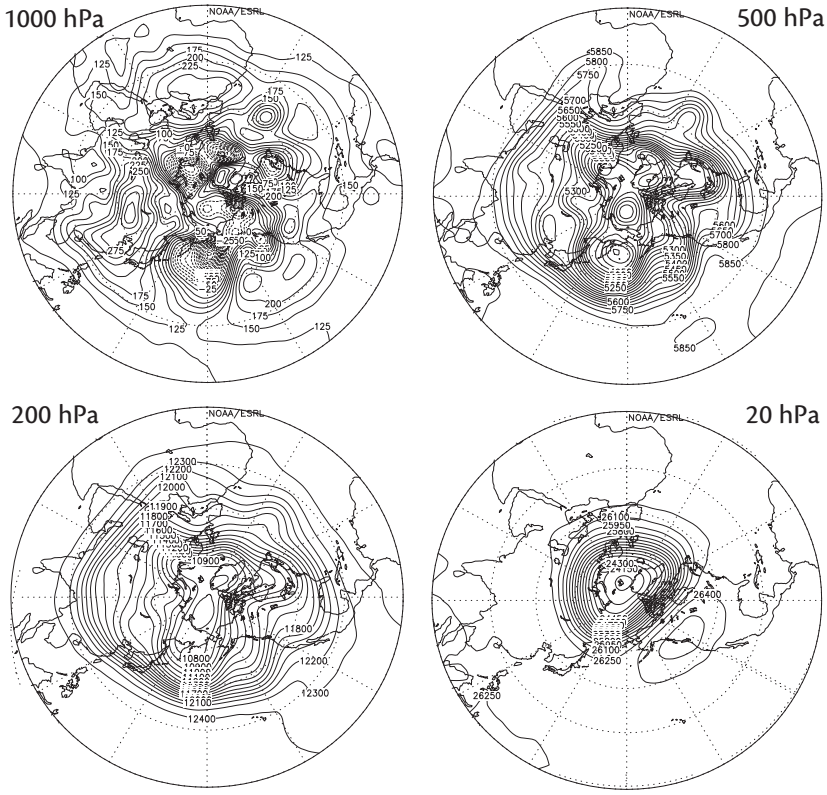

Fig. 11.3 The geopotential height on 1 February, 2000, at various levels in the atmosphere — 1000 and 500 hPa are in the troposphere, 200 hPa is around the tropopause and 20 hPa is in the mid-stratosphere, at about 30 km. Note the general increase in the scale of the variations of the geopotential with height.

the troposphere. This is because of Charney–Drazin filtering, summarized in Fig. 16.6: the smaller the wavelength the smaller is the range of zonal winds through which the waves can propagate. If the wind is too high the waves encounter a turning surface, whereas if the wind is too low they encounter a critical layer. Thus, we would expect that the general horizontal scale of motion is larger in the stratosphere than in the troposphere, and this is borne out by inspection of Fig. 17.3, which shows geopotential height at various levels. The complex patterns of the lower and mid-troposphere are well filtered, and in mid-stratosphere the pattern is dominated by wavenumbers 1 and 2. Indeed it seems from the figure (which is typical) that much of the motion is concentrated around a *polar vortex*.

Looking at geopotential (which roughly corresponds to a streamfunction) gives a somewhat misleading impression of the lack of activity away from the poles. Here, because diabatic effects occur on a rather longer time scale than advective processes, the flow may be characterized by the advection of potential vorticity on more slowly evolving isentropic surfaces, as illustrated in Figs. 17.4 and 17.5. Both the potential vorticity and the tracer are evocative of two-dimensional turbulence. We see Rossby waves breaking and vortices stretched into filaments and tendrils, the features of an enstrophy cascade. We also perceive some idea of the spectral non-locality of the enstrophy transfer — a single large vortex overturns and breaks and there is little sense of a spectrally-local cascade of enstrophy to dissipative scales. For this reason, the mid-latitude region is sometimes known as the *surf zone*. It is precisely this wave breaking that gives rise to the enstrophy flux to

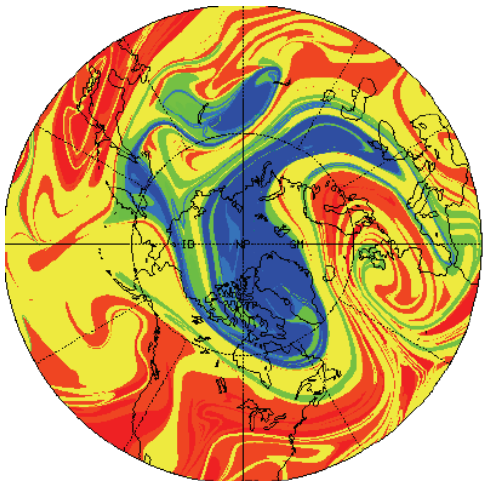

Fig. 11.4 The tracer distribution in the northern hemisphere lower stratosphere on 28 January 1992. The tracer was initialized on 16 January by setting it equal to the potential vorticity field calculated from an observational analysis, and then advected for 12 days by the observed wind fields.[36]

small scales and its dissipation, and which in turn gives rise to the overturning circulation that we discuss below.

The surf-zone does not usually extend to the pole, and in winter dense cold air over the pole forms itself into a cyclonic vortex, apparent in both Fig. 17.3 and 17.5. Although the vortex is ultimately the result of diabatic forcing, and has a preferred location, the tendency of quasi-two-dimensional flow to organize itself into vortices (as we see in Figs. 9.6 and 11.8) contributes to its coherence and isolation from the rest of the hemisphere. The boundary of the vortex, as measured by the value of the potential vorticity or of the tracer, is quite sharp with the value of PV often jumping by a factor of 2 or so, and the vortex is quite persistent — in fact it is a near-permanent feature of the winter hemisphere. Within the vortex potential vorticity tends to homogenize, and once formed the main communication that the vortex has with the surf zone is via occasional wave breaking at its boundary. It is interesting that, although the potential vorticity gradient is strong at the edge of the vortex, the exchange of properties is weak, implying a failure of notions of diffusion, or at least diffusion with a constant value of diffusivity; the edge of the vortex is a *mixing barrier*. We saw this property before, in our discussion of potential vorticity staircases in Section 12.1.3.

Stable as it is, the polar vortex is nevertheless sometimes disrupted by wave activity from below; this tends to occur when the wave activity itself is quite strong, and when the mean conditions are such as to steer that wave activity polewards. Occasionally, this activity is sufficiently strong so as to cause the vortex to break down, or to split into two smaller vortices, and so allow warm mid-latitude air to reach polar latitudes — an event known as a *stratospheric sudden warming*, and one such is illustrated in Fig. 17.22. We come back to the mechanism of such warmings later in the chapter.

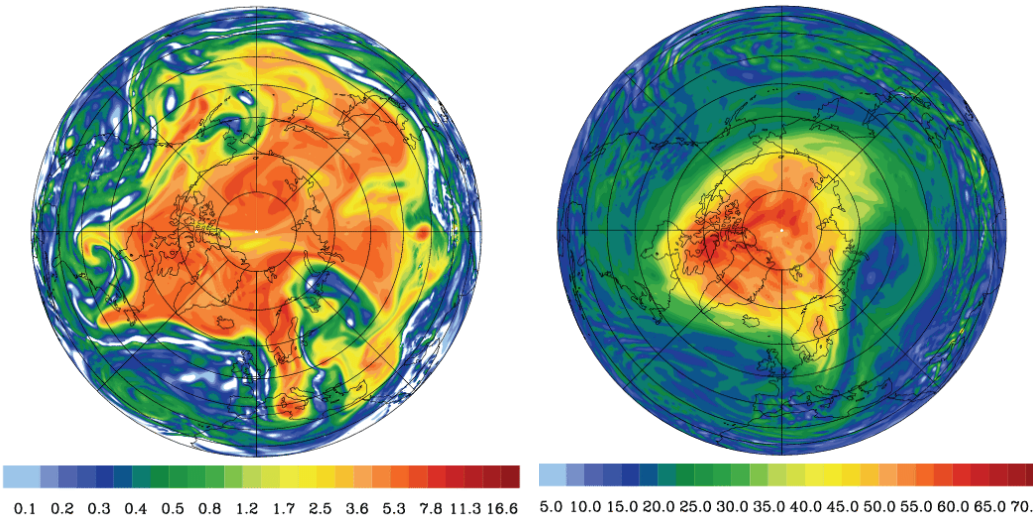

Fig. 11.5 The potential vorticity on two isentropic surfaces, the 310 K surface (left) and the 475 K surface (right), on 19 January, 2005. The shaded bar is in PV units. The 310 K surface is mainly in the troposphere (see Fig. 15.16) where baroclinic instability is abundant. The 475 K surface is at about 20 km altitude, and on it we see a polar stratospheric vortex with a fairly sharp boundary where the PV gradient is high, and a mid-latitude region of smaller-scale features and wave breaking.[37]

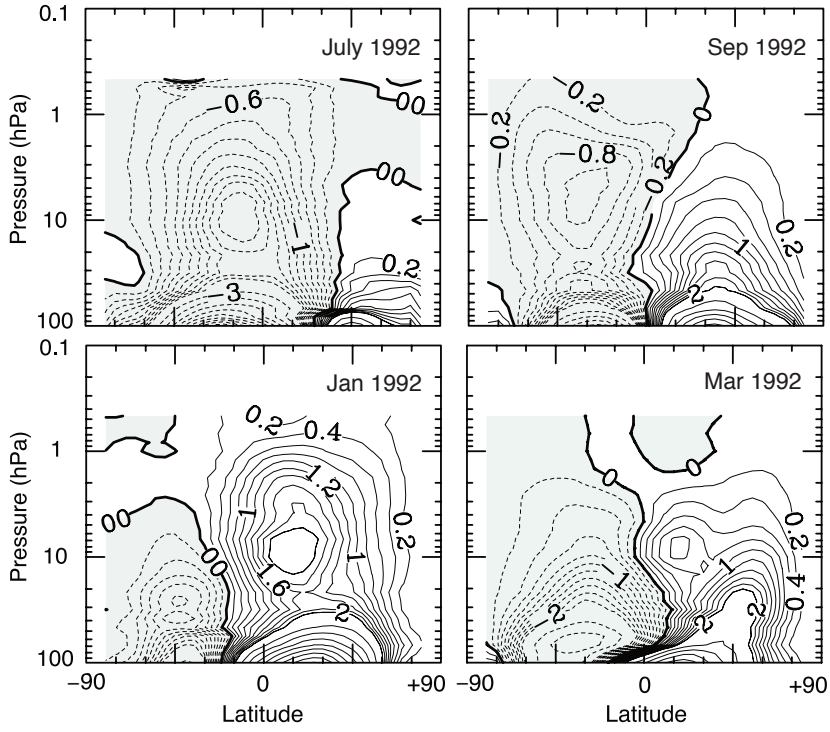

Fig. 11.6 The observed thickness-weighted (residual) streamfunction in the stratosphere, in Sverdrups (10^9 kg s^{-1}). The circulation is clockwise where the contours are solid.

The circulation is stronger in the winter hemispheres, whereas the equinoctial circulations (September, March) are more inter-hemispherically symmetric.[38]

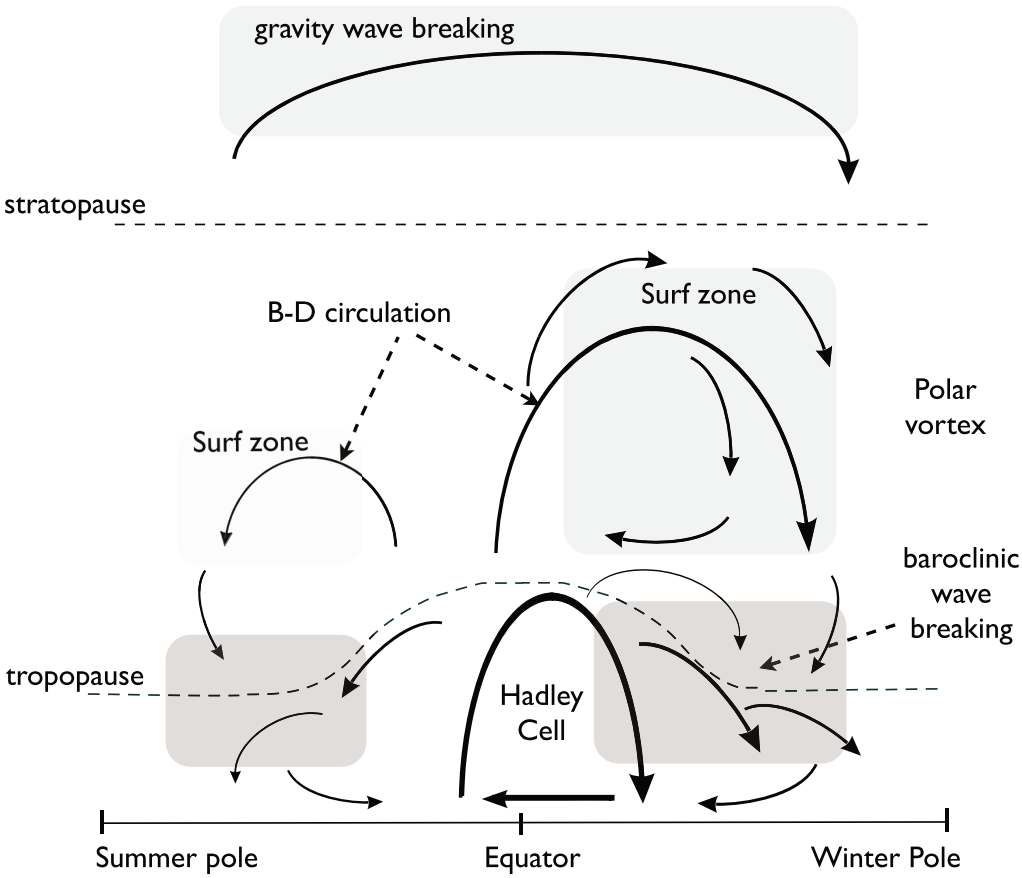

Fig. 11.7 A sketch of the residual mean meridional circulation of the atmosphere. The solid arrows indicate the residual circulation (B-D for Brewer–Dobson) and the shaded areas the main regions of wave breaking (i.e., enstrophy dissipation) associated with the circulation. In the surf zone the breaking is mainly that of planetary Rossby waves, and in the troposphere and lower stratosphere the breaking is that of baroclinic eddies. The surf zone and residual flow are much weaker in the summer hemisphere. Only in the Hadley Cell does the residual circulation consist mainly of the Eulerian mean; elsewhere the eddy component dominates.

I'm singing in the rain, Just singing in the rain,
What a glorious feelin', I'm happy again.
I'm laughing at clouds, So dark up above,
The sun's in my heart, And I'm ready for love .
Lyrics by Arthur Freed, music by Nacio Herb Brown, *Singin' in the Rain,* 1929.

CHAPTER 12

Water Vapour and the Tropical Atmosphere

WATER IS AN ORDINARY SUBSTANCE WITH EXTRAORDINARY EFFECTS. The most obvious is that oceans themselves are made of water, and if our planet were dry this book would perforce be much shorter (if only). Leaving aside the dynamical effects of the oceans, water covers over two-thirds of Earth's surface and because it is warm in some places and cold in others, and because the atmosphere is in motion, water evaporates into the atmosphere in one place and condenses from it elsewhere. The condensation leads to rain, one of the most talked-about aspects of weather and climate. Water also freezes to form ice, so that at any given time water exists on Earth in all three phases. Radiatively, water vapour is a greenhouse gas, meaning that it absorbs infrared radiation that might otherwise be lost to space and so maintains the surface of the planet at a temperature over 20 K higher than an equivalent dry planet. Dynamically, the condensation of water vapour in the atmosphere releases energy, warming the air and tending to make it more unstable than otherwise and leading to convection. Further, the net transport of water vapour from low to high latitudes is effectively a meridional transport of energy.

In this chapter we focus on a small number of these issues, mainly on the kinematics and dynamics of water vapour itself and on some aspects of the dynamics of the tropical atmosphere, where the effects of water vapour are most manifest. The tropics would certainly differ from the mid-latitudes even if the atmosphere were dry — its Coriolis parameter is small among other things — so our attention there is by no means confined to the effects of water vapour. Nevertheless, tropical convection and the attendant 'radiative-convective equilibrium' are greatly influenced by the presence of water. We begin with a discussion of the thermodynamic properties of water vapour itself. We then move on to an essentially kinematic description of the factors determining the large scale distribution of relative humidity, before finally looking at convection and at tropical dynamics more generally.[39]

12.1 A MOIST IDEAL GAS

Water is the compound of hydrogen and oxygen with the chemical formula H_2O, although in informal conversation water is often understood to mean only the liquid form of the compound. *Water vapour* is a gas made up of molecules of H_2O, and *ice* is the solid form of water. *Steam,* in common

parlance, is a mixture of air, water vapour and suspended droplets of water, usually at a very high temperature. Steam is formed when water vapour at temperatures above boiling point cools under contact with air and some of the water vapour condenses, forming a fine mist. Cloud and fog are also mixtures of dry air, water vapour and water droplets, but need not be at high temperature. Our focus will be on water vapour which, as we will see, can exist over a wide range of temperatures; let us first say how we quantify it and how it affects the equation of state. A number of thermodynamic derivations are also given in Appendix A (page 720). Those derivations are more systematic but less pedagogical than those below, and may appeal to some.

12.1.1 Ideal Gas Equation of State

The thermal equation of state for an ideal gas is conventionally written in the form

$$pV = Nk_BT = nR^*T, \tag{12.1}$$

where N is the total number of molecules in the volume V, n is the number of moles in that volume, and $N = nN_A$ where N_A is Avogadro's number. A mole is the amount of a substance that contains the same number of elementary entities, usually atoms or molecules, as there are atoms in 12 grams of carbon-12, that number being Avogadro's number ($N_A \approx 6.02 \times 10^{23}$). Two moles of a substance contains two times Avogadro's number of elementary units. The constants in the above equation are Boltzmann's constant, k_B, and the universal gas constant, R^*, where $R^* \equiv N_Ak_B = 8.314\,\mathrm{J\,mol^{-1}\,K^{-1}}$. As noted in Chapter 1, for any particular gas it is convenient to define the specific gas constant by $R = R^*/\mu$ where μ is the molar mass (mean molecular weight in kg/mol). For a single component gas we then divide (18.1) by the total mass $M = n\mu$ to obtain

$$p = \rho RT. \tag{12.2}$$

Throughout this chapter we will be concerned only with 'simple ideal gases', or 'perfect gases', for which the gas constants at constant composition are, in fact, constant.

For a multi-component ideal gas the partial pressure of each component is independent of the presence of the other components (because the volume of the molecules is negligible) and so is equal to the hypothetical pressure of that gas if it alone occupied the volume of the mixture. The total pressure is therefore the sum of the partial pressures of each gas, a dictum known as Dalton's law of partial pressures. The partial pressure of each constituent in a mixture is proportional to the number of molecules of that constituent, and therefore also proportional to the number of moles. Because of Dalton's dictum we can obtain a simple expression for the equation of state of a mixture, as follows. Denoting the constituents by subscript i, the total pressure is given by

$$p = \sum_i p_i = \sum_i \frac{1}{V} n_iR^*T = \sum_i \left(\frac{M}{V}\right) \frac{n_i\mu_i}{M\mu_i} R^*T. \tag{12.3}$$

Let us define the effective molar mass, μ_e, by

$$\frac{1}{\mu_e} = \sum_i \frac{n_i\mu_i}{M\mu_i} = \sum_i \frac{\varphi_i}{\mu_i}, \tag{12.4}$$

where $\varphi_i = (n_i\mu_i)/M$ is the mass fraction of the i-th constituent. We then have

$$p = \rho RT, \qquad \text{where} \qquad R = \frac{R^*}{\mu_e} = \sum_i \varphi_i R_i\,, \tag{12.5a,b}$$

and $R_i = R^*/\mu_i$. The effective gas constant of the mixture is thus the mass-weighted mean of the specific gas constants of its constituents. Any given gas has a specific gas constant that is inversely

proportional to its molecular weight. Thus, for a given fluid density and temperature a gas with a higher molecular weight will exert a lower pressure than one that has a smaller molecular weight, because it will have fewer molecules per unit mass. Similar expressions apply to the heat capacities c_p and c_v, so that a heavier gas (higher molecular weight) has a smaller specific heat capacity.

12.1.2 Application to Moist Air

Dry air has virtually constant composition and its mean molar mass is $\mu^d = 29.0 \times 10^{-3}\,\mathrm{kg\,mol^{-1}}$, giving $R^d = R^*/\mu^d = 287\,\mathrm{J\,kg^{-1}\,K^{-1}}$. Water vapour has a molar mass of $\mu^v = 18.014{\times}10^{-3}\,\mathrm{kg\,mol^{-1}}$ giving $R^v = 461.5\,\mathrm{J\,kg^{-1}\,K^{-1}}$. The two gas constants are related by

$$\frac{R^v}{R^d} = \frac{\mu^d}{\mu^v} \equiv \frac{1}{\epsilon} \approx 1.608. \tag{12.6}$$

Now consider a mixture of dry air and water vapour.

Measures of moisture

When mixtures are present we use superscripts d, v and l to denote thermodynamic quantities associated with dry air, water vapour and liquid water. The *absolute humidity* is the amount of water vapour per unit volume, with units of $\mathrm{kg\,m^{-3}}$, or informally $\mathrm{g\,m^{-3}}$. The *mixing ratio, w*, is the ratio of the mass of water vapour, m^v, to that of dry air, m^d, in some volume of air and is thus

$$w \equiv \frac{m^v}{m^d} = \frac{\rho^v}{\rho^d}. \tag{12.7}$$

It is a nondimensional measure but it is often expressed in terms of grams per kilogram. In the atmosphere values range from close to zero to about $20\,\mathrm{g\,kg^{-1}}$ (2×10^{-2}) in the tropics on a humid day.

The *specific humidity, q*, is the ratio of the mass of water vapour to the total mass of air — dry air plus water vapour — and so is

$$q \equiv \frac{m^v}{m^d + m^v} = \frac{w}{1+w} \quad \text{and} \quad w = \frac{q}{1-q}. \tag{12.8a,b}$$

The specific humidity is just the mass concentration of water vapour in air. In most circumstances in Earth's atmosphere $m^v \ll m^d$ so that $q \approx w$, usually to an accuracy of about one percent. In most of this chapter we will ignore the differences between w and q, but this is not appropriate for all planetary atmospheres.

The partial pressure of water vapour in air, e, is the pressure exerted by water molecules and is proportional to the number of moles of water vapour in the volume. It is given by

$$e = \frac{n^v}{n^d + n^v} p = \frac{m^v/\mu^v}{m^d/\mu^d + m^v/\mu^v} p, \tag{12.9}$$

where n^v and n^d are the number of moles of water vapour and dry air in the mixture and p is the total pressure. Using (18.7) we can write (18.9) as

$$e = \frac{wp}{w+\epsilon} \quad \text{or} \quad w = \frac{\epsilon e}{p-e}. \tag{12.10}$$

In terms of q instead of w these expressions are

$$e = \frac{qp}{q+\epsilon(1-q)} \quad \text{and} \quad q = \frac{\epsilon e}{p-e(1-\epsilon)}, \tag{12.11}$$

In Earth's atmosphere $w \ll 1$ so that

$$e \approx w\frac{p}{\epsilon} = 1.61wp \qquad \text{and} \qquad q \approx w \approx \epsilon\frac{e}{p}. \tag{12.12}$$

If the mixing ratio of water vapour is $10\,\mathrm{g\,kg^{-1}}$ (a typical tropical value) and $p = 1000\,\mathrm{hPa}$ then $e \approx 16\,\mathrm{hPa}$.

The *relative humidity*, $\mathcal{H}$, is the ratio of the actual vapour pressure to the saturation vapour pressure, e_s, which is the maximum vapour pressure that can occur at a given temperature before condensation occurs, as will be discussed in Section 18.1.4. Thus, $\mathcal{H} = e/e_s \approx q/q_s$ where q_s is the specific humidity at saturation.

12.1.3 Equation of State and Virtual Temperature

Using (18.5b) the effective gas constant of moist air varies with humidity according to

$$R = \frac{m^d R^d + m^v R^v}{m^d + m^v} = (1-q)R^d + qR^v = R^d\left[1 + q\left(\frac{1}{\epsilon} - 1\right)\right], \tag{12.13}$$

with similar expressions for c_p and c_v. In humid air, with $R^d = 287\,\mathrm{J\,kg^{-1}\,K^{-1}}$ and $q = 0.02$ say, we have $R = R^d(1 + 0.02 \times 0.61) = 290.5\,\mathrm{J\,kg^{-1}\,K^{-1}}$,

The heat capacity of water vapour can be estimated from its molecular properties. Water vapour is a triatomic molecule with three translational and three rotational degrees of freedom. If these were the only degrees of freedom then the internal energy would be given by $I = 6R^vT/2$, whence $c_v^v \approx 3R^v = 1384\,\mathrm{W\,m^{-2}}$ and $c_p^v = R^v + c_v^v = 1846\,\mathrm{J\,kg^{-1}\,K^{-1}}$, where c_v^v and c_p^v are the specific heat capacities for water vapour at constant volume and pressure, respectively. In fact vibrational degrees of freedom can sometimes be excited and the measured values are a little higher, namely $c_v^v = 1397\,\mathrm{J\,kg^{-1}\,K^{-1}}$ and $c_p^v = 1859\,\mathrm{J\,kg^{-1}\,K^{-1}}$ (at 273 K, increasing very slightly with temperature). The heat capacity of moist air is thus slightly higher than that of dry air, but since values of q are small the difference is only about 1%.

The variation of gas constant with humidity can be inconvenient in numerical models. A workaround is to define a so-called virtual temperature, T_v, which is the temperature that dry air would need to be in order to have the same density and pressure as moist air. That is, by definition,

$$p = \rho RT = \rho R^d T_v, \tag{12.14}$$

where R is given by (18.13). Using (18.13) we obtain

$$p = \rho R^d T_v, \quad \text{where} \quad T_v = T\left[1 + q\left(\frac{1}{\epsilon} - 1\right)\right] \approx T(1 + 0.61q). \tag{12.15}$$

The virtual temperature, T_v, increases with specific humidity and if $q = 20\,\mathrm{g\,kg^{-1}}$ then T_v is about 12%, or 3 K, larger than the actual temperature. Such a temperature is often used in numerical models of the atmosphere because it enables various thermodynamic equations to keep their original form, with gas constants that actually are constant.

Because the concentration of water vapour in Earth's atmosphere is so small, the variations of the heat capacities are small and constant values are often used to calculate quantities such as the potential temperature and the adiabatic lapse rate. This is not always appropriate, and Appendix A of this chapter indicates how, in principle, more accurate calculations could be made.

12.1.4 Saturation Vapour Pressure

Vapour pressure is the partial pressure of water vapour in the atmosphere. At any given temperature, there is a maximum value of that vapour pressure beyond which condensation normally

occurs and this is known as the *saturation vapour pressure*. Why should this be so, and why don't other atmospheric gases, such as oxygen or carbon dioxide, also condense? To understand this, we have to understand the thermodynamic equilibrium between a liquid and a gas.

Equilibration of the Gibbs function

Consider a system that consists of an enclosed, insulated container partially filled with liquid, and with vapour above it. The two subsystems can exchange mass and energy, with liquid potentially evaporating into vapour and vapour condensing into the liquid. Energy is required to evaporate the liquid into a vapour to overcome the molecular forces in the liquid and this is given by $M(h^v - h^l)$, where M is the mass that has evaporated, h^v is the specific enthalpy of the vapour and h^l is the specific enthalpy of the liquid. The enthalpy of vaporization, more commonly called the *latent heat of evaporation,* is defined by the difference between the two enthalpies at a temperature T, namely,

$$L(T) \equiv h^v - h^l, \tag{12.16}$$

with L having units of J kg^{-1}. It is a function of temperature, because the enthalpies of liquid water and water vapour are both functions of temperature, and a very weak function of pressure — see Appendix A for details. For water, L diminishes almost linearly by about 10% going from 0° C to 100° C, from 2.5×10^6 to 2.26×10^6 J kg^{-1}.

Now suppose we leave the container alone for a long time so that the liquid and vapour come into equilibrium at a temperature T. If a mass M is to evaporate from liquid into vapour then the energy required, E, can be related to the entropy difference between the liquid and vapour phases,

$$E = ML = M(h^v - h^l) = MT(\eta^v - \eta^l), \tag{12.17}$$

where η^v and η^l are the specific entropies of the vapour and liquid, and the temperature is fixed because all the energy put into the liquid is used for evaporation. Re-arranging we find

$$h^v - T\eta^v = h^l - T\eta^l \qquad \text{or} \qquad g^v = g^l, \tag{12.18a,b}$$

where $g^l \equiv h^l - T\eta^l$ and $g^v \equiv h^v - T\eta^v$ are the specific Gibbs functions for the liquid and vapour (Section 1.5.2). That is, *the specific Gibbs functions for the liquid and water phases of a substance are the same at equilibrium.* The result follows directly from (18.17): the energy required to evaporate a mass of liquid, which is equal to the mass times the specific enthalpy difference between the vapour and the liquid, is also equal to the mass times the specific entropy difference between the vapour and liquid. The equality is true only at equilibrium, when temperature remains fixed, so that (18.18b) is an equation, not an identity.

Another way to derive the above result is to begin with the fact that the total Gibbs function, for the entire system, must remain constant. That is, if M_l and M^v are the masses of liquid and water, then

$$G = M_l g^l + M^v g^v \tag{12.19}$$

and

$$\delta G = M_l \delta g^l + M^v \delta g^v + (g^v - g^l)\delta M = 0, \tag{12.20}$$

where δM is the mass exchanged between liquid and vapour arising from a small fluctuation. Now, from (1.78) changes in Gibbs functions arise because of changes in temperature and pressure; that is, in general,

$$\delta g = -\eta\, \delta T + \alpha\, \delta p, \tag{12.21}$$

and given this, (18.20) becomes

$$\delta G = M_l(-\eta^l\, \delta T + \alpha^l\, \delta p) + M^v(-\eta^v\, \delta T + \alpha^v\, \delta p) + (g^v - g^l)\delta M = 0, \tag{12.22}$$

where α_l and α^v are the specific volumes (the inverse density) of the liquid and vapour, respectively. But the temperature and pressure are fixed, and thus, in order that $\delta G = 0$ we must have that $g^v = g^l$. The reason for equality of the two Gibbs functions — as opposed to the equality of some other thermodynamic potential — stems from the fact that the Gibbs function is the only potential for which the natural variables are intensive, namely temperature and pressure. The derivation we have given exploits this directly, for we kept p and T fixed.

12.1.5 Clausius–Clapeyron Equation

Now suppose that the temperature of the liquid-vapour system changes by an amount δT, leading to a change in the vapour pressure and in the specific Gibbs functions for the liquid and water vapour. Using (18.21) the change in the two Gibbs functions is given by

$$\delta g^l = -\eta^l \delta T + \alpha^l \delta p, \qquad \delta g^v = -\eta^v \delta T + \alpha^v \delta p, \tag{12.23}$$

and, since the two changes must be the same, $\delta g^l = \delta g^v$. Re-arranging (18.23) and taking the limit of small changes then gives

$$\frac{\mathrm{d}p}{\mathrm{d}T} = \frac{\eta^l - \eta^v}{\alpha^v - \alpha^l}. \tag{12.24}$$

Using (18.16) and (18.17) this equation can be written

$$\frac{\mathrm{d}p}{\mathrm{d}T} = \frac{h^l - h^v}{T(\alpha^v - \alpha^l)} = \frac{L}{T(\alpha^v - \alpha^l)}, \tag{12.25}$$

where to obtain the rightmost expression we use the definition of L. The quantity p is the vapour pressure of the vapour above the liquid, which we are denoting e. Furthermore, it is the *saturation* vapour pressure, e_s, because the vapour is in equilibrium with the liquid: if more vapour were added it would immediately condense. Using this notation, the *saturation vapour pressure* of a condensible gas above a liquid is given by

$$\frac{\mathrm{d}e_s}{\mathrm{d}T} = \frac{L}{T(\alpha^v - \alpha^l)}. \tag{12.26}$$

This is the *Clausius–Clapeyron* equation, and it tells us how the pressure of a vapour that is in thermodynamic equilibrium with an adjacent liquid varies with temperature. If for some reason the vapour pressure is higher than this value, and if there is an adjacent surface of liquid water, then the vapour will condense into a liquid — a common manifestation of which is the formation of clouds and rain. Evidently, since $L > 0$ and $\alpha^v > \alpha^l$, the saturation vapour pressure increases with temperature so that a reduction in temperature can lead to saturation. At the temperature at which the saturation vapour pressure of a substance equals that of the ambient pressure then any liquid present will *boil*. For water at a pressure of 1000 hPa this occurs at about 100° C, with a lower temperature needed at a lower pressure, which is why it takes longer to properly boil an egg at high altitude.

The presence of a liquid surface is crucial to the derivation, and it means that the equation only applies to a condensible. For gases such as carbon dioxide or oxygen at temperatures encountered on Earth, the saturation vapour pressure is very much higher than the actual pressure at the Earth's surface and the gas never condenses; the partial pressure of the gas is then determined by the ideal gas relation and not by (18.26). On Mars, temperatures are sufficiently low that carbon dioxide (the main constituent of the Martian atmosphere) is a condensate and as much as 25% of the Martian atmosphere will condense in winter. On Titan temperatures are even lower and methane is a condensate, and methane lakes are scattered over the dystopian surface.

On Earth, the partial pressure of water vapour, however, is constrained by (18.26), meaning that the partial pressure will often reach the saturated value and the vapour will then normally condense. Condensation is not, however, guaranteed, and to see this imagine a container that contains unsaturated water vapour and no liquid water, and suppose its temperature is then lowered; the pressure of the vapour will then fall following the ideal gas law. The saturation vapour pressure falls more quickly than this and so at some temperature the vapour pressure will exceed the saturation vapour pressure, but the vapour will not automatically condense since there is no liquid present and (18.26) does not apply. The vapour is then said to be *supersaturated*. A supersaturated state is unstable and condensation will eventually occur and liquid water will form, and subsequent changes in temperature induce pressure changes that satisfy the Clausius–Clapeyron equation. Supersaturated water vapour is fairly rare in Earth's atmosphere because there is usually no shortage of condensation nuclei.

At the other end of the temperature scale, liquid water can exist at temperatures well below freezing when there is insufficient water for the molecules to become organized into a crystalline structure, and super-cooled water droplets rather than ice then result — a common situation in clouds. If the liquid that is present is in the form of small spherical droplets then the saturation vapour pressure will differ slightly from that when the vapour is over a flat surface, because surface tension will affect the energy required for a molecule to escape from the droplet and so the latent heat of vaporization will differ. If the vapour is in contact with ice instead of water then its saturation vapour pressure will differ again, because the specific enthalpy of ice is different from that of liquid water.

Application to an ideal gas

In a mixture of ideal gases the partial pressure of one gas is unaffected by the presence of the other gases (because the volume of the gas molecules is assumed to be negligible) and in particular the saturation vapour pressure for a particular component is independent of the presence of other components. We can then, at least approximately, integrate (18.26) to see how the saturation vapour pressure of a particular component varies with temperature. Let us assume that density of the vapour is much less than that of the liquid, so that $\alpha^v \gg \alpha^l$. Given that the partial pressure of the vapour satisfies the ideal gas law, namely $e^v \alpha^v = R^v T$, where R^v is the specific gas constant for the vapour, the Clausius–Clapeyron equation becomes

$$\frac{\mathrm{d}e_s}{\mathrm{d}T} = \frac{Le_s}{R^v T^2} \,. \tag{12.27}$$

This is the form of Clausius–Clapeyron equation that is normally used in atmospheric applications. If we further assume that L is a constant then (18.27) can be integrated to give

$$e_s = e_0 \exp\left[\frac{L}{R^v}\left(\frac{1}{T_0} - \frac{1}{T}\right)\right], \tag{12.28}$$

where e_0 and T_0 are constants, for example $T_0 = 273\,\mathrm{K}$ and $e_0 = 6.12\,\mathrm{hPa}$. Equation (18.28) is a good approximation if the temperature range is not too wide, and as seen in Fig. 18.1 the saturation vapour pressure of water increases approximately exponentially over commonly encountered terrestrial temperatures. Note that the expression for saturation vapour pressure does not depend on the presence or otherwise of dry air.

The fact that water vapour content cannot normally exceed the saturation value distinguishes the distribution of water from other tracers in the atmosphere, even without taking the heating effects of condensation into account. Note finally that if the atmosphere were motionless it would everywhere be in thermodynamic equilibrium with the moist surface and the surface layers would be saturated, and diffusion of water vapour upwards would then saturate the rest of the atmosphere. Thus, *the relative humidity of the atmosphere is determined by its circulation,* as we now discuss.

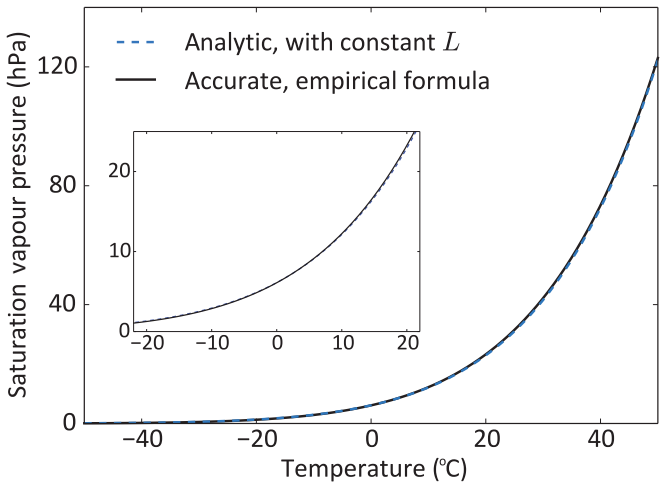

Fig. 12.1 The saturation vapour pressure of water vapour, calculated using the analytic formula (18.28), which assumes that L is constant (dashed line), and using a more accurate, semi-empirical formula (solid line).[40] The inset is the same plot over a smaller range.
The parameters used in the analytic formula are $T_0 = 273\,\mathrm{K}$, $e_0 = 6.12\,\mathrm{hPa}$, $L = 2.44 \times 10^6\,\mathrm{J\,kg^{-1}}$ and $R^v = 462\,\mathrm{J\,kg^{-1}\,K^{-1}}$.

12.2 THE DISTRIBUTION OF RELATIVE HUMIDITY

To a first approximation, the distribution of water in the atmosphere is determined by the distribution of temperature. This is because of the near-exponential dependence of absolute humidity on temperature through the Clausius–Clapeyron equation, so that variations of relative humidity of even an order of magnitude, from 10% to 100% say, are barely noticeable in the specific humidity distribution, as seen in Fig. 18.2. It is, however, the relative humidity that determines such basic quantities as rainfall, and its distribution (Fig. 18.3 and Fig. 18.4) shows a quite different picture, with the following features evident:

- High, near-saturated values close to the ground.
- Low relative humidity in the subtropics at latitudes between 15° to 40° (depending on season) in both hemispheres.
- High values near the equator extending up to the tropopause.
- Vertically near-uniform values in mid- and high latitudes, increasing with latitude close to the pole in some cases.
- Very low values over much of the stratosphere.

The gross distribution of zonally-averaged temperature can be understood, at least in a rough way, using fairly simple arguments. The incoming solar radiation at the top of the atmosphere would lead, in the absence of atmospheric motion, to a strong meridional radiative equilibrium temperature gradient, as in Fig. 14.1. The meridional transport of heat by the Hadley Cell and by mid-latitude baroclinic eddies flattens that temperature gradient, and one might crudely model this transport as a diffusion. In the vertical heat is transported upwards by convection and baroclinic eddies, which might be modelled as a relaxation back to some specified neutrally stable profile or specified isentropic slope. However, arguments of this type cannot capture some basic features of the relative humidity distribution, and diffusive arguments in particular can be quite misleading. The effects of advection, either explicitly or as represented by a stochastic process, are crucial, and in this section we consider advection-diffusion-condensation models of the general form

$$\frac{\partial q}{\partial t} + \boldsymbol{v} \cdot \nabla q = \nabla \cdot \kappa \nabla q - S, \tag{12.29}$$

where q is the specific humidity, $\boldsymbol{v}$ is a specified velocity field, κ is a diffusion coefficient and S is the condensational sink.[42] Condensation in the atmosphere involves complicated microphysical processes but the basic effect is to remove liquid water once the volume becomes saturated and to

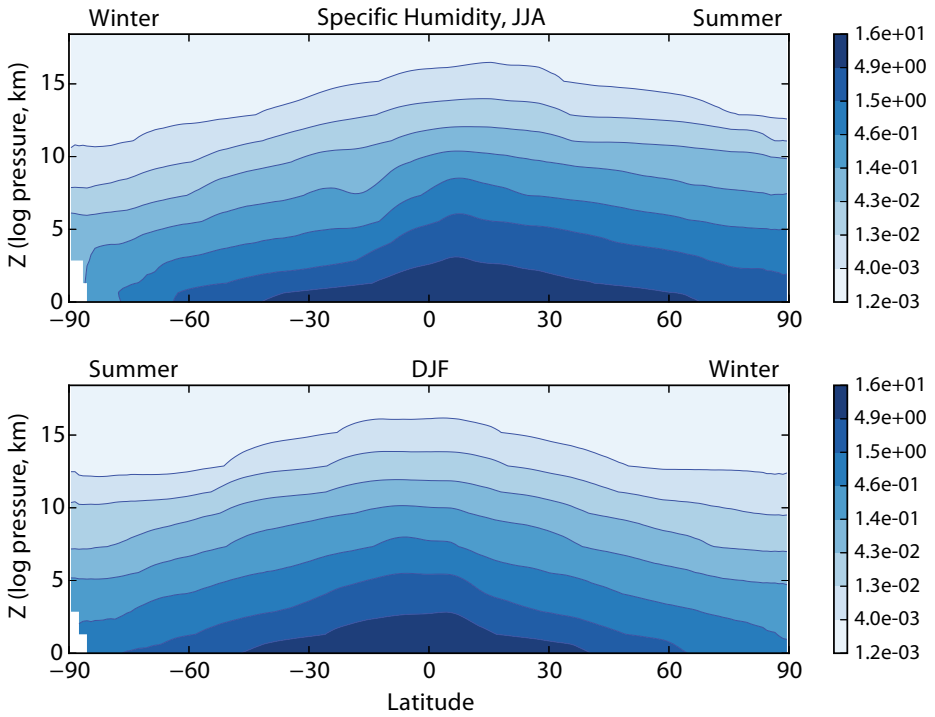

Fig. 12.2 Zonally-averaged specific humidity distribution (g/kg) in the atmosphere, as retrieved from a microwave satellite, for boreal summer in 2008 (top) and boreal winter 2008–2009 (bottom).[41] Note the logarithmic scale.

largely prevent relative humidity from exceeding 100% (although supersaturation can occur locally if there are no particulates in the air onto which the water vapour may condense). A simple analytic way to represent such a condensation process is to let

$$S = \begin{cases} 0, & q \le q_s, \\ (q - q_s)/\tau, & q > q_s, \end{cases} \tag{12.30}$$

where the time τ is much smaller than any large scale diffusion time, L^2/κ, where L is a characteristic length. Such a sink effectively prevents q from exceeding q_s except by a tiny amount. In (18.29) we may consider the advection and diffusion terms as representing larger scale processes and the sink as representing small-scale microphysical processes. We begin our exploration by omitting advection, and a summary can be found on page 683.

12.2.1 A Diffusion-Condensation Model

If we omit advection in (18.29) we have a simple diffusion-condensation model

$$\frac{\partial q}{\partial t} = \nabla \cdot \kappa \nabla q - S. \tag{12.31}$$

Although superficially plausible, such a model is too-often unable to reproduce locally unsaturated regions. For simplicity consider the one-dimensional case satisfying

$$\frac{\partial q}{\partial t} = \kappa \frac{\partial^2 q}{\partial x^2} - S, \tag{12.32}$$

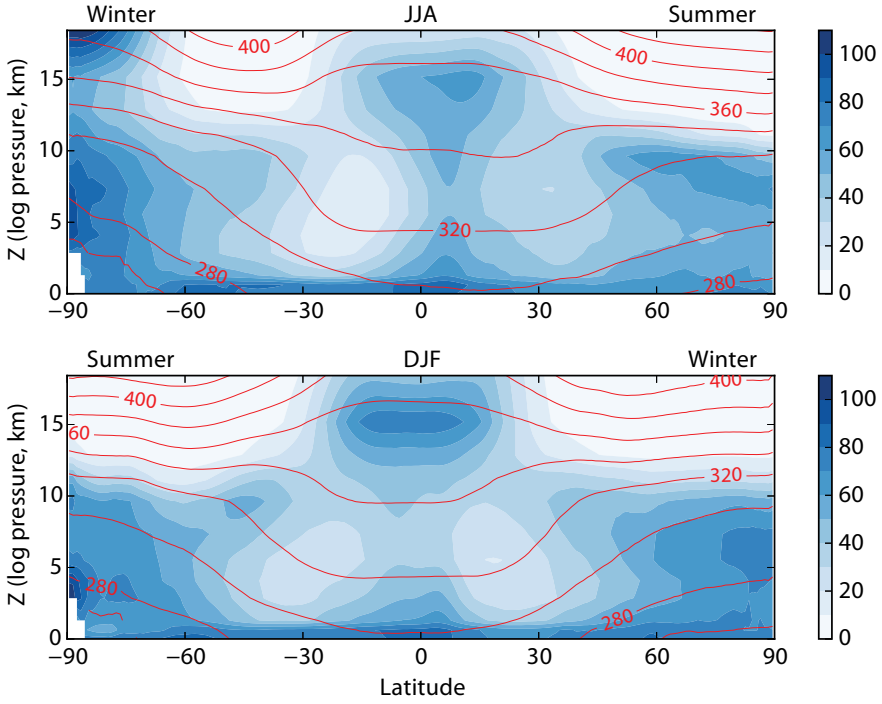

Fig. 12.3 Zonally-averaged relative humidity distribution in the atmosphere (in percent, shading), and isolines of equivalent potential temperature (contours), inferred from satellite as in Fig. 18.2. (Equivalent potential temperature is a modification of potential temperature to account for water vapour, and is a approximately an adiabat; see Section 18.3.2.)

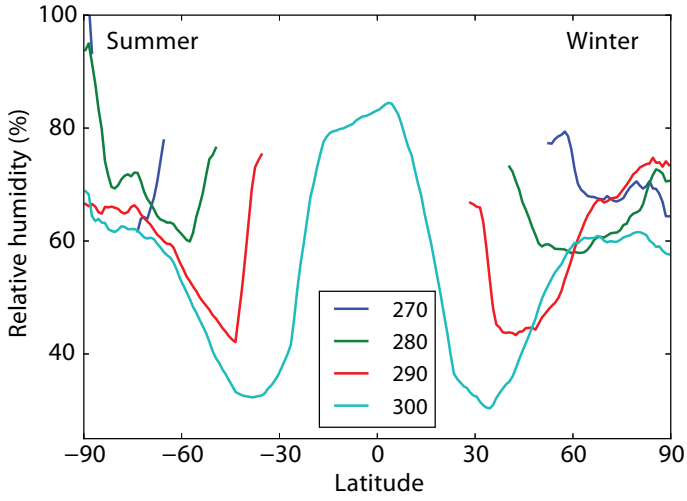

Fig. 12.4 Values of zonally-averaged relative humidity in boreal winter plotted along isolines of equivalent potential temperature (red contours in Fig. 18.3), with values of θ_{eq} as indicated in the legend.

Water Vapour Transport and Relative Humidity

- Water vapour in the atmosphere is primarily transported by advection, much of this on large, near planetary scales but also by convection and smaller scale turbulence. Specific humidity is materially conserved in the absence of condensation and diffusion.
- If the vapour pressure exceeds the saturated value (as given by the Clausius–Clapeyron relation) condensation will occur provided condensation nuclei or liquid water are present. The condensation normally occurs much more quickly than large-scale advective processes, and this situation is known as the *fast condensation limit*.
- When dealing with large-scale flows in Earth's atmosphere the limit is a good approximation. Levels of relative humidity are then determined mainly by advective processes rather than the microphysical details of the condensation process. Specifically, the relative humidity of a parcel is determined by the temperature at the location of last saturation, as in (18.35).
- If the advection is not fully resolved — for example if there is some small-scale turbulence in the flow — then introducing some diffusion seems natural, as is commonly done for tracers, but a large diffusivity can give unrealistic results because of the irreversible nature of condensation. Diffusion is then not a good representation of small-scale quasi-random flow and is overly prone to produce saturation.
- In Earth's atmosphere some of the large-scale features of the relative humidity distribution may be explained as follows:
  - High levels of relative humidity close to the surface. These are due to transport from a saturated surface, especially over the ocean and moist ground.
  - High levels of relative humidity in the ascending branch of the Hadley Cell. These are due to upward advection from a nearly saturated surface. The branch is, however, not saturated on the zonal-average, because of the presence of smaller scale motion such as downdrafts that unsaturate the air.
  - A subtropical minimum of relative humidity. This largely arises because of the mean descending motion, advecting water vapour into a warmer region and decreasing its relative humidity.
  - Variable relative humidity in mid- and high latitudes, with locally strong gradients. Chaotic advection by baroclinic eddies takes moisture upwards and polewards into cooler regions where it becomes saturated, but also downwards and equatorwards so reducing relative humidity.
  - Very low levels of relative humidity in the stratosphere. The tropopause is a cold trap and so relative humidity is very low beyond it. The cold-trap effect occurs in both advective and diffusive models. In Earth's atmosphere, the little water vapour that is in the stratosphere mainly enters advectively through the tropical tropopause.

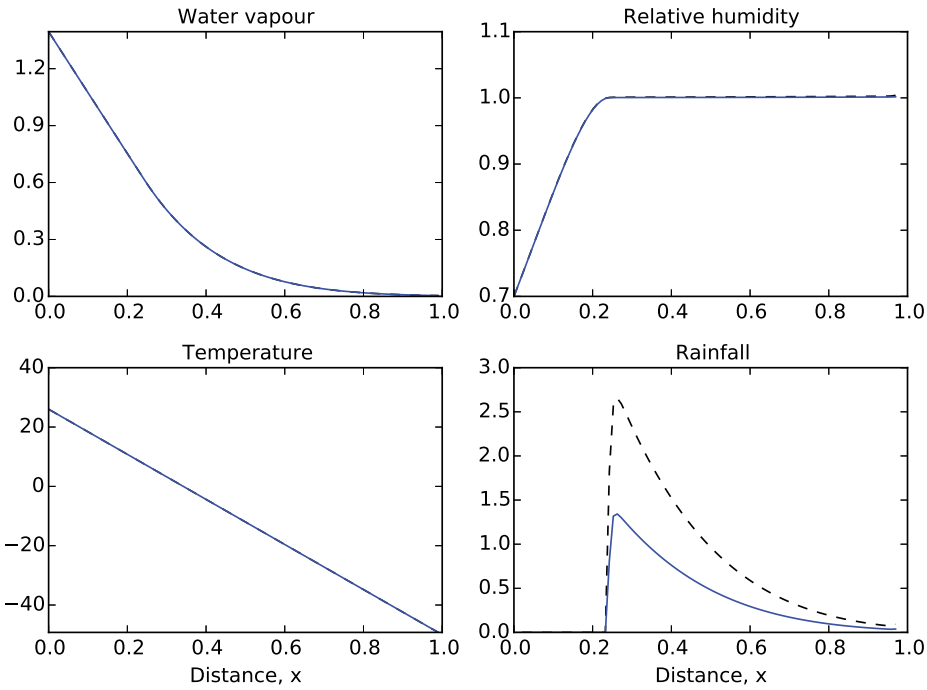

Fig. 12.5 Steady solution of the diffusion-condensation model (18.32) and (18.33), with $\mathcal{H}_b = 0.7$ at $x = 0$ and temperature (°C) falling linearly from $x = 0$ as shown. Water vapour falls linearly away from the boundary at $x = 0$ until it becomes saturated at $x = 0.23$, after which the region is saturated. Two solutions are plotted, the one with dashed lines showing the solution with twice the diffusivity as that with solid lines. The two solutions are nearly identical except for the sink term, the rainfall.

with constant κ. In this model, any interior minimum of q_s will lead to saturation in that neighbourhood. To see this, note that in any region where moisture is present and that has $\partial^2 q/\partial x^2 > 0$ and $q < q_s$, there will be a net flux of water vapour into that region. Saturation must eventually occur, at which point q remains very close to the value of q_s. If $\partial^2 q_s/\partial x^2 > 0$ then the diffusive flux will maintain the saturated state. Given the monotonic dependence of q_s on temperature this result means that, in a moist atmosphere in which water vapour is transported diffusively, the neighbourhood of an interior minimum of temperature will become saturated.

A corollary of this result is that, unless there is a source of moisture at a boundary, a region with $\partial^2 q_s/\partial x^2 > 0$ everywhere will under many conditions eventually lose *nearly all* its moisture. Suppose that $\partial q/\partial x = 0$ at $x = 0$ and that q_s has a maximum at $x = 0$, and that the region extends to infinity and is initially saturated. (Envision a semi-infinite domain with temperature decreasing linearly away from a no-flux boundary, and therefore with no source of moisture, at $x = 0$.) Moisture is transported to higher values of x where condensation occurs and moisture is removed. As time progresses the region of saturation moves to higher and higher vales of x, but nevertheless water is continuously removed. In a finite domain, with no flux boundary conditions at either end, a small amount of moisture will remain in the system for all time because a finite amount of water vapour is needed for condensation to occur.

Now consider the more atmospherically relevant situation with a moisture source at $x = 0$, with q_s decreasing monotonically away and with the other boundary either extending to infinity or being a no-flux boundary at finite x. Such a situation might represent an atmosphere sitting

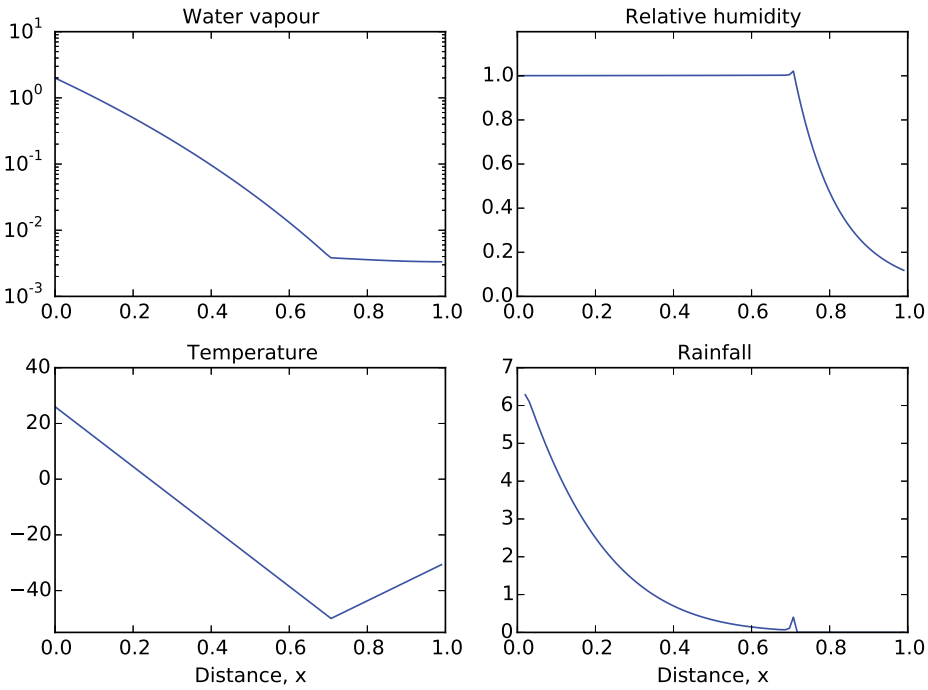

Fig. 12.6 As for Fig. 18.5, but now with $\mathcal{H}_b = 1$ and an interior temperature minimum, a 'cold trap', at $x = 0.7$ (see temperature panel), and water vapour has a log scale. Relative humidity falls rapidly beyond the cold trap and the rainfall there is zero.

atop a moist surface with temperature decreasing with height. Consider the case

$$\begin{aligned} q &= \mathcal{H}_b q_s(T_0), \qquad && x = 0, \\ \frac{\partial q}{\partial x} &= 0, && x = 1, \end{aligned} \tag{12.33}$$

where $\mathcal{H}_b$ is a parameter such that if the boundary is effectively saturated then $\mathcal{H}_b = 1$, and $\mathcal{H}_b < 1$ otherwise, and we suppose that T decreases between T_0 at $x = 0$ and T_1 at $x = x_1$. Consider first the case with $H_b = 1$. If T falls linearly then the value of q_s falls approximately exponentially between $x = 0$ and $x = 1$, with $\partial^2 q_s/\partial x^2 > 0$, and the steady solution of this problem is that the domain is saturated everywhere. To see this, suppose that $q < q_s$ is some region so that $S = 0$. Water vapour will then diffuse into that region until condensation begins, maintaining $q \approx q_s$ everywhere, with, if (18.30) applies, q in fact exceeding q_s by a very small amount so that the diffusion into the region is balanced by condensation. If $H_b < 1$ then the region next to the surface will not be saturated and in steady state the water vapour content will decrease linearly, to satisfy $\partial^2 q/\partial x^2 = 0$, until at some value of x, x_s say, the atmosphere becomes saturated and remains so for $x > x_s$. The actual solution is

$$q(x) = \begin{cases} \mathcal{H}_b q_s(0) + x\Delta q/x_s, & x < x_s, \\ q_s(x), & x \geq x_s, \end{cases} \tag{12.34}$$

where $\Delta q = (q_s(x_s) - \mathcal{H}_b q_s(0))$ and x_s is such that the flux is continuous there. A moment's thought reveals that $x_s = \Delta q/(\partial q_s/\partial x)_{x=x_s}$ and $x_s = 0$ if $\mathcal{H}_b = 1$. It is interesting that the values of water vapour in the solution (plotted in Fig. 18.5) do not depend upon κ and only very weakly on τ. In the fast condensation limit (in which τ is small compared to the diffusion time) variations of τ determine only the tiny amount by which q exceeds q_s. The amount of condensation is actually

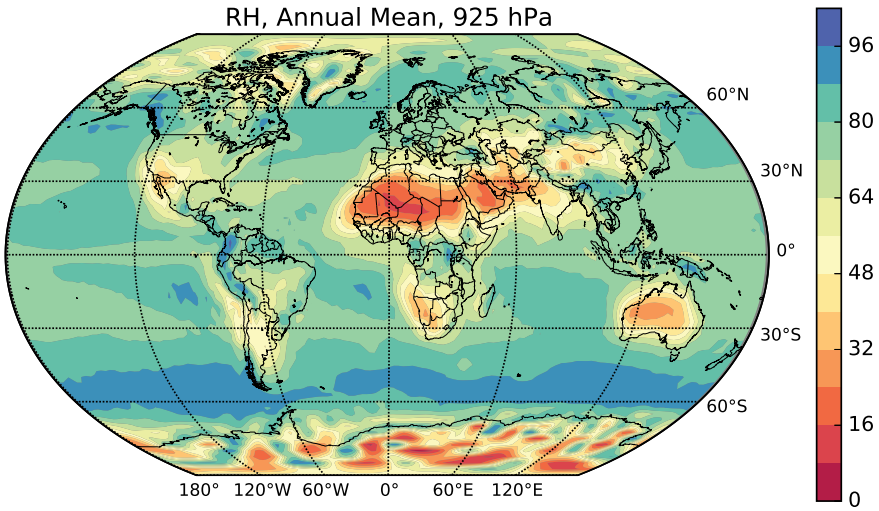

Fig. 12.7 Annually-averaged relative humidity (in percent) at 925 hPa, about 750 m above sea level. The contrast over land and ocean is apparent especially in the subtropics. (In regions of high topography values are interpolated.)

largely determined by the value of κ: large values of κ lead to a stronger diffusion of water vapour into dryer regions where it is almost immediately removed by condensation. This result illustrates the tenet that on large scales precipitation is at leading order determined by the motion of the fluid (here represented by diffusion), with variations in τ (crudely representing complex microphysical processes) being of less import. Microphysical processes are nevertheless important in many ways — a weather forecast model with poor microphysics would likely have little skill in forecasting the onset of precipitation, even if the climatology of the model were good.

Although the above model is over-simple in some respects, the dependence of the solution on $\mathcal{H}_b$ does capture the dependence of relative humidity in the lower atmosphere on the nature of the surface beneath, as seen in Fig. 18.7 showing relative humidity at 925 hPa. Over the desert regions the relative humidity is unsurprisingly low. Perhaps what is surprising is that the general dryness of the subtropics cannot be seen over the oceans — the surface moisture source simply overwhelms the drying effects of descending air (discussed more below).

A variation on the above theme introduces a temperature minimum, or 'cold trap', in the interior of the domain, as at $x = 0.7$ in Fig. 18.6. This configuration is a crude model of the tropopause, with temperatures increasing in the stratosphere beyond. Water vapour has to pass through the cold trap and so, since the specific humidity cannot be higher than the saturated value at the cold trap, the atmosphere will be unsaturated beyond it with relative humidity decreasing rapidly, as is seen in the real atmosphere in Fig. 18.3.

Although informative, diffusive-condensation models are fundamentally limited in what they can achieve, because of the deficiencies of diffusion in parameterizing the motion of a tracer in the presence of condensation. In particular, in the absence of a cold trap, diffusive models are prone to produce saturation everywhere. If the atmosphere obeyed (18.31) with a saturated surface, then the atmosphere would become saturated everywhere up to the tropopause, which from Fig. 18.3 is manifestly not the case. To remedy this we turn our attention to the effects of advection.

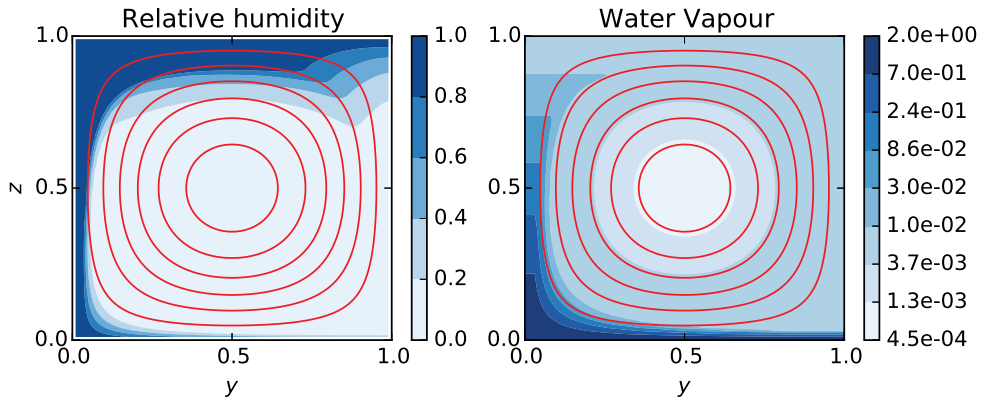

Fig. 12.8 Steady-state distributions of relative humidity (filled contours, left) and water vapour (right) in a single cell as defined by the streamfunction (red contours, clockwise flow. so air rising at the 'equator' at $y = 0$) in a closed domain. The domain boundary is saturated at the bottom, and temperature decreases linearly with height. The diffusivity $\kappa = 0.001$ and so the Peclet number, $Pe \equiv UL/\kappa \sim 1000$.

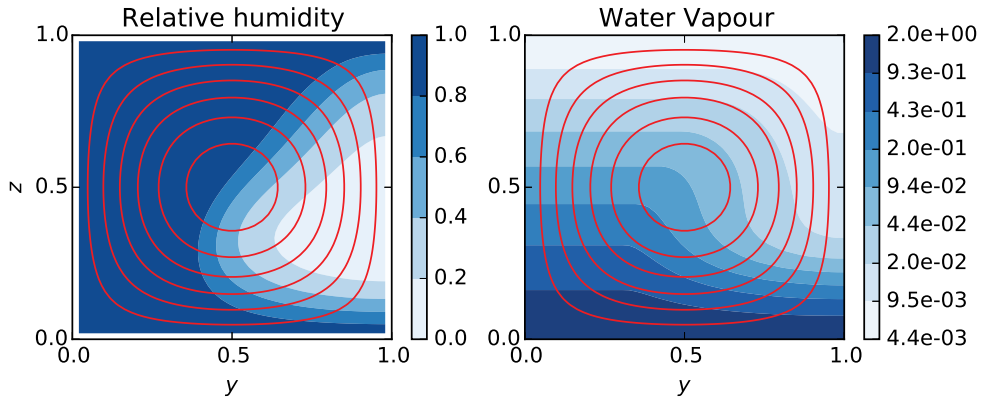

Fig. 12.9 As for Fig. 18.8, but with bigger diffusivity, $\kappa = 0.1$ and $Pe \sim 10$. Most of the domain is now much wetter.

Part IV

LARGE-SCALE OCEANIC CIRCULATION

As I ebb'd with the ocean of life,
As I wended the shores I know,
As I walk'd where the ripples continually wash you Paumanok …
As the ocean so mysterious rolls toward me closer and closer …
I perceive I have not really understood any thing,
not a single object, and that no man ever can,
Nature here in sight of the sea taking advantage of me
to dart upon me and sting me,
Because I have dared to open my mouth to sing at all.

Walt Whitman, *As I Ebb'd with the Ocean of Life,* from *Leaves of Grass,* 1881.

CHAPTER 13

Wind-Driven Gyres

UNDERSTANDING THE CIRCULATION OF THE OCEAN involves a combination of observations, comprehensive numerical modelling, and more conceptual modelling or theory.[43] All are essential, but in this chapter and the ones following our emphasis is on the last of the triad. Its (continuing) role is not to explain every feature of the observed ocean circulation, nor to necessarily describe details best left to numerical simulations. Rather, it is to provide a conceptual and theoretical framework for understanding the circulation of the ocean, for interpreting observations and suggesting how new observations may best be made, and to aid the development and interpretation of numerical models.

The aspect of the ocean that most affects the climate is the sea-surface temperature (SST), as illustrated in Fig. 19.1, and aside from the expected latitudinal variation there is significant zonal variation too — the western tropical Pacific is particularly warm, and the western Atlantic is warmer than the corresponding latitude in the east. These variations owe their existence to ocean currents, and the main ones are sketched — in a highly schematic and non-quantitative fashion — in Fig. 19.2. Over most of the ocean, the vertically averaged currents have a similar sense to the surface currents, one exception being at the equator where the surface currents are mainly westward but the vertical integral is dominated by the eastward undercurrent. Two dichotomous aspects of this picture stand out: (i) the complexity of the currents as they interact with topography and the geography of the continents; (ii) the simplicity and commonality of the large-scale structures in the major ocean basins, and in particular the ubiquity of subtropical and subpolar gyres. Indeed these gyres, sweeping across the great oceans carrying vast quantities of water and heat, are perhaps the single most conspicuous feature of the circulation. The subtropical gyres are anticyclonic, extending polewards to about 45°, and the subpolar gyres are cyclonic and polewards of this, primarily in the Northern Hemisphere. The existence of the great gyres, and that they are strongest in the west, has been known for centuries; this *western intensification* leads to such well-known currents as the Gulf Stream in the Atlantic (charted by Benjamin Franklin), the Kuroshio in the Pacific, and the Brazil Current in the South Atlantic.

For much of this chapter we consider a model, and variations about it, that explains the large-scale features of ocean gyres and that lies at the core of ocean circulation theory — the steady, forced-dissipative, homogeneous model of the ocean circulation first formulated by Stommel.[44] In all of the geosciences there is perhaps no other model that combines elegance and as relevance as much as this one.

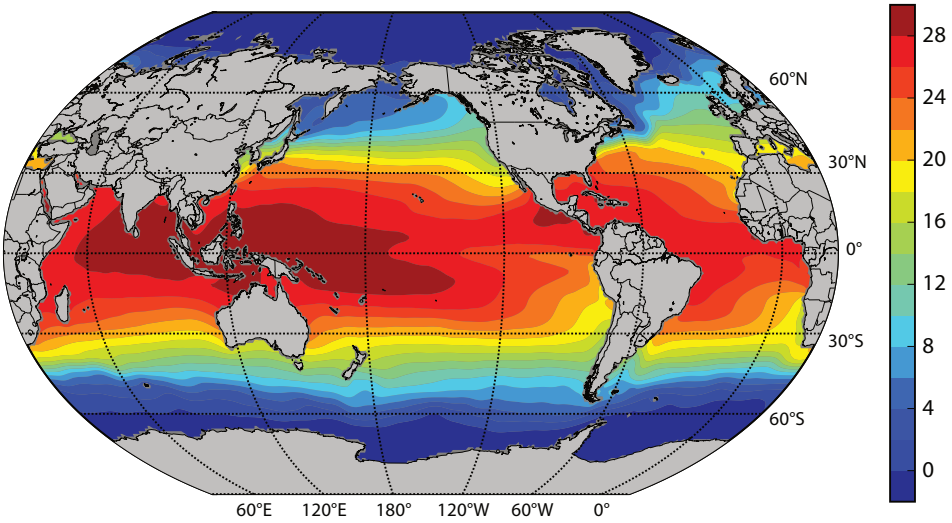

Fig. 13.1 The sea-surface temperature (SST, ° C) of the world's ocean, as determined from a great many observations, combined in the World Ocean Circulation Experiment (WOCE).

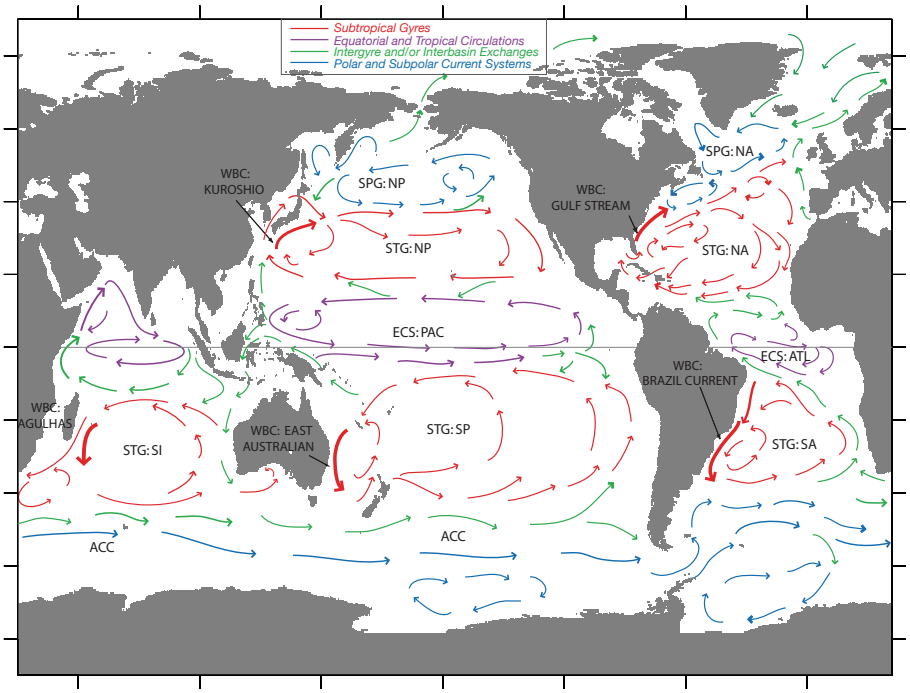

Fig. 13.2 Idealization of the main currents of the global ocean. Key: STG – Subtropical Gyre; SPG – Subpolar Gyre; WBC – Western Boundary Current; ECS – Equatorial Current System; NA – North Atlantic; SA – South Atlantic; NP – North Pacific; SP – South Pacific; SI – South Indian; ACC – Antarctic Circumpolar Current; ATL – Atlantic; PAC – Pacific. The figure is only a qualitative representation of the actual flow. Most of the currents are manifested at the surface, but near the equator the figure shows the undercurrent which flows in the opposite way to the surface current.

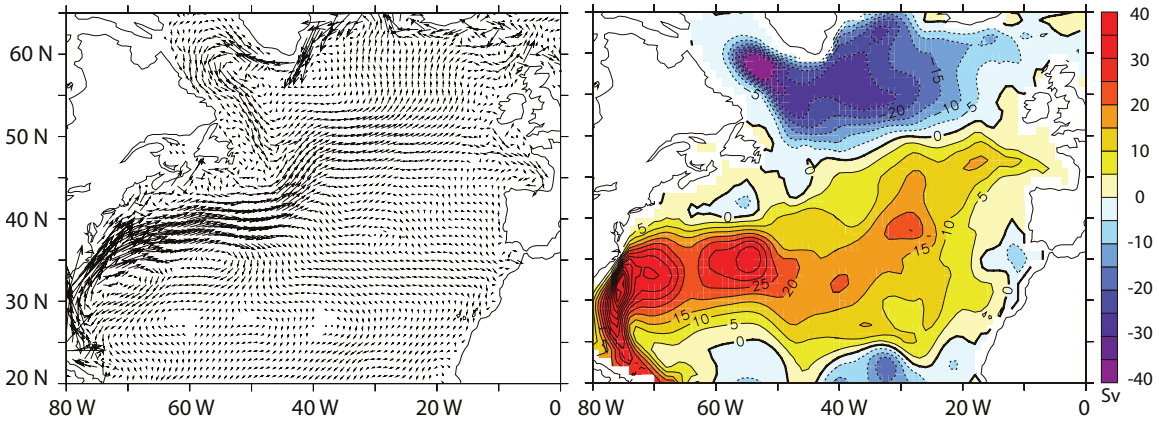

Fig. 13.3 Left: the time averaged velocity field at a depth of 75 m in the North Atlantic, obtained by constraining a numerical model to observations (so giving a 'state estimate'). Right: the streamfunction of the vertically integrated flow, in Sverdrups ($1\,\mathrm{Sv} = 10^9\,\mathrm{kg\,s^{-1}}$). Note the presence of an anticyclonic subtropical gyre (clockwise circulation, shaded red), a cyclonic subpolar gyre (anticlockwise, blue), and intense western boundary currents.[46]

13.1 THE DEPTH INTEGRATED WIND-DRIVEN CIRCULATION

Although even today we barely have sufficient observations to produce a detailed synoptic map of the ocean currents, except at the surface, the large-scale mean currents are fairly well mapped and Fig. 19.3 illustrates the average current pattern of the North Atlantic using a combination of observations and a numerical model, and the Gulf Stream is clearly visible. Similar features are seen in all the major ocean basins (Fig. 19.4) where we see subtropical and subpolar gyres, all of them intensified in the west.[45] Our goal in this chapter is to explain the main features seen in these figures in as simple and straightforward a manner as is possible.

The equations that govern the large-scale flow in the oceans are the planetary-geostrophic equations. Greatly simplified as these are compared to the Navier–Stokes equations, or even the hydrostatic Boussinesq equations, they are still quite daunting: a prognostic equation for buoyancy is coupled to the advecting velocity via hydrostatic and geostrophic balance, and the resulting problem is formidably nonlinear. However, it turns out that thermodynamic effects can effectively be eliminated by the simple device of vertical integration; the resulting equations are linear, and the only external forcing is that due to the wind stress. The resulting model then, at the price of some comprehensiveness, gives a useful picture of the *wind-driven* circulation of the ocean. We will consider the vertical structure of this flow in the next chapter.

13.1.1 The Stommel Model

The planetary-geostrophic equations for a Boussinesq fluid are:

$$\frac{\mathrm{D}b}{\mathrm{D}t} = \dot{b}, \qquad \nabla_3 \cdot \boldsymbol{v} = 0, \tag{13.1a,b}$$

$$\boldsymbol{f} \times \boldsymbol{u} = -\nabla\phi + \frac{1}{\rho_0}\frac{\partial \boldsymbol{\tau}}{\partial z}, \qquad \frac{\partial \phi}{\partial z} = b. \tag{13.2a,b}$$

These equations are, respectively, the thermodynamic equation (19.1a), the mass continuity equation (19.1b), the horizontal momentum equation (19.2a), (i.e., geostrophic balance, plus a stress

term), and the vertical momentum equation (19.2b) — that is, hydrostatic balance. These equations are derived more fully in Chapter 5, but they are essentially the Boussinesq primitive equations with the advection terms omitted from the horizontal momentum equation, on the basis of small Rossby number. In this chapter we will henceforth absorb the factor of ρ_0 into the $\boldsymbol{\tau}$, so that $\boldsymbol{\tau}$ denotes the kinematic stress, and the gradient operator will be two dimensional, in the x-y plane, unless noted.

Take the curl of (19.2a) (that is, cross differentiate its x and y components) and integrate over the depth of the ocean to give

$$\int f \nabla \cdot \boldsymbol{u} \, dz + \frac{\partial f}{\partial y} \int v \, dz = \text{curl}_z(\boldsymbol{\tau}_T - \boldsymbol{\tau}_B), \tag{13.3}$$

where the operator curl_z is defined by $\text{curl}_z \boldsymbol{A} \equiv \partial A^y/\partial x - \partial A^x/\partial y = \mathbf{k} \cdot \nabla \times \boldsymbol{A}$, and the subscripts T and B are for top and bottom. The divergence term vanishes if the vertical velocity is zero at the top and bottom of the ocean. Strictly, at the top of the ocean the vertical velocity is given by the material derivative of height of the ocean's surface, Dh/Dt, but on the large-scales this has a negligible effect and we may make the rigid-lid approximation and set it to zero. At the bottom of the ocean the vertical velocity is only zero if the ocean is flat-bottomed; otherwise it is $\boldsymbol{u} \cdot \nabla \eta_B$, where η_B is the orographic height at the ocean floor. The neglect of this topographic term is probably the most restrictive single approximation in the model. Given this neglect, (19.3) becomes

$$\beta \overline{v} = \text{curl}_z(\boldsymbol{\tau}_T - \boldsymbol{\tau}_B), \tag{13.4}$$

where henceforth, in this section, quantities with an overbar are understood to be the vertical integral over the depth of the ocean. If the stresses depend only on the velocity fields then thermodynamic fields do not affect the vertically integrated flow.

At the top of the ocean, the stress is given by the wind. At the bottom, in the absence of topography we assume that the stress may be parameterized by a linear drag, or Rayleigh friction, as might be generated by an Ekman layer; it is this assumption that particularly characterizes this model as being due to Stommel. (Note that we parameterize the friction by a drag acting on the vertically integrated velocity. Using the velocity at the bottom of the ocean would be more realistic, but this wrinkle is beyond the scope of vertically integrated models.) Equation (19.4) then becomes

$$\beta \overline{v} = -r\overline{\zeta} + F_\tau(x, y), \tag{13.5}$$

where $F_\tau = \text{curl}_z \boldsymbol{\tau}_T$ is the wind-stress curl at the top of the ocean and is a known function. Because the velocity is divergence-free, we can define a streamfunction ψ such that $\overline{u} = -\partial\psi/\partial y$ and $\overline{v} = \partial\psi/\partial x$. Equation (19.5) then becomes

$$r\nabla^2\psi + \beta \frac{\partial \psi}{\partial x} = F_\tau(x, y). \tag{13.6}$$

This equation is often referred to as the *Stommel problem* or the *Stommel model,* and may be posed in a variety of two dimensional domains.

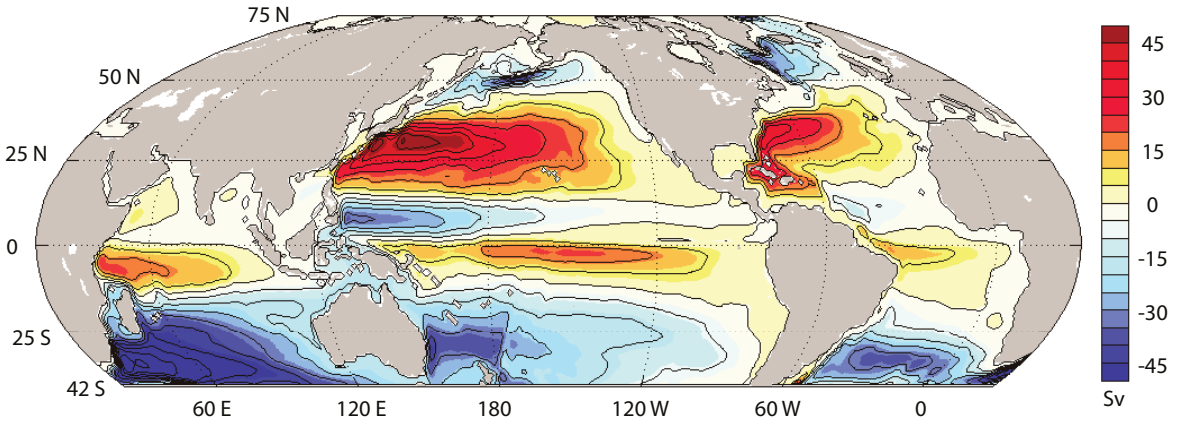

Fig. 13.4 A state estimate of the streamfunction of the vertically integrated flow for the near global ocean. Red shading indicates clockwise flow, and blue shading anticlockwise, but in both hemispheres the subtropical (subpolar) gyres are anticyclonic (cyclonic).[47]

There is a tide in the affairs of men,
which, taken at the flood, leads on to fortune.
Omitted, all the voyage of their life is bound in shallows and in miseries.
On such a full sea are we now afloat,
and we must take the current when it serves, or lose our ventures.
William Shakespeare, *Julius Caesar,* c. 1599.

CHAPTER 14

Structure of the Upper Ocean

IN THE PREVIOUS CHAPTER we developed an understanding of the vertically integrated flow of the worlds oceans. If we are to proceed further we must develop an understanding of the *vertical structure* of the oceans, and that is the subject of this chapter. Our main focus will be on the upper ocean and we will proceed as follows:

1. We first explore the vertical structure of the wind-driven circulation, largely as a continuation of the investigation of the previous chapter. We use the quasi-geostrophic equations to understand why the subsurface ocean moves at all, and we introduce the notion of potential vorticity homogenization.

2. A limitation of the quasi-geostrophic approach is that these equations take the stratification, $N(z)$, as a given and therefore cannot provide a answer to the question as to what produces the density structure itself. Thus, beginning in Section 20.4, we relax the quasi-geostrophic restriction and, using the *planetary-geostrophic* equations, we try to understand the dynamics that give rise to the vertical structure of density itself. We focus on the *main thermocline,* the region of the upper ocean in which temperature and density vary most rapidly, in all seasons, and we discuss the structure of both the internal thermocline and the ventilated thermocline, the meaning of which will become apparent later.

As with many fluid problems, the dynamics becomes intertwined with the thermodynamics, and the mean flow becomes intertwined with the smaller, turbulent, baroclinic eddies, in rather subtle ways that, to this day, are not fully understood and that large numerical models are only beginning to properly simulate. We begin by looking at the vertical structure of the wind-driven gyres, and if and how the influence of the wind can be communicated to the subsurface ocean.

14.1 VERTICAL STRUCTURE OF THE WIND-DRIVEN CIRCULATION

14.1.1 A Two-layer Quasi-Geostrophic Model

We pose the problem using the quasi-geostrophic equations, taking the background stratification of the ocean as a given.[48] The simplest system that has vertical structure is a two-layer model and that is where we start. We don't yet wish to consider the effects of mesoscale eddies, so we'll limit ourselves to motion larger than the deformation scale, although not so large that the quasi-geostrophic system itself does not hold.

Scales of motion

On scales that are sufficiently larger than the deformation radius we can ignore the relative vorticity compared to planetary vortex stretching and the β-effect. Since quasi- geostrophic scaling itself applies only to scales that are not significantly larger than the deformation scale, our analysis will be formally valid under the following set of inequalities:

$$\begin{aligned} \beta L &\ll f_0 && \text{(small variations in Coriolis parameter),} \\ \beta L &> U/L && \text{(to ignore relative vorticity compared to planetary vorticity),} \\ L^2 &> L_d^2 && \text{(to ignore relative vorticity compared to vortex stretching),} \\ Ro\, L^2 &\ll L_d^2 && \text{(to keep the variations in stratification small),} \end{aligned}$$

where L_d is the deformation radius and L the scale of the motion. The first and last of the above inequalities are standard quasi-geostrophic requirements, with the '$\gg$' symbol denoting the asymptotic ordering. The middle two inequalities are taken within the quasi-geostrophic dynamics, and are needed in order to ignore relative vorticity and give a balance between the β-effect and vortex stretching. The simultaneous satisfaction of all these conditions may seem restrictive, but the plangent dynamics contained within the quasi-geostrophic equations and the generality of the method employed below will suggest that the principal results obtained may transcend the limitations of the equations used. In the mid-latitude ocean $L_d \approx 10^5$ m and the above inequalities are reasonably well satisfied for $L \approx 10^6$ m and $U \approx 0.1\,\mathrm{m\,s^{-1}}$ with $\beta = 10^{-11}\,\mathrm{m^{-1}\,s^{-1}}$ and $f_0 = 10^{-4}\,\mathrm{s^{-1}}$.

Constructing the model

We now make the following simplifications for our model ocean:

(i) We use the two-layer quasi-geostrophic equations, with layers of equal thickness.

(ii) We seek only statistically-steady solutions.

(iii) We include a frictional term coming from a downgradient flux of potential vorticity. Given the neglect of relative vorticity, this is equivalent to an interfacial drag.

(iv) We neglect the western boundary layer.

Because of the equal-layer-thickness assumption, which makes the algebra simpler, it is best considered as a model for the upper ocean above a level where the vertical velocity is approximately zero. The equations of motion are then

$$J(\psi_1, q_1) = \frac{1}{H_0}\mathrm{curl}_z \boldsymbol{\tau}_T - \nabla\cdot\boldsymbol{T}_1, \qquad J(\psi_2, q_2) = -\nabla\cdot\boldsymbol{T}_2 \tag{14.1a,b}$$

where

$$q_1 = \beta y + F(\psi_2 - \psi_1), \qquad q_2 = \beta y + F(\psi_1 - \psi_2). \tag{14.2a,b}$$

Here, $F = f_0^2/(g' H_0) = 1/L_d^2$ is a measure of the stratification, where H_0 is the thickness of either layer, and the $\nabla\cdot\boldsymbol{T}$ terms represent interfacial eddy stresses, which, if needed, we will parameterize by a downgradient flux of potential vorticity,

$$\boldsymbol{T}_1 = -\kappa\nabla q_1 = -\kappa(F\nabla(\psi_2 - \psi_1) + \beta\mathbf{j}), \qquad \boldsymbol{T}_2 = -\kappa\nabla q_2 = -\kappa(F\nabla(\psi_1 - \psi_2) + \beta\mathbf{j}), \tag{14.3}$$

where κ is a constant. We will mostly be interested in the limit of small κ, or more specifically $UL/\kappa \gg 1$, which is a large Péclet number condition. (The Péclet number is similar to a Reynolds number, but with the diffusivity replacing the kinematic viscosity.) So first consider the case when κ is identically zero. An *exact* solution to (20.1) has $\psi_2 = 0$, so that (20.1a) becomes $\beta\partial\psi_1/\partial x = H_0^{-1}\mathrm{curl}_z\boldsymbol{\tau}_T$, with solution

$$\psi_1 = -\frac{1}{H_0\beta}\int_x^{x_E} \mathrm{curl}_z\boldsymbol{\tau}_T\,\mathrm{d}x. \tag{14.4}$$

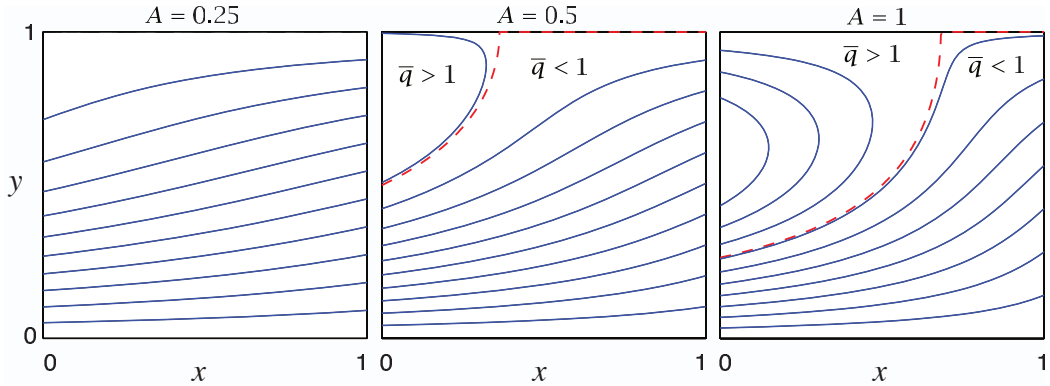

Fig. 14.1 Contours of $\overline{q} = \beta y + A \sin \pi y(1 - x)$, with $\beta = 1$, for three values of A. The red dashed line is $\overline{q} = 1$, which separates the blocked region to the east ($\overline{q} < 1$) from the closed region to the west ($\overline{q} > 1$). See Fig. 20.2 for plots of the other fields.

That is, *there is no flow in the lower layer*, and the upper layer solution is given by Sverdrup balance. The solution satisfies $\psi_1 = 0$ at $x = x_E$ and, because $\psi_2 = 0$, the nonlinear term on the left-hand side of (20.1a) vanishes identically. This is both counter-intuitive and counter-observations, for we know the subsurface ocean is not quiescent. Is there another solution?

A general solution

We now construct the solution without assuming $\psi_2 = 0$. Although the equations are nonlinear, we can obtain a linear equation for a streamfunction by adding (20.1a) and (20.1b), giving

$$J(\psi_1, \beta y + F(\psi_2 - \psi_1)) + J(\psi_2, \beta y + F(\psi_1 - \psi_2)) = \frac{1}{H_0} \mathrm{curl}_z \boldsymbol{\tau}_T. \tag{14.5}$$

The nonlinear terms cancel leaving

$$J(\overline{\psi}, \beta y) = \frac{1}{H_0} \mathrm{curl}_z \boldsymbol{\tau}_T, \qquad \text{where} \quad \overline{\psi} = \psi_1 + \psi_2, \tag{14.6a,b}$$

with solution, as in (20.4),

$$\overline{\psi} = -\frac{1}{H_0 \beta} \int_x^{x_E} \mathrm{curl}_z \boldsymbol{\tau}_T \, \mathrm{d}x'. \tag{14.7}$$

This simply says that the vertically integrated flow obeys Sverdrup balance. For the canonical wind stress

$$\boldsymbol{\tau}_T = -\tau_0 \cos \pi y \, \mathbf{i}, \tag{14.8}$$

and we obtain $\overline{\psi} = (\pi \tau_0 / \beta H_0)(x_E - x) \sin \pi y$. It is useful to define

$$\overline{q} \equiv (\beta y + F\overline{\psi}), \tag{14.9}$$

and then $\overline{q} = \beta[y + A(1 - x) \sin \pi y]$, where $A = \pi \tau_0 / (\beta H_0)$ parameterizes the wind strength, and this is plotted in Fig. 20.1. For $\overline{q} < 1$ (below and to the right of the dashed line) all the geostrophic contours intersect the eastern boundary and the flow is 'blocked'. For $\overline{q} > 1$ the flow is 'closed'.

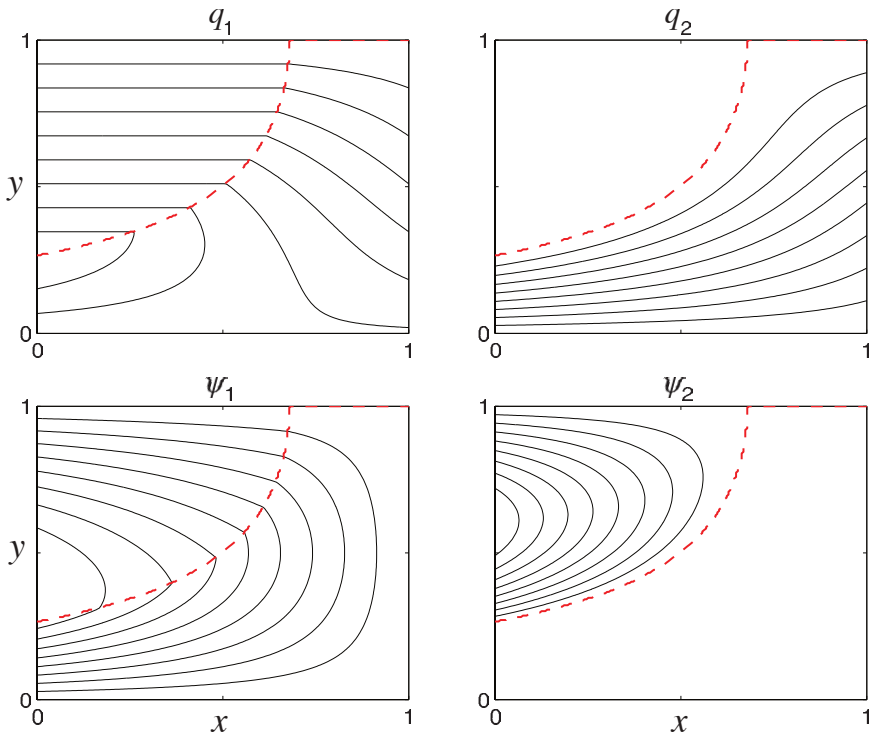

Fig. 14.2 Upper- and lower-level potential vorticity and streamfunction for the canonical wind stress (20.8). The field of $\overline{q}$ is that of Fig. 20.1 with $A = 1$. The dashed line divides the blocked region from the closed region. The lower layer streamfunction ψ_2 is non-zero only in the closed region, and here $q_2 = \beta L$ and $q_1 = 2\beta y - \beta L$. In the blocked region the upper layer carries all of the Sverdrup transport. Both the streamfunction and potential vorticity are continuous at the divide: $\psi_2 = 0$ and $q_2 = \overline{q} = \beta L$.

Lower layer

Although the full equations are nonlinear, using (20.9) we can obtain a linear equation for the lower layer. Because the Jacobian of a field with itself vanishes, (20.1b) and (20.2b) imply that

$$J(\psi_2, \overline{q}) = -\nabla \cdot \boldsymbol{T}_2, \tag{14.10}$$

and this is useful because $\overline{q}$ is a function of the wind, using (20.9). If $\nabla \cdot \boldsymbol{T}_2 = 0$ then

$$J(\psi_2, \overline{q}) = 0. \tag{14.11}$$

As well as the possibility that $\psi_2 = 0$ we now have the more general solution

$$\psi_2 = G(\overline{q}), \tag{14.12}$$

where G is an *arbitrary* function of its argument. Isolines of ψ_2 and $\overline{q}$ are then coincident. (Contours that are isolines of both streamfunction and potential vorticity are known as geostrophic contours.)

Our heads are round so our thoughts may change direction.
Francis Picabia (1879–1953).

Paradigms Lost.
Apologies to John Milton.

CHAPTER 15

The Meridional Overturning Circulation and the Antarctic Circumpolar Current

THE *MERIDIONAL OVERTURNING CIRCULATION,* or the MOC, of the ocean is the circulation associated with sinking mostly at high latitudes and upwelling elsewhere, with much of the meridional transport taking place below the main thermocline. Understanding this circulation is one of the main goals of this chapter. The theory explaining the MOC is not nearly as settled as that of the quasi-horizontal wind-driven circulation discussed in Chapter 19, but considerable progress has been made, in particular with a significant re-thinking of the fundamentals occurring in the late 20th and early 21st century, as we will discover. Our other main goal is to glean an understanding of the Antarctic Circumpolar Current, or ACC, the theory of which has also undergone a transformation over that same period. The ACC is important not only in its own right, but because it mediates the MOCs of the individual ocean basins, connecting them into a global circulation.

That there *is* a deep circulation has been known for a long time, largely from observations of tracers such as temperature, salinity, and constituents such as dissolved oxygen and silica.[49] We can also take advantage of numerical models that are able to assimilate observations (from hydrographic measurements, floats and satellites) and produce a state estimate of the overturning circulation that is consistent with both the observations and the equations of motion, and one such estimate is illustrated in Fig. 21.1. We see that the water does not all upwell in the subtropics as we tacitly assumed in the previous chapter. In fact, much of the mid-depth circulation more-or-less follows the isopycnals that span the two hemispheres (Fig. 21.2), sinking in the North Atlantic and upwelling in the Southern Ocean, with the transport in between being, at least in part, adiabatic.

The MOC used to be known as the 'thermohaline' circulation, reflecting the belief that it was primarily driven[50] by buoyancy forcing arising from gradients in temperature and salinity. Such a circulation requires that the diapycnal mixing must be sufficiently large, but many measurements have suggested this is not the case and that has led to a more recent view that the MOC is at least partially, and perhaps primarily, mechanically driven, mostly by winds, and so *along* isopycnals instead of across them. However, the situation is not wholly settled, and it is almost certain that both buoyancy and wind forcing, as well as diapycnal diffusion, all contribute. The possible role of multiple basins (Atlantic, Pacific, etc.) on the MOC is likewise not fully understood.

In the first half of the chapter we mainly discuss somewhat classical topics associated with the buoyancy forcing. Then, beginning in Section 21.6, we discuss the role of wind forcing in

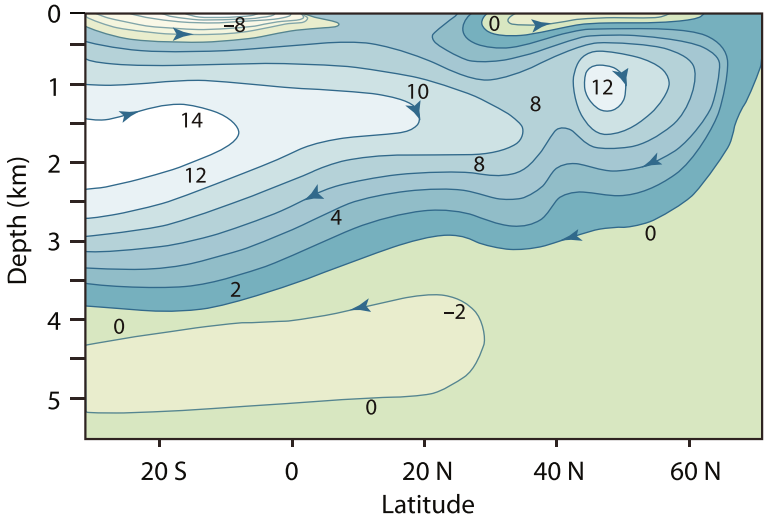

Fig. 15.1 An estimate of the mean meridional overturning circulation of the Atlantic (i.e., the streamfunction of the zonally averaged meridional flow) in Sverdrups.[51]

producing a MOC. This forces us to take an extended diversion into the dynamics of the ACC in Section 21.7 and then, in the last two sections, we present a theory of the MOC that incorporates both wind and buoyancy effects. We start by considering a simple but revealing fluid model of buoyancy forcing at the surface in a very idealised setting.

15.1 SIDEWAYS CONVECTION

Perhaps the simplest and most obvious fluid dynamical model of the overturning circulation is that of *sideways convection*. The physical situation is sketched in Fig. 21.3. A fluid (two- or three-dimensional) is held in a container that is insulated on all of its sides and its bottom, but its upper surface is non-uniformly heated and cooled. In the purest fluid dynamical problem the heat enters the fluid solely by conduction at the upper surface, and one may suppose that here the temperature is imposed. Thus, for a simple Boussinesq fluid the equations of motion are

$$\frac{\mathrm{D}\boldsymbol{v}}{\mathrm{D}t} + \boldsymbol{f}\times\boldsymbol{v} = -\nabla\phi + b\mathbf{k} + \nu\nabla^2\boldsymbol{v}, \qquad \frac{\mathrm{D}b}{\mathrm{D}t} = \kappa\nabla^2 b, \qquad \nabla\cdot\boldsymbol{v} = 0, \tag{15.1a,b,c}$$

where $\boldsymbol{f}\, f\mathbf{k}$, and with boundary conditions

$$b(x, y, 0, t) = g(x, y), \tag{15.2}$$

where $g(x, y)$ is a specified field, and $\partial_n b = 0$ on the other boundaries, meaning that the derivative normal to the boundary, and so the buoyancy flux, is zero. The oceanographic relevance of (21.1) and (21.2) should be clear: the ocean is heated *and* cooled from above, and although the thermal forcing in the real ocean may differ in detail (being in part a radiative flux, and in part a sensible and latent heat transfer from the atmosphere), (21.2) is a useful idealization. An alternative upper boundary condition would be to impose a flux condition whereby

$$\text{flux} = \kappa\frac{\partial}{\partial z}b(x, y, 0, t) = h(x, y), \tag{15.3a}$$

where $h(x, y)$ is given. In some numerical models of the ocean, the heat input at the top is parameterized by way of a relaxation to some specified temperature. This is a form of flux condition in which

$$\kappa\frac{\partial b}{\partial z} = C(b^*(x, y) - b), \tag{15.3b}$$

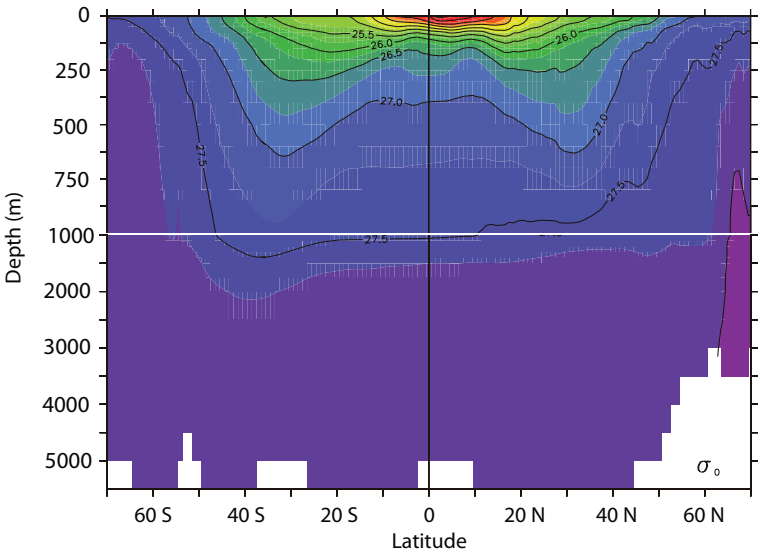

Fig. 15.2 The climatological zonally-averaged potential density (σ_θ) in the Atlantic ocean. Note the break in the vertical scale at 1000 m.

The region of rapid change of density (and temperature) is concentrated in the upper kilometre, in the main thermocline, below which the density is more uniform. The flow of the MOC is largely, but not exactly, parallel to the isopycnals. [52]

and C is an empirical constant and $b^*(x, y)$ is given.[53] Although this may be a little more relevant than (21.2) for the real ocean, which of the three boundary conditions is chosen will not affect the arguments below, and we use (21.2).

15.1.1 Two-dimensional Convection

We may usefully restrict attention to the two-dimensional problem, in latitude and height. This is a poor model of the actual overturning circulation of the ocean, but the results do not depend on this idealization. The incompressibility of the flow then allows one to define a streamfunction such that

$$v = -\frac{\partial \psi}{\partial z}, \quad w = \frac{\partial \psi}{\partial y}, \qquad \zeta = \nabla_x^2 \psi = \left(\frac{\partial^2 \psi}{\partial y^2} + \frac{\partial^2 \psi}{\partial z^2} \right), \tag{15.4}$$

where ζ is the vorticity in the meridional plane. We will omit the subscript x on the Laplacian operator where there is no ambiguity.

Taking the curl of Boussinesq equations of motion (21.1) then gives

$$\frac{\partial \nabla^2 \psi}{\partial t} + J(\psi, \nabla^2 \psi) = \frac{\partial b}{\partial y} + \nu \nabla^4 \psi, \tag{15.5a}$$

$$\frac{\partial b}{\partial t} + J(\psi, b) = \kappa \nabla^2 b, \tag{15.5b}$$

where $J(a, b) \equiv (\partial_y a)(\partial_z b) - (\partial_z a)(\partial_y b)$.

Nondimensionalization and scaling

We nondimensionalize (21.5) by formally setting

$$b = \Delta b \, \hat{b}, \qquad \psi = \Psi \hat{\psi}, \qquad y = L\hat{y}, \qquad z = H\hat{z}, \qquad t = \frac{LH}{\Psi} \hat{t}, \tag{15.6}$$

where the hatted variables are nondimensional, Δb is the temperature difference across the surface, L is the horizontal size of the domain, and Ψ, and ultimately the vertical scale H, are to be

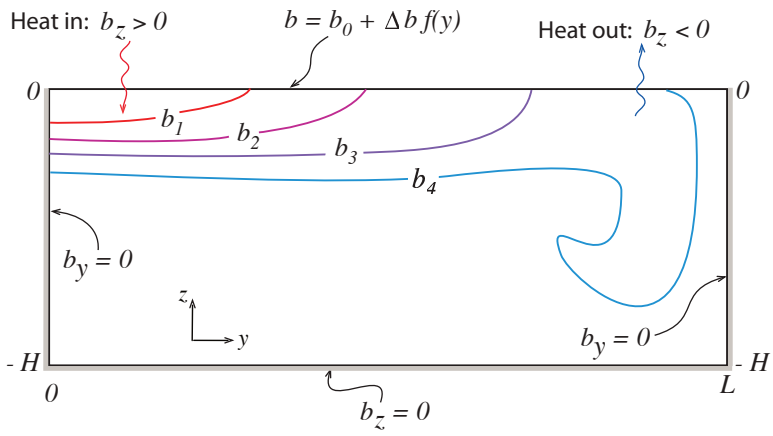

Fig. 15.3 Sketch of sideways convection. The fluid is differentially heated and cooled along its top surface, whereas all the other walls are insulating.

The result is, typically, a small region of convective instability and sinking near the coldest boundary, with generally upwards motion elsewhere.[54]

determined. Substituting (21.6) into (21.5) gives

$$\frac{\partial \widehat{\nabla}^2 \widehat{\psi}}{\partial \hat{t}} + \hat{J}(\widehat{\psi}, \nabla^2 \widehat{\psi}) = \frac{H^3 \Delta b}{\Psi^2} \frac{\partial \hat{b}}{\partial \hat{y}} + \frac{\nu L}{\Psi H} \widehat{\nabla}^4 \widehat{\psi}, \tag{15.7a}$$

$$\frac{\partial \hat{b}}{\partial \hat{t}} + \hat{J}(\widehat{\psi}, \hat{b}) = \frac{\kappa L}{\Psi H} \widehat{\nabla}^2 \hat{b}, \tag{15.7b}$$

where $\widehat{\nabla}^2 = (H/L)^2 \partial^2/\partial \hat{y}^2 + \partial^2/\partial \hat{z}^2$ and the Jacobian operator is similarly nondimensional. If we now use (21.7b) to choose Ψ as

$$\Psi = \frac{\kappa L}{H}, \tag{15.8}$$

so that $t = H^2 \hat{t}/\kappa$, then (21.7) becomes

$$\frac{\partial \widehat{\nabla}^2 \widehat{\psi}}{\partial \hat{t}} + \hat{J}(\widehat{\psi}, \widehat{\nabla}^2 \widehat{\psi}) = Ra \sigma \alpha^5 \frac{\partial \hat{b}}{\partial \hat{y}} + \sigma \widehat{\nabla}^4 \widehat{\psi}, \tag{15.9}$$

$$\frac{\partial \hat{b}}{\partial \hat{t}} + \hat{J}(\widehat{\psi}, \hat{b}) = \widehat{\nabla}^2 \hat{b}. \tag{15.10}$$

It is possible to make different scaling choices, but they all lead to the appearance of the same non dimensional parameters, or combinations thereof, and the three that govern the behaviour of the system are

$$Ra = \left(\frac{\Delta b L^3}{\nu \kappa} \right), \qquad \text{(the Rayleigh number)}, \tag{15.11a}$$

$$\sigma = \frac{\nu}{\kappa}, \qquad \text{(the Prandtl number)}, \tag{15.11b}$$

$$\alpha = \frac{H}{L}, \qquad \text{(the aspect ratio)}. \tag{15.11c}$$

Sometimes H is used instead of L in the Rayleigh number definition; we use L here because it is an external parameter. The Rayleigh number is a measure of the strength of the buoyancy forcing relative to the viscous term, and in the ocean it will be very large indeed, perhaps $\sim 10^{24}$ if molecular values are used.

For steady non-turbulent flows, and also perhaps for statistically steady flows, we can demand that the buoyancy term in (21.9) is $\mathcal{O}(1)$. If it is smaller then the flow is not buoyancy driven, and

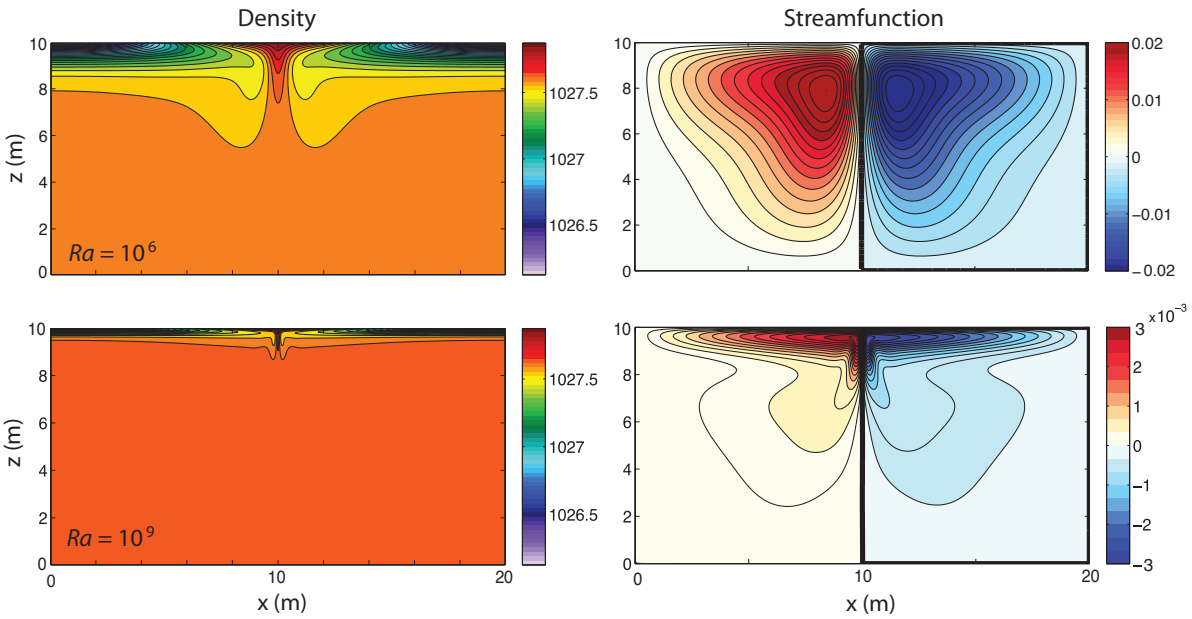

Fig. 15.4 The density and streamfunction in two numerical simulations of two-dimensional sideways convection, with Rayleigh numbers of 10^6 (top) and 10^9 (bottom). The imposed temperature at the top linearly decreases from the centre outward, the side and bottom walls are insulating, and the Prandtl number is 10. The two density plots use the same colourmap, but the streamfunction plots do not. There is a sinking plume at the centre, with a weaker circulation and a thinner thermocline at the higher Rayleigh number.[56]

if it is larger there is nothing to balance it. Our demand can be satisfied only if the vertical scale of the motion adjusts appropriately and, for $\sigma = \mathcal{O}(1)$, this suggests the scalings:[55]

$$H = L\sigma^{-1/5}Ra^{-1/5} = \left(\frac{\kappa^2 L^2}{\Delta b}\right)^{1/5}, \qquad \Psi = Ra^{1/5}\sigma^{-4/5}\nu = (\kappa^3 L^3 \Delta b)^{1/5}. \tag{15.12a,b}$$

The vertical scale H arises as a consequence of the analysis, and the vertical size of the domain plays no direct role. [For $\sigma \gg 1$ we might expect the nonlinear terms to be small and if the buoyancy term balances the viscous term in (21.9) the right-hand sides of (21.12) are multiplied by $\sigma^{1/5}$ and $\sigma^{-1/5}$. For seawater, $\sigma \approx 7$ using the molecular values of κ and ν. If small scale turbulence exists, then the eddy viscosity will likely be similar to the eddy diffusivity and $\sigma \approx 1$.] Numerical experiments (an example is shown in Fig. 21.4) provide support for the scaling of (21.12), and a few simple and robust points that have relevance to the real ocean emerge:

- Most of the box fills up with the densest available fluid, with a boundary layer in temperature near the surface required in order to satisfy the top boundary condition. The boundary gets thinner with decreasing diffusivity, consistent with (21.12). This is a diffusive prototype of the oceanic thermocline.
- The horizontal scale of the overturning circulation is large, nearly the scale of the box.
- The downwelling regions (the regions of convection) are of smaller horizontal scale than the upwelling regions, especially as the Rayleigh number increases.

Let us now try to explain some of the features in a simple and heuristic way, beginning with the scale of the motion.

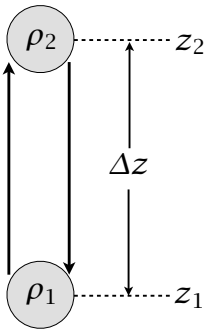

Fig. 15.5 Two fluid parcels, of density ρ_1 and ρ_2 and initially at positions z_1 and z_2 respectively, are interchanged. If $\rho_2 > \rho_1$ then the final potential energy is lower than the initial potential energy, with the difference being converted into kinetic energy.

15.1.2 The Relative Scale of Convective Plumes and Diffusive Upwelling

Why is the downwelling region narrower than the upwelling? The short answer is that high Rayleigh number convection is much more efficient than diffusive upwelling, so that the convective buoyancy flux can match the diffusive flux only if the convective plumes cover a much smaller area than diffusion.[57] Suppose that the basin is initially filled with water of an intermediate temperature, and that surface boundary conditions of a temperature decreasing linearly from low latitudes to high latitudes are imposed. The deep water will be convectively unstable, and convection at high latitudes (where the surface is coldest) will occur, quickly filling the abyss with dense water. After this initial adjustment the deep, dense water at lower latitudes will be slowly warmed by diffusion, but at the same time surface forcing will maintain a cold high latitude surface, thus leading to high latitude convection. A steady state or statistically steady state is eventually reached with the deep water having a slightly lower potential density than the surface water at the highest latitudes, and so maintaining continual convection, but convection that takes place only at the highest latitudes.

To see this more quantitatively consider the respective efficiencies of the convective heat flux and the diffusive heat flux. Consider an idealized re-arrangement of two parcels, initially with the heavier one on top as illustrated in Fig. 21.5. The potential energy released by the re-arrangement, ΔP is given by

$$\Delta P = P_{\text{final}} - P_{\text{initial}} \tag{15.13}$$

$$= g\left[(\rho_1 z_2 + \rho_2 z_1) - (\rho_1 z_1 + \rho_2 z_2)\right] \tag{15.14}$$

$$= g(z_2 - z_1)(\rho_1 - \rho_2) = \rho_0 \Delta b \Delta z, \tag{15.15}$$

where $\Delta z = z_2 - z_1$ and $\Delta b = g(\rho_1 - \rho_2)/\rho_0$.

The kinetic energy gained by this re-arrangement, ΔK is given by $\Delta K = \rho_0 w^2$ and equating this to (21.13) gives

$$w^2 = -\Delta b \Delta z. \tag{15.16}$$

If the heavier fluid is initially on top then $\rho_2 > \rho_1$ and, as defined, $\Delta b < 0$. The vertical convective buoyancy flux per unit area, B_c, is given by $B_c = w\Delta b$ and using (21.16) we find

$$B_c = (-\Delta b)^{3/2}(\Delta z)^{1/2}. \tag{15.17}$$

The upwards diffusive flux, B_d, per unit area is given by

$$B_d = \kappa \frac{\Delta b}{H}, \tag{15.18}$$

where H is the thickness of the layer over which the flux occurs. In a steady state the total diffusive flux must equal the convective flux so that, from (21.17) and (21.18),

$$(-\Delta b)^{3/2}(\Delta z)^{1/2}\delta = \kappa \frac{\Delta b}{H}, \tag{15.19}$$

where δ is the fractional area over which convection occurs. If we set $\Delta z = H$, and use (21.12a) we find

$$(-\Delta b)^{3/2}\left(\frac{\kappa^2 L^2}{\Delta b}\right)^{1/10}\delta = \kappa\frac{\Delta b}{(\kappa^2 L^2/\Delta b)^{1/5}}, \tag{15.20}$$

giving

$$\delta = \left(\frac{\kappa^2}{\Delta b L^3}\right)^{1/5} = (Ra\,\sigma)^{-1/5}. \tag{15.21}$$

For geophysically relevant situations this is a very small number, usually smaller than 10^{-5}. Although the details of the above calculation may be questioned (for example, the use of the same buoyancy difference and vertical scale in the convection and the diffusion), the physical basis for the result is transcendent: for realistic choices of the diffusivity the convection is much more efficient than the diffusion and so will occur over a much smaller area.

15.1.3 Phenomenology of the Overturning Circulation

No water can be denser (or, more accurately, have a greater potential density) than the densest water at the surface. If the surface water is denser than the water at depth then it will be convectively unstable and sink in a plume.[58] The plume slowly entrains the warmer water that surrounds it, and then spreads horizontally when it reaches the bottom or when its density becomes similar to that of its surroundings. The presence of water denser than its surroundings creates a horizontal pressure gradient, and the ensuing flow will displace any adjacent lighter fluid, and so the domain fills with the densest available fluid. This process is a continuous one: the plumes take cold water into the interior, where the water slowly warms by diffusion, and the source of cold water at the surface is continuously replenished. If diffusion is small, the end result is that the potential density of the fluid in the interior will be slightly less than that of the densest fluid formed at the surface. (Because diffusion can act only to reduce extrema, no fluid in the interior can be colder than the coldest fluid formed at the surface.)

However, the value at the surface is given by the boundary condition $b(x, y, z = 0) = f(x, y)$. Thus, the interior cannot fill all the way to the surface with this cold water and there must be a boundary layer connecting the cold, dense interior with the surface; its thickness δ is given by the height scale of (21.12a); that is $\delta \sim H = (\kappa^2 L^2/\Delta b)^{1/5}$. Such a strong boundary layer will not necessarily be manifest in the velocity field, however, because the no-normal flow boundary condition on the velocity field is satisfied by setting $\psi = 0$ as a boundary condition to the elliptic problem $\nabla^2\psi = \zeta$, where ζ is the prognostic variable in (21.5a), and this boundary condition has a global effect on the velocity field.

Why is the horizontal scale of the circulation large? The circulation transfers heat meridionally, and it is far more efficient to do this by a single overturning cell than by a multitude of small cells; hence, although we cannot entirely eliminate the possibility that some instability will produce such small scales of motion, it seems likely the horizontal scale of the mean circulation will be determined by the domain scale. (At low Rayleigh number we can in fact explicitly calculate an approximate analytic solution for the flow, demonstrating this.) For higher Rayleigh number perturbation approaches fail and we must resort to numerical solutions; these (e.g., Fig. 21.4), do show the circulation dominated by a single overturning circulation rather than many small convective cells over a large range of Rayleigh number.

Finally, it is important to realize that *even for large diffusion and viscosity there is no stationary solution:* as soon as we impose a temperature gradient at the top the fluid begins to circulate, a manifestation of the dictum that a baroclinic fluid is a moving fluid, encountered in Section 4.2. Put simply, a temperature gradient leads a density gradient, which in turn leads to a pressure gradient.

The pressure gradient leads to motion: viscosity cannot prevent that, for it can have an effect only if the velocity is non-zero.

'In the afternoon they came unto a land
'In which it seemed always afternoon.
All round the coast the languid air did swoon,
'Breathing like one that hath a weary dream.
Alfred Tennyson, *The Lotus Eaters*, 1832.

CHAPTER 16

Equatorial Circulation and El Niño

EQUATORIAL OCEANOGRAPHY DECEIVES US, hiding fascinating, non-intuitive dynamics beneath the languorous tropical air. The mid-latitudes give us the great gyres with their intense western boundary currents and mesoscale eddies, and by comparison the equatorial currents may seem, on the surface, featureless and vapid. Yet the equatorial regions are home to the resolute equatorial undercurrents that tunnel across the basins, opposite in bearing to the winds that drive them. And the equatorial ocean and atmosphere — in a collaboration that is more tango than waltz — give rise to the marvellous phenomenon that is El Niño, the most dramatic example of climate variability on human timescales that this planet has to offer. Such phenomena are the subjects of this chapter.

The defining feature of equatorial dynamics is that the Coriolis parameter becomes small, at least by comparison with the mid-latitudes, and balanced and unbalanced dynamics become intertwined, as we encountered in Chapter 8. Yet if we move more than a few degrees away from the equator the Rossby number again becomes quite small, suggesting that familiar ways of investigating the dynamics — Sverdrup balance for example — might yet play a role. Let's first see what we are trying to understand and if the observations can give us some intuition.

16.1 OBSERVATIONAL PRELIMINARIES

In mid-latitudes the gyres are very robust features, existing in all the basins, and may be understood as the direct response to the curl of the wind stress. In the equatorial regions the currents also display some robust and distinctive features, illustrated in Fig. 22.1 and the top panel of Fig. 22.2, but their relation to the winds is less obvious. The main features are as follows:

1. A shallow westward[59] flowing surface current, typically confined to the upper 50 m or less, strongest within a few degrees of the equator, although not always symmetric about the equator. Its speed is typically a few tens of centimetres per second.

2. A strong coherent eastward undercurrent extending to about 200 m depth, confined to within a few degrees of the equator. Its speed is up to a metre per second or a little more, and it is this current that dominates the vertically integrated transport at the equator. Beneath the undercurrent the flow is relatively weak.

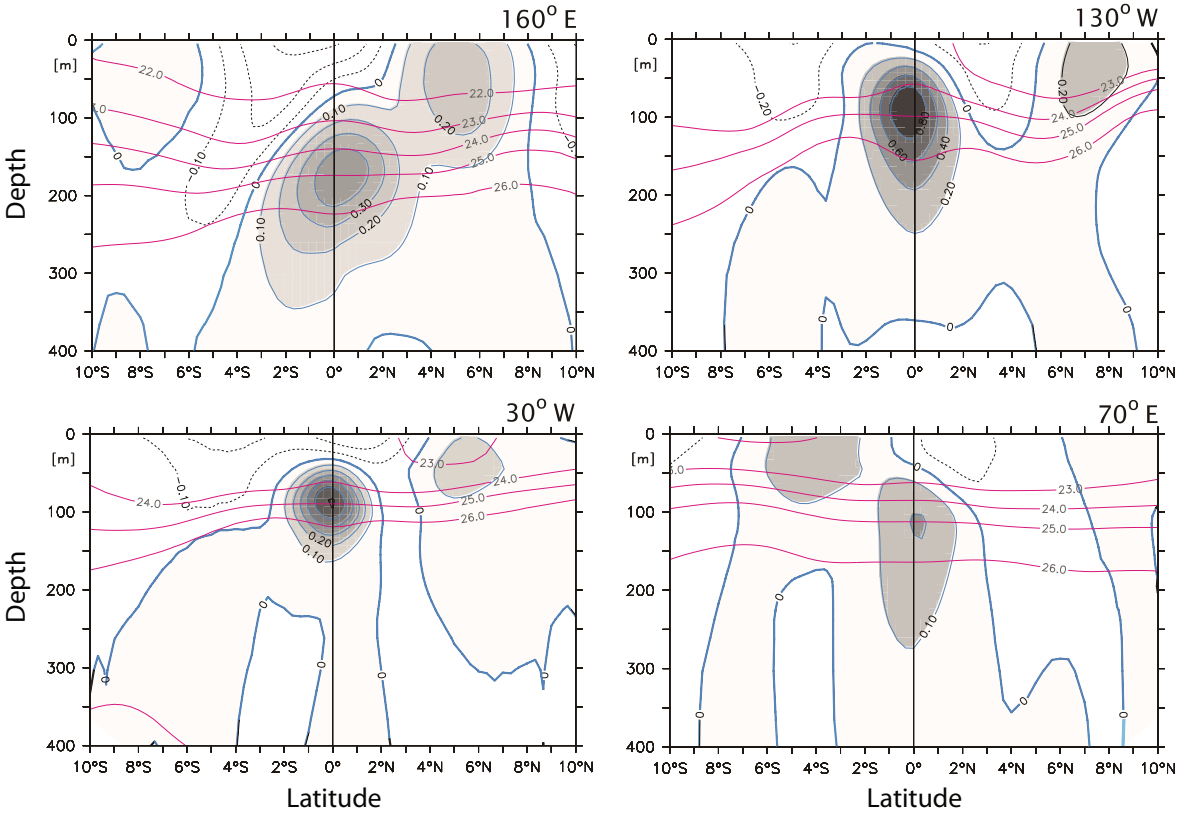

Fig. 16.1 Sections of the observed mean zonal current (shading and associated contours) at two longitudes in the Pacific (upper panels), in the Atlantic (lower left) and in the Indian Ocean (lower right). The contours are every 20 cm s^{-1} in the upper two panels and every 10 cm s^{-1} in the lower panels. Note the well-defined eastward undercurrent at the equator in all panels, and a weaker eastward countercurrent at about 6° N and/or 6° S. The red, more horizontal, lines are isolines of potential density.[60]

3. Westward flow on either side of the undercurrent, with eastward countercurrents poleward of this. In the Pacific the countercurrent is strongest in the Northern Hemisphere where it reaches the surface.

16.2 DYNAMICAL PRELIMINARIES

In mid-latitudes the large scale currents system may be understood using the planetary geostrophic equations of motion. Applying these allows us to understand formation of the great wind-driven gyres, with Sverdrup balance providing a solid foundation on which to build. As we approach lower latitudes the Coriolis parameter, f, decreases and the Rossby number increases and one might expect that dynamics based on geostrophic balance will ultimately fail. A little surprisingly, it is only very close to the equator that the Rossby number exceeds unity: if we take a velocity of 0.5 m s^{-1} and a length scale of 500 km then the Rossby number at 5° latitude is 0.08, at 2°, 0.2 and at 1°, 0.4. These numbers suggest that until we are virtually at the equator (where the Rossby number is infinite) we can use some of the familiar tools from the mid-latitude dynamics. At the equator the Coriolis parameter switches sign and this leads to some interesting features. The vertical structure is also a little complex so let us first see the extent to which the familiar Sverdrup balance can

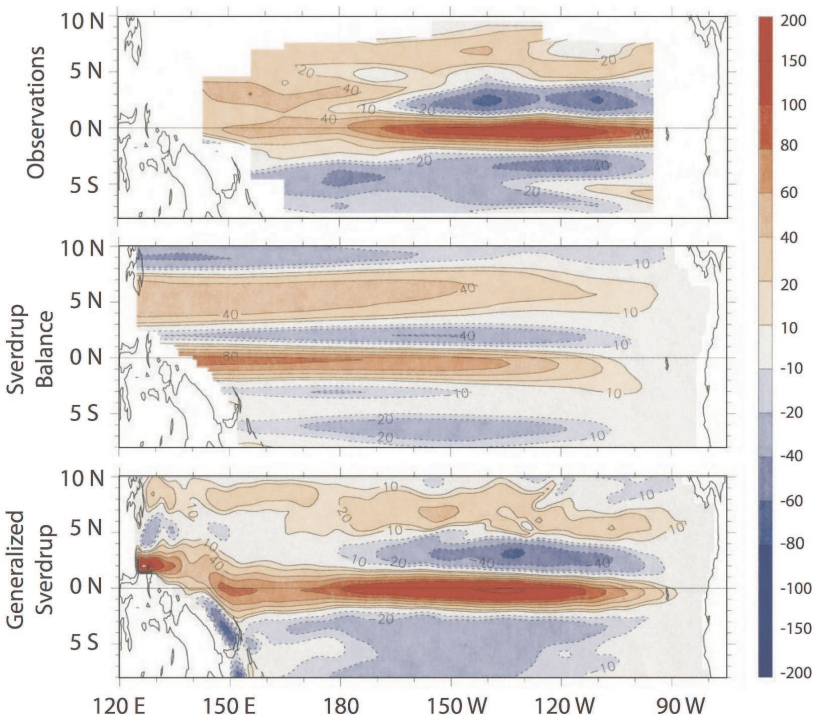

Fig. 16.2 Vertically integrated zonal transport in the Pacific. Red colours indicate eastward flow, blue colours westward. The top panel shows the observed flow, the middle panel shows the flow calculated using Sverdrup balance with the observed wind, and the bottom panel shows the flow calculated with a 'generalized' Sverdrup balance that includes the nonlinear terms in a diagnostic way.[61]

explain the vertically integrated flow.

16.2.1 The Vertically Integrated Flow and Sverdrup Balance

The horizontal momentum may be written

$$\frac{\partial \boldsymbol{u}}{\partial t} + \boldsymbol{u}\cdot\nabla\boldsymbol{u} + \boldsymbol{f}\times\boldsymbol{u} = -\nabla\phi + \frac{1}{\rho_0}\frac{\partial \boldsymbol{\tau}}{\partial z}, \tag{16.1}$$

where $\boldsymbol{\tau}$ is the stress on the fluid. The mass conservation equation is

$$\frac{\partial u}{\partial x} + \frac{\partial v}{\partial y} + \frac{\partial w}{\partial z} = 0, \tag{16.2}$$

which, on vertical integration over the depth of the ocean, gives

$$\frac{\partial U}{\partial x} + \frac{\partial V}{\partial y} = 0, \tag{16.3}$$

where U and V are the vertically integrated zonal and meridional velocities (e.g., $U = \int u\,\mathrm{d}z$) and we assume the ocean has a flat bottom and a rigid lid at the top. If we assume the flow is steady and integrate (22.1) vertically, then take the curl and use (22.3), we obtain

$$\beta V = \mathrm{curl}_z(\tilde{\boldsymbol{\tau}}_T - \tilde{\boldsymbol{\tau}}_B) + \mathrm{curl}_z \boldsymbol{N}, \tag{16.4}$$

where $\tilde{\boldsymbol{\tau}}$ is the kinematic stress ($\tilde{\boldsymbol{\tau}} = \boldsymbol{\tau}/\rho_0$ where ρ_0 is the reference density of seawater) with the subscripts T and B denoting top and bottom, $\boldsymbol{N}$ represents all the nonlinear terms and curl_z is defined by $\mathrm{curl}_z \boldsymbol{A} \equiv \partial A^y/\partial x - \partial A^x/\partial y = \mathbf{k}\cdot\nabla_3\times\boldsymbol{A}$. Equations (22.4) and (22.3) are closed equations for the vertically averaged flow. In oceanography we very often deal with the kinematic

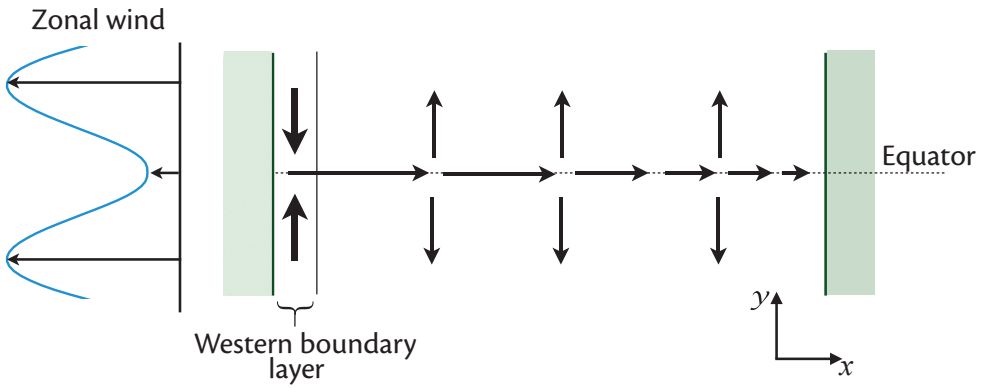

Fig. 16.3 Schema of Sverdrup flow at the equator between two meridional boundaries. The mean winds are all westward, but with a minimum in magnitude at the equator. By Sverdrup balance, (22.5), the wind stress produces the divergent meridional flow shown, which in turn induces an eastward equatorial zonal flow, strongest in the western part of the basin.

stress rather than the stress itself, so henceforth we will drop the tilde over the τ symbol as well as the adjective 'kinematic'. In the cases that we need to refer to the actual stress we will denote this by τ^*; thus, $\tau = \tau^*/\rho_0$.

If we neglect the nonlinear terms and the stress at the bottom (we'll come back to these terms later) then (22.4) becomes

$$\beta V = \mathrm{curl}_z \boldsymbol{\tau}_T. \tag{16.5}$$

This is just Sverdrup balance, familiar from Chapter 19. The zonal transport is obtained by differentiating (22.5) with respect to y, using (22.3) to replace $\partial_y V$ with $\partial_x U$, and then integrating from the eastern boundary (x_E). This procedure gives

$$U = -\frac{1}{\beta}\int_{x_E}^{x} \frac{\partial}{\partial y}\mathrm{curl}_z \boldsymbol{\tau}_T \, \mathrm{d}x' + U(x_E, y). \tag{16.6}$$

We don't integrate from the western boundary because a boundary layer can be expected there, whereas the value of U at the eastern boundary will be small.

If $U(x_E, y) = 0$ and the stress is zonal and uniform, then (22.6) becomes

$$U(x, y) = \frac{1}{\beta}(x - x_E)\frac{\partial^2 \tau_T^x}{\partial y^2}. \tag{16.7}$$

That is, the depth integrated flow is proportional to the second derivative of the zonal wind stress, and because $x < x_E$ we have $U \propto -\partial^2 \tau_T^x/\partial y^2$. Evidently, the result will depend rather sensitively on the wind pattern. Although the zonal wind is generally westward in the tropics there is a minimum in the magnitude of that wind near the equator (that is, a local maximum as schematized in Fig. 22.3) so that $\partial^2 \tau_T^x/\partial y^2$ is negative. Thus, using (22.7), U will generally be positive at the equator. Using the observed wind field the Sverdrup flow — that is, the solution of (22.6) with $U(x_E, y) = 0$ — can be calculated and this is plotted in the middle panel of Fig. 22.2. There is a good but not perfect agreement with the observations: the observed flow has its maximum further east. Further, in the western equatorial Pacific the observed eastward flow is quite broad whereas the eastward Sverdrup flow is narrow, flanked on either side by westward flow. Some of the discrepancy can be attributed to the role of the nonlinear and frictional terms, as illustrated in the bottom panel of Fig. 22.2. To obtain the flow illustrated, the calculation proceeds from (22.4) in the same way as before, but now includes the nonlinear terms and a representation of frictional effects in

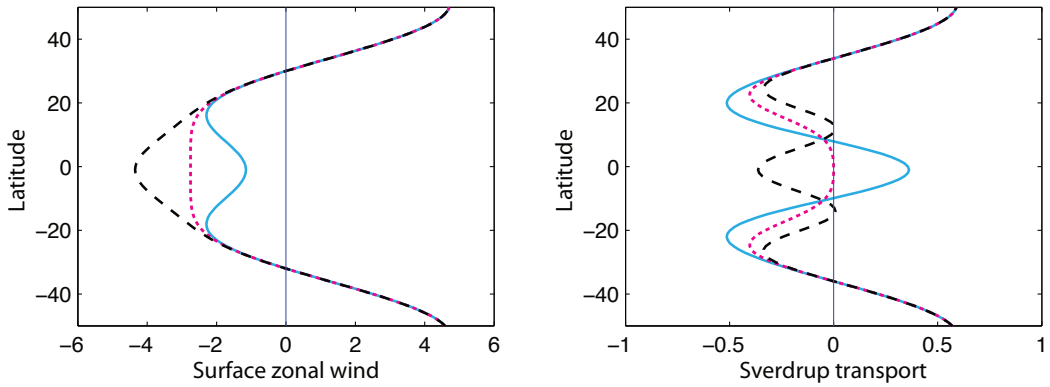

Fig. 16.4 The left panel shows three putative surface zonal (atmospheric) winds, u, all with westward winds in the tropics and with the solid line being the most realistic. The right panel shows the corresponding negative of the second derivative, $-\partial^2 u/\partial y^2$, proportional to the (oceanic) Sverdrup transport, in arbitrary units. The wind represented by solid (blue) line gives an eastward transport at the equator, as is observed, with the others differing markedly.

a diagnostic fashion. Thus, for example, the nonlinear terms of the form $\mathrm{curl}_z(\int \boldsymbol{u} \cdot \nabla \boldsymbol{u}\, dz)$ are evaluated and used to calculate a generalized Sverdrup flow, where the velocities are taken from a nonlinear model forced by the observed winds. Of the nonlinear terms, the largest ones involve the meridional derivatives of the zonal flow, for example $\partial_y(uu_x)$. The effect of the nonlinear terms is to decelerate the eastward flow in the eastern Pacific, with friction tending to damp the flow especially in the central Pacific, and the resulting flow is evidently closer to the observations than is linear Sverdrup balance. Of course the full solution (22.4) must give a vertically integrated flow that closely resembles the observations, because there are only very weak approximations made in deriving it. The success of the Sverdrup theory lies in the extent to which the vertically integrated flow can be satisfied by the simple linear balance (22.5), and then improved by adding nonlinear and dissipative terms in a diagnostic fashion.

16.2.2 Sensitivity of the Sverdrup Flow

Although the calculations of Sverdrup flow do show good agreement with observations, the calculation — and, most likely, the observed flow — is rather sensitive to the precise form of the winds, as in Fig. 22.4. The figure shows three surface zonal wind distributions, with the 'w' shaped solid line having a minimum in the westward flow (i.e., a minimum in the trade winds) at the equator and so being the most realistic. The right-hand panel shows the negative of the second derivative of the winds which is proportional to the zonal Sverdrup flow. Only in the one case does the wind produce an eastward Sverdrup flow. In fact, in the case illustrated with the dashed lines, the small changes in the meridional gradient of the wind between 15° and 20° produce large variations in the Sverdrup transport. Given this delicacy, the small difference in the latitudinal variation of the Sverdrup flow and the observed flow, illustrated in the top and middle panels of Fig. 22.2, is not surprising and cannot be considered a major failure of the theory. However, the difference in the longitudinal structure of the two fields is indicative of the importance of other terms in the vorticity balance.

References

Abarbanel, H. D. I. & Young, W. R., Eds., 1987. *General Circulation of the Ocean*. Springer-Verlag, 291 pp.

Abbe, C., 1901. The physical basis of long-range weather forecasts. *Mon. Wea. Rev.*, **29**, 551–561.

Ablowitz, M. J., 2011. *Nonlinear dispersive waves: asymptotic analysis and solitons*. Vol. 47, Cambridge University Press, 311 pp.

Abramowitz, M. & Stegun, I. A., 1965. *Handbook of Mathematical Functions*. Dover Publications, 1046 pp.

Allen, J. S., 1993. Iterated geostrophic intermediate models. *J. Phys. Oceanogr.*, **23**, 2447–2461.

Allen, J. S., Barth, J. A. & Newberger, P. A., 1990a. On intermediate models for barotropic continental shelf and slope flow fields. Part I: Formulation and comparison of exact solutions. *J. Phys. Oceanogr.*, **20**, 1017–1042.

Allen, J. S., Barth, J. A. & Newberger, P. A., 1990b. On intermediate models for barotropic continental shelf and slope flow fields. Part II: Comparison of numerical model solutions in doubly periodic domains. *J. Phys. Oceanogr.*, **20**, 1043–1082.

Allen, J. S., Holm, D. D. & Newberger, P. A., 2002. Extended-geostrophic Euler–Poincaré models for mesoscale oceanographic flow. In J. Norbury & I. Roulstone, Eds., *Large-scale Atmosphere–Ocean Dynamics I*. Cambridge University Press.

Ambaum, M. H. P., 2010. *Thermal Physics of the Atmosphere*. Wiley, 239 pp.

Andrews, D. G., 1987. On the interpretation of the Eliassen–Palm flux divergence. *Quart. J. Roy. Meteor. Soc.*, **113**, 323–338.

Andrews, D. G., 2010. *An Introduction to Atmospheric Physics*. Cambridge University Press, 237 pp.

Andrews, D. G., Holton, J. R. & Leovy, C. B., 1987. *Middle Atmosphere Dynamics*. Academic Press, 489 pp.

Andrews, D. G. & McIntyre, M. E., 1976. Planetary waves in horizontal and vertical shear: the generalized Eliassen–Palm relation and the mean zonal acceleration. *J. Atmos. Sci.*, **33**, 2031–2048.

Andrews, D. G. & McIntyre, M. E., 1978. Generalized Eliassen–Palm and Charney–Drazin theorems for waves on axisymmetric mean flows in compressible atmospheres. *J. Atmos. Sci.*, **35**, 175–185.

Angell, J. K. & Korshover, J., 1964. Quasi-biennial variations in temperature, total ozone, and tropopause height. *J. Atmos. Sci.*, **21**, 479–492.

Arakawa, A., 2004. The cumulus parameterization problem: Past, present, and future. *J. Climate*, **17**, 13, 2493–2525.

Arakawa, A. & Schubert, W. H., 1974. Interaction of a cumulus cloud ensemble with the large-scale environment, part i. *J. Atmos. Sci.*, **31**, 3, 674–701.

Arbic, B. K., Flierl, G. R. & Scott, R. B., 2007. Cascade inequalities for forced-dissipated geostrophic turbulence. *J. Phys. Oceanogr.*, **37**, 1470–1487.

Arnold, V. I., 1965. Conditions for nonlinear stability of stationary plane curvilinear flows of an ideal fluid. *Dokl. Akad. Nauk SSSR*, **162**, 975–978. Engl. transl.: *Sov. Math.* **6**, 773–777 (1965).

Arnold, V. I., 1966. On an a priori estimate in the theory of hydrodynamic stability. *Izv. Vyssh. Uchebn. Zaved. Math.*, **54**, 3–5. Engl. transl.: *Am Mat. Soc. Transl. Ser.*, 2, **79**, 267–289 (1969).

Assmann, R., 1902. Über die Existenz eines wärmeren Luftstromes in der Höhe von 10 bis 15 km. (On the existence of a warmer airflow at heights from 10 to 15 km). *Sitzber. Königl. Preuss. Akad. Wiss. Berlin*, **24**, 495–504.

Aubin, D. & Dahan Dalmedico, A., 2002. Writing the history of dynamical systems and chaos: *longue durée* and revolution, disciplines and cultures. *Historia Mathematica*, **29**, 1–67.

Baldwin, M. P., Gray, L. J., Dunkerton, T. J., Hamilton, K. *et al.*, 2001. The quasi-biennial oscillation. *Rev. Geophys.*, **39**, 179–229.

Ball, J. M. & James, R. D., 2002. The scientific life and influence of Clifford Ambrose Truesdell III. *Arch. Rational Mech. Anal.*, **161**, 1–26.

Bannon, P. R., 1995. Potential vorticity conservation, hydrostatic adjustment, and the anelastic approximation. *J. Atmos. Sci.*, **52**, 2301–2312.

Bannon, P. R., 1996. On the anelastic equation for a compressible atmosphere. *J. Atmos. Sci.*, **53**, 3618–3628.

Bartello, P. & Warn, T., 1996. Self-similarity of decaying two-dimensional turbulence. *J. Fluid Mech.*, **326**, 357–372.

Batchelor, G. K., 1953a. The conditions for dynamical similarity of motions of a frictionless perfect-gas atmosphere. *Quart. J. Roy. Meteor. Soc.*, **79**, 224–235.

Batchelor, G. K., 1953b. *The Theory of Homogeneous Turbulence*. Cambridge University Press, 197 pp.

Batchelor, G. K., 1959. Small-scale variation of convected quantities like temperature in turbulent fluid. Part 1: General discussion and the case of small conductivity. *J. Fluid Mech.*, **5**, 113–133.

Batchelor, G. K., 1967. *An Introduction to Fluid Dynamics*. Cambridge University Press, 615 pp.

Batchelor, G. K., 1969. Computation of the energy spectrum in homogeneous two-dimensional turbulence. *Phys. Fluids Suppl.*, **12**, II–233—II–239.

Battisti, D. S., 1988. Dynamics and thermodynamics of a warming event in a coupled tropical atmosphere–ocean model. *J. Atmos. Sci.*, **45**, 2889–2919.

Baumert, H. Z., Simpson, J. & Sündermann, J., Eds., 2005. *Marine Turbulence: Theories, Observations and Models*. Cambridge University Press, 630 pp.

Bell, E. T., 1937. *Men of Mathematics*. Simon & Schuster, 590 pp.

Bell, M. J., 2015a. Meridional overturning circulations driven by surface wind and buoyancy forcing. *J. Phys. Oceanogr.*, **45**, 2701–2714.

Bell, M. J., 2015b. Water mass transformations driven by Ekman upwelling and surface warming in subpolar gyres. *J. Phys. Oceanogr.*, **45**, 2356–2380.

Bender, C. M. & Orszag, S. A., 1978. *Advanced Mathematical Methods for Scientists and Engineers*. McGraw-Hill, 593 pp.

Berrisford, P., Marshall, J. C. & White, A. A., 1993. Quasi-geostrophic potential vorticity in isentropic coordinates. *Quart. J. Roy. Meteor. Soc.*, **119**, 778–782.

Betts, A. K., 1973. Non-precipitating convection and its parameterization. *Quart. J. Roy. Meteor. Soc.*, **99**, 178–196.

Betts, A. K., 1986. A new convective adjustment scheme. Part I: Observational and theoretical basis. *Quart. J. Roy. Meteor. Soc.*, **112**, 677–691.

Betts, A. K. & Miller, M. J., 1986. A new convective adjustment scheme. Part II: Single column test using GATE wave, BOMEX, ATEX and Arctic air mass data sets. *Quart. J. Roy. Meteor. Soc.*, **112**, 693–709.

Birner, T., 2006. Fine-scale structure of the extratropical tropopause region. *J. Geophys. Res.*, **111**, D04104.

Birner, T., Dörnbrack, A. & Schumann, U., 2002. How sharp is the tropopause at midlatitudes? *Geophys. Res. Lett.*, **29**, 1700.

Bjerknes, J., 1919. On the structure of moving cyclones. *Geofys. Publ*, **1** (2), 1–8.

Bjerknes, J., 1937. Die Theorie der aussertropischen Zyklonenbildung (The theory of extra-tropical cyclone formation). *Meteor. Zeitschr*, **12**, 460–466.

Bjerknes, J., 1959. Atlantic air–sea interaction. In *Advances in Geophysics*, Vol. 10, pp. 1–82. Academic Press.

Bjerknes, J., 1969. Atmospheric teleconnections from the equatorial Pacific. *Mon. Wea. Rev.*, **97**, 163–172.

Bjerknes, V., 1898a. Über die Bildung von Cirkulationsbewegungen und Wirbeln in reibunglosen Flüssigkeiten (On the generation of circulation and vortices in inviscid fluids). *Skr. Nor. Vidensk.-Akad. 1: Mat.-Naturvidensk. Kl.*, **5**, 3–29.

Bjerknes, V., 1898b. Über einen hydrodynamischen Fundamentalsatz und seine Anwendung besonders auf die Mechanik der Atmosphäre und des Weltmeeres (On a fundamental principle of hydrodynamics and its application particularly to the mechanics of the atmosphere and the world's oceans). *Kongl. Sven. Vetensk. Akad. Handlingar*, **31**, 1–35.

Bjerknes, V., 1902. Cirkulation relativ zu der Erde (Circulation relative to the Earth). *Meteor. Z.*, **37**, 97–108.

Bjerknes, V., 1904. Das Problem der Wettervorhersage, betrachtet vom Standpunkte der Mechanik und der Physic (The problem of weather forecasting as a problem in mathematics and physics). *Meteor. Z.*, January, 1–7. Engl. transl.: Y. Mintz, in Shapiro and Grønas (1999), pp. 1–7.

Blumen, W., 1968. On the stability of quasi-geostrophic flow. *J. Atmos. Sci.*, **25**, 929–933.

Boccaletti, G., Pacanowski, R. C., Philander, S. G. H. & Fedorov, A. V., 2004. The thermal structure of the upper ocean. *J. Phys. Oceanogr.*, **34**, 888–902.

Boer, G. J. & Shepherd, T. G., 1983. Large-scale two-dimensional turbulence in the atmosphere. *J. Atmos. Sci.*, **40**, 164–184.

Boffetta, G. & Ecke, R. E., 2012. Two-dimensional turbulence. *Ann. Rev. Fluid Mech.*, **44**, 427–451.

Bohren, C. F. & Albrecht, B. A., 1998. *Atmospheric thermodynamics*. Oxford University Press, 416 pp.

Bolton, D., 1980. The computation of equivalent potential temperature. *Mon. Wea. Rev.*, **108**, 1046–1053.

Booker, J. R. & Bretherton, F. P., 1967. The critical layer for internal gravity waves in a shear flow. *J. Fluid Mech.*, **27**, 513–539.

Boussinesq, J., 1903. Théorie analytique de la chaleur (Analytic theory of heat). *Tome, Paris, Gauthier-Villars*, **II**, 170–172.

Box, G. E. P., 1976. Science and statistics. *J. Am. Stat. Assoc*, **71**, 791–799.

Box, G. E. P., 1979. Robustness in the strategy of scientific model building. In R. L. Launer & G. N. Wilkinson, Eds., *Robustness in Statistics*, pp. 201–236. Academic Press.

Boyd, J. P., 1976. The noninteraction of waves with the zonally averaged flow on a spherical Earth and the interrelationships of eddy fluxes of energy, heat and momentum. *J. Atmos. Sci.*, **33**, 2285–2291.

Boyd, J. P., 1978. The effects of latitudinal shear on equatorial waves. Part 1. Theory and method. *J. Atmos. Sci.*, **35**, 2236–2258.

Boyd, J. P., 1980. The nonlinear equatorial Kelvin wave. *J. Phys. Oceanogr.*, **10**, 1–11.

Branscome, L. E., 1983. The Charney baroclinic stability problem: approximate solutions and modal structures. *J. Atmos. Sci.*, **40**, 1393–1409.

Bretherton, C. S. & Schär, C., 1993. Flux of potential vorticity substance: a simple derivation and a uniqueness property. *J. Atmos. Sci.*, **50**, 1834–1836.

Bretherton, C. S. & Smolarkiewicz, P. K., 1989. Gravity waves, compensating subsidence and detrainment around cumulus clouds. *J. Atmos. Sci.*, **46**, 740–759.

Bretherton, C. S. & Sobel, A. H., 2002. A simple model of a convectively coupled Walker circulation using the weak temperature gradient approximation. *J. Climate*, **15**, 2907–2920.

Bretherton, C. S. & Sobel, A. H., 2003. The Gill model and the weak temperature gradient approximation. *J. Atmos. Sci.*, **60**, 451–460.

Bretherton, F. P., 1964. Low frequency oscillations trapped near the equator. *Tellus*, **16**, 181–185.

Bretherton, F. P., 1966a. Baroclinic instability and the short wavelength cut-off in terms of potential vorticity. *Quart. J. Roy. Meteor. Soc.*, **92**, 335–345.

Bretherton, F. P., 1966b. Critical layer instability in baroclinic flows. *Quart. J. Roy. Meteor. Soc.*, **92**, 325–334.

Bretherton, F. P., 1969. Momentum transport by gravity waves. *Quart. J. Roy. Meteor. Soc.*, **95**, 213–243.

Brewer, A. W., 1949. Evidence for a world circulation provided by the measurements of helium and water vapour distribution in the stratosphere. *Quart. J. Roy. Meteor. Soc.*, **75**, 251–363.

Brillouin, L., 1926. La mécanique ondulatoire de Schrödinger; une méthode générale de resolution par approximations successives (The wave mechanics of Schrödinger: a general method of solution by successive approximation). *Comptes Rendus*, **183**, 24–26.

Browning, G., Kreiss, H. & Schubert, W., 2000. The role of gravity waves in slowly varying in time tropospheric motions near the equator. *J. Atmos. Sci.*, **57**, 4008–4019.

Bryan, F., 1986. High-latitude salinity effects and interhemispheric thermohaline circulations. *Nature*, **323**, 301–304.

Bryden, H. & Brady, E. C., 1985. Diagnostic study of the three-dimensional circulation of the upper equatorialPacific Ocean. *J. Phys. Oceanogr.*, **15**, 1255–1273.

Buchanan, J. Y., 1886. On the similarities in the physical geography of the great oceans. *Proc. Roy. Geogr. Soc.*, **8**, 753–770.

Bühler, O., 2009. *Waves and Mean Flows*. Cambridge University Press, 370 pp.

Burger, A., 1958. Scale considerations of planetary motions of the atmosphere. *Tellus*, **10**, 195–205.

Burke, A., Stewart, A. L., Adkins, J. F., Ferrari, R. *et al.*, 2015. The glacial mid-depth radiocarbon bulge and its implications for the overturning circulation. *Paleoceanog.*, **30**, 1021–1039.

Caballero, R., 2014. *Physics of the Atmosphere*. IOP Publishing, 132 pp.

Callen, H. B., 1985. *Thermodynamics and an Introduction to Themostatistics*. John Wiley & Sons, 493 pp.

Cane, M. A., 1979a. The response of an equatorial ocean to simple wind stress patterns: I. Model formulation and analytic results. *J. Mar. Res.*, **37**, 232–252.

Cane, M. A., 1979b. The response of an equatorial ocean to simple wind stress patterns: II. Numerical results. *J. Mar. Res.*, **37**, 355–398.

Cane, M. A. & Zebiak, S. E., 1985. A theory for El Niño and the Southern Oscillation. *Science*, **228**, 1084–1087.

Carillo, C. N., 1892. Desertacion sobre las corrientes y estudios de la corriente Peruana de Humboldt. (Dissertation on currents and studies of the Peruvian Humboldt current). *Bol. Soc. Geogr. Lima*, **11**, 72–110.

Carlini, F., 1837. Ricerche sulla convergenza della serie che serva alla soluzione del problema di Keplero (Research on the convergence of series for the solution of Kepler's problem). Milan.

Cessi, P., 2001. Thermohaline circulation variability. In *Conceptual Models of the Climate, Woods Hole Program in Geophysical Fluid Dynamics* (2001). Also available from http://gfd.whoi.edu/proceedings/2001/PDFvol2001.html.

Cessi, P. & Fantini, M., 2004. The eddy-driven thermocline. *J. Phys. Oceanogr.*, **34**, 2642–2658.

Cessi, P. & Young, W. R., 1992. Multiple equilibria in two-dimensional thermohaline circulation. *J. Fluid Mech.*, **241**, 291–309.

Chai, J., 2016. Understanding geostrophic turbulence in a hierarchy of models. Ph. D thesis, Princeton University.

Chandrasekhar, S., 1961. *Hydrodynamic and Hydromagnetic Stability*. Oxford University Press, 652 pp. Reprinted by Dover Publications, 1981.

Chang, E. K. M. & Orlanski, I., 1994. On energy flux and group velocity of waves in baroclinic flows. *J. Atmos. Sci.*, **51**, 3823–3828.

Chang, P., Ji, L., Li, H. & Flügel, M., 1996. Chaotic dynamics versus stochastic processes in El Niño–Southern Oscillation in coupled ocean–atmosphere models. *Physica D*, **98**, 301–320.

Chapman, D. C., Malanotte-Rizzoli, P. & Hendershott, M., 1989. Wave motions in the ocean. Unpublished notes based on lectures by Myrl Hendershott.

Chapman, S. & Lindzen, R. S., 1970. *Atmospheric Tides*. Gordon and Breach, 200 pp.

Charlton, A. J. & Polvani, L. M., 2007. A new look at stratospheric sudden warmings. Part I: Climatology and modeling benchmarks. *J. Climate*, **20**, 449–469.

Charlton, A. J., Polvani, L. M., Perlwitz, J., Sassi, F. *et al.*, 2007. A new look at stratospheric sudden warmings. Part II: Evaluation of numerical model simulations. *J. Climate*, **20**, 470–488.

Charney, J. G., 1947. The dynamics of long waves in a baroclinic westerly current. *J. Meteor.*, **4**, 135–162.

Charney, J. G., 1948. On the scale of atmospheric motion. *Geofys. Publ. Oslo*, **17** (2), 1–17.

Charney, J. G., 1955. The Gulf Stream as an inertial boundary layer. *Proc. Nat. Acad. Sci.*, **41**, 731–740.

Charney, J. G., 1960. Non-linear theory of a wind-driven homogeneous layer near the equator. *Deep-Sea Res.*, **6**, 303–310.

Charney, J. G., 1963. A note on large-scale motions in the tropics. *J. Atmos. Sci.*, **20**, 607–609.

Charney, J. G., 1971. Geostrophic turbulence. *J. Atmos. Sci.*, **28**, 1087–1095.

Charney, J. G. & Drazin, P. G., 1961. Propagation of planetary scale disturbances from the lower into the upper atmosphere. *J. Geophys. Res.*, **66**, 83–109.

Charney, J. G. & Eliassen, A., 1949. A numerical method for predicting the perturbations of the mid-latitude westerlies. *Tellus*, **1**, 38–54.

Charney, J. G. & Eliassen, A., 1964. On the growth of the hurricane depression. *J. Atmos. Sci.*, **21**, 68–75.

Charney, J. G., Fjørtoft, R. & Neumann, J. V., 1950. Numerical integration of the barotropic vorticity equation. *Tellus*, **2**, 237–254.

Charney, J. G. & Stern, M. E., 1962. On the stability of internal baroclinic jets in a rotating atmosphere. *J. Atmos. Sci.*, **19**, 159–172.

Charnock, H., Green, J., Ludlam, F., Scorer, R. & Sheppard, P., 1966. Dr. E. T. Eady, B. A. (Obituary). *Quart. J. Roy. Meteor. Soc.*, **92**, 591–592.

Chasnov, J. R., 1991. Simulation of the inertial-conductive subrange. *Phys. Fluids A*, **3**, 1164–1168.

Chelton, D. B., de Szoeke, R. A., Schlax, M. G., Naggar, K. E. & Siwertz, N., 1998. Geographical variability of the first-baroclinic Rossby radius of deformation. *J. Phys. Oceanogr.*, **28**, 433–460.

Christiansen, B., 1999. Stratospheric vacillations in a general circulation model. *J. Atmos. Sci.*, **56**, 1858–1872.

Christiansen, B., 2000. Chaos, quasiperiodicity, and interannual variability: studies of a stratospheric vacillation model. *J. Atmos. Sci.*, **57**, 3161–3173.

Clarke, A. J., 2008. *An Introduction to the Dynamics of El Niño and the Southern Oscillation*. Elsevier, 308 pp.

Clarke, A. J., Van Gorder, S. & Colantuono, G., 2007. Wind stress curl and ENSO discharge/recharge in the equatorial Pacific. *J. Phys. Oceanogr.*, **37**, 1077–1091.

Colin de Verdière, A., 1980. Quasi-geostrophic turbulence in a rotating homogeneous fluid. *Geophys. Astrophys. Fluid Dyn.*, **15**, 213–251.

Colin de Verdière, A., 1989. On the interaction of wind and buoyancy driven gyres. *J. Mar. Res.*, **47**, 595–633.

Conkright, M. E., Antonov, J., Baranova, O., Boyer, T. P. *et al.*, 2001. World ocean database 2001, vol. 1. In S. Levitus, Ed., *NOAA Atlas NESDIS 42*, pp. 167. US Government Printing Office, Washington DC.

Coriolis, G. G., 1832. Mémoire sur le principe des forces vives dans les mouvements relatifs des machines (On the principle of kinetic energy in the relative movement of machines). *J. Ec. Polytech*, **13**, 268–301.

Coriolis, G. G., 1835. Mémoire sur les équations du mouvement relatif des systèmes de corps (On the equations of relative motion of a system of bodies). *J. Ec. Polytech*, **15**, 142–154.

Corrsin, S., 1951. On the spectrum of isotropic temperature fluctuations in an isotropic turbulence. *J. Appl. Phys.*, **22**, 469–473. Erratum: *J. Appl. Phys.* **22,** 1292, (1951).

Craig, G. C. & Gray, S. L., 1996. CISK or WISHE as the mechanism for tropical cyclone intensification. *J. Atmos. Sci.*, **53**, 3528–3540.

Cressman, G. P., 1996. The origin and rise of numerical weather prediction. In J. R. Fleming, Ed., *Historical Essays on Meteorology 1919–1995*, pp. 617. American Meteorological Society.

Cromwell, T., 1953. Circulation in a meridional plane in the central equatorial Pacific. *J. Mar. Res.*, **12**, 196–213.

Da Vinci, L., 1500. *The notebooks of Leonardo da Vinci*, Vol. 2. J. P. Richter, Ed. Dover Publications, 1970.

Danielsen, E. F., 1990. In defense of Ertel's potential vorticity and its general applicability as a meteorological tracer. *J. Atmos. Sci.*, **47**, 2353–2361.

Danilov, S. & Gryanik, V., 2002. Rhines scale and spectra of the β-plane turbulence with bottom drag. *Phys. Rev. E*, **65**, 067301–1–067301–3.

Danilov, S. & Gurarie, D., 2001. Quasi-two-dimensional turbulence. *Usp. Fiz. Nauk.*, **170**, 921–968.

Davidson, P., 2015. *Turbulence: An Introduction for Scientists and Engineers*. Oxford University Press, 688 pp.

Davies-Jones, R., 2003. Comments on "A generalization of Bernoulli's theorem". *J. Atmos. Sci.*, **60**, 2039–2041.

Davis, R. E., de Szoeke, R., Halpern, D. & Niiler, P., 1981. Variability in the upper ocean during MILE. Part I: The heat and momentum balances. *Deep-Sea Res.*, **28**, 1427–1452.

De Morgan, A., 1872. *A Budget of Paradoxes*. Thoemmmes Continuum, 814 pp.

de Szoeke, R. & Bennett, A. F., 1993. Microstructure fluxes across density surfaces. *J. Phys. Oceanogr.*, **24**, 2254–2264.

de Szoeke, R. A., 2000. Equations of motion using thermodynamic coordinates. *J. Phys. Oceanogr.*, **30**, 2814–2829.

de Szoeke, R. A., 2004. An effect of the thermobaric nonlinearity of the equation of state: A mechanism for sustaining solitary Rossby waves. *J. Phys. Oceanogr.*, **34**, 2042–2056.

Dee, D., Uppala, S., Simmons, A., Berrisford, P. *et al.*, 2011. The ERA-interim reanalysis: Configuration and performance of the data assimilation system. *Quart. J. Roy. Meteor. Soc.*, **137**, 553–597.

Defant, A., 1921. Die Zirkulation der Atmosphäre in den gemäßigten Breiten der Erde. Grundzüge einer Theorie der Klimaschwankungen (The circulation of the atmosphere in the Earth's mid-latitudes. Basic features of a theory of climate fluctuations). *Geograf. Ann.*, **3**, 209–266.

Dellar, P. J., 2011. Variations on a beta-plane: derivation of non-traditional beta-plane equations from Hamilton's principle on a sphere. *J. Fluid Mech.*, **674**, 174–195.

Dewar, W. K. & Huang, R. X., 1995. Fluid flow in loops driven by freshwater and heat fluxes. *J. Fluid Mech.*, **297**, 153–191.

Dewar, W. K., Samelson, R. S. & Vallis, G. K., 2005. The ventilated pool: a model of subtropical mode water. *J. Phys. Oceanogr.*, **35**, 137–150.

Dias, J. & Kiladis, G. N., 2014. Influence of the basic state zonal flow on convectively coupled equatorial waves. *Geophys. Res. Lett.*, **41**, 6904–6913.

Dickinson, R. E., 1968. Planetary Rossby waves propagating vertically through weak westerly wind wave guides. *J. Atmos. Sci.*, **25**, 984–1002.

Dickinson, R. E., 1969. Theory of planetary wave–zonal flow interaction. *J. Atmos. Sci.*, **26**, 73–81.

Dickinson, R. E., 1980. Planetary waves: theory and observation. In *Orographic Effects on Planetary Flows*, Number 23 in GARP Publication Series. World Meteorological Organization.

Dijkstra, H. A., 2008. *Dynamical Oceanography*. Springer, 407 pp.

Dima, I. & Wallace, J. M., 2003. On the seasonality of the Hadley Cell. *J. Atmos. Sci.*, **60**, 1522–1527.

Dobson, G. M. B., 1956. Origin and distribution of the polyatomic molecules in the atmosphere. *Proc. Roy. Soc. Lond. A*, **236**, 187–193.

Döös, K. & Coward, A., 1997. The Southern Ocean as the major upwelling zone of the North Atlantic. *Int. WOCE Newsletter* 27, 3–4.

Drazin, P. G. & Reid, W. H., 1981. *Hydrodynamic Stability*. Cambridge University Press, 527 pp.

Drijfhout, S. S. & Hazeleger, W., 2001. Eddy mixing of potential vorticity versus temperature in an isopycnic ocean model. *J. Phys. Oceanogr.*, **31**, 481–505.

Dritschel, D. & McIntyre, M., 2008. Multiple jets as PV staircases: The Phillips effect and the resilience of eddy-transport barriers. *J. Atmos. Sci.*, **65**, 855–874.

Dunkerton, T., Hsu, C.-P. & McIntrye, M. E., 1981. Some Eulerian and Lagrangian diagnostics for a model stratosphere warming. *JAS*, **38**, 819–843.

Dunkerton, T. J., 1980. A Lagrangian-mean theory of wave, mean-flow interaction with applications to non-acceleration and its breakdown. *Rev. Geophys. Space Phys.*, **18**, 387–400.

Dunkerton, T. J., 1982. Shear zone asymmetry in the observed and simulated quasi-biennial oscillation. *J. Atmos. Sci.*, **38**, 461–469.

Dunkerton, T. J., 1997. The role of gravity waves in the quasi-biennial oscillation. *JGR*, **102**, 26053–26076.

Dunkerton, T. J., Delisi, D. P. & Baldwin, M. P., 1988. Distribution of major stratospheric warmings in relation to the quasi-biennial oscillation. *Geophys. Res. Lett.*, **115**, 136–139.

Durran, D. R., 1989. Improving the anelastic approximation. *J. Atmos. Sci.*, **46**, 1453–1461.

Durran, D. R., 1990. Mountain waves and downslope winds. *Meteor. Monogr.*, **23**, 59–81.

Durran, D. R., 1993. Is the Coriolis force really responsible for the inertial oscillations? *Bull. Am. Meteor. Soc.*, **74**, 2179–2184.

Durran, D. R., 2015. Lee waves and mountain waves. *Encycl. Atmos. Sci.*, 2nd edn, **4**, 95–102.

Durst, C. S. & Sutcliffe, R. C., 1938. The effect of vertical motion on the "geostrophic departure" of the wind. *Quart. J. Roy. Meteor. Soc.*, **64**, 240.

Dutton, J. A., 1986. *The Ceaseless Wind: An Introduction to the Theory of Atmospheric Motion*. Dover Publications, 617 pp.

Eady, E. T., 1949. Long waves and cyclone waves. *Tellus*, **1**, 33–52.

Eady, E. T., 1950. The cause of the general circulation of the atmosphere. In *Cent. Proc. Roy. Meteor. Soc.* (1950), pp. 156–172.

Eady, E. T., 1954. The maintenance of the mean zonal surface currents. *Proc. Toronto Meteor. Conf. 1953*, **138**, 124–128. Royal Meteorological Society.

Eady, E. T., 1957. The general circulation of the atmosphere and oceans. In D. R. Bates, Ed., *The Earth and its Atmosphere*, pp. 130–151. New York, Basic Books.

Eady, E. T. & Sawyer, J. S., 1951. Dynamics of flow patterns in extra-tropical regions. *Quart. J. Roy. Meteor. Soc.*, **77**, 531–551.

Ebdon, R. A., 1960. Notes on the wind flow at 50 mb in tropical and subtropical regions in January 1957 and in 1960. *Quart. J. Roy. Meteor. Soc.*, **86**, 540–542.

Eden, C. & Willebrand, J., 1999. Neutral density revisited. *Deep Sea Res., Part II*, **46**, 33–54.

Edmon, H. J., Hoskins, B. J. & McIntyre, M. E., 1980. Eliassen–Palm cross sections for the troposphere. *J. Atmos. Sci.*, **37**, 2600–2616.

Egger, J., 1976. Linear response of a two-level primitive equation model to forcing by topography. *Mon. Wea. Rev.*, **104**, 351–364.

Ekman, V. W., 1905. On the influence of the Earth's rotation on ocean currents. *Arch. Math. Astron. Phys.*, **2**, 1–52.

Eliassen, A. & Palm, E., 1961. On the transfer of energy in stationary mountain waves. *Geofys. Publ.*, **22**, 1–23.

Eluszkiewicz, J., Crisp, D., Grainger, R. G., Lambert, A. *et al.*, 1997. Sensitivity of the residual circulation diagnosed from the UARS data to the uncertainties in the input fields and to the inclusion of aerosols. *J. Atmos. Sci.*, **54**, 1739–1757.

Emanuel, K., 2007. Quasi-equilibrium dynamics of the tropical atmosphere. In T. Schneider & A. Sobel, Eds., *The Global Circulation of the Atmosphere: Phenomena, Theory, Challenges*, pp. 143–185. Princeton University Press.

Emanuel, K. A., 1987. An air-sea interaction model of intraseasonal oscillations in the tropics. *J. Atmos. Sci.*, **44**, 2324–2340.

Emanuel, K. A., 1994. *Atmospheric Convection*. Oxford University Press, 580 pp.

Emanuel, K. A., 2011. Edward Norton Lorenz, 1917–2008. In *Biog. Memoirs*, pp. 1–28. Nat'l. Acad. Sci.

Emanuel, K. A., Neelin, J. D. & Bretherton, C. S., 1994. On large-scale circulations in convecting atmospheres. *Quart. J. Roy. Meteor. Soc.*, **120**, 1111–1143.

Er-El, J. & Peskin, R., 1981. Relative diffusion of constant-level balloons in the Southern Hemisphere. *J. Atmos. Sci.*, **38**, 2264–2274.

Ertel, H., 1942a. Ein neuer hydrodynamischer Wirbelsatz (A new hydrodynamic eddy theorem). *Meteorol. Z.*, **59**, 277–281.

Ertel, H., 1942b. Über des Verhältnis des neuen hydrodynamischen Wirbelsatzes zum Zirculationssatz von V. Bjerknes (On the relationship of the new hydrodynamic eddy theorem to the circulation theorem of V. Bjerknes). *Meteorol. Z.*, **59**, 385–387.

Ertel, H. & Rossby, C.-G., 1949a. Ein neuer Erhaltungs-satz der Hydrodynamik (A new conservation theorem of hydrodynamics). *Sitzungsber. d. Deutschen Akad. Wissenschaften Berlin*, **1**, 3–11.

Ertel, H. & Rossby, C.-G., 1949b. A new conservation theorem of hydrodynamics. *Geofis. Pura Appl.*, **14**, 189–193.

Fang, M. & Tung, K. K., 1996. A simple model of nonlinear Hadley circulation with an ITCZ: analytic and numerical solutions. *J. Atmos. Sci.*, **53**, 1241–1261.

Fang, M. & Tung, K. K., 1999. Time-dependent nonlinear Hadley circulation. *J. Atmos. Sci.*, **56**, 1797–1807.

Farrell, B., 1984. Modal and non-modal baroclinic waves. *J. Atmos. Sci.*, **41**, 668–673.

Farrell, B. & Ioannou, P. J., 1995. Stochastic dynamics of the midlatitude atmospheric jet. *J. Atmos. Sci.*, **52**, 1642–1656.

Farrell, B. F. & Ioannou, P. J., 1996. Generalized stability theory. Part I: autonomous operators. *J. Atmos. Sci.*, **53**, 2025–2040.

Farrell, B. F. & Ioannou, P. J., 2008. Formation of jets by baroclinic turbulence. *J. Atmos. Sci.*, **65**, 3353–3375.

Feistel, R., 2008. A Gibbs function for seawater thermodynamics for −6° C to 80° C and salinity up to 120 g kg^{-1}. *Deep-Sea Res.*, **55**, 1639–1671.

Feistel, R., Wright, D., Kretzschmar, H.-J., Hagen, E. *et al.*, 2010. Thermodynamic properties of sea air. *Oce. Sci.*, **6**, 91–141.

Ferrari, R., Griffies, S. M., Nurser, G. & Vallis, G. K., 2010. A boundary-value problem for the parameterized mesoscale eddy transport. *Oce. Model.*, **32**, 143–156.

Ferrari, R., Jansen, M. F., Adkins, J. F., Burke, A. *et al.*, 2014. Antarctic sea ice control on ocean circulation in present and glacial climates. *Proceedings of the National Academy of Sciences*, **111**, 8753–8758.

Ferrel, W., 1856a. An essay on the winds and currents of the ocean. *Nashville J. Med. & Surg.*, **11**, 287–301.

Ferrel, W., 1856b. The problem of the tides. *Astron. J*, **4**, 173–176.

Ferrel, W., 1858. The influence of the Earth's rotation upon the relative motion of bodies near its surface. *Astron. J.*, **V**, No. 13 (109), 97–100.

Ferrel, W., 1859. The motion of fluids and solids relative to the Earth's surface. *Math. Monthly*, **1**, 140–148, 210–216, 300–307, 366–373, 397–406.

Fjørtoft, R., 1950. Application of integral theorems in deriving criteria for laminar flows and for the baroclinic circular vortex. *Geophys. Publ.*, **17**, 1–52.

Fjørtoft, R., 1953. On the changes in the spectral distribution of kinetic energy for two-dimensional nondivergent flow. *Tellus*, **5**, 225–230.

Fleming, E. L., Chandra, S., Schoeberl, M. R. & Barnett, J. J., 1988. Monthly mean global climatology of temperature, wind, geopotential height, and pressure for 0-120 km. Technical report, NASA/Goddard Space Flight Center, Greenbelt, MD. NASA Tech. Memo. 100697.

Fofonoff, N. P., 1954. Steady flow in a frictionless homogeneous ocean. *J. Mar. Res.*, **13**, 254–262.

Fofonoff, N. P., 1959. Interpretation of oceanographic measurements – thermodynamics. In *Physical and Chemical Properties of Sea Water*, Vol. 600. Nat. Acad. Sci., Nat. Res. Counc., Publ.

Fofonoff, N. P. & Montgomery, R. B., 1955. The equatorial undercurrent in the light of the vorticity equation. *Tellus*, **7**, 518–521.

Fox-Kemper, B. & Pedlosky, J., 2004. Wind-driven barotropic gyre I: Circulation control by eddy vorticity fluxes to an enhanced removal region. *J. Mar. Res.*, **62**, 169–193.

Franklin, W. S., 1898. Review of P. Duhem, *Traité Elementaire de Méchanique Chimique fondée sur la Thermodynamique*, Two volumes. Paris, 1897. *Phys. Rev.*, **6**, 170–175.

Friedman, R. M., 1989. *Appropriating the Weather: Vilhelm Bjerknes and the Construction of a Modern Meteorology*. Cornell University Press, 251 pp.

Frierson, D. M. W., Lu, J. & Chen, G., 2007. Width of the Hadley cell in simple and comprehensive general circulation models. *Geophys. Res. Lett.*, **34**, L18804.

Fu, L. L. & Flierl, G. R., 1980. Nonlinear energy and enstrophy transfers in a realistically stratified ocean. *Dyn. Atmos. Oceans*, **4**, 219–246.

Gage, K. S. & Nastrom, G. D., 1986. Theoretical interpretation of atmospheric wavenumber spectra of wind and temperature observed by commercial aircraft during GASP. *J. Atmos. Sci.*, **43**, 729–740.

Galanti, E. & Tziperman, E., 2000. Enso's phase locking to the seasonal cycle in the fast-SST, fast-wave, and mixed-mode regimes. *J. Atmos. Sci.*, **57**, 2936–2950.

Galperin, B. & Read, P. L., Eds., 2017. *Zonal Jets: Phenomenology, Genesis, Physics*. Cambridge University Press, 431 pp.

Galperin, B., Sukoriansky, S. & Dikovskaya, N., 2010. Geophysical flows with anisotropic turbulence and dispersive waves: flows with a β-effect. *Ocean Dynamics*, **60**, 427–441.

Galperin, B., Sukoriansky, S., Dikovskaya, N., Read, P. *et al.*, 2006. Anisotropic turbulence and zonal jets in rotating flows with a β-effect. *Nonlinear Proc. Geophys.*, **13**, 83–98.

Garcia, R. R., 1987. On the mean meridional circulation of the stratosphere. *J. Atmos. Sci.*, **44**, 2599–2609.

Gardiner, C. W., 1985. *Handbook of Stochastic Methods*. Springer-Verlag, 442 pp.

Gent, P. R. & McWilliams, J. C., 1990. Isopycnal mixing in ocean circulation models. *J. Phys. Oceanogr.*, **20**, 150–155.

Gent, P. R., Willebrand, J., McDougall, T. J. & McWilliams, J. C., 1995. Parameterizing eddy-induced transports in ocean circulation models. *J. Phys. Oceanogr.*, **25**, 463–474.

Gierasch, P. J., 1975. Meridional circulation and the maintenance of the Venus atmospheric rotation. *J. Atmos. Sci.*, **32**, 1038–1044.

Gill, A. E., 1971. The equatorial current in a homogeneous ocean. *Deep-Sea Res.*, **18**, 421–431.

Gill, A. E., 1975. Models of equatorial currents. In *Proceedings of Numerical Models of Ocean Circulation*, pp. 181–203. National Academy of Science.

Gill, A. E., 1980. Some simple solutions for heat induced tropical circulation. *Quart. J. Roy. Meteor. Soc.*, **106**, 447–462.

Gill, A. E., 1982. *Atmosphere–Ocean Dynamics*. Academic Press, 662 pp.

Gill, A. E. & Clarke, A. J., 1974. Wind-induced upwelling, coastal currents and sea-level changes. *Deep-Sea Res.*, **21**, 325–345.

Gill, A. E., Green, J. S. A. & Simmons, A. J., 1974. Energy partition in the large-scale ocean circulation and the production of mid-ocean eddies. *Deep-Sea Res.*, **21**, 499–528.

Gille, S. T., 1997. The Southern Ocean momentum balance: evidence for topographic effects from numerical model output and altimeter data. *J. Phys. Oceanogr.*, **27**, 2219–2232.

Gilman, P. A. & Glatzmaier, G. A., 1981. Compressible convection in a rotating spherical shell. I. Anelastic equations. *Astrophys. J. Suppl. Ser.*, **45**, 335–349.

Giorgetta, M. A., Manzini, E. & Roeckner, E., 2002. Forcing of the quasi-biennial oscillation from a broad spectrum of atmospheric waves. *Geophys. Res. Lett.*, **29**, 1245.

Gnanadesikan, A., 1999. A simple predictive model for the structure of the oceanic pycnocline. *Science*, **283**, 2077–2079.

Godske, C. L., Bergeron, T., Bjerknes, J. & Budgaard, R. C., 1957. *Dynamic Meteorology and Weather Forecasting*. American Meteorological Society, 864 pp.

Goody, R. M. & Yung, Y. L., 1995. *Atmospheric radiation: theoretical basis*. Oxford University Press, 544 pp.

Gough, D. O., 1969. The anelastic approximation for thermal convection. *J. Atmos. Sci.*, **216**, 448–456.

Graham, F. S. & McDougall, T. J., 2013. Quantifying the nonconservative production of conservative temperature, potential temperature and entropy. *J. Phys. Oceanogr.*, **43**, 838–862.

Grant, H. L., Hughes, B. A., Vogel, W. M. & Moilliet, A., 1968. The spectrum of temperaure fluctuation in turbulent flow. *J. Fluid Mech.*, **344**, 423–442.

Grant, H. L., Stewart, R. W. & Moilliet, A., 1962. Turbulent spectra from a tidal channel. *J. Fluid Mech.*, **12**, 241–268.

Gray, D. D. & Giorgini, A., 1976. The validity of the Boussinesq approximation for liquids and gases. *Int. J. Heat and Mass Transfer*, **19**, 545–551.

Gray, L. J., 2010. Stratospheric equatorial dynamics. In *The Stratosphere: Dynamics, Transport, and Chemistry*, Geophys. Monogr. Ser, Vol. 190 (2010).

Gray, L. J., Crooks, S., Pascoe, C. & Palmer, M., 2001. Solar and QBO influences on the timing of stratospheric sudden warmings. *J. Atmos. Sci.*, **61**, 2777–2796.

Gray, L. J., Phipps, S. J., Dunkerton, T. J., Baldwin, M. P. *et al.*, 2001. A data study of the influence of the upper stratosphere on northern hemisphere stratospheric warmings. *Quart. J. Roy. Meteor. Soc.*, **127**, 1985–2003.

Greatbatch, R. J., 1998. Exploring the relationship between eddy-induced transport velocity, vertical momentum transfer, and the isopycnal flux of potential vorticity. *J. Phys. Oceanogr.*, **28**, 422–432.

Green, G., 1837. On the motion of waves in a variable canal of small depth and width. *Trans. Camb. Phil. Soc.*, **6**, 457–462.

Green, J. S. A., 1960. A problem in baroclinic stability. *Quart. J. Roy. Meteor. Soc.*, **86**, 237–251.

Green, J. S. A., 1970. Transfer properties of the large-scale eddies and the general circulation of the atmosphere. *Quart. J. Roy. Meteor. Soc.*, **96**, 157–185.

Green, J. S. A., 1977. The weather during July 1976: some dynamical considerations of the drought. *Weather*, **32**, 120–128.

Green, J. S. A., 1999. *Atmospheric Dynamics*. Cambridge University Press, 213 pp.

Greenspan, H., 1962. A criterion for the existence of inertial boundary layers in oceanic circulation. *Proc. Nat. Acad. Sci.*, **48**, 2034–2039.

Gregg, M. C., 1998. Estimation and geography of diapycnal mixing in the stratified ocean. In J. Imberger, Ed., *Physical Processes in Lakes and Oceans*, pp. 305–338. American Geophysical Union.

Griffies, S. M., 1998. The Gent–McWilliams skew flux. *J. Phys. Oceanogr.*, **28**, 831–841.

Griffies, S. M., 2004. *Fundamentals of Ocean Climate Models*. Princeton University Press, 518 pp.

Grose, W. & Hoskins, B., 1979. On the influence of orography on large-scale atmospheric flow. *J. Atmos. Sci.*, **36**, 223–234.

Hadley, G., 1735. Concerning the cause of the general trade-winds. *Phil. Trans. Roy. Soc.*, **29**, 58–62.

Haine, T. W. N. & Marshall, J., 1998. Gravitational, symmetric, and baroclinic instability of the ocean mixed layer. *J. Phys. Oceanogr.*, **28**, 634–658.

Hallberg, R. & Gnanadesikan, A., 2001. An exploration of the role of transient eddies in determining the transport of a zonally reentrant current. *J. Phys. Oceanogr.*, **31**, 3312–3330.

Hamilton, K., Wilson, R. J. & Hemler, R. S., 2001. Spontaneous QBO-like oscillations simulated by the GFDL SKYHI general circulation mode. *J. Atmos. Sci.*, **58**, 3271–3292.

Hamilton, K. P., 1998. Dynamics of the tropical middle atmosphere: a tutorial review. *Atmosphere–Ocean*, **36**, 319–354.

Haney, R. L., 1971. Surface thermal boundary condition for ocean circulation models. *J. Phys. Oceanogr.*, **1**, 241–248.

Harnik, N. & Heifetz, E., 2007. Relating overreflection and wave geometry to the counterpropagating Rossby wave perspective: Toward a deeper mechanistic understanding of shear instability. *J. Atmos. Sci.*, **64**, 7, 2238–2261.

Haurwitz, B., 1941. *Dynamic meteorology*. Haurwitz press, 380 pp. Reprinted in 2007.

Hayes, M., 1977. A note on group velocity. *Proc. Roy. Soc. Lond. A*, **354**, 533–535.

Haynes, P., 2005. Stratospheric dynamics. *Ann. Rev. Fluid Mech.*, **37**, 263–293.

Haynes, P. H., 2015. Critical layers. *Encycl. Atmos. Sci.*, 2nd edn, **2**, 317–323.

Haynes, P. H., Marks, C. J., McIntyre, M. E., Shepherd, T. G. & Shine, K. P., 1991. On the "downward control" of extratropical diabatic circulations by eddy-induced mean zonal forces. *J. Atmos. Sci.*, **48**, 651–678.

Haynes, P. H. & McIntyre, M. E., 1987. On the evolution of vorticity and potential vorticity in the presence of diabatic heating and frictional or other forces. *J. Atmos. Sci.*, **44**, 828–841.

Haynes, P. H. & McIntyre, M. E., 1990. On the conservation and impermeability theorem for potential vorticity. *J. Atmos. Sci.*, **47**, 2021–2031.

Heckley, W. & Gill, A., 1984. Some simple analytical solutions to the problem of forced equatorial long waves. *Quart. J. Roy. Meteor. Soc.*, **110**, 203–217.

Heifetz, E. & Caballero, R., 2014. An alternative view on the role of the β-effect in the Rossby wave propagation mechanism. *Tellus A*, **66**, 1–6.

Held, I. M., 1982. On the height of the tropopause and the static stability of the troposphere. *J. Atmos. Sci.*, **39**, 412–417.

Held, I. M., 1983. Stationary and quasi-stationary eddies in the extratropical troposphere: theory. In B. Hoskins & R. P. Pearce, Eds., *Large-Scale Dynamical Processes in the Atmosphere*, pp. 127–168. Academic Press.

Held, I. M., 1985. Pseudomomentum and the orthogonality of modes in shear flows. *J. Atmos. Sci.*, **42**, 2280–2288.

Held, I. M., 2000. The general circulation of the atmosphere. In *Woods Hole Program in Geophysical Fluid Dynamics* (2000), pp. 66.

Held, I. M. & Hou, A. Y., 1980. Nonlinear axially symmetric circulations in a nearly inviscid atmosphere. *J. Atmos. Sci.*, **37**, 515–533.

Held, I. M. & Larichev, V. D., 1996. A scaling theory for horizontally homogeneous, baroclinically unstable flow on a beta-plane. *J. Atmos. Sci.*, **53**, 946–952.

Held, I. M., Tang, M. & Wang, H., 2002. Northern winter stationary waves: theory and modeling. *J. Climate*, **15**, 2125–2144.

Helmholtz, H., 1858. Über Integrale der hydrodynamischen Gleichungen welche den Wirbelbewengungen entsprechen (On the integrals of the hydrodynamic equations that correspond to eddy motion). *J. Reine Angew. Math*, **25**, 25–55. Engl. transl.: C. Abbe, *Smithson. Misc. Collect.*, no. 34, pp. 78–93, Smithsonian Institution, Washington DC, 1893.

Helmholtz, H., 1868. Über discontinuirliche Flüssigkeitsbewegungen (On discontinuous liquid motion). *Monats. Königl. Preuss. Akad. Wiss. Berlin*, **23**, 215–228. Engl. trans.: F. Guthrie: On discontinuous movements of fluids. *Phil. Mag.*, **36**, 337–346 (1868).

Hendershott, M., 1987. Single layer models of the general circulation. In H. Abarbanel & W. R. Young, Eds., *General Circulation of the Ocean*, pp. 202–267. Springer-Verlag.

Henning, C. C. & Vallis, G. K., 2004. The effect of mesoscale eddies on the main subtropical thermocline. *J. Phys. Oceanogr.*, **34**, 2428–2443.

Henning, C. C. & Vallis, G. K., 2005. The effects of mesoscale eddies on the stratification and transport of an ocean with a circumpolar channel. *J. Phys. Oceanogr.*, **35**, 880–896.

Hide, R., 1969. Dynamics of the atmospheres of major planets with an appendix on the viscous boundary layer at the rigid boundary surface of an electrically conducting rotating fluid in the presence of a magnetic field. *J. Atmos. Sci.*, **26**, 841–853.

Hilborn, R. C., 2004. Sea-gulls, butterflies, and grasshoppers: a brief history of the butterfly effect in nonlinear dynamics. *Am. J. Phys.*, **72**, 425–427.

Hirst, A. C., 1986. Unstable and damped equatorial modes in simple coupled ocean–atmosphere models. *J. Atmos. Sci.*, **43**, 606–632.

Hockney, R., 1970. The potential calculation and some applications. In *Methods of Computational Physics*, Vol. 9, pp. 135–211. Academic Press.

Hogg, N., 2001. Quantification of the deep circulation. In G. Siedler, J. Church, & J. Gould, Eds., *Ocean Circulation and Climate: Observing and Modelling the Global Ocean*, pp. 259–270. Academic Press.

Hoinka, K. P., 1997. The tropopause: discovery, definition and demarcation. *Meteorol. Z.*, **6**, 281–303.

Holland, W. R., Keffer, T. & Rhines, P. B., 1984. Dynamics of the oceanic circulation: The potential vorticity field. *Nature*, **308**, 698–705.

Holloway, G. & Hendershott, M. C., 1977. Stochastic closure for nonlinear Rossby waves. *J. Fluid Mech.*, **82**, 747–765.

Holm, D. D., Marsden, J. E., Ratiu, T. & Weinstein, A., 1985. Nonlinear stability of fluid and plasma equilibria. *Phys. Rep.*, **123**, 1–116.

Holmes, M. H., 2013. *Introduction to Perturbation Methods*. 2nd edn. Springer, 436 pp.

Holton, J. R., 1974. Forcing of mean flows by stationary waves. *J. Atmos. Sci.*, **31**, 942–945.

Holton, J. R., 1992. *An Introduction to Dynamic Meteorology*. 3rd edn. Academic Press, 507 pp.

Holton, J. R. & Hakim, G., 2012. *An Introduction to Dynamic Meteorology*. 5th edn. Academic Press, 552 pp.

Holton, J. R., Haynes, P. R., McIntyre, M. E., Douglass, A. R. *et al.*, 1995. Stratosphere-troposphere exchange. *Rev. Geophys.*, **33**, 403–439.

Holton, J. R. & Lindzen, R. S., 1972. An updated theory for the quasi-biennial cycle of the tropical stratosphere. *J. Atmos. Sci.*, **29**, 1076–1080.

Holton, J. R. & Mass, C., 1976. Stratospheric vacillation cycles. *J. Atmos. Sci.*, **33**, 2218–2215.

Holton, J. R. & Tan, H.-C., 1980. The influence of the equatorial quasi-biennial oscillation on the global circulation at 50 mb. *J. Atmos. Sci.*, **37**, 2200–2208.

Holton, J. R. & Tan, H.-C., 1982. The quasi-biennial oscillation in the northern hemisphere lower stratosphere. *J. Meteor. Soc. Japan*, **60**, 140–158.

Hoskins, B. J. & Karoly, D. J., 1981. The steady linear response of a spherical atmosphere to thermal and orographic forcing. *J. Atmos. Sci.*, **38**, 1179–1196.

Hough, S. S., 1897. On the application of harmonic analysis to the dynamical theory of the tides. Part I: On Laplace's "Oscillations of the first species", and on the dynamics of ocean currents. *Phil. Trans. (A)*, **189 (IX)**, 201–258.

Hough, S. S., 1898. On the application of harmonic analysis to the dynamical theory of the tides. Part II: On the general integration of Laplace's dynamical equations. *Phil. Trans. (A)*, **191 (V)**, 139–186.

Huang, R. X., 1998. Mixing and available potential energy in a Boussinesq ocean. *J. Phys. Oceanogr.*, **28**, 669–678.

Huang, R. X., 1999. Mixing and energetics of the oceanic thermohaline circulation. *J. Phys. Oceanogr.*, **29**, 727–746.

Huang, R. X., 2010. *Ocean Circulation*. Cambridge University Press, 791 pp.

Hughes, C. W., 2002. Sverdrup-like theories of the Antarctic Circumpolar Current. *J. Mar. Res.*, **60**, 1–17.

Hughes, C. W. & de Cuevas, B., 2001. Why western boundary currents in realistic oceans are inviscid: a link between form stress and bottom pressure torques. *J. Phys. Oceanogr.*, **31**, 2871–2885.

Hughes, G. O. & Griffiths, R. W., 2008. Horizontal convection. *Ann. Rev. Fluid Mech.*, **185–2008**, 40.

Ierley, G. R. & Ruehr, O. G., 1986. Analytic and numerical solutions of a nonlinear boundary value problem. *Stud. Appl. Math.*, **75**, 1–36.

Ilicak, M. & Vallis, G. K., 2012. Simulations and scaling of horizontal convection. *Tellus A*, **64**, 1–17.

Il'in, A. M. & Kamenkovich, V. M., 1964. The structure of the boundary layer in the two-dimensional theory of ocean currents (in Russian). *Okeanologiya*, **4** (5), 756–769.

Ingersoll, A. P., 2005. Boussinesq and anelastic approximations revisited: potential energy release during thermobaric instability. *J. Phys. Oceanogr.*, **35**, 1359–1369.

IOC, SCOR & IAPSO, 2010. The international thermodynamic equation of seawater – 2010: Calculation and use of thermodynamic properties. Technical report, Intergovernmental Oceanographic Commission, Manuals and Guides No. 56, UNESCO (English).

Iwayama, T., Shepherd, T. G. & Watanabe, T., 2002. An 'ideal' form of decaying two-dimensional turbulence. *J. Fluid Mech.*, **456**, 183–198.

Jackett, D. R. & McDougall, T. J., 1997. A neutral density variable for the world's oceans. *J. Phys. Oceanogr.*, **28**, 237–263.

Jackson, L., Hughes, C. W. & Williams, R. G., 2006. Topographic control of basin and channel flows: the role of bottom pressure torques and friction. *J. Phys. Oceanogr.*, **36**, 1786–1805.

Jansen, M. & Ferrari, R., 2012. Macroturbulent equilibration in a thermally forced primitive equation system. *J. Atmos. Sci.*, **69**, 695–713.

Jansen, M. & Ferrari, R., 2013. Equilibration of an atmosphere by adiabatic eddy fluxes. *J. Atmos. Sci.*, **70**, 2948–2962.

Jeffreys, H., 1924. On certain approximate solutions of linear differential equations of the second order. *Proc. London Math. Soc.*, **23**, 428–436.

Jeffreys, H., 1926. On the dynamics of geostrophic winds. *Quart. J. Roy. Meteor. Soc.*, **51**, 85–104.

Jeffreys, H. & Jeffreys, B. S., 1946. *Methods of Mathematical Physics*. Cambridge University Press, 728 pp.

Jin, F.-F., 1997a. An equatorial ocean recharge paradigm for ENSO. Part I: Conceptual model. *J. Atmos. Sci.*, **54**, 811–829.

Jin, F.-F., 1997b. An equatorial ocean recharge paradigm for ENSO. Part II: A stripped-down coupled model. *J. Atmos. Sci.*, **54**, 830–847.

Johnson, G. C. & Bryden, H. L., 1989. On the size of the Antarctic Circumpolar Current. *Deep-Sea Res.*, **36**, 39–53.

Jones, D. B. A., Schneider, H. R. & McElroy, M. B., 1998. Effects of the quasi-biennial oscillation on the zonally averaged transport of tracer. *J. Geophys. Res.*, **103**, 11235–11249.

Jones, W. L., 1967. Propagation of internal gravity waves in fluids with shear flow and rotation. *J. Fluid Mech.*, **30**, 439–448.

Jucker, M., 2014. Scientific visualisation of atmospheric data with ParaView. *J. Open Res. Software*, **2**, e4.

Jucker, M., Fueglistaler, S. & Vallis, G. K., 2013. Maintenance of stratospheric structure in an idealized general circulation model. *J. Atmos. Sci.*, **70**, 3341–3358.

Jucker, M., Fueglistaler, S. & Vallis, G. K., 2014. Stratospheric sudden warmings in an idealized GCM. *J. Geophys. Res. (Atmospheres)*, **119**, 11054–11064.

Juckes, M. N., 2000. The static stability of the midlatitude troposphere: the relevance of moisture. *J. Atmos. Sci.*, **57**, 3050–3057.

Juckes, M. N., 2001. A generalization of the transformed Eulerian-mean meridional circulation. *Quart. J. Roy. Meteor. Soc.*, **127**, 147–160.

Kalnay, E., 1996. The NCEP/NCAR 40-year reanalysis project. *Bull. Amer. Meteor. Soc.*, **77**, 437–471.

Karsten, R., Jones, H. & Marshall, J., 2002. The role of eddy transfer in setting the stratification and transport of a circumpolar current. *J. Phys. Oceanogr.*, **32**, 39–54.

Keffer, T., 1985. The ventilation of the world's oceans: maps of potential vorticity. *J. Phys. Oceanogr.*, **15**, 509–523.

Kessler, W. S., Johnson, G. C. & Moore, D. W., 2003. Sverdrup and nonlinear dynamics of the Pacific equatorial currents. *J. Phys. Oceanogr.*, **33**, 994–1008.

Kevorkian, J. & Cole, J. D., 2011. *Multiple Scale and Singular Perturbation Methods*. Springer-Verlag, 648 pp.

Kibel, I., 1940. Priloozhenie k meteorogi uravnenii mekhaniki baroklinnoi zhidkosti (Application of baroclinic fluid dynamic equations to meteorology). *SSSR Ser. Geogr. Geofiz.*, **5**, 627–637.

Kiladis, G. N., Straub, K. H. & Haertel, P. T., 2005. Zonal and vertical structure of the Madden–Julian oscillation. *J. Atmos. Sci.*, **62**, 2790–2809.

Kiladis, G. N., Wheeler, M. C., Haertel, P. T., Straub, K. H. & Roundy, P. E., 2009. Convectively coupled equatorial waves. *Rev. Geophys.*, **47**, RG2003.

Killworth, P. D., 1987. A continuously stratified nonlinear ventilated thermocline. *J. Phys. Oceanogr.*, **17**, 1925–1943.

Killworth, P. D., 1997. On the parameterization of eddy transfer. Part I: theory. *J. Marine Res.*, **55**, 1171–1197.

Killworth, P. D. & McIntyre, M. E., 1985. Do Rossby-wave critical layers absorb, reflect, or over-reflect? *J. Fluid Mech.*, **161**, 449–492.

Kim, H.-K. & Lee, S., 2001. Hadley cell dynamics in a primitive equation model. Part II: Nonaxisymmetric flow. *J. Atmos. Sci.*, **58**, 19, 2859–2871.

Kimoto, M. & Ghil, M., 1993. Multiple flow regimes in the northern hemisphere winter. Part 1: Methodology and hemispheric regimes. *J. Atmos. Sci.*, **50**, 2625–2643.

Kolmogorov, A. N., 1941. The local structure of turbulence in incompressible viscous fluid for very large Reynolds numbers. *Dokl. Acad. Sci. USSR*, **30**, 299–303.

Kolmogorov, A. N., 1962. A refinement of previous hypotheses concerning the local structure of turbulence in a viscous incompressible fluid at high Reynolds numbers. *J. Fluid Mech.*, **13**, 82–85.

Kraichnan, R., 1967. Inertial ranges in two-dimensional turbulence. *Phys. Fluids*, **10**, 1417–1423.

Kraichnan, R. & Montgomery, D., 1980. Two-dimensional turbulence. *Rep. Prog. Phys.*, **43**, 547–619.

Kramers, H. A., 1926. Wellenmechanik und halbzahlige Quantisierung (Wave mechanics and semi-integral quantization). *Zeit. fur Physik A*, **39**, 828–840.

Kundu, P., Allen, J. S. & Smith, R. L., 1975. Modal decomposition of the velocity field near the Oregon coast. *J. Phys. Oceanogr.*, **5**, 683–704.

Kundu, P., Cohen, I. M. & Dowling, D. R., 2015. *Fluid Mechanics*. Academic Press, 928 pp.

Kuo, H.-l., 1949. Dynamic instability of two-dimensional nondivergent flow in a barotropic atmosphere. *J. Meteorol.*, **6**, 105–122.

Kuo, H.-l., 1951. Vorticity transfer as related to the development of the general circulation. *J. Meteorol.*, **8**, 307–315.

Kushner, P. J., 2010. Annular modes of the troposphere and stratosphere. In *The Stratosphere: Dynamics, Transport, and Chemistry*, Geophys. Monogr. Ser (2010).

Kushnir, Y., Robinson, W. A., Bladé, I., Hall, N. M. J. *et al.*, 2002. Atmospheric GCM response to extratropical SST anomalies: synthesis and evaluation. *J. Climate*, **15**, 2233–2256.

Labitzke, K., Kunze, M. & Bronnimann, S., 2006. Sunspots, the qbo and the stratosphere in north polar regions —- 20 years later. *Meteor. Z.*, **15**, 355–363.

LaCasce, J. H. & Ohlmann, C., 2003. Relative dispersion at the surface of the Gulf of Mexico. *J. Mar. Res.*, **65**, 285–312.

Lait, L. R., 1994. An alternative form for potential vorticity. *J. Atmos. Sci.*, **51**, 1754–1759.

Lamb, H., 1932. *Hydrodynamics*. Cambridge University Press, reissued by Dover Publications 1945, 768 pp.

Lanczos, C., 1970. *The Variational Principles of Mechanics*. University of Toronto Press, Reprinted by Dover Publications 1980, 418 pp.

Landau, L. D., 1944. On the problem of turbulence. *Dokl. Akad. Nauk SSSR*, **44**, 311–314.

Landau, L. D. & Lifshitz, E. M., 1987. *Fluid Mechanics* (Course of Theoretical Physics, v. 6). 2nd edn. Pergamon Press, 539 pp.

Larichev, V. D. & Held, I. M., 1995. Eddy amplitudes and fluxes in a homogeneous model of fully developed baroclinic instability. *J. Phys. Oceanogr.*, **25**, 2285–2297.

Latif, M. & Barnett, T., 1996. Decadal climate variability over the North Pacific and North America: dynamics and predictability. *J. Climate*, **10**, 219–239.

Lau, K.-M., 1981. Oscillations in a simple equatorial climate system. *J. Atmos. Sci.*, **38**, 248–261.

Lawrence, M. G., 2005. The relationship between relative humidity and the dewpoint temperature in moist air: A simple conversion and applications. *Bull. Am. Meteor. Soc.*, **86**, 225–233.

LeBlond, P. H. & Mysak, L. A., 1980. *Waves in the Ocean*. Elsevier, 616 pp.

Ledwell, J., Watson, A. & Law, C., 1998. Mixing of a tracer released in the pycnocline. *J. Geophys. Res.*, **103**, 21499–21529.

Lee, M.-M., Marshall, D. P. & Williams, R. G., 1997. On the eddy transfer of tracers: advective or diffusive? *J. Mar. Res.*, **55**, 483–595.

Lee, T. D., 1951. Difference between turbulence in a two-dimensional fluid and in a three-dimensional fluid. *J. Appl. Phys.*, **22**, 524.

Leetmaa, A., Niiler, P. & Stommel, H., 1977. Does the Sverdrup relation account for the mid-Atlantic circulation? *J. Mar. Res.*, **35**, 1–10.

Leith, C. E., 1968. Diffusion approximation for two-dimensional turbulence. *Phys. Fluids*, **11**, 671–672.

Lesieur, M., 1997. *Turbulence in Fluids: Third Revised and Enlarged Edition*. Kluwer, 515 pp.

Levinson, N., 1950. The 1st boundary value problem for $\epsilon\Delta U + A(x,y)U_x + B(x,y)U_y + C(x,y)U = D(x,t)$ for small epsilon. *Ann. Math.*, **51**, 429–445.

Lewis, R., Ed., 1991. *Meteorological Glossary*. 6th edn. Her Majesty's Stationery Office, 335 pp.

Lighthill, J., 1978. *Waves in Fluids*. Cambridge University Press, 504 pp.

Lighthill, M. J., 1965. Group velocity. *J. Inst. Math. Appl.*, **1**, 1–28.

Lighthill, M. J., 1969. Dynamic response of the Indian Ocean to onset of the southwest monsoon. *Phil. Trans. Roy. Soc. Lond. A*, **265**, 45–92.

Lilly, D. K., 1969. Numerical simulation of two-dimensional turbulence. *Phys. Fluid Suppl. II*, **12**, 240–249.

Lilly, D. K., 1996. A comparison of incompressible, anelastic and Boussinesq dynamics. *Atmos. Res*, **40**, 143–151.

Limpasuvan, V., Thompson, D. W. J. & Hartmann, D. L., 2000. The life cycle of the Northern Hemisphere sudden stratospheric warmings. *J. Climate*, **17**, 2584–2596.

Lindborg, E., 1999. Can the atmospheric kinetic energy spectrum be explained by two-dimensional turbulence? *J. Fluid Mech.*, **388**, 259–288.

Lindborg, E. & Alvelius, K., 2000. The kinetic energy spectrum of the two-dimensional enstrophy turbulence cascade. *Phys. Fluids*, **12**, 945–947.

Lindzen, R. S. & Farrell, B., 1980. The role of the polar regions in global climate, and a new parameterization of global heat transport. *Mon. Wea. Rev.*, **108**, 2064–2079.

Lindzen, R. S. & Holton, J. R., 1968. A theory of the quasi-biennial oscillation. *J. Atmos. Sci.*, **25**, 1095–1107.

Lindzen, R. S. & Hou, A. Y., 1988. Hadley circulation for zonally averaged heating centered off the equator. *J. Atmos. Sci.*, **45**, 2416–2427.

Lindzen, R. S., Lorenz, E. N. & Plazman, G. W., Eds., 1990. *The Atmosphere — a Challenge: the Science of Jule Gregory Charney*. American Meteorological Society, 321 pp.

Lindzen, R. S. & Nigam, S., 1987. On the role of sea surface temperature gradients in forcing low-level winds and convergence in the tropics. *J. Atmos. Sci.*, **44**, 2418–2436.

Liouville, J., 1837. Sur le développement des fonction ou parties de fonction en séries (On the development of functions of parts of functions in series). *J. Math. Pures Appl.*, **2**, 16–35.

Lipps, F. B. & Hemler, R. S., 1982. A scale analysis of deep moist convection and some related numerical calculations. *J. Atmos. Sci.*, **39**, 2192–2210.

Longuet-Higgins, M. S., 1964. Planetary waves on a rotating sphere, I. *Proc. Roy. Soc. Lond. A*, **279**, 446–473.

Longuet-Higgins, M. S., 1968. The eigenfunctions of Laplace's tidal equations over a sphere. *Proc. Roy. Soc. Lond. A*, **262**, 511–607.

Lorenz, E. N., 1955. Available potential energy and the maintenance of the general circulation. *Tellus*, **7**, 157–167.

Lorenz, E. N., 1963. Deterministic nonperiodic flow. *J. Atmos. Sci.*, **20**, 130–141.

Lorenz, E. N., 1967. *The Nature and the Theory of the General Circulation of the Atmosphere*. WMO Publications, Vol. 218, World Meteorological Organization.

Lozier, S., Owens, W. B. & Curry, R. G., 1996. The climatology of the North Atlantic. *Prog. Oceanog.*, **36**, 1–44.

Ludlam, F. H., 1966. Cumulus and cumulonimbus convection. *Tellus*, **18**, 687–698.

Lumpkin, R. & Speer, K., 2007. Global ocean meridional overturning. *J. Phys. Oceanogr.*, **37**, 2550–2562.

Luyten, J. R., Pedlosky, J. & Stommel, H., 1983. The ventilated thermocline. *J. Phys. Oceanogr.*, **13**, 292–309.

Madden, R. A. & Julian, P. R., 1971. Detection of a 40–50 day oscillation in the zonal wind in the tropical Pacific. *J. Atmos. Sci.*, **28**, 702–708.

Madden, R. A. & Julian, P. R., 1972. Description of global-scale circulation cells in the tropics with a 40–50 day period. *J. Atmos. Sci.*, **29**, 1109–1123.

Majda, A. J. & Klein, R., 2003. Systematic multiscale models for the tropics. *J. Atmos. Sci.*, **60**, 393–408.

Majda, A. J. & Stechmann, S. N., 2009. The skeleton of tropical intraseasonal oscillations. *Proc. Nat. Acad. Sci.*, **106**, 8417–8422.

Maltrud, M. E. & Vallis, G. K., 1991. Energy spectra and coherent structures in forced two-dimensional and beta-plane turbulence. *J. Fluid Mech.*, **228**, 321–342.

Manabe, S. & Stouffer, R. J., 1988. Two stable equilibria of a coupled ocean–atmosphere model. *J. Climate*, **1**, 841–866.

Manabe, S. & Strickler, R. F., 1964. Thermal equilibrium of the atmosphere with a convective adjustment. *J. Atmos. Sci.*, **21**, 361–385.

Manabe, S. & Wetherald, R. T., 1980. On the distribution of climate change resulting from an increase in CO_2 content of the atmosphere. *J. Atmos. Sci.*, **37**, 99–118.

Mapes, B. E., 1997. Equilibrium vs. activation control of large-scale variations of tropical deep convection. In R. K. Smith, Ed., *The Physics and Parameterization of Moist Atmospheric Convection*, pp. 321–358. Springer.

Mapes, B. E., 1998. The large-scale part of tropical mesoscale convective system circulations: A linear vertical spectral band model. *J. Meteor. Soc. Japan*, **76**, 29–55.

Mapes, B. E., 2000. Convective inhibition, subgrid-scale triggering energy, and stratiform instability in a toy tropical wave model. *J. Atmos. Sci.*, **57**, 1515–1535.

Marcus, P. S., 1993. Jupiter's Great Red Spot and other vortices. *Ann. Rev. Astron. Astrophys*, **31**, 523–573.

Margules, M., 1903. Über die Energie der Stürme (On the energy of storms). *Jahrb. Kais.-kön Zent. für Met. und Geodynamik, Vienna*, 26 pp. Engl. transl.: C. Abbe, *Smithson. Misc. Collect.*, no. 51, pp. 533-595, Smithsonian Institution, Washington D. C., 1910.

Marotzke, J., 1989. Instabilities and multiple steady states of the thermohaline circulation. In D. L. T. Anderson & J. Willebrand, Eds., *Oceanic Circulation Models: Combining Data and Dynamics*, pp. 501–511. NATO ASI Series, Kluwer.

Marshall, D. P., Maddison, J. R. & Berloff, P. S., 2012. A framework for parameterizing eddy potential vorticity fluxes. *J. Phys. Oceanogr.*, **42**, 539–557.

Marshall, D. P., Williams, R. G. & Lee, M.-M., 1999. The relation between eddy-induced transport and isopycnic gradients of potential vorticity. *J. Phys. Oceanogr.*, **29**, 1571–1578.

Marshall, J. & Plumb, R. A., 2008. *Atmosphere, Ocean and Climate Dynamics: An Introductory Text*. Academic Press, 344 pp.

Marshall, J. & Speer, K., 2012. Closure of the meridional overturning circulation through southern ocean upwelling. *Nature Geosciences*, **5**, 171–180.

Marshall, J. C., 1981. On the parameterization of geostrophic eddies in the ocean. *J. Phys. Oceanogr.*, **11**, 257–271.

Marshall, J. C. & Nurser, A. J. G., 1992. Fluid dynamics of oceanic thermocline ventilation. *J. Phys. Oceanogr.*, **22**, 583–595.

Marshall, J. C. & Radko, T., 2003. Residual-mean solutions for the Antarctic Circumpolar Current and its associated overturning circulation. *J. Phys. Oceanogr.*, **22**, 2341–2354.

Marshall, J. C. & Schott, F., 1999. Open-ocean convection: observations, theory, and models. *Rev. Geophys.*, **37**, 1–64.

Matsuno, T., 1966. Quasi-geostrophic motions in the equatorial area. *J. Meteor. Soc. Japan*, **44**, 25–43.

Matsuno, T., 1971. A dynamical model of the sudden stratospheric warming. *J. Atmos. Sci.*, **28**, 1479–1494.

Maze, G. & Marshall, J., 2011. Diagnosing the observed seasonal cycle of Atlantic subtropical mode water using potential vorticity and its attendant theorems. *J. Phys. Oceanogr.*, **41**, 1986–1999.

McCarthy, M. C. & Talley, L. D., 1999. Three-dimensional isoneutral potential vorticity structure in the Indian Ocean. *J. Geophys. Res. (Oceans)*, **104**, 13251–13267.

McCreary, J. P., 1981. A linear stratified ocean model of the equatorial undercurrent. *Phil. Trans. Roy. Soc. Lond.*, **A298**, 603–635.

McCreary, J. P., 1985. Modeling equatorial ocean circulation. *Ann. Rev. Fluid Mech.*, **17**, 359–407.

McCreary, J. P. & Lu, P., 1994. Interaction between the subtropical and equatorial ocean circulations: the subtropical cell. *J. Phys. Oceanogr.*, **24**, 466–497.

McDougall, T. J., 1987. Neutral surfaces. *J. Phys. Oceanogr.*, **17**, 1950–1964.

McDougall, T. J., 1998. Three-dimensional residual mean theory. In E. P. Chassignet & J. Verron, Eds., *Ocean Modeling and Parameterization*, pp. 269–302. Kluwer Academic.

McDougall, T. J., 2003. Potential enthalphy: a conservative oceanic variable for evaluating heat content and heat fluxes. *J. Phys. Oceanogr.*, **33**, 945–963.

McIntosh, P. C. & McDougall, T. J., 1996. Isopycnal averaging and the residual mean circulation. *J. Phys. Oceanogr.*, **26**, 1655–1660.

McIntyre, M. E. & Norton, W. A., 1990. Dissipative wave–mean interactions and the transport of vorticity or potential vorticity. *J. Fluid Mech.*, **212**, 403–435.

McIntyre, M. E. & Norton, W. A., 2000. Potential vorticity inversion on a hemisphere. *J. Atmos. Sci.*, **57**, 1214–1235.

McIntyre, M. E. & Shepherd, T. G., 1987. An exact local conservation theorem for finite-amplitude disturbances to nonparallel shear flows, with remarks on Hamiltonian structure and on Arnol'd's stability theorems. *J. Fluid Mech.*, **181**, 527–565.

McKee, W. D., 1973. The wind-driven equatorial circulation in a homogeneous ocean. *Deep-Sea Res.*, **20**, 889–899.

McPhaden, M. J., Timmermann, A., Widlansky, M. J., Balmaseda, M. A. & Stockdale, T. N., 2015. The curious case of the El Niño that never happened: A perspective from 40 years of progress in climate research and forecasting. *Bull. Am. Meteor. Soc.*, **96**, 1647–1665.

McWilliams, J. C., 1984. The emergence of isolated coherent vortices in turbulent flow. *J. Fluid Mech.*, **146**, 21–43.

Mihaljan, J. M., 1962. A rigorous exposition of the Boussinesq approximations applicable to a thin layer of fluid. *Astrophysical J.*, **136**, 1126–1133.

Millero, F. J., Feistel, R., Wright, D. G. & McDougall, T. J., 2008. The composition of standard seawater and the definition of the reference-composition salinity scale. *Deep Sea Res., Part I*, **55**, 50–72.

Moffatt, H. K., 1983. Transport effects associated with turbulence with particular attention to the influence of helicity. *Rep. Progress Phys.*, **46**, 621–664.

Monin, A. S. & Yaglom, A. M., 1971. *Statistical Fluid Mechanics: Mechanics of Turbulence, Vols. 1 and 2*. MIT Press and Dover Publications, 1680 pp.

Morel, P. & Larcheveque, M., 1974. Relative dispersion of constant-level balloons in the 200 mb general circulation. *J. Atmos. Sci.*, **31**, 2189–2196.

Mundt, M., Vallis, G. K. & Wang, J., 1997. Balanced models for the large- and meso-scale circulation. *J. Phys. Oceanogr.*, **27**, 1133–1152.

Munk, W. H., 1950. On the wind-driven ocean circulation. *J. Meteorol*, **7**, 79–93.

Munk, W. H., 1966. Abyssal recipes. *Deep-Sea Res.*, **13**, 707–730.

Munk, W. H. & Palmén, E., 1951. Note on dynamics of the Antarctic Circumpolar Current. *Tellus*, **3**, 53–55.

Munk, W. H. & Wunsch, C., 1998. Abyssal recipes II: energetics of tidal and wind mixing. *Deep-Sea Res.*, **45**, 1976–2009.

Namias, J., 1959. Recent seasonal interaction between North Pacific waters and the overlying atmospheric circulation. *J. Geophys. Res.*, **64**, 631–646.

Neelin, J. D., 1988. A simple model for surface stress and low-level flow in the tropical atmosphere driven by prescribed heating. *Quart. J. Roy. Meteor. Soc.*, **114**, 747–770.

Neelin, J. D. & Zeng, N., 2000. A quasi-equilibrium tropical circulation model—formulation. *J. Atmos. Sci.*, **57**, 1741–1766.

Newell, A. C., 1969. Rossby wave packet interactions. *J. Fluid Mech.*, **35**, 255–271.

Newman, P. A., Coy, L., Pawson, S. & Lait, L. R., 2016. The anomalous change in the QBO in 2015–2016. *Geophys. Res. Lett.*, **43**, 8791–8797. doi:10.1002/2016GL070373.

Nicholls, S., 1985. Aircraft observations of the Ekman layer during the joint air-sea interaction experiment. *Quart. J. Roy. Meteor. Soc.*, **111**, 391–426.

Nikurashin, M. & Vallis, G. K., 2011. A theory of deep stratification and overturning circulation in the ocean. *J. Phys. Oceanogr.*, **41**, 485–502.

Nikurashin, M. & Vallis, G. K., 2012. A theory of the interhemispheric meridional overturning circulation and associated stratification. *J. Phys. Oceanogr.*, **42**, 1652–1667.

Nof, D., 2003. The Southern Ocean's grip on the northward meridional flow. In *Progress in Oceanography*, Vol. 56, pp. 223–247. Pergamon.

Novikov, E. A., 1959. Contributions to the problem of the predictability of synoptic processes. *Izv. An. SSSR Ser. Geophys.*, **11**, 1721. Eng. transl.: *Am. Geophys. U. Transl.*, 1209-1211.

Nycander, J., 2011. Energy conversion, mixing energy, and neutral surfaces with a nonlinear equation of state. *J. Phys. Oceanogr.*, **41**, 28–41.

Nycander, J. & Roquet, F., 2015. The nonlinear equation of state of sea water and the global water mass distribution. *Geophys. Res. Lett.*, **42**, 7714–7721. In press.

Oberbeck, A., 1879. Über die Wärmeleitung der Flüssigkeiten bei Berücksichtigung der Strömungen infolge vor Temperaturdifferenzen (On the thermal conduction of liquids taking into account flows due to temperature differences). *Ann. Phys. Chem., Neue Folge*, **7**, 271–292.

Oberbeck, A., 1888. Über die Bewegungserscheinungen der Atmosphäre (On the phenomena of motion in the atmosphere). *Sitzb. K. Preuss. Akad. Wiss*, **7**, 383–395 and 1129–1138. Engl trans.: in B. Saltzman, Ed.,*Theory of Thermal Convection*, Dover, 162–183.

Obukhov, A. M., 1941. Energy distribution in the spectrum of turbulent flow. *Izv. Akad. Nauk. SSR, Ser. Geogr. Geofiz.*, **5**, 453–466.

Obukhov, A. M., 1949. Structure of the temperature field in turbulent flows. *Izv. Akad. Nauk. SSR, Ser. Geogr. Geofiz.*, **13**, 58–63.

Obukhov, A. M., 1962. On the dynamics of a stratified liquid. *Dokl. Akad. Nauk SSSR*, **145**, 1239–1242. Engl. transl.: *Soviet Physics–Dokl.* 7, 682–684.

Oetzel, K. & Vallis, G. K., 1997. Strain, vortices, and the enstrophy inertial range in two-dimensional turbulence. *Phys. Fluids*, **9**, 2991–3004.

O'Gorman, P. A., Lamquin, N., Schneider, T. & Singh, M. S., 2011. The relative humidity in an isentropic advection–condensation model: Limited poleward influence and properties of subtropical minima. *J. Atmos. Sci.*, **68**, 3079–3093.

O'Gorman, P. A. & Pullin, D. I., 2005. Effect of Schmidt number of the velocity-scaler cospectrum in isotropic turbulence with a mean scalar gradient. *J. Fluid Mech.*, **532**, 111–140.

Ogura, Y. & Phillips, N. A., 1962. Scale analysis of deep and shallow convection in the atmosphere. *J. Atmos. Sci.*, **19**, 173–179.

Olbers, D., 1998. Comments on "On the obscurantist physics of 'form drag' in theorizing about the Circumpolar Current". *J. Phys. Oceanogr.*, **28**, 1647–1654.

Olbers, D., Borowski, D., Völker, C. & Wolff, J.-O., 2004. The dynamical balance, transport and circulation of the Antarctic Circumpolar Current. *Antarctic Science*, **16**, 439–470.

Olbers, D., Willebrand, J. & Eden, C., 2012. *Ocean Dynamics*. Springer, 704 pp.

Ollitrault, M., Gabillet, C. & Colin de Verdière, A., 2005. Open ocean regimes of relative dispersion. *J. Fluid Mech.*, **533**, 381–407.

Onsager, L., 1931. Reciprocal relations in irreversible processes. II. *Phys. Rev.*, **38**, 2265–2279.

Onsager, L., 1949. Statistical hydrodynamics. *Nuovo Cim. (Suppl.)*, **6**, 279–287.

Ooyama, K. ., 1963. A dynamical model for the study of tropical cyclone development. New York University, 26pp, unpublished manuscript.

Ooyama, K. V., 1982. Conceptual evolution of the theory and modeling of the tropical cyclone. *J. Meteor. Soc. Japan*, **60**, 369–380.

Orlanski, I. & Sheldon, J. P., 1995. Stages in the energetics of baroclinic systems. *Tellus A*, **47**, 605–628.

Osprey, S. M., Butchart, N., Knight, J. R., Scaife, A. *et al.*, 2016. An unexpected disruption of the atmospheric quasi-biennial oscillation. *Science*, **353**, 1424–1427.

Paldor, N., Rubin, S. & Mariono, A. J., 2007. A consistent theory for linear waves of the shallow-water equations on a rotating plane in midlatitudes. *J. Atmos. Sci.*, **37**, 115–128.

Paldor, N. & Sigalov, A., 2011. An invariant theory of the linearized shallow water equations with rotation and its application to a sphere and a plane. *Dyn. Atmos. Oceans*, **51**, 26–44.

Palmer, T. N., 1981. Diagnostic study of a wavenumber-2 stratospheric sudden warming in a transformed Eulerian-mean formalism. *J. Atmos. Sci.*, **38**, 844–855.

Palmer, T. N., 1997. A nonlinear dynamical perspective on climate prediction. *J. Climate*, **12**, 575–591.

Palmer, T. N., 2009. Edward Lorenz, 1917–2008. *Biogr. Mems Fell. R. Soc.*, **55**, 139–155.

Paparella, F. & Young, W. R., 2002. Horizontal convection is non-turbulent. *J. Fluid Mech.*, **466**, 205–214.

Pascoe, C. L., Gray, L. J., Crooks, S. A., Juckes, M. N. & Baldwin, M. P., 2005. The quasi-biennial oscillation: Analysis using ERA-40 data. *J. Geophys. Res.*, **110**, D08105.

Pauluis, O., 2007. Sources and sinks of available potential energy in a moist atmosphere. *J. Atmos. Sci.*, **64**, 2627–2641.

Pauluis, O., 2008. Thermodynamic consistency of the anelastic approximation for a moist atmosphere. *J. Atmos. Sci.*, **65**, 2719–2729.

Pedlosky, J., 1964. The stability of currents in the atmosphere and ocean. Part I. *J. Atmos. Sci.*, **21**, 201–219.

Pedlosky, J., 1987a. *Geophysical Fluid Dynamics*. 2nd edn. Springer-Verlag, 710 pp.

Pedlosky, J., 1987b. An inertial theory of the equatorial undercurrent. *J. Phys. Oceanogr.*, **17**, 1978–1985.

Pedlosky, J., 1996. *Ocean Circulation Theory*. Springer-Verlag, 453 pp.

Pedlosky, J., 2003. *Waves in the Ocean and Atmosphere: Introduction to Wave Dynamics*. Springer-Verlag, 260 pp.

Peixoto, J. P. & Oort, A. H., 1992. *Physics of Climate*. American Institute of Physics, 520 pp.

Peltier, W. R. & Stuhne, G., 2002. The upscale turbulence cascade: shear layers, cyclones and gas giant bands. In R. P. Pearce, Ed., *Meteorology at the Millennium*, pp. 43–61. Academic Press.

Persson, A., 1998. How do we understand the Coriolis force? *Bull. Am. Meteor. Soc.*, **79**, 1373–1385.

Philander, S. G., 1990. *El Niño, La Niña, and the Southern Oscillation*. Academic Press, 289 pp.

Phillips, N. A., 1954. Energy transformations and meridional circulations associated with simple baroclinic waves in a two-level, quasi-geostrophic model. *Tellus*, **6**, 273–286.

Phillips, N. A., 1956. The general circulation of the atmosphere: a numerical experiment. *Quart. J. Roy. Meteor. Soc.*, **82**, 123–164.

Phillips, N. A., 1963. Geostrophic motion. *Rev. Geophys.*, **1**, 123–176.

Phillips, N. A., 1966. The equations of motion for a shallow rotating atmosphere and the traditional approximation. *J. Atmos. Sci.*, **23**, 626–630.

Phillips, N. A., 1973. Principles of large-scale numerical weather prediction. In P. Morel, Ed., *Dynamic Meteorology*, pp. 1–96. Riedel.

Phillips, O., 1972. Turbulence in a strongly stratified fluid—is it unstable? In *Deep Sea Research and Oceanographic Abstracts*, Vol. 19 (1972), pp. 79–81. Elsevier.

Pierini, S. & Vulpiani, A., 1981. Nonlinear stability analysis in multi-layer quasigeostrophic system. *J. Phys. A*, **14**, L203–L207.

Pierrehumbert, R. T., 2010. *Principles of Planetary Climate*. Cambridge University Press, 652 pp.

Pierrehumbert, R. T., Brogniez, H. & Roca, R., 2007. On the relative humidity of the atmosphere. In T. Schneider & A. Sobel, Eds., *The Global Circulation of the Atmosphere: Phenomena, Theory, Challenges*, pp. 143–185. Princeton University Press.

Pierrehumbert, R. T. & Swanson, K. L., 1995. Baroclinic instability. *Ann. Rev. Fluid Mech.*, **27**, 419–467.

Plumb, R., 1981. Instability of the distorted polar night vortex: A theory of stratospheric warmings. *J. Atmos. Sci.*, **38**, 2514–2531.

Plumb, R. & McEwan, A., 1978. The instability of a forced standing wave in a viscous stratified fluid: A laboratory analogue of. the Quasi-Biennial Oscillation. *J. Atmos. Sci.*, **35**, 1827–1839.

Plumb, R. A., 1977. The interaction of two internal waves with the mean flow: Implications for the theory of the Quasi-Biennial Oscillation. *J. Atmos. Sci.*, **34**, 1847–1858.

Plumb, R. A., 1979. Eddy fluxes of conserved quantities by small-amplitude waves. *J. Atmos. Sci.*, **36**, 1699–1704.

Plumb, R. A., 1984. The quasi-biennial oscillation. In J. R. Holton & T. Matsuno, Eds., *Dynamics of the Middle Atmosphere*, pp. 217–251. Terra Scientific Publishing.

Plumb, R. A., 1990. A nonacceleration theorem for transient quasi-geostrophic eddies on a three-dimensional time-mean flow. *J. Atmos. Sci.*, **47**, 1825–1836.

Plumb, R. A., 2002. Stratospheric transport. *J. Meteor. Soc. Japan*, **80**, 793–809.

Plumb, R. A. & Bell, R. C., 1982. An analysis of the quasi-biennial oscillation on an equatorial beta-plane. *Quart. J. Roy. Meteor. Soc.*, **108**, 335–352.

Poincaré, H., 1893. *Théorie des Tourbillons (Theory of Vortices [literally, Swirls])*. Georges Carré, Éditeur. Reprinted by Éditions Jacques Gabay, 1990, 211 pp.

Poincaré, H., 1908. *Science and Method*. T. Nelson and Sons. Engl. transl.: F. Maitland. Reprinted in *The Value of Science: Essential Writings of Henri Poincaré*, Ed. S. J. Gould, Random House, 584 pp.

Polzin, K. L., Toole, J. M., Ledwell, J. R. & Schmidt, R. W., 1997. Spatial variability of turbulent mixing in the abyssal ocean. *Science*, **276**, 93–96.

Pope, S. B., 2000. *Turbulent Flows*. Cambridge University Press, 754 pp.

Price, J. F., Weller, R. A. & Schudlich, R. R., 1987. Wind-driven ocean currents and Ekman transport. *Science*, **238**, 1534–1538.

Proudman, J., 1916. On the motion of solids in liquids. *Proc. Roy. Soc. Lond. A*, **92**, 408–424.

Queney, P., 1948. The problem of air flow over mountains: A summary of theoretical results. *Bull. Am. Meteor. Soc.*, **29**, 16–26.

Quinn, W. H., 1974. Monitoring and predicting El Niño invasions. *J. Appl. Meteor.*, **13**, 825–830.

Quon, C. & Ghil, M., 1992. Multiple equilibria in thermosolutal convection due to salt-flux boundary conditions. *J. Fluid Mech.*, **245**, 449–484.

Randall, D. A., 2015. *An Introduction to the Global Circulation of the Atmosphere*. Princeton University Press, 456 pp.

Randel, W. J., Wu, F., Swinbank, R., Nash, J. & O'Neill, A., 1999. Global QBO circulation derived from UKMO stratospheric analyse. *J. Atmos. Sci.*, **56**, 457–474.

Rayleigh, Lord, 1880. On the stability, or instability, of certain fluid motions. *Proc. London Math. Soc.*, **11**, 57–70.

Rayleigh, Lord, 1894. *The Theory of Sound, Volume II*. 2nd edn. Macmillan, 522 pp. Reprinted by Dover Publications, 1945.

Rayleigh, Lord, 1912. On the propagation of waves through a stratified medium, with special reference to the question of reflection. *Proc. Roy. Soc. Lond. A*, **86**, 207–226.

Raymond, D. J., 1995. Regulation of moist convection over the west Pacific warm pool. *J. Atmos. Sci.*, **52**, 3945–3959.

Raymond, D. J., 1997. Boundary layer quasi-equilibrium. In R. K. Smith, Ed., *The Physics and Parameterization of Moist Atmospheric Convection*, pp. 387–397. Springer.

Raymond, D. J. & Fuchs, Ž., 2009. Moisture modes and the Madden–Julian oscillation. *J. Climate*, **22**, 3031–3046.

Read, P. L., 2001. Transition to geostrophic turbulence in the laboratory, and as a paradigm in atmospheres and oceans. *Surveys Geophys.*, **33**, 265–317.

Reed, R. J., 1960. The structure and dynamics of the 26-month oscillation. Paper presented at the 40th anniversary meeting of the Am. Meter. Soc., Boston.

Reed, R. J., Campbell, W. J., Rasmussen, L. A. & Rogers, D. G., 1961. Evidence of a downward-propagating annual wind reversal in the equatorial stratosphere. *J. Geophys. Res.*, **66**, 813–818.

Reif, F., 1965. *Fundamentals of Statistical and Thermal Physics*. McGraw-Hill, 651 pp.

Rhines, P. B., 1975. Waves and turbulence on a β-plane. *J. Fluid. Mech.*, **69**, 417–443.

Rhines, P. B., 1977. The dynamics of unsteady currents. In E. A. Goldberg, I. N. McCane, J. J. O'Brien, & J. H. Steele, Eds., *The Sea*, Vol. 6, pp. 189–318. J. Wiley and Sons.

Rhines, P. B. & Holland, W. R., 1979. A theoretical discussion of eddy-driven mean flows. *Dyn. Atmos. Oceans*, **3**, 289–325.

Rhines, P. B. & Young, W. R., 1982a. Homogenization of potential vorticity in planetary gyres. *J. Fluid Mech.*, **122**, 347–367.

Rhines, P. B. & Young, W. R., 1982b. A theory of wind-driven circulation. I. Mid-ocean gyres. *J. Mar. Res. (Suppl)*, **40**, 559–596.

Richardson, L. F., 1920. The supply of energy from and to atmospheric eddies. *Proc. Roy. Soc. Lond. A*, **97**, 354–373.

Richardson, L. F., 1922. *Weather Prediction by Numerical Process*. Cambridge University Press, 236 pp. Reprinted by Dover Publications.

Richardson, L. F., 1926. Atmospheric diffusion on a distance-neighbour graph. *Proc. Roy. Soc. Lond. A*, **110**, 709–737.

Richardson, P. L., 1983. Eddy kinetic-energy in the North Atlantic from surface drifters. *J. Geophys. Res.*, **88**, 4355–4367.

Riehl, H. & Fultz, D., 1957. Jet stream and long waves in a steady rotating-dishpan experiment: structure of the circulation. *Quart. J. Roy. Meteor. Soc.*, **82**, 215–231.

Rintoul, S. R., Hughes, C. & Olbers, D., 2001. The Antarctic Circumpolar Current system. In G. Siedler, J. Church, & J. Gould, Eds., *Ocean Circulation and Climate*, pp. 271–302. Academic Press.

Ripa, P., 1981. On the theory of nonlinear wave–wave interactions among geophysical waves. *J. Fluid Mech.*, **103**, 87–115.

Robinson, A. R., 1966. An investigation into the wind as the cause of the equatorial undercurrent. *J. Mar. Res.*, **24**, 179–204.

Robinson, A. R., Ed., 1984. *Eddies in Marine Science*. Springer-Verlag, 609 pp.

Robinson, A. R. & McWilliams, J. C., 1974. The baroclinic instability of the open ocean. *J. Phys. Oceanogr.*, **4**, 281–294.

Robinson, A. R. & Stommel, H., 1959. The oceanic thermocline and the associated thermohaline circulation. *Tellus*, **11**, 295–308.

Rooth, C., 1982. Hydrology and ocean circulation. *Prog. Oceanogr.*, **11**, 131–149.

Roquet, F., Madec, G., Brodeau, L. & Nycander, J., 2015. Defining a simplified yet 'realistic' equation of state for seawater. *J. Phys. Oceanogr.*, **45**, 2564–2579.

Roquet, F., Madec, G., McDougall, T. J. & Barker, P. M., 2015. Accurate polynomial expressions for the density and specific volume of seawater using the TEOS-10 standard. *Oce. Model.*, **90**, 29–43.

Rossby, C.-G., 1936. Dynamics of steady ocean currents in the light of experimental fluid dynamics. *Papers Phys. Oceanog. Meteor.*, **5**, 1–43.

Rossby, C.-G., 1938. On the mutual adjustment of pressure and velocity distributions in certain simple current systems, II. *J. Mar. Res.*, **5**, 239–263.

Rossby, C.-G., 1939. Relations between variation in the intensity of the zonal circulation and the displacements of the semi-permanent centers of action. *J. Marine Res.*, **2**, 38–55.

Rossby, C.-G., 1940. Planetary flow patterns in the atmosphere. *Quart. J. Roy. Meteor. Soc.*, **66,** suppl., 68–87.

Rossby, C.-G., 1949. On the nature of the general circulation of the lower atmosphere. In G. P. Kuiper, Ed., *The Atmospheres of the Earth and Planets*, pp. 16–48. University of Chicago Press.

Rossby, H. T., 1965. On thermal convection driven by non-uniform heating from below: an experimental study. *Deep-Sea Res.*, **12**, 9–16.

Ruddick, B., McDougall, T. & Turner, J., 1989. The formation of layers in a uniformly stirred density gradient. *Deep-Sea Res.*, **36**, 597–609.

Rudnick, D. L. & Weller, R. A., 1993. Observations of superinertial and near-inertial wind-driven flow. *J. Phys. Oceanogr.*, **23**, 2351–2359.

Ruelle, D. & Takens, F., 1971. On the nature of turbulence. *Commun. Math. Phys.*, **20**, 167–192.

Salmon, R., 1980. Baroclinic instability and geostrophic turbulence. *Geophys. Astrophys. Fluid Dyn.*, **10**, 25–52.

Salmon, R., 1983. Practical use of Hamilton's principle. *J. Fluid Mech.*, **132**, 431–444.

Salmon, R., 1990. The thermocline as an internal boundary layer. *J. Mar. Res.*, **48**, 437–469.

Salmon, R., 1998. *Lectures on Geophysical Fluid Dynamics*. Oxford University Press, 378 pp.

Saltzman, B., 1962. Finite amplitude free convection as an initial value problem. *J. Atmos. Sci.*, **19**, 329–341.

Samelson, R. M., 1999a. Geostrophic circulation in a rectangular basin with a circumpolar connection. *J. Phys. Oceanogr.*, **29**, 3175–3184.

Samelson, R. M., 1999b. Internal boundary layer scaling in 'two-layer' solutions of the thermocline equations. *J. Phys. Oceanogr.*, **29**, 2099–2102.

Samelson, R. M., 2004. Simple mechanistic models of middepth meridional overturning. *J. Phys. Oceanogr.*, **34**, 2096–2103.

Samelson, R. M., 2011. *The Theory of Large-Scale Ocean Circulation*. Cambridge University Press, 193 pp.

Samelson, R. M. & Tziperman, E., 2001. Instability of the chaotic ENSO: the growth-phase predictability barrier. *J. Atmos. Sci.*, **58**, 3613–3625.

Samelson, R. M. & Vallis, G. K., 1997. Large-scale circulation with small diapycnal diffusion: the two-thermocline limit. *J. Mar. Res.*, **55**, 223–275.

Sandström, J. W., 1908. Dynamische Versuche mit Meerwasser (Dynamical experiments with seawater). *Annal. Hydrogr. Marit. Meteorol.*, **36**, 6–23.

Sandström, J. W., 1916. Meteorologische Studien im Schwedischen Hochgebirge (Meteorological studies in the Swedish high mountains). *Goteborgs Kungl. Vetenskaps-och Vitterhets-Samhalles, Handingar*, **27**, 1–48.

Sarachik, E. S. & Cane, M. A., 2010. *The El Niño-Southern Oscillation Phenomenon*. Cambridge University Press, 369 pp.

Sarkisyan, A. & Ivanov, I., 1971. Joint effect of baroclinicity and relief as an important factor in the dynamics of sea currents. *Izv. Akad. Nauk Atmos. Ocean. Phys.*, **7**, 116–124.

Scaife, A., Butchart, N., Warner, C. D. & Swinbank, R., 2002. Impact of a spectral gravity wave parameterization on the stratosphere in the Met Office Unified Model. *J. Atmos. Sci.*, **59**, 1473–1489.

Scaife, A. & James, I. N., 2000. Response of the stratosphere to interannual variability of tropospheric planetary waves. *Quart. J. Roy. Meteor. Soc.*, **126**, 275–297.

Schär, C., 1993. A generalization of Bernoulli's theorem. *J. Atmos. Sci.*, **50**, 1437–1443.

Schmidtko, S., Johnson, G. C. & Lyman, J. M., 2013. MIMOC: a global monthly isopycnal upper-ocean climatology with mixed layers. *J. Geophys. Res. (Oceans)*, **118**, 4, 1658–1672.

Schmitz, W. J., 1995. On the interbasin-scale thermohaline circulation. *Rev. Geophysics*, **33**, 151–173.

Schneider, E. K., 1977. Axially symmetric steady-state models of the basic state for instability and climate studies. Part II: nonlinear calculations. *J. Atmos. Sci.*, **34**, 280–297.

Schneider, T., Held, I. & Garner, S. T., 2003. Boundary effects in potential vorticity dynamics. *J. Atmos. Sci.*, **60**, 1024–1040.

Schneider, T., O'Gorman, P. A. & Levine, X. J., 2010. Water vapor and the dynamics of climate changes. *Rev. Geophys.*, **48**, RG3001.

Schneider, T. & Sobel, A., Eds., 2007. *The Global Circulation of the Atmosphere*. Princeton University Press.

Schneider, T. & Walker, C. C., 2006. Self-organization of atmospheric macroturbulence into critical states of weak nonlinearity. *J. Atmos. Sci.*, **63**, 1569–1586.

Schoeberl, M. R., 1978. Stratospheric warmings: observations and theory. *Revs. Geophys. Space Phys.*, **16**, 521–538.

Schubert, W. H., Hausman, S. A., Garcia, M., Ooyama, K. V. & Kuo, H.-C., 2001. Potential vorticity in a moist atmosphere. *J. Atmos. Sci.*, **58**, 3148–3157.

Schubert, W. H. & Masarik, M. T., 2006. Potential vorticity aspects of the MJO. *Dyn. Atmos. Oceans*, **42**, 127–151.

Schubert, W. H., Ruprecht, E., Hertenstein, R., Nieto Ferreira, R. *et al.*, 2004. English translations of twenty-one of Ertel's papers on geophysical fluid dynamics. *Meteor. Z.*, **13**, 527–576.

Scinocca, J. F. & Shepherd, T. G., 1992. Nonlinear wave-activity conservation laws and Hamiltonian structure for the two-dimensional anelastic equations. *J. Atmos. Sci.*, **49**, 5–28.

Scorer, R. S. & Ludlam, F. H., 1951. Bubble theory of penetrative convection. *Q. J. Mech. Appl. Maths*, **3**, 107–112.

Scott, R. B., 2001. Evolution of energy and enstrophy containing scales in decaying, two-dimensional turbulence with friction. *Phys. Fluids*, **13**, 2739–2742.

Scott, R. K. & Dritschel, D. G., 2012. The structure of zonal jets in geostrophic turbulence. *J. Fluid Mech.*, **711**, 576–598.

Scott, R. K. & Haynes, P. H., 1998. Internal interannual variability of the extratropical stratospheric circulation: The low latitude flywheel. *Quart. J. Roy. Meteor. Soc.*, **124**, 2149–2173.

Scott, R. K. & Haynes, P. H., 2000. Internal vacillations in stratosphere-only models. *J. Atmos. Sci.*, **57**, 2333–2350.

Shapiro, M. & Grønas, S., Eds., 1999. *The Life Cycles of Extratropical Cyclones*. American Meteorological Society, 359 pp.

Shepherd, T. G., 1983. Mean motions induced by baroclinic instability in a jet. *Geophys. Astrophys. Fluid Dyn.*, **27**, 35–72.

Shepherd, T. G., 1987. A spectral view of nonlinear fluxes and stationary-transient interaction in the atmosphere. *J. Atmos. Sci.*, **44**, 1166–1179.

Shepherd, T. G., 1990. Symmetries, conservation laws, and Hamiltonian structure in geophysical fluid dynamics. *Adv. Geophys.*, **32**, 287–338.

Shepherd, T. G., 1993. A unified theory of available potential energy. *Atmosphere–Ocean*, **31**, 1–26.

Sherwood, S. C., Roca, R., Weckwerth, T. M. & Andronova, N. G., 2010. Tropospheric water vapor, convection and climate. *Rev. Geophys.*, **48**, RG2001.

Shutts, G. J., 1983. Propagation of eddies in diffluent jet streams: eddy vorticity forcing of blocking flow fields. *Quart. J. Roy. Meteor. Soc.*, **109**, 737–761.

Silberstein, L., 1896. O tworzeniu sie wirow, w plynie doskonalym (On the creation of eddies in an ideal fluid). *W Krakaowie Nakladem Akademii Umiejetnosci (Proc. Cracow Acad. Sci.)*, **31**, 325–335.

Simmonds, J. G. & Mann, J. E., 1998. *A First Look at Perturbation Theory*. Dover Publications, 139 pp.

Simmons, A. & Hoskins, B., 1978. The life-cycles of some nonlinear baroclinic waves. *J. Atmos. Sci.*, **35**, 414–432.

Sjoberg, J. P. & Birner, T., 2012. Transient tropospheric forcing of sudden stratospheric warmings. *J. Atmos. Sci.*, **69**, 3420–3432.

Smagorinsky, J., 1953. The dynamical influences of large-scale heat sources and sinks on the quasi-stationary mean motions of the atmosphere. *Quart. J. Roy. Meteor. Soc.*, **79**, 342–366.

Smagorinsky, J., 1969. Problems and promises of deterministic extended range forecasting. *Bull. Am. Meteor. Soc.*, **50**, 286–311.

Smith, K. S., Boccaletti, G., Henning, C. C., Marinov, I. *et al.*, 2002. Turbulent diffusion in the geostrophic inverse cascade. *J. Fluid Mech.*, **469**, 13–48.

Smith, K. S. & Vallis, G. K., 1998. Linear wave and instability properties of extended range geostrophic models. *J. Atmos. Sci.*, **56**, 1579–1593.

Smith, K. S. & Vallis, G. K., 2001. The scales and equilibration of mid-ocean eddies: freely evolving flow. *J. Phys. Oceanogr.*, **31**, 554–571.

Smith, K. S. & Vallis, G. K., 2002. The scales and equilibration of mid-ocean eddies: forced-dissipative flow. *J. Phys. Oceanogr.*, **32**, 1669–1721.

Smith, L. M. & Waleffe, F., 1999. Transfer of energy to two-dimensional large scales in forced, rotating three-dimensional turbulence. *Phys. Fluids*, **11**, 1608–1622.

Smith, R. B., 1979. The influence of mountains on the atmosphere. In B. Saltzman, Ed., *Advances in Geophysics*, vol. 21, pp. 87–230. Academic Press.

Smith, R. K., 1997. On the theory of CISK. *Quart. J. Roy. Meteor. Soc.*, **123**, 407–418.

Sobel, A. & Maloney, E., 2013. Moisture modes and the eastward propagation of the MJO. *J. Atmos. Sci.*, **70**, 187–192.

Sobel, A. H., Nilsson, J. & Polvani, L., 2001. The weak temperature gradient approximation and balanced tropical moisture waves. *J. Atmos. Sci.*, **58**, 3650–3665.

Spall, M. A., 2000. Generation of strong mesoscale eddies by weak ocean gyres. *J. Mar. Res.*, **58**, 97–116.

Spiegel, E. A. & Veronis, G., 1960. On the Boussinesq approximation for a compressible fluid. *Astrophys. J.*, **131**, 442–447. (Correction: *Astrophys. J.*, **135,** 655–656).

Squire, H., 1933. On the stability of three-dimensional disturbances of viscous flow between parallel walls. *Proc. Roy. Soc. Lond. A*, **142**, 621–628.

Srinivasan, K. & Young, W., 2012. Zonostrophic instability. *J. Atmos. Sci.*, **69**, 1633–1656.

Stammer, D., 1997. Global characteristics of ocean variability estimated from regional TOPEX/Poseidon altimeter measurements. *J. Phys. Oceanogr.*, **27**, 1743–1769.

Starr, V. P., 1948. An essay on the general circulation of the Earth's atmosphere. *J. Meteor.*, **78**, 39–43.

Starr, V. P., 1968. *Physics of Negative Viscosity Phenomena*. McGraw-Hill, 256 pp.

Stechmann, S. N. & Ogrosky, H. R., 2014. The Walker circulation, diabatic heating, and outgoing longwave radiation. *Geophys. Res. Lett.*, **41**, 9097–9105.

Steers, J. A., 1962. *An Introduction to the Study of Map Projections*. Univ. of London Press, 288 pp.

Stern, M. E., 1963. Trapping of low frequency oscillations in an equatorial boundary layer. *Tellus*, **15**, 246–250.

Stevens, D. P. & Ivchenko, V. O., 1997. The zonal momentum balance in an eddy-resolving general-circulation model of the southern ocean. *Quart. J. Roy. Meteor. Soc.*, **123**, 929–951.

Stewart, G. R., 1941. *Storm*. Random House, 349 pp.

Stewartson, K., 1977. The evolution of the critical layer of a Rossby wave. *Geophys. Astrophys. Fluid Dyn.*, **9**, 185–200.

Stips, A., 2005. Dissipation measurement: theory. In H. Z. Baumert, J. Simpson, & J. Sündermann, Eds., *Marine Turbulence*. Cambridge University Press.

Stommel, H., 1958. The abyssal circulation. *Deep-Sea Res.*, **5**, 80–82.

Stommel, H., 1960. Wind-drift near the equator. *Deep-Sea Res.*, **6**, 298–302.

Stommel, H., 1961. Thermohaline convection with two stable regimes of flow. *Tellus*, **13**, 224–230.

Stommel, H. & Arons, A. B., 1960. On the abyssal circulation of the world ocean—I. Stationary planetary flow patterns on a sphere. *Deep-Sea Res.*, **6**, 140–154.

Stommel, H., Arons, A. B. & Faller, A. J., 1958. Some examples of stationary planetary flow patterns in bounded basins. *Tellus*, **10**, 179–187.

Stommel, H. & Moore, D. W., 1989. *An Introduction to the Coriolis Force*. Columbia University Press, 297 pp.

Stommel, H. & Webster, J., 1963. Some properties of the thermocline equations in a subtropical gyre. *J. Mar. Res.*, **44**, 695–711.

Stone, P. H., 1972. A simplified radiative-dynamical model for the static stability of rotating atmospheres. *J. Atmos. Sci.*, **29**, 405–418.

Stone, P. H., 1978. Baroclinic adjustment. *J. Atmos. Sci.*, **35**, 561–571.

Stone, P. H. & Nemet, B., 1996. Baroclinic adjustment: a comparison between theory, observations, and models. *J. Atmos. Sci.*, **53**, 1663–1674.

Straub, D. N., 1993. On the transport and angular momentum balance of channel models of the Antarctic Circumpolar Current. *J. Phys. Oceanogr.*, **23**, 776–782.

Straub, D. N., 1999. On thermobaric production of potential vorticity in the ocean. *Tellus A*, **51**, 314–325.

Suarez, M. & Schopf, P., 1988. A delayed action oscillator for *ENSO*. *J. Atmos. Sci.*, **45**, 323–3287.

Sukhatme, J. & Young, W. R., 2011. The advection–condensation model and water-vapour probability density functions. *Quart. J. Roy. Meteor. Soc.*, **137**, 1561–1572.

Sukoriansky, S., Dikovskaya, N. & Galperin, B., 2007. On the arrest of inverse energy cascade and the Rhines scale. *J. Atmos. Sci.*, **64**, 3312–3327.

Sutcliffe, R. C., 1939. Cyclonic and anticylonic development. *Quart. J. Roy. Meteor. Soc.*, **65**, 518–524.

Sutcliffe, R. C., 1947. A contribution to the problem of development. *Quart. J. Roy. Meteor. Soc.*, **73**, 370–383.

Sutherland, B., 2010. *Internal Gravity Waves*. Cambridge University Press, 394 pp.

Swallow, J. C. & Worthington, V., 1961. An observation of a deep countercurrent in the western North Atlantic. *Deep-Sea Res.*, **8**, 1–19.

Tailleux, R., 2016. Neutrality versus materiality: A thermodynamic theory of neutral surfaces. *Fluids*, **1**, 32.

Takahashi, M., 1996. Simulation of the stratospheric quasi-biennial oscillation using a general circulation model. *Geophys. Res. Lett.*, **23**, 661–664.

Talley, L., 1988. Potential vorticity distribution in the North Pacific. *J. Phys. Oceanogr.*, **18**, 89–106.

Talley, L. D., Pickard, G., Emery, W. J. & Swift, J. H., 2011. *Descriptive Physical Oceanography: An Introduction*. Academic press, 555 pp.

Taylor, G. I., 1921a. Diffusion by continuous movements. *Proc. London Math. Soc.*, **2** (20), 196–211.

Taylor, G. I., 1921b. Experiments with rotating fluids. *Proc. Roy. Soc. Lond. A*, **100**, 114–121.

Tennekes, H. & Lumley, J. L., 1972. *A First Course in Turbulence*. The MIT Press, 330 pp.

Tesserenc De Bort, L. P., 1902. Variations de la température de l'air libre dans la zone comprise 8 km et 13 km d'altitude (Variations in the temperature of the free air in the zone between 8 km and 13 km of altitude). *C. R. Hebd. Séances Acad. Sci.*, **134**, 987–989.

Thompson, A. F., Stewart, A. L. & Bischoff, T., 2016. A multibasin residual-mean model for the global overturning circulation. *J. Phys. Oceanogr.*, **46**, 2583–2604.

Thompson, A. F. & Young, W. R., 2006. Scaling baroclinic eddy fluxes: vortices and energy balance. *J. Phys. Oceanogr.*, **36**, 720–738.

Thompson, P. D., 1957. Uncertainty of initial state as a factor in the predictability of large scale atmospheric flow patterns. *Tellus*, **9**, 275–295.

Thompson, R. O. R. Y., 1971. Why there is an intense eastward current in the North Atlantic but not in the South Atlantic. *J. Phys. Oceanogr.*, **1**, 235–237.

Thompson, R. O. R. Y., 1980. A prograde jet driven by Rossby waves. *J. Atmos. Sci.*, **37**, 1216–1226.

Thomson, J., 1892. Bakerian lecture. On the grand currents of atmospheric circulation. *Phil. Trans. Roy. Soc. Lond. A*, **183**, 653–684.

Thomson, W. (Lord Kelvin), 1869. On vortex motion. *Trans. Roy. Soc. Edinburgh*, **25**, 217–260.

Thomson, W. (Lord Kelvin), 1871. Hydrokinetic solutions and observations. *Phil. Mag. and J. Science*, **42**, 362–377.

Thomson, W. (Lord Kelvin), 1879. On gravitational oscillations of rotating water. *Proc. Roy. Soc. Edinburgh*, **10**, 92–100.

Thorncroft, C. D., Hoskins, B. J. & McIntyre, M. E., 1993. Two paradigms of baroclinic-wave life-cycle behaviour. *Quart. J. Roy. Meteor. Soc.*, **119**, 17–55.

Thorpe, A. J., Volkert, H. & Ziemianski, M. J., 2003. The Bjerknes' circulation theorem: a historical perspective. *Bull. Am. Meteor. Soc.*, **84**, 471–480.

Thual, O. & McWilliams, J. C., 1992. The catastrophe structure of thermohaline convection in a two-dimensional fluid model and a comparison with low-order box models. *Geophys. Astrophys. Fluid Dyn.*, **64**, 67–95.

Thuburn, J., 2017. Use of the Gibbs thermodynamic potential to express the equation of state in atmospheric models. *Quart. J. Roy. Meteor. Soc.*. submitted.

Thuburn, J. & Craig, G. C., 1997. GCM tests of theories for the height of the tropopause. *J. Atmos. Sci.*, **54**, 869–882.

Thuburn, J. & Craig, G. C., 2000. Stratospheric influence on tropopause height: the radiative constraint. *J. Atmos. Sci.*, **57**, 17–28.

Tobias, S. & Marston, J., 2013. Direct statistical simulation of out-of-equilibrium jets. *Phys. Rev. Lett.*, **110**, 10, 104502.

Toggweiler, J. R. & Samuels, B., 1995. Effect of Drake Passage on the global thermohaline circulation. *Deep-Sea Res.*, **42**, 477–500.

Toggweiler, J. R. & Samuels, B., 1998. On the ocean's large-scale circulation in the limit of no vertical mixing. *J. Phys. Oceanogr.*, **28**, 1832–1852.

Toole, J. M., Polzin, K. L. & Schmitt, R. W., 1994. Estimates of diapycnal mixing in the abyssal ocean. *Science*, **264**, 1120–1123.

Tort, M. & Dubos, T., 2014. Dynamically consistent shallow-atmosphere equations with a complete Coriolis force. *Quart. J. Roy. Meteor. Soc.*, **140**, 684, 2388–2392.

Tréguier, A. M., Held, I. M. & Larichev, V. D., 1997. Parameterization of quasi-geostrophic eddies in primitive equation ocean models. *J. Phys. Oceanogr.*, **29**, 567–580.

Trenberth, K. E., 1997. The definition of El Niño. *Bull. Am. Meteor. Soc.*, **78**, 2771–2777.

Trenberth, K. E. & Caron, J. M., 2001. Estimates of meridional atmosphere and ocean heat transports. *J. Climate*, **14**, 3433–3443.

Tritton, D. J., 1988. *Physical Fluid Dynamics*. Oxford University Press, 519 pp.

Truesdell, C., 1951. Proof that Ertel's vorticity theorem holds in average for any medium suffering no tangential acceleration on the boundary. *Geofis Pura Appl.*, **19**, 167–169.

Truesdell, C., 1954. *The Kinematics of Vorticity*. Indiana University Press, 232 pp.

Truesdell, C., 1969. *Rational Thermodynamics*. McGraw Hill, 208 pp.

Tsang, Y.-K. & Vanneste, J., 2016. Advection-condensation of water vapor in a model of coherent stirring. Submitted to *Proc. Roy. Soc. A*.

Tudhope, A. W., Chilcott, C. P., McCulloch, M. T., Cook, E. R. *et al.*, 2001. Variability in the El Niño Southern Oscillation through a glacial-interglacial cycle. *Science*, **291**, 1511–1517.

Tung, K. K., 1979. A theory of stationary long waves. Part III: quasi-normal modes in a singular wave guide. *Mon. Wea. Rev.*, **107**, 751–774.

Tziperman, E., Stone, L., Cane, M. A. & Jarosh, H., 1994. El Niño chaos: Overlapping of resonances between the seasonal cycle and the Pacific ocean-atmosphere oscillator. *Science*, **264**, 72–73.

Valdes, P. J. & Hoskins, B. J., 1988. Baroclinic instability of the zonally averaged flow with boundary layer damping. *J. Atmos. Sci.*, **45**, 1584–1593.

Vallis, G. K., 1982. A statistical dynamical climate model with a simple hydrology cycle. *Tellus*, **34**, 211–227.

Vallis, G. K., 1985. Instability and flow over topography. *Geophys. Astrophys. Fluid Dyn.*, **34**, 1–38.

Vallis, G. K., 1988a. Conceptual models of El Niño and the Southern Oscillation. *J. Geophys. Res.*, **93**, 13979–13991.

Vallis, G. K., 1988b. Numerical studies of eddy transport properties in eddy-resolving and parameterized models. *Quart. J. Roy. Meteor. Soc.*, **114**, 183–204.

Vallis, G. K., 1996. Potential vorticity and balanced equations of motion for rotating and stratified flows. *Quart. J. Roy. Meteor. Soc.*, **122**, 291–322.

Vallis, G. K., 2000. Large-scale circulation and production of stratification: effects of wind, geometry and diffusion. *J. Phys. Oceanogr.*, **30**, 933–954.

Vallis, G. K. & Maltrud, M. E., 1993. Generation of mean flows and jets on a beta plane and over topography. *J. Phys. Oceanogr.*, **23**, 1346–1362.

Vallis, G. K., Zurita-Gotor, P., Cairns, C. & Kidston, J., 2015. The response of the large-scale structure of the atmosphere to global warming. *Quart. J. Roy. Meteor. Soc.*, **141**, 1479–1501.

Vanneste, J. & Shepherd, T. G., 1998. On the group-velocity property for wave-activity conservation laws. *J. Atmos. Sci.*, **55**, 1063–1068.

Verkley, W. T. M. & van der Velde, I. R., 2010. Balanced dynamics in the tropics. *Quart. J. Roy. Meteor. Soc.*, **136**, 41–49.

Veronis, G., 1960. An approximate theoretical analysis of the equatorial undercurrent. *Deep-Sea Res.*, **6**, 318–327.

Veronis, G., 1966a. Wind-driven ocean circulation – Part 1: Linear theory and perturbation analysis. *Deep-Sea Res.*, **13**, 17–29.

Veronis, G., 1966b. Wind-driven ocean circulation – Part 2: Numerical solutions of the non-linear problem. *Deep-Sea Res.*, **13**, 30–55.

Veronis, G., 1969. On theoretical models of the thermocline circulation. *Deep-Sea Res.*, **31** Suppl., 301–323.

Veryard, R. G. & Ebdon, R. A., 1961. Fluctuations in tropical stratospheric winds. *Meteor. Mag*, **90**, 125–143.

Visbeck, M., Marshall, J., Haine, T. & Spall, M., 1997. Specification of eddy transfer coefficients in coarse-resolution ocean circulation models. *J. Phys. Oceanogr.*, **27**, 381–402.

Von Neumann, J., 1955. Methods in the physical sciences. In L. G. Leary, Ed., *The Unity of Knowledge*. Doubleday.

Walker, C. & Schneider, T., 2005. Response of idealized Hadley circulations to seasonally varying heating. *Geophys. Res. Lett.*, **32**, L06813. doi:10.1029/2004GL022304.

Wallace, J. M., 1973. General circulation of the tropical lower stratosphere. *Rev. Geophys.*, **11**, 191–222.

Wallace, J. M., 1983. The climatological mean stationary waves: observational evidence. In B. Hoskins & R. P. Pearce, Eds., *Large-Scale Dynamical Processes in the Atmosphere*, pp. 27–63. Academic Press.

Wallace, J. M. & Hobbs, P. V., 2006. *Atmospheric Science: An Introductory Survey*. 2nd edn. Elsevier, 483 pp.

Wallace, J. M. & Holton, J. R., 1968. A diagnostic numerical model of the quasi-biennial oscillation. *J. Atmos. Sci.*, **25**, 280–292.

Warn, T., Bokhove, O., Shepherd, T. G. & Vallis, G. K., 1995. Rossby number expansions, slaving principles, and balance dynamics. *Quart. J. Roy. Meteor. Soc.*, **121**, 723–739.

Warn, T. & Warn, H., 1976. On the development of a Rossby wave critical level. *J. Atmos. Sci.*, **33**, 2021–2024.

Warren, B. A., 1981. Deep circulation of the world ocean. In B. A. Warren & C. Wunsch, Eds., *Evolution of Physical Oceanography*, pp. 6–41. The MIT Press.

Warren, B. A., 1999. Approximating the energy transport across oceanic sections. *J. Geophys. Res.*, **104**, 7915–7920.

Warren, B. A., 2006. The first law of thermodynamics in a salty ocean. *Progress in Oceanography*, **70**, 2, 149–167.

Warren, B. A., LaCasce, J. H. & Robbins, P. E., 1996. On the obscurantist physics of form drag in theorizing about the Circumpolar Current. *J. Phys. Oceanogr.*, **26**, 2297–2301.

Wasow, W., 1944. Asymptotic solution of boundary value problems for the differential equation $\Delta U + \lambda(\partial/\partial x)U = \lambda f(x, y)$. *Duke Math J.*, **11**, 405–415.

Watson, A., Vallis, G. K. & Nikurashin, M., 2015. Southern Ocean buoyancy forcing of ocean ventilation and glacial atmospheric CO_2. *Nature Geosciences*, **8**, 861–864. doi:10.1038/ngeo2538.

Webb, D. J. & Suginohara, N., 2001. Vertical mixing in the ocean. *Nature*, **409**, 37.

Weinstock, R., 1952. *Calculus of Variations*. McGraw-Hill. Reprinted by Dover Publications, 1980, 328 pp.

Welander, P., 1959. An advective model of the ocean thermocline. *Tellus*, **11**, 309–318.

Welander, P., 1968. Wind-driven circulation in one- and two-layer oceans of variable depth. *Tellus*, **20**, 1–15.

Welander, P., 1971a. Some exact solutions to the equations describing an ideal-fluid thermocline. *J. Mar. Res.*, **29**, 60–68.

Welander, P., 1971b. The thermocline problem. *Phil. Trans. Roy. Soc. Lond. A*, **270**, 415–421.

Welander, P., 1973. Lateral friction in the ocean as an effect of potential vorticity mixing. *Geophys. Fluid Dyn.*, **5**, 101–120.

Welander, P., 1986. Thermohaline effects in the ocean circulation and related simple models. In J. Willebrand & D. L. T. Anderson, Eds., *Large-scale Transport Processes in Oceans and Atmospheres*, pp. 163–200. Reidel.

Wentzel, G., 1926. Eine Verallgemeinerung der Quantenbedingungen für die Zwecke der Wellenmechanik (A generalization of the quantum conditions for the purposes of wave mechanics). *Zeit. fur Physic A*, **38**, 518–529.

Wheeler, M. & Kiladis, G. N., 1999. Convectively coupled equatorial waves: Analysis of clouds and temperature in the wavenumber-frequency domain. *J. Atmos. Sci.*, **56**, 374–399.

White, A. A., 1977. Modified quasi-geostrophic equations using geometric height as vertical co-ordinate. *Quart. J. Roy. Meteor. Soc.*, **103**, 383–396.

White, A. A., 2002. A view of the equations of meteorological dynamics and various approximations. In J. Norbury & I. Roulstone, Eds., *Large-Scale Atmosphere-Ocean Dynamics I*, pp. 1–100. Cambridge University Press.

White, A. A., 2003. The primitive equations. In J. Holton, J. Pyle, & J. Curry, Eds., *Encyclopedia of Atmospheric Science*, pp. 694–702. Academic Press.

White, A. A., Hoskins, B. J., Roulstone, I. & Staniforth, A., 2005. Consistent approximate models of the global atmosphere: shallow, deep, hydrostatic, quasi-hydrostatic and non-hydrostatic. *Quart. J. Roy. Meteor. Soc.*, **131**, 609, 2081–2107.

Whitehead, J. A., 1975. Mean flow generated by circulation on a beta-plane: An analogy with the moving flame experiment. *Tellus*, **27**, 358–364.

Whitehead, J. A., 1995. Thermohaline ocean processes and models. *Ann. Rev. Fluid Mech.*, **27**, 89–113.

Whitham, G. B., 1974. *Linear and Nonlinear Waves*. Wiley-Interscience, 656 pp.

Williams, G. P., 1978. Planetary circulations: 1. Barotropic representation of Jovian and terrestrial turbulence. *J. Atmos. Sci.*, **35**, 1399–1426.

Wittenberg, A. T., 2009. Are historical records sufficient to constrain ENSO simulations? *Geophys. Res. Lett.*, **36**, L12702. doi:10.1029/2009GL038710.

Wolfe, C. L. & Cessi, P., 2010. What sets the middepth stratification of eddying ocean models? *J. Phys. Oceanogr.*, **40**, 1520–1538.

Wolfe, C. L. & Cessi, P., 2011. The adiabatic pole-to-pole overturning circulation. *J. Phys. Oceanogr.*, **41**, 1795–1810.

World Meteorological Organization, 1957. Definition of the tropopause. *WMO Bulletin*, **6**, 136.

Wunsch, C., 2002. What is the thermohaline circulation? *Science*, **298**, 1179–1180.

Wunsch, C., 2015. *Modern Observational Physical Oceanography*. Princeton University Press, 481 pp.

Wunsch, C. & Ferrari, R., 2004. Vertical mixing, energy, and the general circulation of the oceans. *Ann. Rev. Fluid Mech.*, **36**, 281–314.

Wunsch, C. & Roemmich, D., 1985. Is the North Atlantic in Sverdrup balance? *J. Phys. Oceanogr.*, **15**, 1876–1880.

Wyrtki, K., 1952. Der Einfluss des Windes auf den mittleren Wasserstand Der Nordsee und ihren Wasserhausalt (the influence of the wind on the mean sea level and water budget of the north sea). *Dtsch.. Hydrogr. Z.*, **5**, 21–27.

Wyrtki, K., 1975. El Niño—The dynamic response of the equatorial Pacific ocean to atmospheric forcing. *J. Phys. Oceanogr.*, **5**, 572–584.

Wyrtki, K., 1985. Water displacements in the Pacific and the genesis of El Niño cycles. *J. Geophys. Res.*, **90**, 7129–7132.

Wyrtki, K., Magaard, L. & Hager, J., 1976. Eddy energy in oceans. *J. Geophys. Res.*, **81**, 2641–2646.

Xu, X., Rhines, P. B., Chassignet, E. P. & Schmitz, W. J., 2015. Spreading of Denmark Strait overflow water in the western subpolar North Atlantic: insights from eddy-resolving simulations with a passive tracer. *J. Phys. Oceanogr.*, **45**, 2913–2932.

Yaglom, A. M., 1994. A. N. Kolmogorov as a fluid mechanician and founder of a school in turbulence research. *Ann. Rev. Fluid Mech.*, **26**, 1–22.

Yanai, M. & Maruyama, T., 1966. Stratospheric wave disturbances in the tropical stratosphere. *J. Meteor. Soc. Japan*, **44**, 291–294.

Yoden, S., 1987. Bifurcation properties of a stratospheric vacillation model. *J. Atmos. Sci.*, **44**, 1723–1733.

Yoden, S., 1990. An illustrative model of seasonal and interannual variations of the stratospheric circulation. *J. Atmos. Sci.*, **47**, 1845–1853.

Young, W. R., 2010. Dynamic enthalpy, conservative temperature, and the seawater Boussinesq approximation. *J. Phys. Oceanogr.*, **40**, 394–400.

Young, W. R., 2012. An exact thickness-weighted average formulation of the Boussinesq equations. *J. Phys. Oceanogr.*, **42**, 692–707.

Young, W. R. & Rhines, P. B., 1982. A theory of the wind-driven circulation II. Gyres with western boundary layers. *J. Mar. Res.*, **40**, 849–872.

Zebiak, S. E. & Cane, M. A., 1987. A model El Niño Southern Oscillation. *Mon. Wea. Rev.*, **115**, 2262–2278.

Zeng, N., Neelin, J. D. & Chou, C., 2000. A quasi-equilibrium tropical circulation model – implementation and simulation. *J. Atmos. Sci.*, **57**, 1767–1796.

Zhang, C., 2005. Madden–Julian oscillation. *Rev. Geophys.*, **43**, 1–36.

Zhang, R. & Vallis, G. K., 2007. The role of the bottom vortex stretching on the path of the North Atlantic western boundary current and on the northern recirculation gyre. *J. Phys. Oceanogr.*, **37**, 2053–2080.

Zurita-Gotor, P. & Lindzen, R., 2007. Theories of baroclinic adjustment and eddy equilibration. In T. Schneider & A. Sobel, Eds., *The Global Circulation of the Atmosphere: Phenomena, Theory, Challenges*. Princeton University Press.

Zurita-Gotor, P. & Vallis, G. K., 2009. Equilibration of baroclinic turbulence in primitive equations and quasi-geostrophic models. *J. Atmos. Sci.*, **66**, 837–863.

Zurita-Gotor, P. & Vallis, G. K., 2011. Dynamics of mid-latitude tropopause height in an idealized model. *J. Atmos. Sci.*, **68**, 823–838.

Index

Bold face denotes a primary entry or an extended discussion.

Abbe, Cleveland, 442
Absolute humidity, 675
Abyssal ocean circulation, **818–828**
    wind driven, 829
ACC, **836–845**
    adiabatic model of, 843
    and mesoscale eddies, 837
    form drag in, 844
    momentum balance, 837, 839, 841
Acoustic-gravity waves, **293–296**
Adiabatic lapse rate
    dry, 99
    moist, 692
Adiadbatic lapse rate, 48
Advection-diffusion-condensation models, 686
Advective derivative, 4
Anelastic approximation, **75–78**
Anelastic equations, 76, 78
    energetics of, 78
Angular momentum, 67
    spherical coordinates, 67
Antarctic Circumpolar Current, **836–845**
Antisymmetric turbulent diffusivity, 491
APE, 137
Arnold stability conditions, 406
Asymptotic models
    conservation properties of, 187
    quasi-geostrophy, 188
Atmospheric stratification, **572–581**
Auto-barotropic fluid, 14
Available potential energy, **137–140**
    Boussinesq fluid, 138
    ideal gas, 139

Balanced dynamics
    tropics, 711
Baroclinic adjustment, 576
Baroclinic circulation theorem, 151
Baroclinic eddies, **464–471**
    effect on Hadley Cell, 528
    in atmosphere, 465
    in ocean, 468
    magnitude and scale, 464
Baroclinic eddy diffusivities, 494
Baroclinic fluid, 14
Baroclinic instability, **335**, **347–367**
    beta effect in continuous model, 369
    beta effect in two-layer model, 360
    Eady problem, 351
    effect of stratosphere, 372
    energetics of, 367
    high-wavenumber cut-off, 343, 360, 410, 459
    in ocean, 373
    interacting edge waves, 363
    linear QG equations, 349
    mechanism of, 347
    minimum shear, 361
    necessary conditions for, 351, 408, 410
    neutral curve in two-layer problem, 362
    non-uniform shear and stratification, 372
    sloping convection, 347
    two-layer problem, 356
Baroclinic lifecycle, 466
Baroclinic lifecycles
    in atmosphere, 465
    in ocean, 468, 470
Baroclinic term, 145
Baroclinic triads, 457
Barotropic fluid, 14, 20
Barotropic instability, **335**
Barotropic jet, **540–549**
    and Rossby waves, 542
    and the EP flux, 547

numerical example, 548
Barotropic triads, 457
Batchelor scale, 439
Batchelor spectrum, 439
Bernoulli function, 44
Bernoulli's theorem, 44
and potential vorticity flux, 167
Beta effect, 154, 155
in two-dimensional turbulence, 445
Beta plane vorticity equation, 156
Beta scale, 446, 447
Beta-plane approximation, **69**
Beta-Rossby number, 559, 735
Bjerknes, Jacob, 907
Bjerknes, Vilhelm, 169
Bjerknes-Silberstein circulation theorem, 151
Boiling point, 678
Bolus velocity, 500, 503
Bottom pressure stress, 755
Boundary layers
Ekman, 201
Boussinesq approximation, **70–75**
Boussinesq equations, 71
asymptotic derivation, 101
energetics of, 74
potential vorticity conservation, 163
relation to pressure coordinates, 82
strong and weak versions, 78
summary, 74
Box ocean models, **813–818**
many boxes, 817
two boxes, 814
Breaking waves, 599
Bretherton's boundary layer, 191
Brewer–Dobson circulation, **631–643**, 644, 669
Brunt–Väisälä frequency, 97
Buoyancy frequency, 73, 97
ideal gas, 99
ocean, 99
Buoyancy-driven ocean circulation, 801, 813
Burger number, 173

Cabbeling, 39
CAPE, 695
Centrifugal force, 57
Chaos, 433, 435
a brief history, 443
Charney problem, 369
Charney, Jule, 376
Charney–Drazin condition, 599, 601, 603
Charney–Eliassen problem, 609
Charney–Green number, 370
Charney–Stern–Pedlosky criterion for instability, 351
Chemical potential, 16, 17
CIN, 695
Circular reference, *see* Reference, circular
Circulation, **143–153**
Circulation theorem, 150, **147–156**
baroclinic, 151
barotropic fluid, 150
beta effect, 154
hydrostatic flow, 152
rotating flow, 152
CISK, 727
Clausius–Clapeyron equation, **678–679**
ideal gas, 679
Closure problem of turbulence, 413
Compensating subsidence, 716
Compressible flow, 41
Concentration and mixing ratio, 10
Condensation-diffusion models, 681
Condensation-diffusion-advection models, 686
Conditional instability, 695, 696
Conservative temperature, 36, 39
Conservative tracers, 10
Convection, 699
energetics of, 696
moist, 695
Convective adjustment, 697, 706
Convective instability, 261
Convective plumes, 805
Convective quasi-equilibrium, 698
Conventional equation of state, 13
Coriolis acceleration, 57
Coriolis force, **57–58**
Coriolis, Gaspard Gustave de, 103
Critical layers, 594
gravity wave, 597
Rossy wave, 594
Critical levels, 634
Critical line, 593, **594**, 607
Cyclostrophic balance, 91, 95, 96

Deacon Cell, 833, 841, 843, 852
Deacon cell, 834
Deformation radius, 124, 125
Delayed oscillator model of El Niño, 904
Density
neutral, 32
potential, 24
Dew point, 724
Diffusion
equation of, 473
potential vorticity, 505
turbulent, 473
Diffusion-condensation models, 681
Diffusive fluxes, 490
Diffusive thermocline, **779–785**, 805
Diffusive transport, 473
Diffusivity tensors, 490

Dispersion relation, 215, 216, **219**
  Rossby waves, 228
Divergence equation, 96
Downward control, 648
Dry adiabatic lapse rate, 29, 48, 99
Dumbbell in beta-plane turbulence, 448

Eady problem, **351–356**, 357
  eddy effect on mean-flow, 399
  secondary circulation, 399
  with beta, 371
Eady, Eric, 376
Eddy diffusion, 475
  two-dimensional, 483
Eddy transport
  and the TEM, 506
  velocity, 500
Eddy vicoscity, 202
Edge waves, 340, 341, 343
  Eady problem, 365
  in shear flows, 340
Effective gravity, 59
Egg, boiling, 678
Ekman layers, **201–211**
  integral properties of, 204
  momentum balance, 203
  observed, 209
  stress in, 201
Ekman number, 202
Ekman spiral, 206, 209
El Niño, **886–904**
  toy models, 898
Elephant, 610
Eliassen–Palm flux, **383–387**, 568
  and barotropic jets, 547
  and form drag, 397
  observed, 568
  primitive equations, 581
  spherical coordinates, 581
Eliassen–Palm relation, 384
Energetics
  of quasi-geostrophic equations, 198
Energy budget, 42
  constant density fluid, 42
  variable density fluid, 43
  viscous effects, 45
Energy conservation
  Boussinesq equations, 74
  primitive equations, 65
  shallow water equations, 122
Energy flux, 234
  Bernoulli function, 44
  Rossby waves, 234–236
Energy inertial range
  in two-dimensional turbulence, 429
Energy transfer in two-dimensional flow, 424

ENSO, 886
Enstrophy inertial range, 424, 429
  passive tracer in, 439
Enstrophy transfer in two-dimensional flow, 424
Enthalpy, 17, 45, 49
  dynamic, 37
  fluxes in convection, 705
  generalized, 45
  ideal gas, 21
  of vaporization, 677
  potential, 36, 37, 49
  potential, generalized, 46
Enthalpy of vaporization, 722
Entropy, 14, 24, 48
  moist air, 721
Equation of State, **14**
Equation of state, **13**
  conventional or thermal, 13
  fundamental, 14, 15, 20
  ideal gas, 13
  moist air, 674
  seawater, 13, 33
Equations of motion, **3**
  for tropics, 711
  rotating frame, 55
  tropical atmosphere, 708
Equatorial undercurrent, **865**, 867, 874
  ideal fluid model, **876–885**
  local model, **865–876**
Equatorial waves
  stratosphere, 634
Equivalent potential temperature, 680, **694**, 723
Equivalent topography, 617
Euler, Leonard, 52
Eulerian and Lagrangian, 3
Eulerian derivative, 4
Eulerian viewpoint, 4
Exner function, 136
Explication, 156, 170

f-plane approximation, 69
Ferrel Cell, **534–536**, 571
  eddy fluxes in, 536
  surface flow in, 535
Ferrel, William, 537
Field or Eulerian viewpoint, 4
First law of thermodynamics, 15, **49**
Fjørtoft's criterion for instability, 347, 408
Fluid element, 4
Fofonoff model, 751
Force
  centrifugal, 57
  Coriolis, 58
Form drag, 119
  and Eliassen Palm flux, 397

at ocean bottom, 755
in ACC, 839, 844
Form stress, **119–120**
Four-thirds law, 482
Free energy, 17
Free-slip condition, 741
Frequency, 216
Frictional–geostrophic balance, 202
Froude number, 86, 173, 494
Frozen in property of vorticity, 147
Fundamental equation of state, 14, 15, 20
ideal gas, 25, **47–49**
Fundamental postulate of thermodynamics, 14
Fundamental thermodynamic relation, 16

Gas constant, 674
Generalized enthalpy, 46
Gent–McWilliams scheme, 499
Geopotential surfaces, 60
Geostrophic adjustment, **127–134**
energetics of, 130
Rossby problem, 128
Geostrophic balance, **87–93**, 95, 118
a variational perspective, 133
frictional, 202
in shallow water equations, 118
pressure coordinates, 91
Geostrophic contours, 764
Geostrophic scaling, 171
in continuously stratified equations, 174
in shallow water equations, 171
Geostrophic turbulence, **445**, 460
Larichev–Held model, 460
stratified, 454
two layers, 455
two-dimensional, beta-plane, 445
Gibbs function, 17, 18
equilibration, 677
for seawater, 33
ideal gas, 25, **47**
moist air, 720
Gradient wind balance, 91, 96, **94–97**
in Eulerian equations, 96
Gravity waves, 100, 101, **251**
acoustic, 293
critical line, 594
hydrostatic, 261
stratosphere, 634
Green and Stone turbulent transport, 494
Group velocity, **220–224**, **240**
internal waves, 264
property for wave activity, 384
Group velocity property, **242–246**
Gyres, 731

Hadley Cell, **516–534**
angular-momentum-conserving model, 516
effects of eddies on, 528, 532
effects of moisture on, 522
poleward extent, 517
radiative equilibrium solution, 523
seasonal effects and hemispheric asymmetry, 525
shallow water model of, 524
strength of, 517
Hadley, George, 537
Haney boundary condition, 802, 858
Heat capacity, 21
Held–Hou model of Hadley Cell, 516
Helmholtz function, 18
Hermite polynomials, **330**
Hide's theorem, 523, 537
Holton, Jim, 104
Homentropic fluid, 14, 20, 53
Homogenization of a tracer, **487–489**
Horizontal convection, **802–813**
maintenance of, 808
Humidty
measures of, 675
Hurricanes , 727
Hydrostasy, 12
accuracy, 86
scaling for, 83, 84
Hydrostatic approximation
accuracy, 86
in deriving primitive equations, 64
Hydrostatic balance, 12, **87**
effects of rotation, 92
effects of stratification, 85
scaling for, 84, 93, **83–93**
Hydrostatic equations
potential vorticity conservation, 164
Hydrostatic internal waves, 261

Ideal gas, 20
buoyancy frequency, 99
enthalpy, 21
equation of state, 13
fundamental equation of state, 25, 47
heat capacity, 21
simple and general, 20
thermodynamics of, 23
Impermeability of potential vorticity, 165
Incompressible flow, 41, **41–42**
conditions for, 41
Inertial flow, 96
Inertial oscillations, 126
Inertial range, **418**, 423
3D, 418
energy in 2D, 429
energy in 3D, 419

enstrophy, 429
two-dimensional turbulence, 427
Inertial western boundary currents, **747**
Inertial-diffusive range, 441
Inflection point criterion, 346
Instability
baroclinic, 335, 347
barotropic, 335
Kelvin–Helmholtz, 335
necessary conditions in baroclinic flow, 351
necessary conditions in shear flow, 345
parallel shear flow, 337
Intermediate models, 186
Intermittency, 423
Internal energy, 20, 48
Internal thermocline, **779–785**
Internal waves, 100, **259–261**
energetics, 267
group velocity, 264, 268
polarization properties, 261
polarization relations, 261
rays, 273
reflection, 268
stratosphere, 634
topographic generation, 283
Inverse cascade, **424**, 429
energy-enstrophy argument, 425
similarity theory, 426
vorticity elongation, 424
Inversion, 147
of vorticity, 147
Inviscid western boundary currents, **753–757**
Isentropic coordinates, **134–137**
and quasi-geostrophy, 196
Boussinesq fluid, 135
ideal gas, 136
Isopycnal coordinates, 135

JEBAR, joint effect of baroclinicity and relief, 756
Jets, **448–453**, **540–549**
and the pseudomomentum budget, 544
and the vorticity budget, 541
atmospheric, 540
eddy-driven, 540
in beta-plane turbulence, 448
numerical simulation of, 449
Joint effect of baroclinicity and relief, 756
Joint effect of beta and friction, 449
Jump conditions, 339
JWKB approximation, 247, 623

K41 theory, 416, 418
Kelvin cat's eye, 597
Kelvin waves, 126, 636
Kelvin's circulation theorem, **150**, 156
Kelvin–Helmholtz instability, **335**, 340
Kinematic stress, 202
Kinematic viscosity, 12
Kinematics
of waves, 215
Kolmogorov scale, 420
Kolmogorov theory, **416–422**
Kolmogorov theory of turbulence, 418
Kolmogorov, A. N., 441

Lagrange, Joseph-Louis, 52
Lagrangian derivative, 4
Lagrangian viewpoint, 3, 4
Lamb waves, 295
Lapse rate, **99**
adiabatic, of density, 27
adiabatic, of temperature, 29
dry adiabatic, 29, 99
dry ideal gas, 99
of seawater, 34
saturated, 692
Latent heat, 722
Latent heat of evaporation, 677
Level of free convection, 695
Lifecycle of baroclinic waves, 466
in atmosphere, 465
in ocean, 468, 470
Lifting condensation level, 695
Liouville–Green approximation, 247
Locality in turbulence, 423
Log-pressure coordinates, 82
Lorenz equations, 433
Lorenz, Edward, 141, 142
LPS model, 785
Luyten–Pedlosky–Stommel model, 785

M equation, 779
one-dimensional model, 780
Mach number, 42
Macro-turbulence, 445
Madden–Julian oscillation, 717
Main thermocline, 774
Margules relation, 119
Mass continuity, **7–10**
Eulerian derivation, 7
in a rotating frame, 58
in Boussinesq equations, 72
Lagrangian derivation, 9
Mass continuity equation
shallow water, 107
Material derivative, **4–7**
finite volume, 5
fluid property, 5
Material viewpoint, 4
Maxwell relations, **17**, **19**
Mercator coordinates, 621
Meridional overturning circulation, 801

atmospheric, Eulerian, 514
of atmosphere, 514
of ocean, 801
wind-driven, ocean, 829
Mid-latitude atmospheric circulation, **549–571**
Minimum shear for baroclinic instability, 361
Mixing length theory, **484–487**
Mixing ratio, 675
Mixing ratio and concentration, 10
MJO, 717
MOC, 514, 801
stratosphere, 644
wind-driven, ocean, 829
Moist convection, **695–700**
Moist thermodynamics, 720
Moisture
effect on potential vorticity, 160
effects on Hadley Cell, 522
Momentum equation, **11–13**
in a rotating frame, 58
shallow water, 106
vector invariant form, 66
monsoons, 717
Montgomery potential, 136
Mountain waves, 283
Multi-layer QG equations, 185
Munk wind-driven model, 740
properties of, 741

Natural coodinates, 94
Navier, Claude, 53
Necessary conditions for baroclinic instability, 408, 410
Necessary conditions for instability, **403–411**
baroclinic flow, 351
Charney–Stern–Pedlosky criterion, 351, 404
Fjørtoft's criterion, 347, 408
Rayleigh–Kuo criterion, 346, 404
relation to eddy fluxes, 564
shear flow, 345
use of pseudoenergy, 406
use of pseudomomentum, 403
Neutral density, 32, 33, 53, 774, 799
No-slip condition, 741
Non-acceleration result, 379, 639
Non-acceleration theorem, **394–399**
Non-homentropic term, 145
Nondimensionalization
in rotating flow, 171
nondimensionalization, **46–47**

Oblate spheroid, 59, 60
Observations
MJO, 718
abyssal ocean, 829
Atlantic Ocean, 803
atmospheric meridional overturning circulation, 514, 572
atmospheric stratification, mean, 572
atmospheric wind and temperature, 513
deep ocean circulation, 801
deep western boundary current, 827
Ekman layers, 209
Eliassen–Palm flux, 568, 570
Eliassen–Palm flux divergence, 570
equatorial ocean currents, 861
Global Ocean, 735
global ocean currents, 732
main thermocline, 774
North Atlantic, 827
North Atlantic currents, 733
ocean stratification, 802
oceanic meridional overturning circulation, 801
of the atmosphere, 511
potential vorticity, ocean, 770
reanalysis, 537
relative humidity, 682
surface winds, 514
zonally-averaged atmosphere, 515
zonally-averaged zonal wind, 570
Ocean circulation
abyssal, 821
laboratory model of, 818
scaling for buoyancy-driven, 813
wind-driven, 733
wind-driven abyssal, 829
Ocean currents, 732
Ocean gyres, 731
Omega equation, 192
Outcropping, 788

Parabolic cylinder functions, 330
Parcel method, **97–99**, 695
Passive tracer, **437–441**
in three dimensions, 439
in two dimensions, 439
spectra of, 437
Perfect gas, 47
Phase speed, 217, **216–219**
Phase velocity, 219
Phillips instability problem, 356
Piecewise linear flows, 338
Plane waves, 216
Planetary waves, 585
Planetary-geostrophic equations, **176–180**
for shallow water flow, 176
for stratified flow, 178
Planetary-geostrophic potential vorticity
equation, 178, 179
shallow water, 178

stratified, 179
Poincaré waves, 124, 125, 244
Poincaré, Henri, 141
Polar vortex, 629
Polarization properties of internal waves, 261
Polarization relations, 261
Polytropic fluid, 14
Potential density, 24, 25, 27, 30, **32**
and static instability, 97
of seawater, 27, 32
Potential enthalpy, 36, 46, 49
Potential temperature, 24, 30, 49
equivalent, 694
ideal gas, 25
moist air, 722
of liquids, 28
seawater, 28, 34
Potential vorticity, 143, **156–168**
and Bernoulli's theorem, 167
and the frozen-in property, 158
Boussinesq equations, 163
concentration, 165
conservation of, 156
diffusion of, 505
for baroclinic fluids, 157
for barotropic fluids, 156
homogenization of, 793
hydrostatic equations, 164
impermeability of isentropes, 165
mixing, 575, 576
moisture effect, 160
ocean observations, 770
on isentropic surfaces, 164
planetary-geostrophic, 178
quasi-geostrophic, 190
relation to circulation, 156
salinity effect, 160
shallow water, 120, 162, 182
staircase, 451–453
substance, 165
Potential vorticity flux, 566
Potential vorticity fluxes, atmospheric, 566
Potential vorticity homogenization, 487
Potential vorticity transport
and tropospheric stratification, 574
Prandtl number, 439, 804
Predictability, **433–437**
of Lorenz equations, 433
of turbulence, 435
of weather, 437
Pressure, 11, 17
Pressure coordinates, **79**, 81
and quasi-geostrophy, 192
relation to Boussinesq equations, 82
Primitive equations, **64**
potential vorticity conservation, 164
vector form, 65
Pseudoenergy, 406
and hydrodynamic instability, 406
and wave activity, 407
Pseudomomentum, 384
and hydrodynamic stability, 403
and zonal jets, 544

QBO, **652–662**
essentials, 655
Quasi-biennial oscillation, **652–662**
Quasi-equilibrium, **698**, 699
Quasi-geostrophic
wave–mean-flow interaction, 380
Quasi-geostrophic potential vorticity
equation, 190
relation to Ertel PV, 195
Quasi-geostrophic turbulence, 454
Quasi-geostrophy, **180–195**
asymptotic derivation, 188
buoyancy advection at surface, 191
continuously stratified, 187
energetics, 198
in isentropic coordinates, 196
informal derivation, 193
multi-layer, 185–186
pressure coordinates, 192
shallow water, 180
sheet at boundary, 191
single layer, 180
stratified equations, **187–194**
two-layer, 184–185
two-level, 194

Radiation condition, 543
Radiative equilibrium temperature, 511
Radiative equililibrium, 700–703
Radiative transfer, 724
Radiative-convective equililibrium, 703–706
Radius of deformation, 124, 125
Random walk, 476
Ray theory, **224–226**, 621
Ray tracing, 621
Rayleigh criterion for instability, 345
Rayleigh equation, 338
Rayleigh number, 804
Rayleigh's equation, 338
Rayleigh–Kuo criterion, 346, 404
Rayleigh–Kuo equation, 338
Rays, 226, 273
equatorial, 314
in internal waves, 273
Reanalysis, **537**, 537
Recharge-discharge oscillator, 901
Reduced gravity equations, **110–112**

Reference, circular, *see* Circular reference
Reflection
  internal waves, 268
  Rossby waves, 237
Refractive index, 587, 599
Relative humidity, 675, 676, **680–690**
  in mid-latitudes, 688
Relative vorticity, 152
Residual circulation, 388
  and thickness-weighted circulation, 391
  atmospheric, mid-latitude, 571
  atmospheric, observations of, 572
  stratospheric, 642
Resonance of stationary waves, 610
Reynolds number, 46
Reynolds stress, 415
Reynolds, Osborne, 53
Rhines length, 447
Rhines scale, 446
Rhines–Young model, 761
Richardson number, 494
Richardson's four-thirds law, 482
Richardson, Lewis Fry, 442
Rigid body rotation, 144
Rigid lid, 108, 111
Rossby number, **87**
Rossby wave trains, 611
Rossby waves, **226–240**, 585
  and barotropic jets, 542
  and ray tracing, 621
  and turbulence, 446
  barotropic, 227
  breaking, 599, 642
  continuously stratified, 231, 599
  critical layers, 594
  dispersion relation, 228
  energy flux, **234–236**
  finite deformation radius, 229
  group velocity property, 384
  horizontal propagation, 588
  mechanism of, 229
  meridional propagation, 621
  momentum transport in, 542
  planetary geostrophic, 302
  propagation, 585
  reflection, 237
  topographic, 602
  two layers, 230
  vertical propagation, 599, 603, 605, 606
Rossby, Carl-Gustav, 212
Rotating frame, **55–59**

Salinity, 13, 33
  effect on potential vorticity, 160
  in box models, 814
Salt, 13
Sandström's effect, 809
Saturated adiabatic lapse rate, 692, 695
Saturation vapour pressure, 676
Scale height
  atmosphere, 42
  density, 27
  temperature, 28
Scale height, atmosphere, 83
Scaling, **46–47**
  geostrophic, 171
  in rotating shallow water equations, 171
  in rotating stratified equations, 174
Schwarzchild equations, 724
Seawater, 13, **33**
  adiabatic lapse rate, 34
  equation of state, 13, 33, 34
  heat capacity, 34
  potential temperature, 34
  thermodynamic properties, 33
Shadow zone, 791
Shallow water
  quasi-geostrophic equations, 180
Shallow water equations
  multi-layer, 112
  potential vorticity conservation, 162
  reduced gravity, 110
  rotation effects, 121
Shallow water model of Hadley Cell, 524
Shallow water systems, **105–123**
  conservation properties of, 120
  potential vorticity in, 120
Shallow water waves, **123–127**
Shallow-fluid approximation, 65
Sideways convection, **802–813**
  conditions for maintenance, 809
  energy budget, 808
  limit of small diffusivity, 811
  maintenance of, 808
  mechanical forcing of, 812
  phenomenology, 807
Sigma coordinates, 82
Singing in the rain, 673
Single-particle diffusivity, 478
Skew diffusion, 491
Skew flux, 491
Skew fluxes, 490
Sloping convection, 347
Solenoidal term, 145
Solenoids, 146, 151
Sound waves, 40
Southern Ocean, 836
Southern Oscillation, 888
Specific heat capacities, 20
Specific humidity, 675
Spectra of passive tracers, 437

Spherical coordinates, **59–68**
centrifugal force in, 59
Squire's theorem, 375
Stacked shallow water equations, 112
Staircases of potential vorticity, 451–453
Standard atmosphere, 572
State estimate, 537
Static instability, **97–99**, 695
Stationary phase, 223
Stationary waves, **609–625**
adequacy of linear theory, 614
and ray tracing, 621
Green function, 613
in a single-layer, 609
meridional propagation, 621
one-dimensional wave trains, 611
resonant response, 610
thermal forcing of, 615
Stokes, George, 53
Stommel box models, 813
Stommel wind-driven model, **733**
boundary layer solution, 737
properties of, 741
quasi-geostrophic formulation, 736
the nonlinear problem, 745
Stommel, Henry, 758
Stommel–Arons model, **821**
single-hemisphere, 821
two-hemisphere, 826
Stommel–Arons–Faller model, 818
Stratification
in mid-latitudes, 579
of the atmosphere, 572
Stratified geostrophic turbulence, 454
Stratosphere, 514, 572, **627**
polar vortex, 629
sudden warming of, 631
Stratospheric dynamics, **627–669**
Stratospheric sudden warmings, 663
Stress
Ekman layer, 201
kinematic, 202
Stretching, 149
Sudden warming, 631
Sudden warmings, 663
Super-rotation, 523
Surf zone, 629
Surface drifters, 483
Surface westerlies, 540
Surface winds, 567
observed, 514
Sverdrup balance, 737
near the equator, 863
Sverdrup interior flow, 738
Symmetric diffusivity tensor, 490
Tangent plane, 69
Taylor–Goldstein equation, 597
Taylor–Proudman effect, 90
TEM, 379, 387, 389, 392
TEM equations, **387**
for primitive equations, 581
Temperature, **17**, 724
dew point, 724
potential, 24, 724
wet-bulb, 724
Thermal equation of state, 13, 47
moist air, 721
Thermal wind, 87
in shallow water equations, 118, 119
Thermal wind balance, **87–93**
pressure coordinates, 91
Thermobaric effect, 14, 33
on potential density, 36
on potential vorticity, 161
Thermocline, 761, **774–798**
advective scaling, 777
boundary-layer analysis, 782
diffusive, 805
diffusive scaling, 777
internal, 779
kinematic model, 775
main, 774
one-dimensional model, 780
reduced-gravity, single-layer model, 786
scaling for, 776
summary and overview, 790
ventilated, 785
wind-influenced diffusive scaling, 778
Thermodynamic equation, **21–30**
Boussinesq equations, 72
for liquids, 25, 30
summary table, 26
Thermodynamic equilibrium, 21
Thermodynamic potentials, 17–19
Thermodynamic relations, **14–21**
fundamental, 16
Maxwell, 17
Thermodynamics
first law, 15
fundamental postulate, 14
moist, 720
Thermohaline circulation, 801
Thickness, 83
Thickness diffusion, **502**, 504
Thomas, Dylan, 3
Tilting and tipping, 149
Topographic effects
atmospheric stationary waves, 609
JEBAR, 756
oceanic western boundary current, 753

Toy models, 908
  El Niño, 898
Tracer continuity equation, 10
Tracer homogenization, 487
Traditional approximation, 65
Transformed Eulerian Mean, 379, 392, **387–392**
  and eddy transport, 506
  isentropic coordinates, 389
  primitive equations, 581
  quasi-geostrophic form, 387
  spherical coordinates, 581
Triad interactions, 415
  two-layer geostrophic turbulence, 457
Tropics, 673
Tropopause, 572–581, **706–708**
  definition, 572
Tropopause height
  in mid-latitudes, 579
  theory of, 706, 707, 725
Troposphere, 514, 572
  and potential vorticity transport, 574
  stratification, 572, 574, 578
  ventilation and moist convection, 577
Truesdell, Clifford, 52
Turbulence, **413**
  beta-plane, 448
  closure problem, 413
  degrees of freedom, 422
  fundamental problem, 413
  predictability of, 433
  three-dimensional, 416
  two-dimensional, 423
Turbulent diffusion, **473**, **475**, 490
  and the TEM, 506
  in the atmosphere and ocean, 493
  macroscopic perspective, 487
  requirements for, 485
  thickness, 502
  two-dimensional, 483
Turbulent diffusivity, 478
Turning line, 589, 607
Two-box model, 814
Two-dimensional turbulence, **423–433**
  beta effect, 445
  eddy diffusion in, 483
  energy and enstrophy transfer, 424
  numerical solutions, 432
Two-dimensional vorticity equation, 147
Two-layer instability problem, 356
Two-layer model
  of atmospheric mid-latitudes, 554
Two-layer QG equations, 184
Two-level QG equations, 194
Two-particle diffusivity, 480, 482

Under Milk Wood, 3
Unit vectors
  rate of change on sphere, 62

Vapour pressure
  saturation, 676
Vector invariant momentum equation, 66
Ventilated pool, 794
Ventilated thermocline, **785–798**
  reduced-gravity, single-layer model, 786
  two-layer model, 788
Vertical coordinates, **79–83**
Vertical vorticity equation, 155
Virtual temperature, 674, 676
Viscosity, 12
  effect on energy budget, 45
Viscous scale, 420
Viscous-advective range, 439
Vorticity, 96, **143–153**
  equation for a barotropic fluid, 146
  equation on beta plane, 156
  evolution equation, **145**
  evolution in a rotating frame, 153
  frozen-in property, 147
  in two dimensional fluids, 147
  stretching, 151
  stretching and tilting, 149
  vertical component, 155
Vorticity equation, 96
Vorticity, relative, 152
vr vortex, 144

Walker Cell, 717
Walker circulation, 328, 888, **891**
Water, 673
Water vapour, 673–676
  measures of, 675
Wave activity, 384
  and pseudomomentum, 384
  group velocity property, 384
  orthogonality of modes, 385
Wave breaking, 642
Wave packet, 221
Wave propagation, 585
Wave trains, 611
Wave–mean-flow interaction, **379**, 382
  quasi-geostrophic, 380
Wave–turbulence cross-over, 446
Waveguides
  for equatorial waves, 314
  for internal waves, 274
Wavelength, 217
Waves, **215**
  acoustic-gravity, 293
  barotropic Rossby, 227
  breaking, 642

frequency, 216
group velocity property, 240
hydrostatic gravity, 261
inertial, 126
Kelvin, 126, 636
kinematics, 215
Lamb, 295
Poincaré, 124, 125, 244
Rossby, 226
Rossby dispersion relation, 228
Rossby wave mechanism, 229
Rossby, continuously stratified, 231
Rossby, single-layer, 227
Rossby, two-layer, 230
rotating shallow water, 124
shallow water, 123
sound, 40
wavevector, 216
Wavevector, 216
Weak temperature gradient approximation, 712, 714
adjustment to, 716
for stratified flow, 717
in shallow water equations, 716
Weather predictability, 437
West, Mae, 156
Western boundary currents
topographic and inviscid, 753
Western boundary layer, 739
frictional, 738
inertial, 747
Western intensification, 731
Western pool, 793
Wet-bulb temperature, 724
Wind-driven gyres, 731
Wind-driven ocean circulation, **733–770**
continuously stratified, 767
homogeneous model, 733
two-layer model, 761
vertical structure, 761
WKB approximation, **247–249**, 623
internal waves, 271
Rossby waves, 589, 590, 598

Zonal boundary layers in ocean gyres, 744
Zonal flow in turbulence, 446
Zonal flows in beta-plane turbulence, 448
Zonally-averaged atmospheric circulation, 539